Universidade de Aveiro
2012

Departamento de Biologia

Tatiana Lima de Vilhena Magalhães Costa

Respostas celulares aos erros de tradução do genoma

Cellular responses to genome mistranslation

Universidade de Aveiro
2012

Departamento de Biologia

Tatiana Lima de Vilhena Magalhães Costa

Respostas celulares aos erros de tradução do genoma

Cellular responses to genome mistranslation

Dissertação apresentada à Universidade de Aveiro para cumprimento dos requisitos necessários à obtenção do grau de Doutor em Bioquímica, realizada sob a orientação científica do Doutor Manuel Santos, Professor Associado do Departamento de Biologia da Universidade de Aveiro

Apoio Financeiro: Programa Operacional Potencial Humano (POPH) - QREN, comparticipado pelo Fundo Social Europeu (FSE) e por fundos próprios do MCES.

“One time /one meeting (ichigo-ichie)
This gathering never happened in the past and it will never happen in the future,
as its exact nature will never be the same again”

Sen no Rikyú (1522-1591)

“If we knew what it was we were doing it would not be called research, would it?”

“No amount of experimentation can ever prove me right; a single experiment can prove me wrong.”

Albert Einstein (1879-1955)

o júri

Presidente

Doutor Vitor José Babau Torres
Professor Catedrático da Universidade de Aveiro

Doutor Vítor Manuel Vieira da Costa
Professor Associado, ICBAS- Instituto de Ciências Biomédicas Abel Salazar da Universidade do Porto

Doutora Maria Alexandra Marques Moreira Mourão do Carmo
Investigadora Principal, IBMC- Instituto de Biologia Molecular e Celular da Universidade do Porto

Doutora Maria Paula Polónia Gonçalves
Professora Associada da Universidade de Aveiro

Doutor Manuel António da Silva Santos
Professor Associado da Universidade de Aveiro

Doutora Paula Cristina Costa Alves Monteiro Ludovico
Professora Auxiliar da Escola de Ciências da Saúde da Universidade do Minho

Doutora Laura Cristina da Silva Carreto
Investigadora Auxiliar do CESAM- Centro de Estudos do Ambiente e do Mar da Universidade de Aveiro

Agradecimentos

Acknowledgements

I am thankful to my supervisor Professor Manuel Santos for all these years that I have worked with him. He taught me a great deal about research work and scientific thinking.

I would like to express my gratitude to the members of the Desjardins laboratory, especially to Christiane, Magali and Joe for the warm welcome in their laboratory, and for making my Canadian days less lonely and more fun. And a big thanks to Xana and Paula for helping with my laboratory experiments, for all the discussions and fruitful inputs that meant so much in this last period of my thesis.

Also, I would like to thank to the all the people in the hallway- Isabel, Sofia, Claúdia, Cristina, Andreia, Marta, and Virgilia - and also to the girls upstairs namely Gabi, Sandra V., Sandra and Margarida, for saving my work when something was missing.

A special thanks to Tânia, which was there since the first moment in Aveiro and in the Biology world. Thanks also to Rita Jordão, Márcia Henriques, Rui Adão and also my sweet brother Diogo for being my "study model" in what teaching is concerned. I am sorry if things did not go always as smoothly as they should.

I am most grateful to Dr. Roy Parker and Dr.Daniela Teixeira; Dr.Mathias Petter and Dr. Claudine Kraft; Dr. Oshumi, Dr. Kabeya and Dr. Buchan for sending plasmids and to Dr Klionsky for strains, for the most helpful discussions and interest in my work. And also to Yu-yi Lin for the emails with technical advices and interesting scientific discussions.

During my years in the RNA Biology Laboratory, I have worked with many interesting and fantastic people, several of them became my dear friends. Many thanks to Catarina and Céu for their friendship, encouragement, support, help, advices, critical readings and the most valuable comments. Cristina, João S. (júnior), Rita B., Marisa, Patricia and Laura: thanks for the silly (and not so silly!) conversations, for the company late at night, at weekends and holidays, for the lunches and dinners (Snack, Ramona and Evaristo sempre!), drinks and laughs that we have shared. Thanks for all the help with the experiments too and for making me feel better whenever things seemed upside down. I have the feeling that I have received more than what I gave. Without you it would have been so much difficult! Thanks, João P. (senior) for answering to all my questions. Also, Violeta, thanks for all the administrative work and friendship; Ana S., Jörg, Tobias, and Gabi thank you for the enthusiasm and for your examples.

Thanks, Isabelinha, for all that is behind- the dancing nights, the vacations and wild trips, the horseback riding passion, the talks and the late night pancakes. And today, after all the twists and turns in life and the distance apart, thanks for your continuous support and invaluable friendship.

Thanks to my family too, close relatives and friends in Porto de Mós and surroundings that saw me grow, for all the interest shown in my work and for being such a colorful bunch of people. And, also, to Família Macedo, which has been here for me daily for the last years, making my days much more cheerful.

Mum, Dad and Diogo, thanks for raising me up and making me believe. Thanks for your support, encouragement and trust towards my choices. And for much more that I cannot put into words.

And finally, thank you Bé for being you: someone who urges me on, has faith in me, and makes me smile and laugh. Thanks for being my balance, for your patience and for teaching me to look to the brighter side of life. Thanks for making me incredible happy!

Palavras-chave Tradução do mRNA, erros de tradução, proteoma, proteostasia, tRNA, síntese proteica, autofagia, stress oxidativo, stress proteotoxico

Resumo

Erros no processo da síntese proteica podem ter profundos efeitos na fisiologia celular e no desenvolvimento de doenças, nomeadamente doenças neurodegenerativas, cancro e envelhecimento. A introdução de erros durante a síntese de proteínas e, em particular durante o processo da tradução, é designado por "mistranslation" que é um processo pouco estudado e mal compreendido. Neste projecto, construímos leveduras que, sistemática e constitutivamente, treslêem o codão de leucina CUG como serina, o que corresponde a um aumento de erro de 240 vezes relativamente à taxa de erro basal da síntese proteica (0.001%).

Os resultados obtidos demonstram que os erros de tradução induzem a actividade autofágica, acumulação de proteínas insolúveis, produção de espécies reactivas de oxigénio, disrupção funcional e morfológica das mitocôndrias, não ocorrendo, no entanto, destruição selectiva destas. A expressão do gene *PNC1*, associado ao aumento da longevidade e regulador da actividade da deacetilase Sir2p, é fortemente aumentada em resposta aos erros da tradução. Os genes *PNC1* e *SIR2* estão envolvidos no controlo da autofagia induzida pelos erros de tradução mas não em situações de stress nutricional. O aumento dos erros de tradução leva à formação de P-bodies, mas não induz a formação de grânulos de stress e reduz a expressão de genes que codificam proteínas ribosomais em vez de se verificar destruição selectiva de ribosomas - ribofagia.

Este estudo mostra que as células de levedura são muito mais resistentes aos erros na tradução do que o esperado. Os resultados mostram um papel fundamental da autofagia na resposta celular aos erros de tradução e indicam que estes têm um forte impacto em alterações morfo-funcionais das mitocondrias, sendo este um dos fenótipos mais marcantes nestas células. Considerando que a maior parte dos mecanismos celulares são conservados entre leveduras e células humanas, este estudo mostra que a levedura é um excelente modelo para estudar a resposta celular aos erros de tradução e sugere que o stress oxidativo, a acumulação de espécies reactivas de oxigénio e a acumulação de proteínas insolúveis podem ser a causa da degeneração celular observada em múltiplas doenças humanas associadas a defeitos na síntese proteica.

keywords Translation, mistranslation, proteome,proteostasis, tRNA ,protein synthesis, autophagy, oxidative stress,proteotoxic stress

abstract

Low level protein synthesis errors can have profound effects on normal cell physiology and disease development, namely neurodegeneration, cancer and aging. The biology of errors introduced into proteins during mRNA translation, herein referred as mistranslation, is not yet fully understood. In order to shed new light into this biological phenomenon, we have engineered constitutive codon misreading in *S. cerevisiae*, using a mutant tRNA that misreads leucine CUG codons as serine, representing a 240 fold increase in mRNA translational error relative to typical physiological error (0.0001%).

Our studies show that mistranslation induces autophagic activity, increases accumulation of insoluble proteins, production of reactive oxygen species, and morphological disruption of the mitochondrial network. Mistranslation also up-regulates the expression of the longevity gene *PNC1*, which is a regulator of Sir2p deacetylase activity. We show here that both *PNC1* and *SIR2* are involved in the regulation of autophagy induced by mistranslation, but not by starvation-induced autophagy. Mistranslation leads to P-body but not stress-granule assembly, down-regulates the expression of ribosomal protein genes and increases slightly the selective degradation of ribosomes (ribophagy).

The study also indicates that yeast cells are much more resistant to mistranslation than expected and highlights the importance of autophagy in the cellular response to mistranslation. Morpho-functional alterations of the mitochondrial network are the most visible phenotype of mistranslation. Since most of the basic cellular processes are conserved between yeast and humans, this study reinforces the importance of yeast as a model system to study mistranslation and suggests that oxidative stress and accumulation of misfolded proteins arising from aberrant protein synthesis are important causes of the cellular degeneration observed in human diseases associated to mRNA mistranslation.

Contents

List of abbreviations

2D-PAGE	two dimensional polyacrylamide gel electrophoresis
A	ampére
ADH	alcohol dehidrogenase
APS	ammonium persulphate
ATG genes	Autophagy Related Genes
ATP	adenosine 5'-triphosphate
AZC	azetidine-2-carboxylic acid
cAMP	cyclic adenosine 5'-monohosphate
cDNA	complementary deoxyribonucleic acid
Cm	centimeter
Cy3	cyanine 3
Cy5	cyanine 5
DHE	dihydroethidium
DHR123	dihydrorhodamine 123
DMSO	dimethyl sulfoxide
DNA	deoxyribonucleic acid
DNP	2, 4-dinitrophenylhydrazine
DTT	dithiotreitol
EDTA	ethylenediamine tetracetic acid
ER	endoplasmatic reticulum
ERAD	endoplasmatic reticulum associated degradation
g (mg, μg, ng)	gram (miligram, microgram, nanogram)
GFP	green fluorescent protein
GTP	guanosine 5'-triphosphate
H_2O_2	hydrogen peroxide
HEPES	N-[-2-hydroxyethyl]piperazine-N'-[2-ethanesulfonic acid]
HSP	heat shock protein
kDa	kilodalton
l (ml, μl)	liter (mililiter, microliter)
MCA	4-methylcoumaryl-7-amide
mQ	milliQ
mRNA	messenger ribonucleic acid
mtDNA	mitochondrial DNA
NAD	oxidised nicotinamide adenine dinucleotide
NADPH	reduced nicotinamide adenine dinucleotide phosphate
NADH	reduced nicotinamide adenine dinucleotide
$NADP^+$	oxidised nicotinamide adenine dinucleotide phosphate
nm	nanometers
NP-40	nonylphenyl-polyethylene glycol
$OD_{600/595}$	optical density at 600 nm or 595 nm
PAS	pre-autophagosomal structure
PBS	phosphate buffered saline
PMSF	phenylmethylsulfonyl fluoride
RFU	relative fluorescence units
RNA	ribonucleic acid
ROS	reactive oxygen species
rpm	revolutions per minute
rRNA	ribosomal ribonucleic acid
RT	room temperature
SDS	sodium dodecyl sulphate
SDS-PAGE	sodium dodecyl sulphate-polyacrylamide gel electrophoresis
SMD	synthetic minimal médium
Suc-LLVY-MCA	succinyl-leucyl-leucyl-valyl-tyrosine 4-methylcoumaryl-7-amide
TCA	trichloroacetic acid
TEM	transmission electron microscopy
TEMED	N,N,N,'N,'-tetramethylethylenediamine
Tris	2-amino-2-hydroxymethyl-1,3-propanodiol
tRNA	transfer ribonucleic acid
U	units
Ub	ubiquitin
V	volt
W	watt
YPD	Yeast Peptone Dextrose médium

Background and Thesis Outline

Aims of this study and thesis organization

During the last ten years, our laboratory pioneered a number of studies to elucidate the evolution of genetic code alterations, which are mediated by codon decoding ambiguity, a form of mRNA mistranslation. These studies provide the first insight on how genetic code alterations evolve and raise a number of new biological questions, namely how do organisms tolerate mRNA mistranslation and genetic code alterations? For example, re-construction of a *Candida albicans* genetic code alteration in the close relative *S. cerevisiae* showed that codon ambiguity deregulates gene expression, up-regulates the expression of stress genes and induces the accumulation of trehalose and glycogen. These results show that the experimental system used in our laboratory could be an excellent working model for studying the impact of general mistranslation on cells physiology, which is of biomedical relevance. Here we explore this hypothesis to shed new light on the cellular responses to aberrant protein synthesis.

This thesis is written in the form of three manuscripts (chapters 2-4), as follows:

Chapter 1 provides a general introduction and addresses translational mechanisms, translational fidelity and proteome quality control mechanisms. A brief introduction to the working model used in this thesis is provided at the end of the chapter.

Chapter 2 establishes a link between mRNA mistranslation and autophagy in yeast and explores the role of the *SIR2* gene on protein aggregation and autophagy.

Chapter 3 describes a link between mistranslation and oxidative stress. The data show that mistranslation increases accumulation of reactive oxygen species (ROS) in both wild-type and in several knockout strains. In addition, we describe the effects of mistranslation on mitochondrial homeostasis.

Chapter 4 describes a link between mistranslation and P-body assembly and explores the formation of stress granules by mistranslation.

Finally, **Chapter 5** is a general discussion that integrates the results presented in chapters 2-5. Future perspectives and studies are also presented.

Parts of the work presented in this PhD thesis contributed to the following publications:

- Lima-Costa T, Paredes JA, Rondeau C, Desjardins M, Moura GR, Santos MAS , **Mistranslation of the genetic code induces autophagy in yeast**, International Conference on Yeast Genetics and Molecular Biology. Yeast. 2009 Jul;26(S1): S176-S208
- Silva RM, Duarte IC, Paredes JA, Lima-Costa T, Perrot M, Boucherie H, Goodfellow BJ, Gomes AC, Mateus DD, Moura GR, Santos MAS, **The yeast PNC1 longevity gene is up-regulated by mRNA mistranslation**, PLoS One. 2009; 4(4):e5212.
- Silva RM, Paredes JA, Moura GR, Manadas B, Lima-Costa T, Rocha R, Miranda I, Gomes AC, Koerkamp MJG, Perrot M, Holstege FCP, Boucherie H, Santos MAS, **Genetic Code Alteration Plays a Critical Role in the Evolution of Candida Genes Quantitative Analysis of Single Amino Acid Changes using a 4000 QTRAP® system**(2007),Applied Byosystems technical note.
- Silva RM, Paredes JA, Moura GR, Manadas BR, Lima-Costa T, Rocha R, Miranda I, Gomes AC, Koerkamp MJ, Perrot M, Holstege FC, Boucherie H, and Santos MAS. 2007. **Critical roles for a genetic code alteration in the evolution of the genus *Candida***. *EMBO J.* 26:4555-4565.

The results described in this thesis were presented at the following scientific meetings:

- VI Simpósio Pós-Graduação do Departamento de Biologia da Universidade de Aveiro, May, 2007, Aveiro, Portugal (Oral presentation)
- EMBO Conference on Protein Synthesis and Translational Control, 12th -16th Setember, 2007, Heidelberg, Germany (Poster presentation)
- RNA 2008-Thirteenth Annual Meeting of the RNA Society, 28thJuly- 3rdAugust, 2008, Berlin, Germany (Poster presentation)

- EMBO conference on Autophagy: Cell Biology, Physiology and Pathology 18th - 21st October, 2009,Ascona, Switzerland (Poster presentation)
- 23rd tRNA Workshop,28th January-1st Feb, 2010, Aveiro, Portugal (Poster presentation) Yeast Genetics and Molecular Biology Meeting, 27thJuly- 1stAugust, 2010, University of British Columbia, Vancouver, Canada (Poster presentation)

Chapter 1
Literature Overview

From genes to proteins: a process (almost) perfect

Gene expression is a highly efficient and accurate molecular process that is tightly regulated. However, synthesis of functional proteins is not error free. Mistranslation is a general term used for describing translational errors. Over the last 45 years, many attempts have been made to quantify the error rate of gene translation, however little is still known about such errors and their biological relevance remains poorly understood.

Gene translation errors can occur at replication, transcription, translation and post-translational level (Figure 1). During replication and transcription, polymerase slippage or nucleotide misincorporations can occur. Indeed, the bacterium *Escherichia coli* has a typical replication error rate of approximately 10^{-8}– 10^{-9} per base pair (Kunkel and Bebenek, 2000), and uses specific mechanisms like editing and repair to correct such errors. In eukaryotes, DNA replication error rates are even lower, being in the order of 10^{-10}– 10^{-11} (Matsuda et al., 2000). The error rate of transcription *in vivo* in *E. coli* has been estimated at $1.4x10^{-4}$ per nucleotide (Rosenberger and Foskett, 1981; Ninio, 1991) and more recent *in vitro* studies have shown that the rate of misincorporation of UTP at G sites during transcription is in the order of $2x10^{-6}$ (Kireeva et al., 2008). On the other hand, studies in HeLa cells (Fox-Walsh and Hertel, 2009) and *Schizosaccharomyces pombe* (Wilhelm et al., 2008) have shown that mRNA splicing can also account for mistranslation through exon skipping and failure in removing introns. These errors occur at rates of $\approx 10^{-2}$- 10^{-6}(Drummond and Wilke, 2009). Translation, the last step in the gene expression process, is the most error prone, with average error

rate of approximately 1 amino acid per 10^4 codons (10^{-4}). This means that 15% of all average-length protein molecules contain at least one misincorporated amino acid (Reynolds et al., 2010). Even when correctly transcribed and translated, that is, in cases where proteins have the correct amino acid sequence, post-translational modifications errors as well as folding errors alter their function, but their relevance and frequency are still obscure. For instance, Winklhofer and coworkers (Winklhofer et al., 2008) have suggested that misphosphorylation of the microtubule-binding protein tau is a pathological signature of Alzheimer's disease and that it contributes to misfolding and aggregation of this protein. Additionally, mutations that alter glycosilation have been described as being extremely deleterious (Freeze, 2006; Freeze, 2006).

As this work is focused on the consequences of erroneous amino acid incorporation into proteins, a brief overview of the eukaryotic mRNA translation mechanism is provided below.

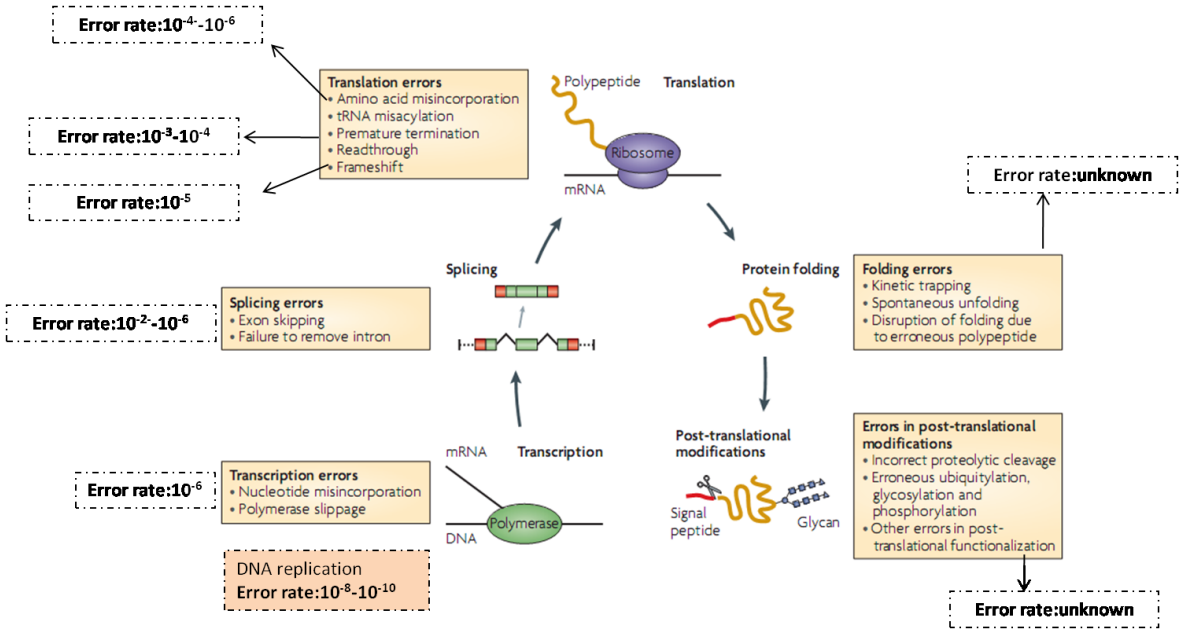

Figure 1 - Errors in genetic information flow. Errors arise at many stages, from the transcription of genetic information to the folding and post-translational modification of the finished polypeptide. Estimated error rates are shown. Adapted from Drummond and Wilke, 2009.

Eukaryotic translation

Translation is the last step of gene expression and is divided into three steps: initiation, elongation and termination. Initiation and termination have mechanistic differences between eukaryotes, bacteria and archea, while elongation is semi-conserved across the three kingdoms of life (Kapp and Lorsch, 2004). During initiation, all the events that are needed for the positioning of the ribosome at the start codon take place. Polypeptide synthesis occurs during the elongation step and the completed peptide is released during termination.

During initiation the assembly of a ribosome with an initiator-methionyl-transfer-RNA (met-$tRNA_i^{Met}$) in its peptidyl (P-) site located on the initiation codon of the mRNA is accomplished. In order to do so cells use the 5´m7(5´)ppp(5´)N cap structure and the 3'end of the poly(A) tail of the mRNA together with at least 12 eukaryotic initiation factors (eIFs). In contrast, prokaryotes only need three initiation factors (Kapp and Lorsch, 2004b). The initiation step can be divided into several steps (Figure 2), namely (i) assembly of eukaryotic initiation factor 2 (eIF2), GTP and met-$tRNA_i^{Met}$ (ternary complex); (ii) formation of a 43 Svedberg (S) preinitiation complex, comprising the small (40S) ribosomal subunit, initiation factors (eIF1, eIF1A, eIF3) and the ternary complex and probably eIF5; (iii) activation of the mRNA, an ATP-dependent reaction, that implies the unwinding of the mRNA cap-proximal region by eIF4F and eIF4B; (iv)

recruitment of the 43S complex to the (capped) 5'end of the mRNA; (v) scanning of the 5'untranslated region (UTR) of the mRNA by the 43S complexes; (vi) recognition of the start codon (AUG) and formation of 48S initiation complex, leading to an alteration in the conformation and with a consequent displacement of eIF1, allowing eIF5-mediated hydrolysis of eIF2-bound GTP and Pi release; (vii) joining of the large (60S) subunit to assemble a complete (80S) ribosome, and associated displacement of eIF2–GDP and other factors (eIF1, eIF3, eIF4B, eIF4F and eIF5) mediated by eIF5B and (viii) hydrolysis of GTP by eIF5B and release of eIF1A and GDP-bound eIF5B from assembled elongation-competent 80S ribosomes. At this point, the mRNA is positioned so that the next codon can be translated during the elongation step of protein synthesis. As translation is a cyclic process, termination follows elongation and leads to recycling (Figure 2, step 1), which generates separated ribosomal subunits. It is important to note that protein synthesis is mainly regulated during initiation, rather than during elongation or termination.

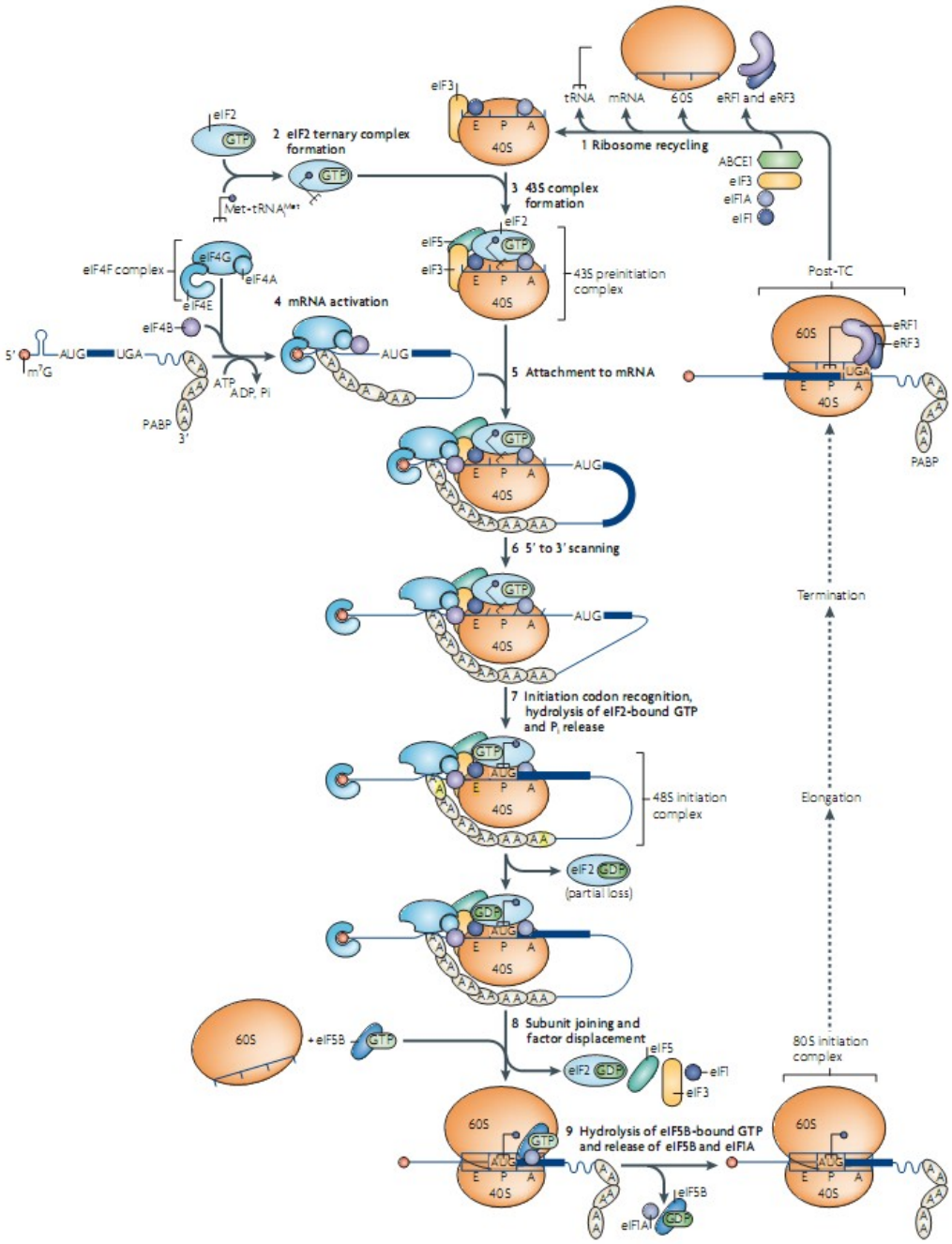

Figure 2- Details of eukaryote translation initiation. Translation initiation is a complex process that can be divided into several steps. It comprises ternary complex formation (2), 43S complex formation (3), mRNA activation (4), attachment of pre-initiation complex to mRNA (5), scanning of the 5'UTR (6), recognition of initiation codon (7), joining of 60S subunit and displacement (8), hydrolysis of eIF5B-GTP bound and eIF5B and eIF1A factor release (9) and ribosome recycling (1). Adapted from Jackson et al., 2010.

During elongation sequential binding of aminoacyl-tRNAs (aa-tRNAs) to the ribosome and the formation of peptide bonds between the amino acids occur (Figure 3, A). This phase is dependent on the activity of several factors, known as elongation factors (EF), and requires substantial amounts of energy. It starts by the recognition of the aa-tRNAs by elongation factor eEF-1 (EF-Tu in bacteria), in the presence of GTP. After the recognition step, the aatRNA-eEF1-GTP complex enters the empty A-site of the ribosome and the anticodon of the incoming aa-tRNA recognizes the mRNA codon positioned in the A–site. Universally conserved bases in the small subunit of the ribosome (16S rRNA, bacteria; 18S eukaryotes) interact with the 2 first bases of the codon/anticodon complex. This interaction stabilizes a specific ribosomal conformation, which allows for verification of whether the correct tRNA is bound. A ribosomal conformational change coupled with the formation of correct codon-anticodon complexes leads to alterations in the position of active site residues bound to eEF1A which, in turn, activates its GTPase activity. The eEF1A•GDP complex releases the aa-tRNA into the A site (Kapp and Lorsch, 2004b). The peptide bond, which is catalyzed in the ribosomal peptidyl transferase center, is then formed between the growing polypeptide, which is located in the P-site of the ribosome, and the new amino acid located in the A-site. At this point, the P-site is free and a new peptidyl-tRNA occupies the A-site. The ribosome moves one codon forward (mRNA translocation) thereby exposing new codons for tRNA binding. Simultaneously with the ribosome movement, the empty tRNA is displaced from the P-site to the E-site as the peptidyl tRNA is translocated from the A-site to the P-site. This process is facilitated by elongation factor eEF-2 (EF2-G in prokaryotes) and GTP, which is hydrolyzed by the elongation factor. After translocation, the peptidyl-tRNA is positioned in the P-site and

the next codon on the mRNA is made available for interaction with a new aa-tRNA in the A-site (Kapp and Lorsch, 2004a). Additionally, ribosome translocation allows another ribosome to initiate on the 5′ end of the mRNA and begin its round of translation. Thus, mRNAs usually have several ribosomes attached to them forming a polysome. These reaction steps are repeated until the ribosome encounters an in-frame stop-codon (UAA, UAG, UGA). After GTP hydrolysis and the release of the aa-tRNA onto the ribosome, the eEF1A•GDP complex is released. In order to participate in successive rounds of polypeptide elongation, it is recycled to its GTP-bound form by eEF1B multifactor complex. Additionally, fungi possess an additional factor, eEF3, that possesses both GTPase and ATPase activity (Dasmahapatra and Chakraburtty, 1981; Skogerson and Engelhardt, 1977) and whose encoding gene is essential for yeast viability (Qin et al., 1990). This factor is found primarily associated with translating cytosolic ribosomes and is required for each round of elongation. It is known to interact with eEF1A (Kovalchuke et al., 1998) and to facilitate the release of the E-site-deacylated tRNA and the binding of the eEF1A-GTP•aa-tRNA ternary complex to the A site of the ribosome (Triana-Alonso et al., 1995). The elongation step can be inhibited by drugs like cycloheximide and lactinidomycin, which specifically block the translocation step (Schneider-Poetsch et al., 2010).

Whenever a stop codon is found in the ribosomal A site, translation termination occurs (Figure 3, B). This results in the release of the completed polypeptide chain, following the hydrolysis of the ester bond that links the polypeptide chain to the P-site tRNA. The hydrolysis reaction is thought to be carried out by the ribosomal peptidyl transferase center. As cells do not have tRNA molecules that recognize stop codons,

release factors are used to recognize the stop signals and terminate protein synthesis. Eukaryotic cells have 2 RFs (eRF-1 and eRF-3). eRF-1 recognizes the stop codons and eRF-3 acts together with the first enhancing its activity. The RF bind to the termination codon in the A site and stimulate hydrolysis of the bond between the tRNA and the polypeptide chain in the P site. The completed polypeptide and the tRNAs are then released from the ribosome while the ribosomal subunits and the mRNA template dissociate.

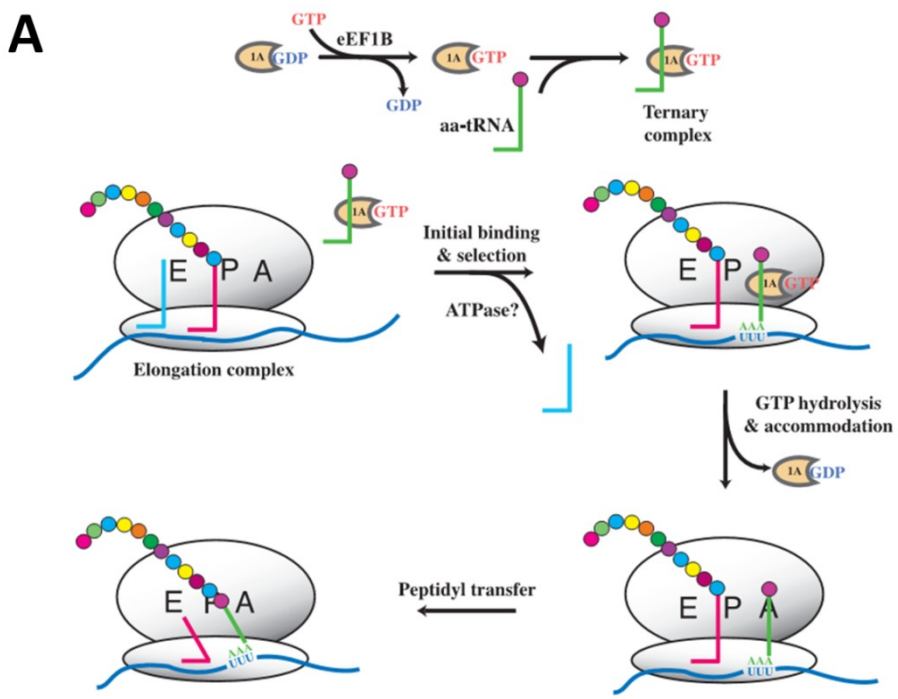

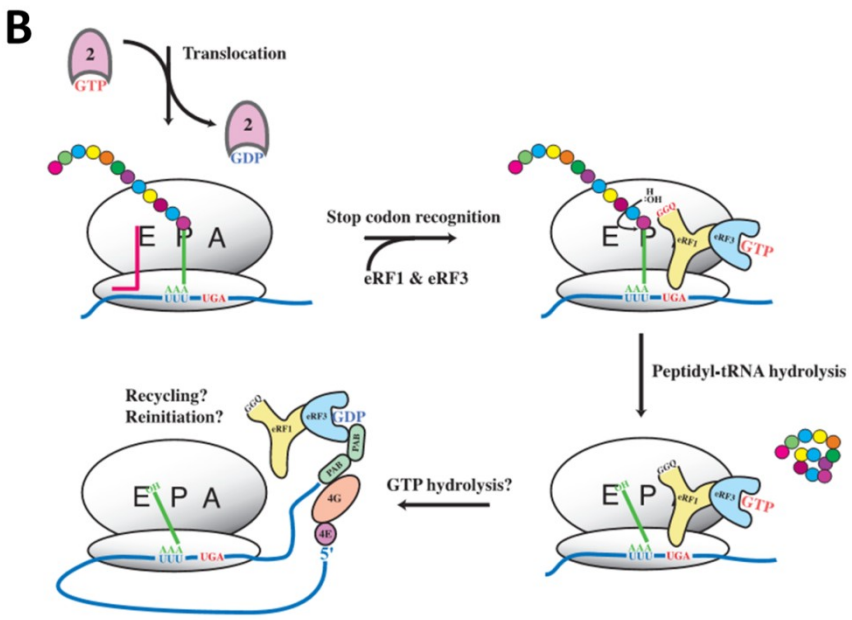

Figure 3- Simplified view of eukaryotic translation elongation and termination. A) Elongation- the elongation factor eEF1A delivers aa-tRNAsto the ribosomal A site. When a codon/anticodon match is detected, eEF1A deposits the aa-tRNA and is itself released from the ribosome. A peptide bond is then formed. eEF2 promotes the GTP-dependent translocation of the nascent protein chain from the A-site to the P-site of the ribosome, positioning the next codon in the A site and allowing the process to repeat **B) Termination** - A termination codon at the A site is recognized by a release factor rather than by a tRNA. The result is the release of the completed polypeptide chain, followed by the dissociation of tRNA and mRNA from the ribosome. Note that not all steps are shown, see text for details. Adapted from Kapp and Lorsch,2004b.

Translation errors and determinant factors

Translation is accurate and occurs at biologically relevant rates. As in many other biological processes, accuracy has its price and therefore, speed and accuracy are a compromise solution, indicating, therefore, that accuracy is not perfect. Indeed, of all the steps of the flow of genetic information from genes to proteins, translation is the most error prone step. Errors occur during tRNA aminoacylation by the aaRS or at the level of mRNA decoding by the ribosome. Phenomena like amino acid

misincorporation, tRNA misacylation, premature termination, stop codon readthrought, ribosome drop-off and frameshifting are frequent (Drummond and Wilke, 2009). Aminoacylation errors are mostly due to abnormal recognition of the tRNAs and amino acids by aaRSs. At the ribosome level missense errors occur when a wrong amino acid is incorporated into the polypeotide chain, while nonsense errors are due to stop codon readthough which ultimately results in proteins with extended C-termini (Figure 4). Processivity errors and frameshifting originate truncated proteins. Frameshifting errors, i.e., errors that occur due to shifting of reading frames during the elongation step, normally result in synthesis of truncated proteins due to premature translation termination (Farabaugh and Bjork, 1999). The mechanisms by which frameshifting occurs is not yet fully understood, but some models have been proposed, namely the pause and slip model (Farabaugh and Bjork, 1999), which postulates that frameshifting is a two step process (Figure 4, B). This type of translational error occurs at a frequency of 10^{-5} in E*. coli* (Curran and Yarus, 1986). Analysis of premature termination in *E. coli* and in *S. cerevisiae* has also shown that this type of error has a frequency in the order of 10^{-4} to 10^{-3} per codon (Arava et al., 2005). Ribosomal accuracy is therefore energetically costly and affects translational speed (Drummond and Wilke, 2009).

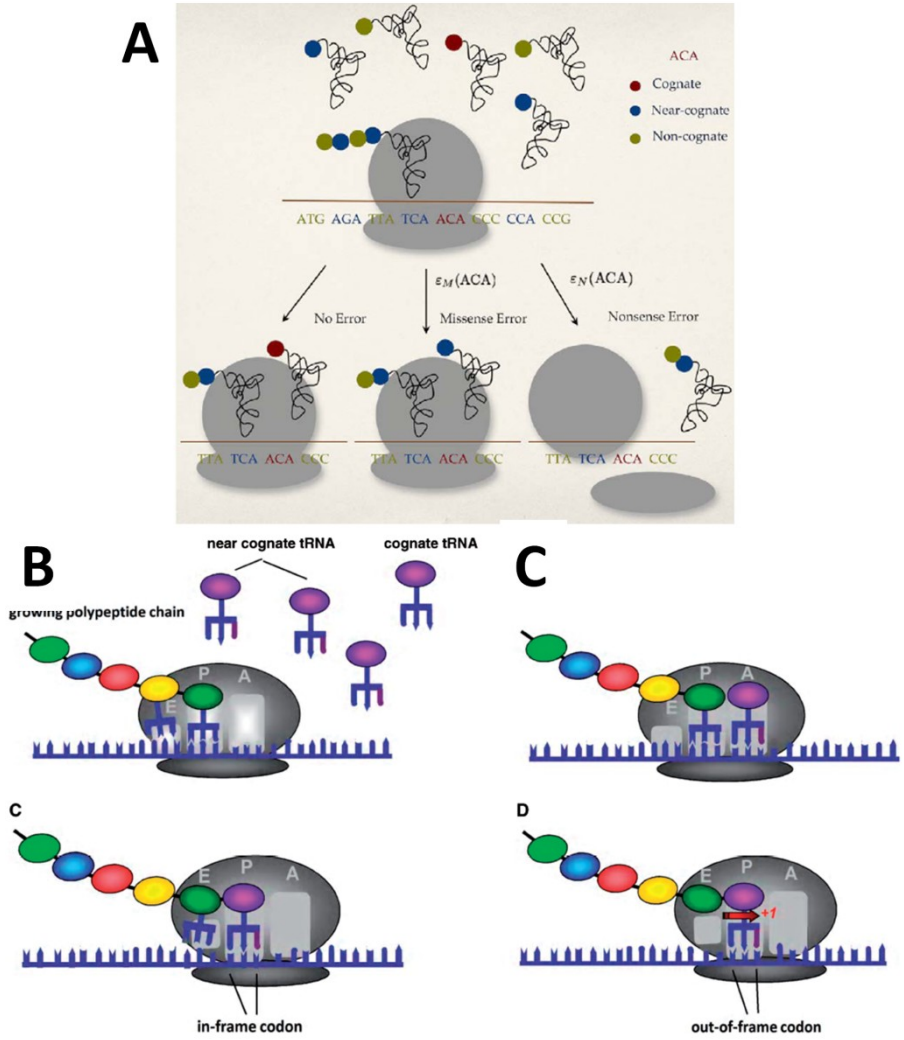

Figure 4- Translation errors at the ribosome level- A) During the translation process the ribosome stops at a codon (in this case ACA), while waiting for a cognate tRNA. At this point 3 things can happen:1) the cognate tRNA arrives and elongation occurs leading accurate translation; 2) a near-cognate tRNA is used and elongation proceeds leading to a missense error (incorporation of a wrong amino acid into the growing peptide chain) or 3) premature termination of translation due to recognition by release factors, spontaneous ribosome drop-off or frameshifting leading to a nonsense error (adapted from Shah and Gilchrist, 2010) **B and C) Frameshifting (Pause-and-Slip model)** +1 frameshifting is shown. In the first step **(B)**, insufficient amount of cognate tRNA results in an empty ribosomal A-site, as the near cognate tRNA forms a suboptimal bond with the mRNA, dropping off easily, leading to a translational pause. In the second step **(C)**, when a weak bond is formed between the near-cognate tRNA and the codon, translocation to the P-site occurs. As the interaction tRNA-mRNA is weak, the near-cognate tRNA can “slip” to the right (+1 frameshiting) or to the left (-1 frameshifting).

Amino acid starvation conditions, mRNA structure, codon usage, tRNA abundance and tRNA modifications are known to increase translational errors (Kramer and Farabaugh, 2007; Stahl et al., 2004; Parker and Precup, 1986; Precup and Parker, 1987) . Premature termination and ribosome drop-off, for instance, can happen due to alterations in the concentration of aminoacylated tRNA, as it can transiently stall the ribosomes (Zhang et al., 2010). Codons corresponding to low abundance tRNAs will be more error prone than other codons (Drummond and Wilke, 2009; Kramer and Farabaugh, 2007). Likewise, tRNAs with the right amino acid (cognate) and tRNAs with the wrong amino-acid (near cognate, single codon-anticodon nucleotide mismatch) compete for the ribosomal A-site and the latter may introduce missense errors. An increase in abundance of cognate tRNA decreases missense error and, conversely, an increase in abundance of near-cognate tRNA has the opposite effect (Shah and Gilchrist, 2010; Kramer and Farabaugh, 2007; Zaher and Green, 2009). In higher eukaryotes, tRNA concentration varies among different tissues and stages of differentiation (Dittmar et al., 2006) and in exponentially growing bacteria tRNA concentration can change very quickly (Rocha, 2004; Rocha and Danchin, 2004). Base modifications in tRNAs are known to affect mRNA translation accuracy as they affect their coding capacity and influence codon-anticodon interactions (Bjork, 1995). Despite their importance modified nucleosides are apparently not essential in *E.coli*, which contrasts to the situation of yeast where the lack of certain modifying enzymes is lethal (Persson et al., 1992). In *S.cerevisiae* and bacteria, tRNA modifications have been suggested to act as biological sensors, changing in quantity and quality accordingly to growth conditions. Moreover, nucleoside modification deficiencies have a diverse

range of effects, from decreased virulence in bacteria, neuronal system disease in human, and gene expression and stress response changes in plants.

Protein Quality Control Mechanisms

Errors in DNA replication are repaired by DNA repair systems and errors in transcription and mRNA processing are fixed by mRNA quality control systems, notably by the nonsense mediated decay (NMD) (Amrani et al., 2006; Garneau et al., 2007). Likewise, errors in translation are dealt by protein quality control mechanisms (Reynolds et al., 2010; Koga et al., 2011; Buchberger et al., 2010). Organisms evolved strategies to reduce the frequency of errors. For example, genes tend to select high-fidelity codons which correspond to abundant tRNAs. Furthermore, errors normally occur between chemically similar amino acid, which minimizes their impact on protein structure (Drummond and Wilke, 2009). Therefore, organisms normally tolerate errors because these do not lead to significant changes in fitness. This is known as translational-robustness selection, i.e, a selection pressure that causes proteins to be tolerant to missense errors. In other words, translationally robust proteins fold and function even when mistranslated.

In addition, both aaRS and ribosomes possess mechanisms to avoid and correct errors. If these mechanisms fail and abnormal proteins are synthetized, post-translational quality control mechanisms are activated. The following paragraphs elucidate briefly quality control mechanisms both at translation level and at post translation level.

Translational Quality Control

Aminoacyl-tRNA-synthetases discriminate between cognate and near-cognate amino acids (Figure 5, A). However, this can be a tricky task, because some amino acids are very similar and only differ by as much as one functional group. For instance valine (val) and isoleucine (ile) differ by a single methyl group. Quality control starts at the active site of the enzyme, where amino acid selection occurs. Studies in *S. cerevisiae* and *E.coli* have shown that the activation and attachment of the wrong amino acid to a tRNA can be corrected by pre-transfer editing or post transfer editing (Ling et al., 2009). The first implies the hydrolysis of mischarged aminoacyl adenylates with consequent release of the non-cognate amino acid, AMP and PPi and can be tRNA dependent or tRNA independent (Reynolds et al., 2010). The second case is tRNA dependent, as it requires the tRNA CCA 3' end to move from the synthetic site to the editing site, allowing the hydrolysis of the RNA-amino acid bond. The tRNA is released from the active site and the aa-tRNA rebinds to the aaRS active site. Additionally, some aaRS have the ability to compete with the EF-1A for aa-tRNAs, meaning that a resampling of the mysacilated tRNAs that passed the first editing mechanism exists (Reynolds et al., 2010). EF-1A also contributes to translation accuracy as it binds cognate and non-cognate aa-tRNAs with different affinities (Dale and Uhlenbeck, 2005b; Dale and Uhlenbeck, 2005a).

After aa-tRNA synthesis and EF-1A binding, the complex is transferred to the ribosome. Although not able to discriminate between mischarged tRNAs, this organelle can discriminate between correct and incorrect codon-anticodon interactions. This

interaction is monitored in two 2 steps (Figure 5, B). When the ternary complex binds, the ribosomal 30S subunit monitors the geometry of the interaction. A correct interaction allows for multiple conformational changes that accelerate GTP hydrolysis on eEF-1A. On the other hand, a mismatch will block the conformational change, delaying GTP hydrolysis and increasing the chances of complex dissociation. After GTP hydrolysis, the aa-tRNA is released and either enters the ribosomal 80S subunit or is rejected. An additional quality control step is performed when the new peptidyl-tRNA is translocated from the A site to the P site (Reynolds et al., 2010). The ribosome is still checking for codon-anticodon mismatches and, if they occur, there is a general specificity loss at the A site. This results in either amplification of errors (Zaher and Green, 2009) or premature termination and accelerated peptide release. Besides guaranteeing codon-anticodon interaction accuracy, the ribosome must also ensure the correct reading frame in order to avoid frameshifting errors. Studies indicate that both P and E sites may play important roles in this process (Marquez et al., 2004).

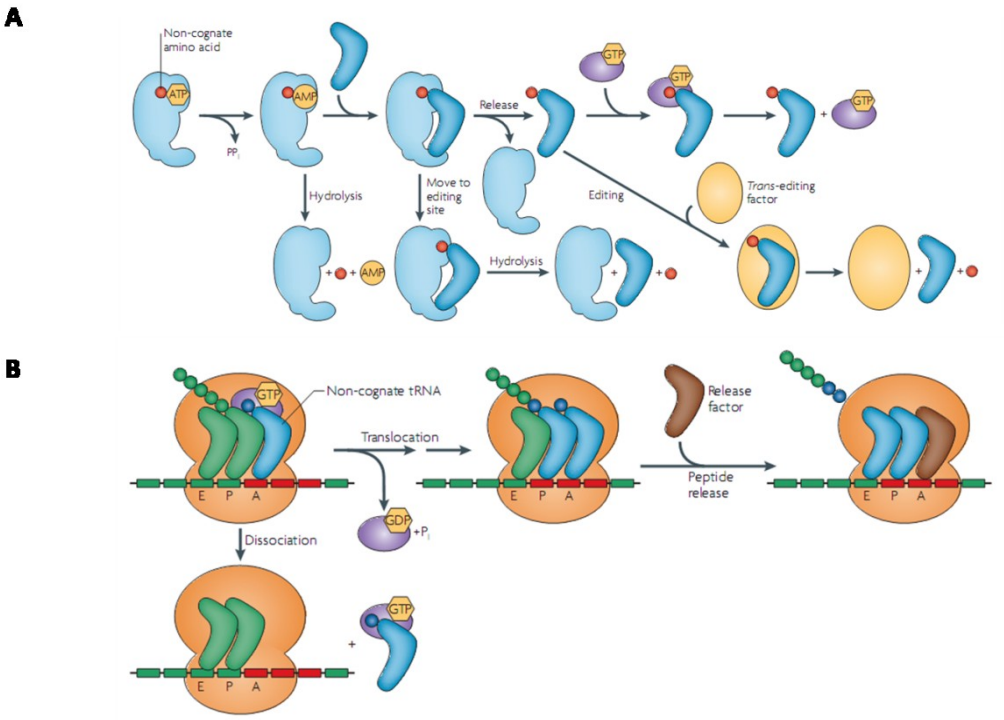

Figure 5- Quality control mechanisms at the translation level. A) At the aminoacyl-tRNA step formation. When non-cognate amino acids are activated, the aminoacyladenilates can be hydrolyzed by the aaRS editing site. Alternatively, misacylated tRNA can be released from the aaRS and be edited by trans-acting factors or aaRS resampling; **B) At the ribosome level –** when incorrect codon-anti-codon interactions occur the most frequent outcome is ternary complex dissociation. On other cases, these incorrect interactions can result in GTP hydrolysis and translocation. If the wrong interactions persist, resulting in wrong amino acid incorporation, ribosomal A site specificity is compromised, release factors bind and the peptide is released. Adapted from Reynolds et al 2010.

Post-translation Quality Control

Despite the defence mechanisms mentioned above, errors still occur ultimately resulting in protein misfolding or malfunction. Therefore, cells possess protein quality control (PQC) mechanisms that act downstream of translation, namely chaperones, the ubiquitin-proteasome pathway, ERAD and autophagy. Their function is to destroy aberrant proteins or refold them (when possible) and ultimately maintain proteostasis

(Figure 6). These PQC's are highly dynamic and react rapidly to proteome quality needs by increasing or decreasing the transcription and translation of their various components. In addition, they may be tissue specific which may explain why certain mutations in proteins that are expressed in all tissues only give rise to cellular dysfunction in one or other tissue. Some components are constitutively expressed, as for instance Hsp70p or the proteasome, while others only appear upon stress. A brief overview of these systems is provided in the following paragraphs.

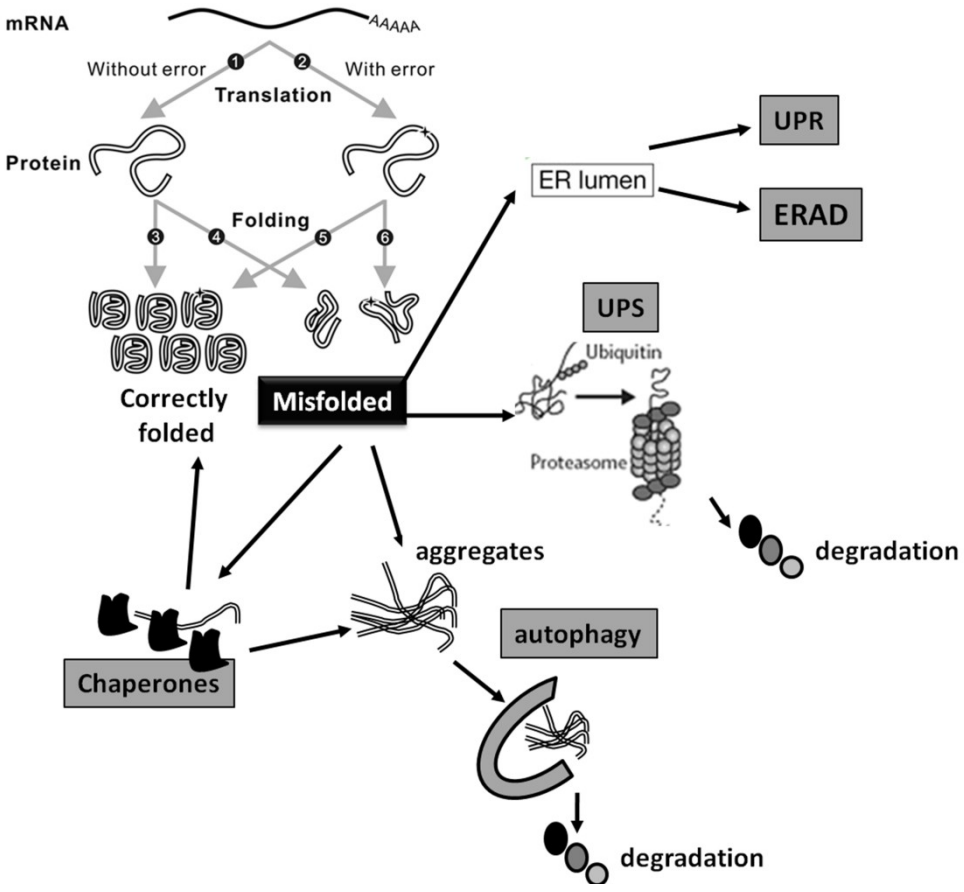

Figure 6- A schematic illustration of protein proteostasis alterations and its relationships to PQC in the cell. When no failures occur at the protein synthesis level, correctly folded proteins are produced. On the other hand, when proofreading activity or any other security system fails, misfolded proteins are released from the ribosome. PQC functions to minimize the

production of abnormal proteins in the cell, remove unsalvageable abnormal proteins, and prevent abnormal proteins from damaging the cell. Chaperones facilitate the folding of nascent polypeptides and the unfolding/refolding of misfolded proteins, prevent the misfolded proteins from aggregating, and escort terminally misfolded proteins for degradation by the UPS. The UPS degrades both misfolded/damaged proteins and most unneeded native proteins in the cell. This process involves two steps: first, covalent attachment of ubiquitin to a target protein by a cascade of chemical events and then the degradation of the target protein by the proteasome. The autophagy pathway participates in PQC by helping remove protein aggregates formed by the misfolded proteins that have escaped from the surveillance of chaperones and the UPS. When misfolded proteins accumulate in the lumen of the endoplasmatic reticulum UPR and ERAD are activated. For simplicity, not all the described and reciprocal relations between the different systems are displayed. See text for details. Adapted from Yang et al., 2010.

In the cytosol

Chaperone Systems

Although cells possess multiple quality control networks, preference is given to chaperone mediated repair (Figure 7) (Buchberger et al., 2010; Stolz and Wolf, 2010). This may be explained by thermodynamics as both degradation and refolding are ATP dependent processes and the overall energetic balance of refolding should be favorable, when compared to degradation followed by *de novo* synthesis. Additionally, under severe conditions, cell survival can be endangered as degradation implies the substitution of missing protein functions by *de novo* synthesis, being this last process comparatively slower than protein repair. Chaperones and, specifically, heat-shock proteins (HSPs), are engaged in folding both newly synthesized and denaturated proteins. They are known to interact with exposed hydrophobic surfaces. In general, aggregation is reduced but in some cases proteins are targeted to the ubiquitin/proteasome machinery for degradation. In addition, molecular chaperones

buffer phenotypic change during development, regulate the onset of tumorigenesis, defend the cell against the effects of stress (such as heat shock, exposure to toxins, heavy metals or viral infections) and assist in translocating newly synthesised proteins to their functional destination (Tomala and Korona, 2008; Calderwood and Ciocca, 2008; Mosser and Morimoto, 2004).

Chaperones can be divided into several classes, according to their molecular weight. Some of the major chaperones (Hsp70p, Hsp90p, small Hsps) are present at high concentrations in non-stressed cells reaching 1–5% of total cellular protein while others are only produced under stress conditions. One of the most prominent class of chaperones is the HSP70 family. This family comprises two different forms of proteins namely the Hsp70p, which are expressed during cellular stress and are homologous heat shock cognate proteins and the Hsc70p, which are constitutively expressed. These proteins can be found in the cytosol (Hsc70p and inducible Hsp70p of higher organism), ER (BiP/kar2) or mitochondria (Hsp75p) (Hartl and Hayer-Hartl, 2002), and in a variety of situations, e.g., protein folding, prevention of protein aggregation, membrane translocation and autophagy (Stolz and Wolf, 2010). The activity of HSP70 is ATP dependent and works in cycles of binding to the substrate and ATP hydrolysis, but Hsp70p hydrolyses ATP inefficiently by itself and needs the help of Hsp40p and nucleotide exchange factors (NEFs) to facilitate it. Therefore, these proteins can be usually found together. When bound to ATP, HSP70p chaperones have low affinity for their substrates but ADP increases the affinity towards the substrates (Stolz et al., 2010).

Hsp40s, also termed J proteins due to their founding member (bacterial DnaJ), act mainly as co-factors and, as stated above, stimulate the ATP hydrolysis step within the Hsp70p reaction cycle. Some Hsp40 proteins, such as bacterial DnaJ and yeast Ydj1, can prevent aggregation by themselves, through ATP-independent transient and rapid association with substrates (Cheetham and Caplan, 1998; Fan et al., 2003). This chaperone family can be found in different cellular compartments and has different substrate affinities.

HSP100 family members are known to interact with other chaperones, namely with Hsp70p/Hsp40p during protein disaggregation and also with co-chaperones, namely Sti1p, Cpr7p and Cnsp1p (Bbas-Terki et al., 2001). Within the HSP100 family of proteins, yeasts express a ~104 kDa form which is necessary to protect cells from various stress conditions such as heat, heavy metals and ethanol. Mutational studies have shown that Hsp104p is not required for normal growth and is expressed at low levels under normal growth conditions (Bosl et al., 2006; Lindquist and Kim, 1996). Also, at normal temperatures, Hsp104p regulates the formation and inheritance of yeast prions. Hsp104p can exist in either inactive monomeric, dimeric or trimeric forms or in an active ring-shaped hexamer form (Bosl et al., 2006)**.** These different forms are considered to exist in a dynamic equilibrium. Several studies have demonstrated that these conformational alterations are regulated by nucleotide and ionic strength as well as by one of the two nucleotide binding domains that characterize this protein family (NBD2). The translocation of the peptide through the protein channel is thought to be driven by the energy provided by ATP hydrolysis, performed by the two NBD, which have ATPase activity. Small heat shock proteins (sHsp) have also been shown to

interact with the Hsp104p system (Cashikar et al., 2005; Haslbeck et al., 2005; Mogk et al., 2003a; Mogk et al., 2003b). Small heat shock proteins (sHSPs) bind substrates rather unspecifically and prevent irreversible aggregation of proteins. However, it remains to be clarified whether the Hsp100 chaperones interact physically with either Hsp40p/70p or sHSPs, or if their relation is only at the functional level.

The members of the Hsp90p family are mainly committed to ATP binding and hydrolysis and, therefore, are characterized by an ATP binding domain in their N-terminal region. These proteins have a helical domain at the C-terminal domain, that allows for dimerization, which is necessary for ATP binding. Additionally, these proteins possess a large hydrophobic patch which is attributed to substrate binding (Stolz and Wolf, 2010). Their function is tightly regulated by numerous co-chaperones (Hessling et al., 2009; Taipale et al., 2010) and they bind to a wide range of substrates, including signal transduction kinases and transcription factors.

Other chaperones, like the Hsp60 (chaperonin) family member TRiC/CCT (TCP1-ring complex or chaperonin containing TCP1), recognize a smaller range of substrates. TRiC/CTT is composed of a double-ring structure of eight different subunits in each ring forming a large cavity in which the polypeptide is folded to a native or near-native form, in a protected environment (Spiess et al., 2004; Buchberger et al., 2010). Its substrate specificity is not well defined and it is not present in the ER.

Although not completely clarified, the emerging picture shows that all chaperone systems cooperate to some level in a multi-chaperone complex network to maintain

protein homeostasis. In yeast, the expression of this protein family is regulated by heat-shock transcription factor 1 (HSF1).

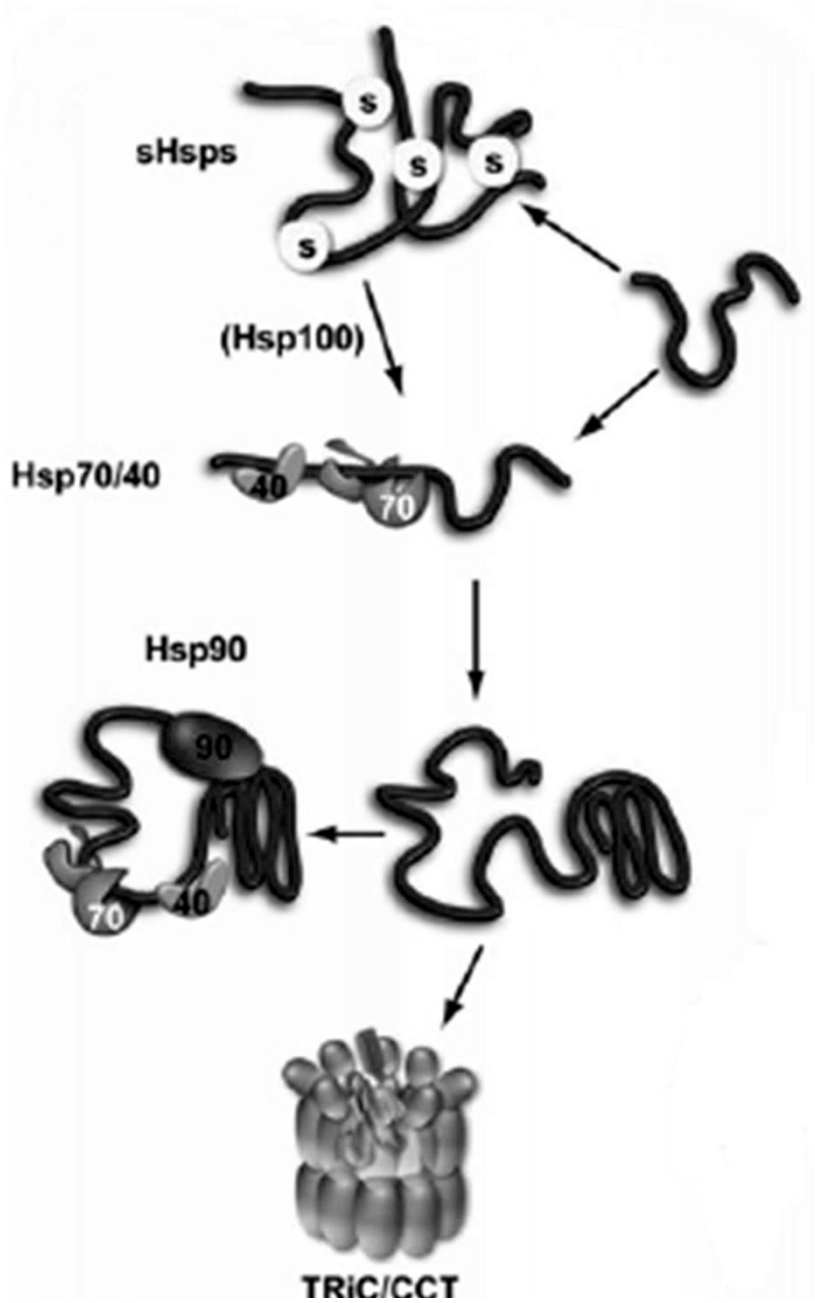

Figure 7- Hsps in the eukaryotic cytoplasm. Unfolded proteins are recognized by Hsp70 that acts together with Hsp40 co-chaperones. More mature folding intermediates are recognized by Hsp90 or TRiC/CTT. Small Hsps promote solubilization and contribute to ameliorate protein aggregation driven by Hsp100 family. Adapted from Buchberger et al., 2010

The ubiquitin-proteasome system

A second line of cytosolic PQC is the ubiquitin-proteasome system (UPS) which represents the main proteolytic pathway in the cell. The UPS is also implicated in intracellular signaling, transcriptional control and regulation of cell death and is highly conserved among eukaryotes. Proteasome substrates are initially tagged with ubiquitin (Ub), preferentially at a lysine side chain. The process is initiated by activation of ubiquitin molecules by the ubiquitin-activating enzyme E1, which forms a high energy Ub-thiol ester bond in the presence of ATP. The activated Ub is then transferred to an Ub-conjugating enzyme, E2, which forms an E2-thiol ester bond. Finally, ubiquitin is transferred to the target substrate protein through an isopeptide linkage between the conserved C-terminal glycine residue of ubiquitin and the *ε*-amino group of lysine substrate residues. In many cases, the transfer of ubiquitin from E2 to target proteins requires the involvement of an ubiquitin ligase, E3. The Ub signal is recognized by intrinsic proteasome receptors and the target proteins are degraded with consequent release of free and reusable ubiquitin. Some proteins may require the attachment of an adaptor molecule before recognition by of the Ub signal by the proteasome and while other proteins do not need to be ubiquitinated for UPS degradation, namely mutant α factor precursor (pαF) and ornithine decarboxylase (ODC) (Coffino, 2001; Wolf and Hilt, 2004).

The 26S proteasome is a large multicatalytic protease complex of approximately 700 kDa (Elofsson et al., 1999) which is present both in the cytoplasm and the nucleus (Navon and Ciechanover, 2009). It consists of the 20S proteolytic core particle (20S, CP) and the 19S regulatory complex (19S, RP). The latter can be found at both ends of the

proteasome and is involved in recognition, binding and unfolding of ubiquitinated proteins and in the regulation of the opening of the 20S core particle (Heinemeyer et al., 1991; Voges et al., 1999; Wolf and Hilt, 2004). It is a highly conserved organelle and has three major catalytic activities, namely a chymotrypsin-like activity, a trypsin-like activity and a post-glutamyl peptide hydrolyzing (PGPH) activity, being capable of catalyzing cleavage of peptide bonds on the carboxyl side of basic, acidic, and hydrophobic amino acid residues in both natural peptides and synthetic substrates (Zhu Y and Gao Q, 2009).

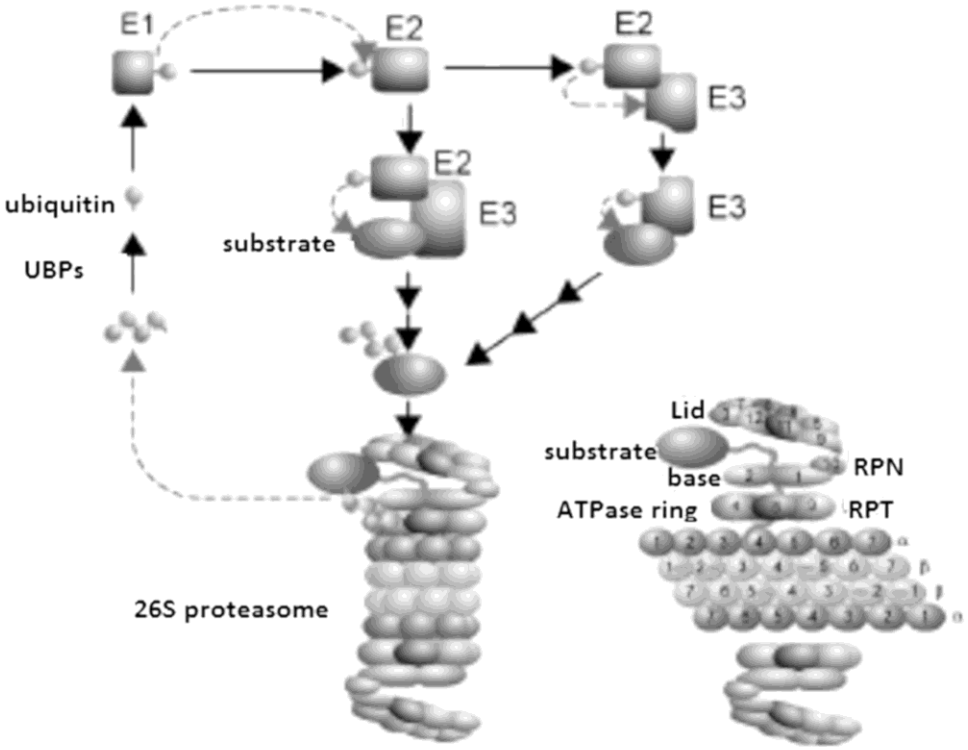

Figure 8- The yeast ubiquitin proteasome system Attachment of ubiquitin to target proteins requires three enzymatic steps. Ubiquitin activating enzymes (E1) activate ubiquitin in an ATP dependent reaction. An activated ubiquitin moiety is then formed and is transferred and bound to ubiquitin-conjugating enzymes (E2) that serve as carrier proteins. Ubiquitin protein ligases (E3) catalyze the covalent attachment of ubiquitin to target protein. Multiple cycles of ubiquitination result in synthesis and attachment of polyubiquitin chains that serve as a

recognition signal for the degradation of the target protein by the 26S proteasome. The 26S proteasome is formed by the 20S catalytic core complex and two 19S regulatory complexes capping the 20S complex at both ends. The 20S complex is composed of four axially stacked rings. Each outer ring consists of seven nonproteolytic subunits. Each of the two inner rings is formed by seven proteolytic subunits. The 19S complex consists of the base and lid subcomplex. The base subcomplex contains six nonredundant ATPases of the AAA superfamily. The lid subcomplex contains at least eight subunits including deubiquitylating enzymes and receptors for ubiquitylated proteins. Polyubiquitinated target proteins enter the 19S regulatory complex and are recognized, deubiquitynated, unfolded, and translocated into the central cavity of the 20S catalytic core complex, where they are degraded by different hydrolytic activities. Degradation peptides are released from the 26S proteasome by diffusion and further degraded to single amino acids by cytosolic peptidases or, in higher eukaryotes, are used for major histocompatibility class I antigen presentation. Adapted from Wolf and Hilt, 2004.

Autophagy

Another defense system that cells possess to overcome protein dysfunction problems is autophagy. The term autophagy refers to the cellular processes of self-digestion which involve the uptake of cellular components for degradation in the vacuole/lysosome (yeasts/mammals) (Levine and Kroemer, 2008). Under vegetative growth conditions, autophagy occurs at a basal level in both yeast and mammalian cells, but the lack of nutrients or other types of stress trigger the process. It can be divided in four pathways, namely macroautophagy, microautophagy, chaperone-mediated autophagy (CMA) and cytosol-to-vacuole targeting pathway (CVT). The first two types are conserved between yeast and mammals, while the other two have only been described in mammals or yeast, respectively. Each of these pathways differ in the way the cytoplasmatic substrates are delivered to the vacuole (Huang and Klionsky, 2007). During macroautophagy (referred as autophagy in this thesis), a portion of the cytoplasm is sequestered by a double-membrane structure named autophagosome and is degraded by vacuolar hydrolases upon fusion of the autophagosome with the

vacuole (Figure 9). In contrast, microautophagy allows direct uptake of cytoplasmic material by invaginations of the vacuolar membrane, while chaperone-mediated autophagy involves the translocation of specific cytosolic proteins that contain a specific signal motif – KFERQ- across the lysosomal membrane (Figure 10). Cytosol-to-vacuole targeting is used for the delivery of the vacuole resident hydrolases through vesicules smaller than autophagosomes.

More than 30 genes (ATG genes, AuTophaGy related), which are mainly conserved in higher eukaryotes, are involved in autophagy regulation. Among the ATG genes, a subset is required for autophagosome formation in all subtypes of autophagy, which is usually referred as the core autophagy machinery. This machinery is composed of three major functional groups: (1) Atg9p and its cycling system, which includes Atg9p, the Atg1p kinase complex (Atg1p and Atg13p), Atg2p and Atg18p; (2) the phosphatidylinositol 3-OH kinase (PI(3)K) complex (vacuolar protein sorting (Vps)34, Vps15p, Atg6p(Vps30) and Atg14p) and (3) the ubiquitin-like protein (Ubl) system, which includes two Ubl proteins (Atg8p and 3Atg12p), an activating enzyme (Atg7p), two analogues of ubiquitin-conjugating enzymes (Atg10p and Atg3p), an Atg8p modifying protease (Atg4p), the protein target of Atg12p attachment (Atg5p) and Atg16p (Kundu and Thompson, 2008).

The autophagic process can be divided into several sequential steps, namely induction, cargo selection and packaging, nucleation and vesicle formation, targeting, docking and fusion, breakdown and export, which share similarities between yeasts and mammals (Figure 9).

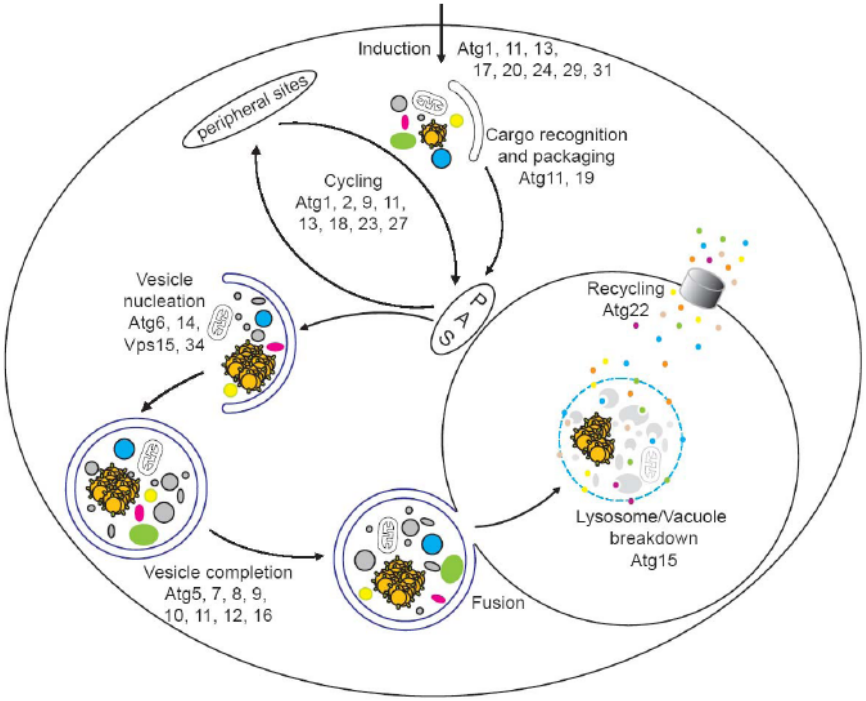

Figure 9- Schematic overview of the autophagic pathway. **Autophagy can be broken down in several discrete steps. Induction:** requires the dephosphorylation of Atg13p which interacts with Atg1p, up-regulating the latter kinase activity. **Cargo selection and packaging:** are specific of selective autophagy pathways and involve several proteins. **Nucleation of vesicle formation**: lipids and proteins that constitute the autophagosome and Cvt vesicles are brought together. Several organelles (ER, mitochondria) have been suggested to be involved in this step, as a lipid source. **Vesicle Expansion and Completion**: Two ubiquitin-like conjugation systems involving the ubiquitin-like proteins Atg8p and Atg12p are needed for vesicle expansion. **Targeting, docking and fusion**: The machinery involved in this step includes the SNARE proteins Vam3p, Vam7p, Vti1p and Ykt6p; the Rab protein Ypt7p; members of the class C Vps/HOPS complex; the NSF, SNAP and GDI homologues Sec17p, Sec18p and Sec19p and Ccz1p and Mon1p. In mammalian cells, the initial fusion may involve an endosome. **Breakdown and export;** autophagosomes are degraded in the interior of the vacuole. Adapted from Huang and Klionsky, 2007.

Until very recently, starvation induced autophagy was considered a non-selective pathway, but numerous observations have shown that autophagy can be a selective process which can eliminate specific proteins, complexes and organelles. These use the conserved core autophagy machinery.The mechanisms that ensure the accurateness in specific selection of the cargo are not well understood. Recent findings suggest that

some specific post-translational modifications and specific key factors may play an important role in this process (Kraft et al., 2009). The selective types of autophagy can be divided into two groups: organellar (ribophagy, mitophagy, pexophagy, reticulophagy and piecemeal autophagy of the nucleus) and non-organellar types of autophagy (Cvt pathway, aggrephagy and xenophagy). A brief explanation of each process is provided below.

The selective degradation of ribosomes is known as ribophagy (Kraft et al., 2008). In *S. cerevisiae*, the degradation of ribosomes occurs faster than cytosolic proteins, which suggests a selective autophagosomal degradation pathway. Indeed, it has been shown that – under nutrient-limiting conditions – mature ribosomes are both non-selectively degraded by the bulk autophagic pathway and rapidly and selectively degraded by a specific macroautophagic process (Figure 10). During extended periods of starvation, ribophagy seems to be essential for cell survival implying that the selective removal of excessive, non-functional or wrongly-assembled ribosomes may be required to attenuate protein synthesis and to provide an important source of new building blocks to maintain cellular homeostasis. Human homologues of the ribophagy process have been identified but do not have yet known functions. However, a critical regulator of autophagy, the Atg1p mammalian homologue Ulk1p, has been implicated in the autophagic clearance of ribosomes during reticulocyte maturation.

When the degradation target is mitochondria, the term mitophagy is used (Figure 10). These organelles are essential as they supply energy to the cell by carrying out metabolic processes such as fatty acid oxidation and oxidative phosphorilation.

However, mitochondria are also a source of potential harmful reactive oxygen species that damage lipids, proteins and DNA and have been implicated in aging, cancer and neurodegeneration. Therefore, controlling the number and quality of mitochondria is crucial for cellular homeostasis. Several different mechanisms have been proposed to mediate mitophagy: non-specific macroautophagy, selective macroautophagy (Priault et al., 2005), selective microautophagy and non selective microautophagy. Interestingly, mitophagy is preferentially mediated by microautophagy in yeasts and macroautophagy in mammals. In either case, the regulatory mechanisms are largely unknown, but osmotic swelling and organelle fragmentation caused by depletion of the mitochondrial inner membrane protein Mdm38, induce mitophagy (Tatsuta and Langer, 2008). It has been suggested that fission of the swollen organelle triggers the autophagic machinery, which is corroborated by the finding that inhibition of the fission protein Dnm1p blocks mitophagy. In mammals, loss of mitochondrial membrane potential and opening of the mitochondrial permeability transition pore seem to be common prerequisites for mitophagy.

Pexophagy is the selective degradation of peroxisomes (Figure 10). These organelles are involved in many aspects of lipid metabolism and the elimination of peroxides and their number also needs to be tightly controlled. In *P.pastori,* at least two basic modes of selective peroxisome degradation have been described, namely macro- and micropexophagy, analogous to macro- and microautophagy. In mammals, pexophagy has also been described but it remains unclear if it is a selective process. Peroxisome unbalance and pexophagy have been described to play important roles in several illnesses namely Zellweger syndrome and Refsum's disease (Shimozawa, 2007).

The ER also appears to be a selective target for autophagic degradation (Bernales et al., 2006), named reticulophagy. This organelle is the entry site of secretory proteins and most of the integral membrane polypeptides, where they are properly folded and modified. Reticulophagy is responsible for removal of surplus ER upon UPR inactivation. It contributes to cells physiology in two ways, namely by reducing ER size after folding stress induced enlargement and by sequestering damaged parts of the ER containing potentially toxic aberrant proteins. This pathway can also occur as a result of starvation, but apparently starvation and UPR induced reticulophagy differ at the morphological level. Also, the two processes depend on different Atg proteins (Mijaljica et al., 2006; Ogata et al., 2006; Bernales et al., 2006).

Piecemeal autophagy of the nucleus (PMN) occurs under starvation conditions and the term refers to the process where nonessential parts of the *S.cerevisiae* yeast nucleus are targeted for degradation in the vacuole. It resembles microautophagy as the cargo is sequestered into an invagination of the vacuolar membrane. So far, no analogous mechanism and no homologous genes have been identified in mammalian cells.

The Cvt pathway is the best characterized type of selective autophagy. It refers to a biosynthetic process that transports certain resident hydrolases such as aminopeptidase I and α-mannosidase to the vacuole where they are enzimatically processed into their mature form. This pathway has only been identified in *S. cerevisiae* and *P. pastoris* (Kraft et al., 2009).

The term aggrephagy refers to the breakdown of toxic protein aggregates in pathological conditions (Figure 10) and is important in the prevention of inclusion bodies formation in healthy individuals (Kraft et al., 2009). It has only been described in higher eukaryotes.

Xenophagy is related to MHC class II crosspresentation and is only known in higher eukaryotes. Interestingly, several pathogens manipulate the autophagic process in their mammalian host cells in order to survive and to establish a persistent infection.

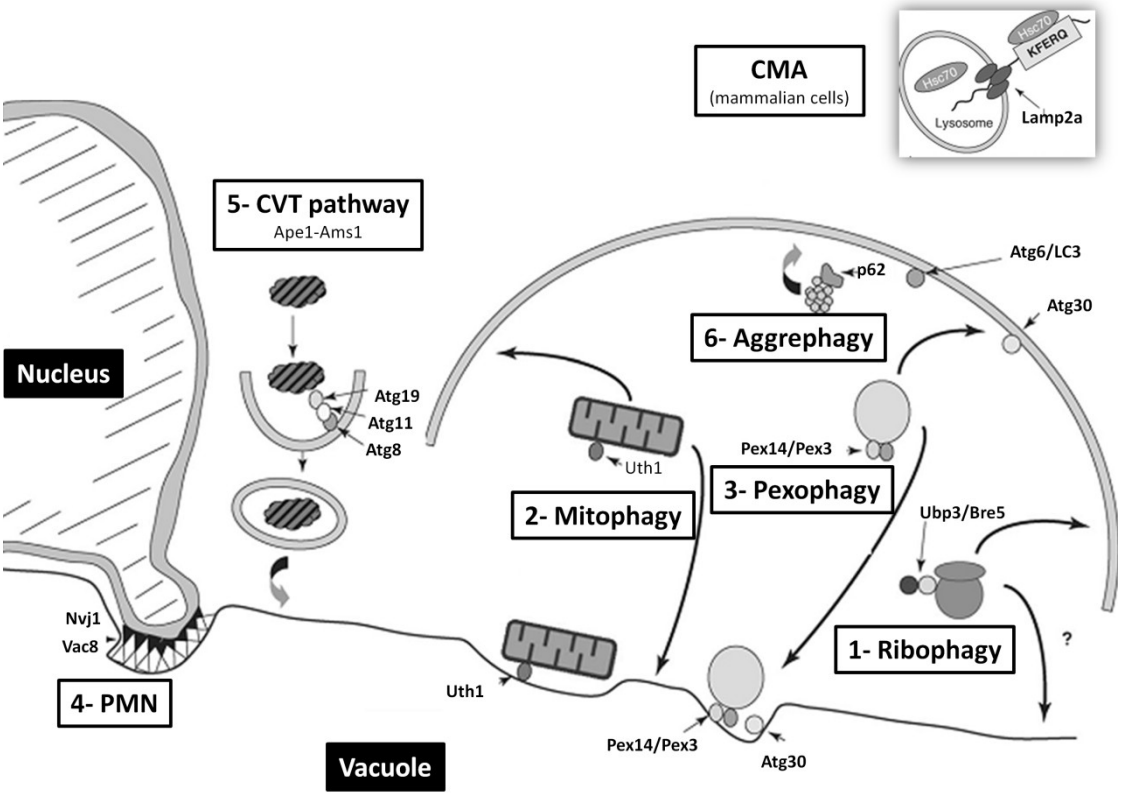

Figure 10- Selective types of autophagy. 1- Ribophagy: refers to ribosome degradation and depends on Atg1p and Atg7p, which are core components of the autophagy machinery, Ccz1p which is necessary for autophagosome fusion to the vacuole and Ubp3p and its cofactor Bre5p which is involved in 60s ribosomal subunit degradation. Rps5p, Cdc48p and Ufd3p may also be involved in this pathway. Ubiquitination of ribosomal subunits or associated factors by Rsp5p may provide a specific engulfment signal and a subsequent Ubp3/Bre5-dependent de-

ubiquitination step may allow the maturation and/or fusion of the autophagosome with the vacuole**. 2- Mitophagy:** In yeasts, Uth1p and Aup1p are indispensable for mitophagy, but a mechanistic model integrating the two proteins is still missing, as several apparent contradictory observations have been made. For instance, deletion of one or the other gene has opposite effects on cell survival: deleting *AUT1* results in loss of cell viability while deletion of *UTH1* results in increase lifespan and viability under starvation conditions. Recently, a new protein, localized on mitochondria (Atg32p) has been identified as a recognition factor for selective mitochondrial sequestration **3- Pexophagy:** At least two mechanisms are known for pexophagy, namely micro and macropexophagy. While similar to other selective pathways, pexophagy requires Atg11p but also specific proteins namely Pex14p and Pex3p. **4-PMN:** occurs in the context of nuclear vacuolar (NV) junctions, which are velcro-like patches between the nucleus and the vacuole, generated by the interaction of Vac8p (a protein form the membrane of the vacuole) and Nvj1p (the outer membrane nuclear protein).Other proteins, namely Osh1p, Tsc13p and the autophagy core machinery, are needed for PMN**. 5- CvT:** makes use of most of the core machinery required for bulk autophagy but additional factors are required to ensure cargo specificity, namely Ubp3p and Bre5p **6-Aggrephagy:** is the degradation of protein toxic aggregates, only occurs in higher eukaryotes and requires Atg8p as well as specific factors, namely p62p. Adapted from Beau et al., 2008.

In the organelles

In the endoplamatic reticulum

Almost all organelles have a PQC system. The unfolded protein response (UPR) is an intra-organellar signal transducting pathway that monitors protein quality control in the ER. The endoplasmatic reticulum (ER) is a membranous system of eukaryotic cells where folding and modification of secretory proteins occurs, prior to their final destination such as the ER itself, Golgi apparatus, plasma membrane, vacuoles/lysosomes and the exterior of the cell. In addition, the ER also works as an important Ca^{2+} reservoir (Hoyer-Hansen and Jaattela, 2007). Proteins of the secretory pathway are imported into the ER either co-translationally (ribosome-coupled) or post-translationally (uncoupled), in an unfolded state. Briefly, proteins are translocated to the ER through the Sec61p translocon complex. When this happens post-

translationally, the cytosolic chaperones Ssa1-4, Ssb and Sse1/2 ensure solubility and prevent aggregation. In the ER lumen, Kar2p/Bip binds to the polypeptides and, in an ATP-dependent cyclic process of release and binding, mediates mature folding of the peptide. Additionally, Pdi and Ero activity allow for disulfide bond formation, a process that produces ROS. Proteins are exported only if the correct conformation is achieved, otherwise non-native or unfolded proteins accumulate in the organelle leading to UPR activation (Gasser et al., 2008). The expression of more than 400 genes is controlled by this signaling pathway through the Ire1p (inositol-requiring kinase 1) regulator, which resides in the ER membrane and can work as a kinase or as an endonuclease. When aberrant proteins are detected in the ER lumen, Ire1p suffers auto-phosphorylation and oligomerization, Kar2p/Bip binds to its amino-acid terminal and induces dimerization and catalyses the alternative splicing of the UPR transcription factor *HAC1* (*XBP1* in mammalian cells). The tRNA ligase Rlg1p is also needed in this process. An intron in *HAC1* mRNA promotes a translational blockage which is relieved by splicing, allowing for production of an activator protein that migrates to the nucleus where it binds unfolded protein response elements (UPRE) in target genes, inducing their expression (Back et al., 2005). In mammalian cells, the unspliced transcript promotes the synthesis of an unstable protein while splicing leads to the formation of a stable transcription activator protein. These cells have another mechanism that slows down translation initiation upon ER stress. This pathway is activated by the ER kinase PERK which phosphorylates the translation initiation factor eIF2α. This is not known to happen in yeast cells. Although UPR is usually regarded as an adaptive response that helps cells to survive acute stress, recent work has shown that it is not always beneficial during chronic stress (Cyr and Hebert, 2009). This pathway can be inhibited in

yeast cells by treatment with dithiothreitol (DTT), a strong reducing agent which prevents disulfide bond formation, or via the drug tunicamycin, which inhibits N-linked glycosylation.

Another PQC that ER possesses is the ER-associated degradation pathway (ERAD). When ER-chaperone and refolding enzymes fail, as sensed by prolonged binding of proteins to either calcinexin or BiP, aberrant proteins are then targeted to degradation via ERAD. After being recognized, terminally misfolded or unassembled proteins are sorted to an ER-membrane-associated dislocation/ubiquitination complex. This complex contains adaptor proteins that recognize the quality control receptor and/or the ERAD substrate directly. Misfolded proteins are then retro-translocated to the cytosol. The retrotranslocation complex (RTC) contains several proteins namely the Hrd-Der ubiquitin ligase complex, which is connected to the Derlin Der1p and the Sec61p translocon on the luminal side of the ER membrane and the Cdc48-Ufd-Npl4 segregation machinery on the cytoplasmatic side. This process can be coupled with ubiquitination by an ER-associated E3 ubiquitin ligase. Additional cytosolic components are also recruited to the retro-translocation complexes, to aid in the extraction of the ERAD substrate from the ER, and prepare it for proteasomal degradation. The Cdc48-Ufd1-Npl4 complex delivers the polybiquitinated proteins to the proteasome. ERAD is also responsible for the degradation of multimeric proteins that are unable to assemble (Gasser et al., 2008).

UPR and ERAD are highly coordinated. Overexpression or accumulation of unfolded proteins due to the absence of components of the ER degradation machinery induces

UPR (Knop et al., 1996). In yeast, loss of function of components of both systems is lethal (Haynes et al., 2004; Kincaid and Cooper, 2007a; Kincaid and Cooper, 2007b).

Recent data indicates that ER stress is also a potent trigger of autophagy and that the latter can work as a backup system to ERAD. This is conserved from yeast to mammals. However, the signaling pathways responsible for autophagy induction and its cellular consequences appear to vary according to cell type and stimulus and, therefore, are not fully understood. In yeast, conditions that trigger UPR also induce the expression of several autophagy related genes (ATG genes) and the activation of Atg1p kinase and ATG-dependent autophagy. Moreover, *IRE1* and *HAC1* are dispensable for the induction of ATG genes in response to ER stress (Yorimitsu et al., 2006; Hoyer-Hansen and Jaattela, 2007).

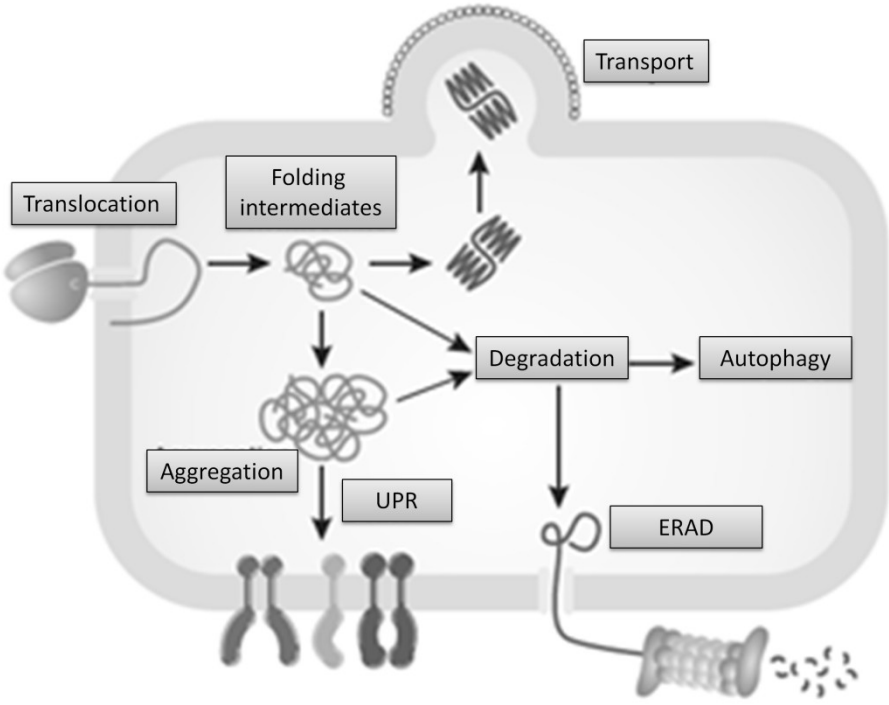

Figure 11- Schematic overview of quality control in the ER. Secretory pathway proteins fold in the lumen or membrane of the ER from where they are sorted to their site of action. When

proteins do not acquire their native conformation and whenever chaperones fail to refold them, the proteins are targeted for degradation. This process relies on retro-translocation to the cytosol and polyubiquitination by the ER associated machinery, followed by proteasomal degradation. Adapted from Cyr and Herbert, 2009.

In the mitochondria

Mitochondria also possess specific PQC systems. They are particularly needed as mitochondrial proteins are subjected to very specific challenges. Despite the majority of the mitochondrial proteins being nuclear encoded, synthesized in the cytosol and subsequently imported into the mitochondria, these organelles possess their own genome making mitochondrial protein biogenesis a quite complex process. This implies that 1) the proteins synthethyzed in the cytosol enter the organelle mainly post-translationally, in an unfolded conformation, through translocation systems that exist in the outer (OM) and inner mitochondrial membranes (IM) (Wiedemann et al., 2004b; Wiedemann et al., 2004a) and 2) the subunits of respiratory chain complexes (RCs) that are synthesized in the mitochondria need to be assembled with imported proteins. Secondly, as mitochondria are major sources of ROS, mitochondrial proteins are continuously exposed to oxidative modification (Tatsuta, 2009). In the mitochondrial matrix, PQCs are similar to those found in α-proteobacteria and include chaperones that are members of Hsp70, Hsp60 and Hsp100 families, and proteolytic systems, namely a set of proteases with AAA^+ domains that resemble the proteasome (Tatsuta and Langer, 2009; Tatsuta, 2009). These proteases are also found in the mitochondrial IM, as well as in OM and IMS. In the IM, the Oma1 protease seems to play an important role in PQC and in the OM HtrA2/Omi has similar functions. It has been assumed that UPS might be involved in the PQC in the OM since it allows direct

access from the cytosol. In mammalian cells a mtUPR has been described but so far a similar pathway seems absent in *S.cerevisiae* cells (Tatsuta, 2009)

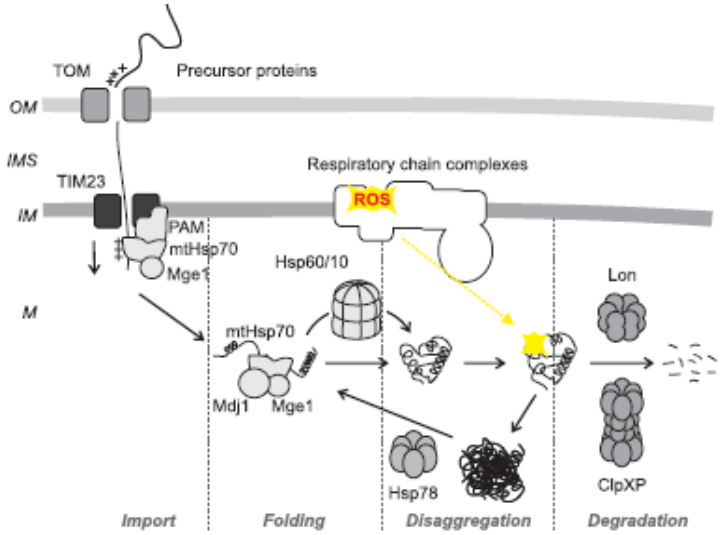

Figure 12- PQC network in the mitochondria. Proteins are imported into the matrix through the Tim23p translocase and a complex (PAM) containing mtHsp70p (Ssc1p in yeast) and co-factors. Folding of proteins is assisted by mtHsp70 and Hsp60 chaperones. ROS can lead to protein aggregation. In yeast mitochondria, Hsp78 disassembles protein aggregates. ATP-dependent proteases degrade aggregation-prone, damaged proteins. Lon is the mammalian homologue for yeast Pim1.OM-outer membrane; IMS- intramembranar space; IM- inner membrane; M-matrix. Adapted from Tatsuta, 2009.

In the nucleus

As there is no functional protein synthesis in the nucleus, there is no apparent need for PQC in this organelle. However, nuclear proteins can be damaged by the same stressors that affect the other cellular proteins and therefore, cells must deal with abnormal proteins that may arise in the nucleus. Few studies have addressed the problem of PQC in the nucleus, however, a number of chaperones have been described as being involved in protein refolding and disaggreagation in this organelle (Parsell et al., 1994; Rossi and Lindquist, 1989). Moreover, San1p, a nuclear-localized ubiquitin ligase, has been implied in targeting misfolded proteins in the nucleus of

yeast cells. Studies in mammalian cells have also identified potential roles in nuclear PQC degradation for the nuclear ubiquitin ligases PML IV and UHRF-2 (Rosenbaum et al., 2011; Gardner et al., 2005; Fu et al., 2005; Iwata et al., 2009; Janer et al., 2006).

Mistranslation: deleterious and beneficial effects

The biological impact of translational errors depends on their effects on protein function and on their frequency. There is a generalized view that mistranslation is a highly deleterious phenomenon and, in fact, small increase in translation error can cause neurodegenerative and metabolic diseases and is relevant to cancer, autoimmune diseases and aging (Reynolds et al., 2010). However, this classical view is changing, as more and more examples of beneficial effects of mistranslation have been described.

In mice, a single mutation in the editing domain of the alanyl-tRNA synthetase (AlaRS) impairs the discrimination between alanine (Ala) and serine (Ser), leading to mischarging of Ala tRNAs with Ser (Ser-tRNA^{Ala}). As a result, mistranslated proteins misfold, aggregate, are extensively ubiquitinated and both autophagy and the UPR are up-regulated, leading to loss of mouse Purkinje cells and premature mouse death (Lee et al., 2006). In humans, mutations in the gene that encodes the glycyl-tRNA synthetase (GlyRS) affect tRNA charging fidelity and induce its mislocalization into granules within cell bodies and in neurite projections of neuronal cells (Antonellis et al., 2003; Xie et al., 2007) and have been described as the cause of some types of the peripheral neuropathy Charcot-Marie-Tooth (CMT). Also, misincorporation of

homocysteine (Hcy) at methionine (Met) codons caused by mischarging of $tRNA^{Met}$ by the methionyl-tRNA synthetase (MetRS), causes proteome N-homocysteinylation in vascular endothelial cells (HUVEC) and is associated with increased risk of vascular disease (Jakubowski et al., 2008). Several diseases like myopathy, encephalopathy, lactic acidosis, stroke-like episodes or myoclonic epilepsy with ragged-red fibres (MELAS/MERRF syndromes) have been liked to mutations in various human mitochondrial tRNA genes (Shoffner et al., 1990; Borner et al., 2000; Enriquez et al., 1995). Furthermore, multiple studies have linked failures in PQC with human diseases, namely Alzheimer's disease, Parkinson's disease, Huntington's disease and other polyglutamine diseases, aging and heart disease (Wang and Robbins, 2006; Villarreal and Lew, 2010; McClellan and Frydman, 2001; Luce et al., 2010; Witt, 2010; Dimcheff et al., 2003a; Dimcheff et al., 2003b; Gregersen et al., 2006). One of the most striking characteristic of the described phenomena is that they do not affect embryonic development and the observed diseases normally appear in adult individuals. This observation suggests that, at least in higher eukaryotes, the consequences of mistranslation are chronic rather than acute.

Several studies also indicate that mistranslation can be tolerated and can even be beneficial under certain circumstances. For instance, misincorporation of Ser at Leu CUG codons allows yeast to growth in presence of high concentrations of several toxics and stress agents (Silva RM et al., 2007; Santos et al., 1999), while epigenetic control of both stop codon read-through and antizyme frameshifting by the yeast [PSI^{+}] prion generates phenotypic diversity and regulates the cellular concentration of polyamines (True and Lindquist, 2000; True et al., 2004; Namy et al., 2008). The human pathogen

Candida albicans possess a unique $tRNA_{CAG}^{Ser}$ which is recognized by both leucyl- and seryl-tRNA synthetases (LeuRS and SerRS) and is aminoacylated *in vitro* with both serine (97%) and leucine (3%). This event generates extensive phenotypic diversity, induces expression of novel colony and cell morphology phenotypes and is associated with the evolution of a genetic code alteration (Gomes et al., 2007; Miranda et al., 2007). In *Acinetobacter baylyi* , when the levels of Ile are limiting and there is excess of valine (Val), substitutions in IleRS that affect editing and allow the mischarging of $tRNA^{ile}$ with Val increase growth rate compared to wild-type bacteria (Bacher and Schimmel, 2007; Bacher et al., 2005). Additional evidences come from *Escherichia coli* where it was shown that the aminoglycosidic antibiotic streptomycin, a mistranslation inducer, and mutant glycine (Gly) tRNAs that misincorporate glycine at aspartate (Asp) codons generate extensive genetic diversity and increase adaptation potential through translational stress induced mutagenesis (TSM) (Dorazi et al., 2002). The potential benefits arising from mistranslation events are also illustrated by the natural reassignments of UGA and UAG stop codons to selenocisteine and pyrolisine, respectively (Namy et al., 2005). Other examples come from studies in mammalian cells (Nangle LA et al., 2007) where methionine misincorporation is associated with increased ROS levels, as it was shown to be a ROS scavenger (Netzer et al., 2009).

In conclusion, mistranslation can have harmful physiological effects being relevant to human diseases, but it is becoming increasingly clear that it also has beneficial effects in antibiotic and stress resistance, metabolic regulation, phenotypic and genetic diversity and is a major driver in the in the evolution of the genetic code (

Figure **13**) (Santos et al., 1999; Reynolds et al., 2010).

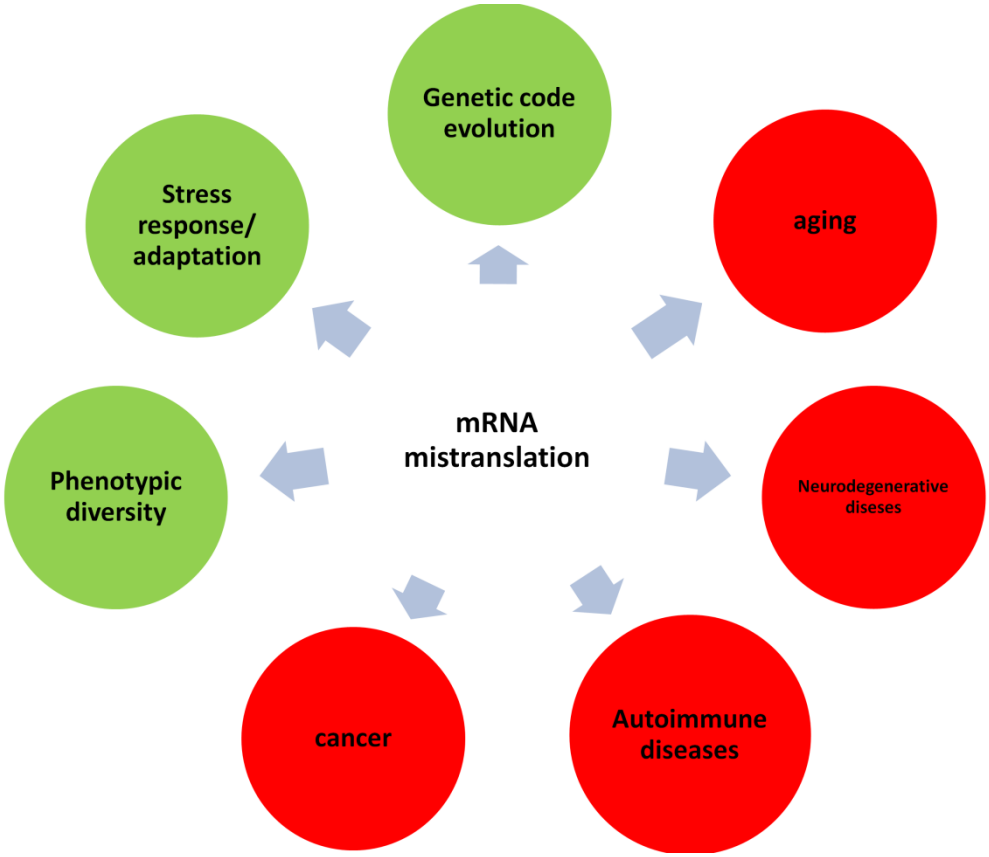

Figure 13 - Possible implications of mRNA mistranslation.

The mistranslation model

Yeast is extensively used as a model system to study cell physiology, cellular mechanisms, signalling pathways and the basic molecular mechanisms of many human diseases. This is due to its eukaryotic nature, availability of the whole sequence high level genome, annotation and a large set of genetic manipulation tools. In addition, yeast genome databases are highly sophisticated and contain useful information about many aspects of yeast biology. Gene expression profiles, protein-protein interaction networks, many well characterized genetic tools and resources for gene disruption, mutation, gene over expression and tagging are available to the scientific community.

Furthermore, more than 30% of the human genes involved in disease have orthologues in yeast.

In this thesis we have also used yeast as a model system to elucidate the biology of mistranslation. For this, we have engineered yeast cells to express serine tRNAs that misread leucine CUG codons as serine. These atypical serine tRNAs occur naturally in the human pathogen *Candida albicans* where the CUG leucine codon is translated as serine (Silva RM et al., 2007; Miranda et al., 2006; Gomes et al., 2007; Santos et al., 1999; Santos et al., 1996). We have used two variant forms of a *C. albicans* $tRNA^{ser}$ gene namely one $tRNA_{CAG}^{Ser}$ containing a guanosine (G) at position 33 (the natural occurring form, G_{33}) and a second tRNA containing a uridine (U) in the same position (U_{33}) (Figure 14, A). The latter decodes CUGs more efficiently than the G_{33} $tRNA_{CAG}^{Ser}$. This tRNA was previously tested *in vivo* in *S. cerevisiae* and is correctly aminoacylated and the levels of serine misincorporation at CUG codons *in vivo* varies from 1.4% to 2.3% (Silva RM et al., 2007), which represents a 140 to 240 fold increase in translational error relative to the typical translation error. Moreover, 88.8% of the *S.cerevisiae* genes contain 30994 CUG codons, allowing to study mistranslation at a global level (Figure 14, B). We have focused our studies on the activation of autophagy and on the effect of mistranslation on oxidative stress and mitochondrial function. Our data show that mistranslation activates autophagy and has a major impact on oxidative stress. We have also observed the mistranslation effects on the assembly of cytoplasmatic granules like P-bodies and stress granules.

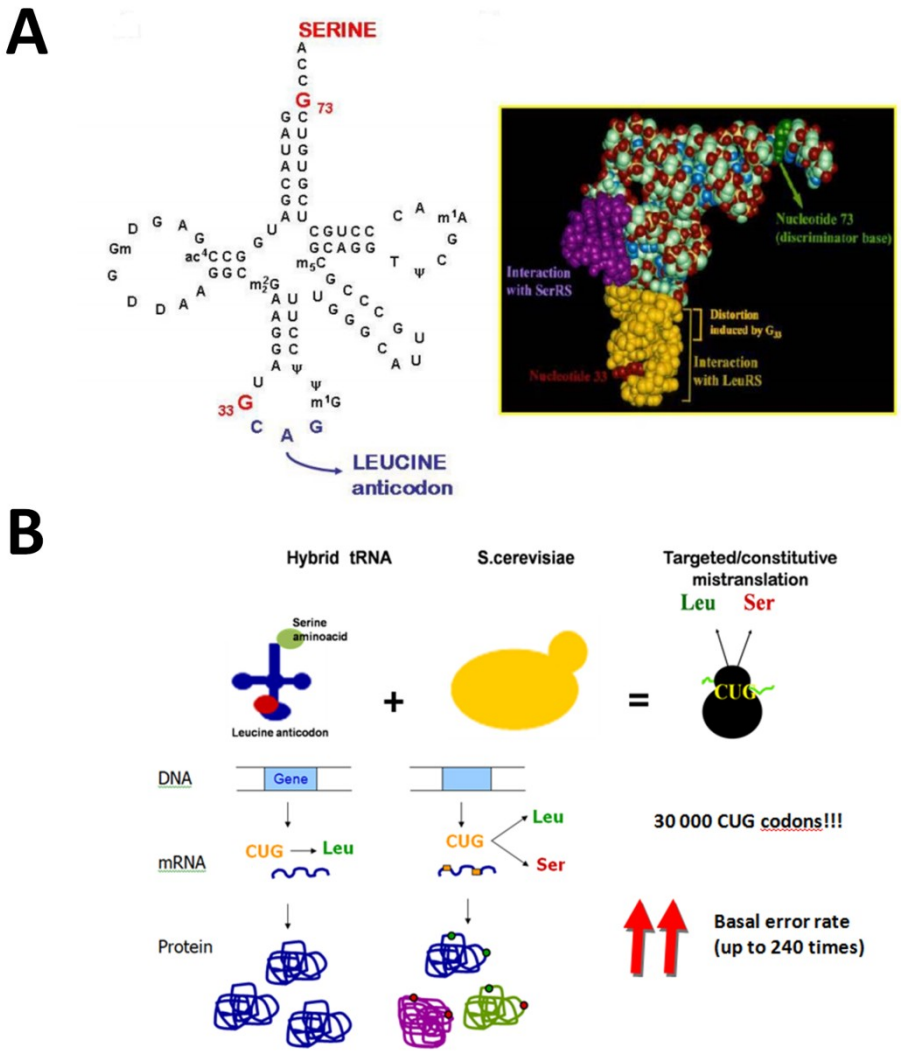

Figure 14 – A) The *Candida albicans* $tRNA_{CAG}^{Ser}$ secondary (left) and tertiary structures (right). This tRNA is a hybrid molecule containing the body of a serine tRNA and the anticodon arm of a leucine tRNA **B) Experimental model of mRNA mistranslation**. Single codon mistranslation in yeast cells was engineered using constitutive expression of mutant tRNA-Ser genes, based on the *C. albicans* ser-$tRNA_{CAG}$ that misreads leucine CUG codons as serine. This tRNA increases mistranslation by 240 fold and affects most of the proteome. Adapted from Silva RM et al., 2007 and Paredes JA, 2010.

References

1. Amrani, N., M.S.Sachs, and A.Jacobson. 2006. Early nonsense: mRNA decay solves a translational problem. *Nat Rev Mol Cell Biol* 7:415-425.
2. Antonellis, A., R.E.Ellsworth, N.Sambuughin, I.Puls, A.Abel, S.Q.Lee-Lin, A.Jordanova, I.Kremensky, K.Christodoulou, L.T.Middleton, K.Sivakumar, V.Ionasescu, B.Funalot, J.M.Vance, L.G.Goldfarb, K.H.Fischbeck, and E.D.Green. 2003. Glycyl tRNA synthetase mutations in Charcot-Marie-Tooth disease type 2D and distal spinal muscular atrophy type V. *Am J Hum. Genet.* 72:1293-1299.
3. Arava, Y., F.E.Boas, P.O.Brown, and D.Herschlag. 2005. Dissecting eukaryotic translation and its control by ribosome density mapping. *Nucleic Acids Res* 33:2421-2432.
4. Bacher, J.M., V.de Crecy-Lagard, and P.R.Schimmel. 2005. Inhibited cell growth and protein functional changes from an editing-defective tRNA synthetase. *Proc. Natl. Acad. Sci. U. S. A* 102:1697-1701.
5. Bacher, J.M. and P.Schimmel. 2007. An editing-defective aminoacyl-tRNA synthetase is mutagenic in aging bacteria via the SOS response. *PNAS* 104:1907-1912.
6. Back, S.H., M.Schr÷der, K.Lee, K.Zhang, and R.J.Kaufman. 2005. ER stress signaling by regulated splicing: IRE1/HAC1/XBP1. *Methods* 35:395-416.
7. bbas-Terki, T., O.Donze, P.A.Briand, and D.Picard. 2001. Hsp104 interacts with Hsp90 cochaperones in respiring yeast. *Mol. Cell Biol.* 21:7569-7575.
8. Beau, I., A.Esclatine, and P.Codogno. 2008. Lost to translation: when autophagy targets mature ribosomes. *Trends Cell Biol* 18:311-314.
9. Bernales, S., K.L.McDonald, and P.Walter. 2006. Autophagy counterbalances endoplasmic reticulum expansion during the unfolded protein response. *PLoS Biol* 4:e423.
10. Bjork, G.R. 1995. Genetic dissection of synthesis and function of modified nucleosides in bacterial transfer RNA. *Prog. Nucleic Acid Res. Mol. Biol.* 50:263-338.
11. Bjork, G.R., J.U.Ericson, C.E.Gustafsson, T.G.Hagervall, Y.H.Jonsson, and P.M.Wikstrom. 1987. Transfer RNA modification. *Annu. Rev. Biochem.* 56:263-287.
12. Borner, G.V., M.Zeviani, V.Tiranti, F.Carrara, S.Hoffmann, K.D.Gerbitz, H.Lochmuller, D.Pongratz, T.Klopstock, A.Melberg, E.Holme, and S.Paabo. 2000. Decreased aminoacylation of mutant tRNAs in MELAS but not in MERRF patients. *Hum. Mol. Genet.* 9:467-475.
13. Bosl, B., V.Grimminger, and S.Walter. 2005. Substrate binding to the molecular chaperone Hsp104 and its regulation by nucleotides. *J. Biol. Chem.* 280:38170-38176.
14. Bosl, B., V.Grimminger, and S.Walter. 2006. The molecular chaperone Hsp104--A molecular machine for protein disaggregation. *Journal of Structural Biology* In Press, Corrected Proof.
15. Buchberger, A., B.Bukau, and T.Sommer. 2010. Protein quality control in the cytosol and the endoplasmic reticulum: brothers in arms. *Mol. Cell* 40:238-252.
16. Calderwood, S.K. and D.R.Ciocca. 2008. Heat shock proteins: stress proteins with Janus-like properties in cancer. *Int. J. Hyperthermia* 24:31-39.
17. Cashikar, A.G., M.Duennwald, and S.L.Lindquist. 2005. A Chaperone Pathway in Protein Disaggregation: Hsp26 alters the nature of protein aggregates to facilitate reactivation by Hsp104. *J. Biol. Chem.* 280:23869-23875.
18. Cheetham, M.E. and A.J.Caplan. 1998. Structure, function and evolution of DnaJ: conservation and adaptation of chaperone function. *Cell Stress. Chaperones.* 3:28-36.
19. Coffino, P. 2001. Antizyme, a mediator of ubiquitin-independent proteasomal degradation. *Biochimie* 83:319-323.
20. Curran, J.F. and M.Yarus. 1986. Base substitutions in the tRNA anticodon arm do not degrade the accuracy of reading frame maintenance. *Proc. Natl. Acad. Sci U. S. A* 83:6538-6542.
21. Cyr, D.M. and D.N.Hebert. 2009. Protein quality control--linking the unfolded protein response to disease. Conference on 'From Unfolded Proteins in the Endoplasmic Reticulum to Disease'. *EMBO Rep.* 10:1206-1210.
22. Dale, T. and O.C.Uhlenbeck. 2005a. Amino acid specificity in translation. *Trends Biochem Sci* 30:659-665.
23. Dale, T. and O.C.Uhlenbeck. 2005b. Binding of misacylated tRNAs to the ribosomal A site. *RNA.* 11:1610-1615.
24. Dasmahapatra, B. and K.Chakraburtty. 1981. Protein synthesis in yeast. I. Purification and properties of elongation factor 3 from Saccharomyces cerevisiae. *J. Biol. Chem.* 256:9999-10004.
25. Dimcheff, D.E., S.Askovic, A.H.Baker, C.Johnson-Fowler, and J.L.Portis. 2003a. Endoplasmic reticulum stress is a determinant of retrovirus-induced spongiform neurodegeneration. *J. Virol.* 77:12617-12629.
26. Dimcheff, D.E., J.L.Portis, and B.Caughey. 2003b. Prion proteins meet protein quality control. *Trends Cell Biol.* 13:337-340.
27. Dittmar, K.A., J.M.Goodenbour, and T.Pan. 2006. Tissue-specific differences in human transfer RNA expression. *PLoS. Genet.* 2:e221.
28. Dorazi, R., J.J.Lingutla, and M.Z.Humayun. 2002. Expression of mutant alanine tRNAs increases spontaneous mutagenesis in Escherichia coli. *Mol Microbiol.* 44:131-141.

29. Drummond, D.A. and C.O.Wilke. 2009. The evolutionary consequences of erroneous protein synthesis. *Nat Rev Genet* 10:715-724.
30. Elofsson, M., U.Splittgerber, J.Myung, R.Mohan, and C.M.Crews. 1999. Towards subunit-specific proteasome inhibitors: synthesis and evaluation of peptide alpha',beta'-epoxyketones. *Chem. Biol.* 6:811-822.
31. Enriquez, J.A., A.Chomyn, and G.Attardi. 1995. MtDNA mutation in MERRF syndrome causes defective aminoacylation of tRNA(Lys) and premature translation termination. *Nat. Genet.* 10:47-55.
32. Fan, C.Y., S.Lee, and D.M.Cyr. 2003. Mechanisms for regulation of Hsp70 function by Hsp40. *Cell Stress. Chaperones.* 8:309-316.
33. Farabaugh, P.J. and G.R.Bjork. 1999. How translational accuracy influences reading frame maintenance. *EMBO J* 18:1427-1434.
34. Fox-Walsh, K.L. and K.J.Hertel. 2009. Splice-site pairing is an intrinsically high fidelity process. *Proc. Natl. Acad. Sci U. S. A* 106:1766-1771.
35. Freeze, H.H. 2006. Genetic defects in the human glycome. *Nat Rev Genet* 7:537-551.
36. Fu, C., K.Ahmed, H.Ding, X.Ding, J.Lan, Z.Yang, Y.Miao, Y.Zhu, Y.Shi, J.Zhu, H.Huang, and X.Yao. 2005. Stabilization of PML nuclear localization by conjugation and oligomerization of SUMO-3. *Oncogene* 24:5401-5413.
37. Gardner, R.G., Z.W.Nelson, and D.E.Gottschling. 2005. Degradation-mediated protein quality control in the nucleus. *Cell* 120:803-815.
38. Gasser, B., M.Saloheimo, U.Rinas, M.Dragosits, E.Rodriguez-Carmona, K.Baumann, M.Giuliani, E.Parrilli, P.Branduardi, C.Lang, D.Porro, P.Ferrer, M.L.Tutino, D.Mattanovich, and A.Villaverde. 2008. Protein folding and conformational stress in microbial cells producing recombinant proteins: a host comparative overview. *Microb. Cell Fact.* 7:11.
39. Gomes, A.C., I.Miranda, R.M.Silva, G.R.Moura, B.Thomas, A.Akoulitchev, and M.A.Santos. 2007b. A genetic code alteration generates a proteome of high diversity in the human pathogen Candida albicans. *Genome Biol.* 8:R206.
40. Gregersen, N., P.Bross, S.Vang, and J.H.Christensen. 2006. Protein misfolding and human disease. *Annu. Rev. Genomics Hum. Genet.* 7:103-124.
41. Hartl, F.U. and M.Hayer-Hartl. 2002. Molecular chaperones in the cytosol: from nascent chain to folded protein. *Science* 295:1852-1858.
42. Haslbeck, M., A.Miess, T.Stromer, S.Walter, and J.Buchner. 2005. Disassembling Protein Aggregates in the Yeast Cytosol: THE COOPERATION OF HSP26 WITH SSA1 AND HSP104. *J. Biol. Chem.* 280:23861-23868.
43. Haslberger, T., J.Weibezahn, R.Zahn, S.Lee, F.T.Tsai, B.Bukau, and A.Mogk. 2007. M domains couple the ClpB threading motor with the DnaK chaperone activity. *Mol. Cell* 25:247-260.
44. Haynes, C.M., E.A.Titus, and A.A.Cooper. 2004. Degradation of misfolded proteins prevents ER-derived oxidative stress and cell death. *Mol. Cell* 15:767-776.
45. Heinemeyer, W., J.A.Kleinschmidt, J.Saidowsky, C.Escher, and D.H.Wolf. 1991. Proteinase yscE, the yeast proteasome/multicatalytic-multifunctional proteinase: mutants unravel its function in stress induced proteolysis and uncover its necessity for cell survival. *EMBO J.* 10:555-562.
46. Hessling, M., K.Richter, and J.Buchner. 2009. Dissection of the ATP-induced conformational cycle of the molecular chaperone Hsp90. *Nat. Struct. Mol. Biol.* 16:287-293.
47. Hoyer-Hansen, M. and M.Jaattela. 2007. Connecting endoplasmic reticulum stress to autophagy by unfolded protein response and calcium. *Cell Death. Differ.* 14:1576-1582.
48. Huang, J. and D.J.Klionsky. 2007. Autophagy and human disease. *Cell Cycle* 6:1837-1849.
49. Iwata, A., Y.Nagashima, L.Matsumoto, T.Suzuki, T.Yamanaka, H.Date, K.Deoka, N.Nukina, and S.Tsuji. 2009. Intranuclear degradation of polyglutamine aggregates by the ubiquitin-proteasome system. *J. Biol. Chem.* 284:9796-9803.
50. Jackson, R.J., C.U.Hellen, and T.V.Pestova. 2010. The mechanism of eukaryotic translation initiation and principles of its regulation. *Nat Rev Mol Cell Biol* 11:113-127.
51. Jakubowski, H., G.H.Boers, and K.A.Strauss. 2008. Mutations in cystathionine beta-synthase or methylenetetrahydrofolate reductase gene increase N-homocysteinylated protein levels in humans. *FASEB J* 22:4071-4076.
52. Janer, A., E.Martin, M.P.Muriel, M.Latouche, H.Fujigasaki, M.Ruberg, A.Brice, Y.Trottier, and A.Sittler. 2006. PML clastosomes prevent nuclear accumulation of mutant ataxin-7 and other polyglutamine proteins. *J. Cell Biol.* 174:65-76.
53. Kapp, L.D. and J.R.Lorsch. 2004a. GTP-dependent recognition of the methionine moiety on initiator tRNA by translation factor eIF2. *J Mol Biol* 335:923-936.
54. Kapp, L.D. and J.R.Lorsch. 2004b. The molecular mechanics of eukaryotic translation. *Annu. Rev Biochem* 73:657-704.
55. Kincaid, M.M. and A.A.Cooper. 2007a. ERADicate ER stress or die trying. *Antioxid. Redox. Signal.* 9:2373-2387.
56. Kincaid, M.M. and A.A.Cooper. 2007b. Misfolded proteins traffic from the endoplasmic reticulum (ER) due to ER export signals. *Mol. Biol. Cell* 18:455-463.

57. Kireeva, M.L., Y.A.Nedialkov, G.H.Cremona, Y.A.Purtov, L.Lubkowska, F.Malagon, Z.F.Burton, J.N.Strathern, and M.Kashlev. 2008. Transient reversal of RNA polymerase II active site closing controls fidelity of transcription elongation. *Mol Cell* 30:557-566.
58. Knop, M., A.Finger, T.Braun, K.Hellmuth, and D.H.Wolf. 1996. Der1, a novel protein specifically required for endoplasmic reticulum degradation in yeast. *EMBO J.* 15:753-763.
59. Kovalchuke, O., R.Kambampati, E.Pladies, and K.Chakraburtty. 1998. Competition and cooperation amongst yeast elongation factors. *Eur. J. Biochem.* 258:986-993.
60. Kraft , C., A.Deplazes, M.Sohrmann, and M.Peter. 2008. Mature ribosomes are selectively degraded upon starvation by an autophagy pathway requiring the Ubp3p/Bre5p ubiquitin protease. *Nat Cell Biol* Apr 6.
61. Kraft, C., F.Reggiori, and M.Peter. 2009. Selective types of autophagy in yeast. *Biochim. Biophys. Acta* 1793:1404-1412.
62. Kramer, E.B. and P.J.Farabaugh. 2007. The frequency of translational misreading errors in E. coli is largely determined by tRNA competition. *RNA* 13:87-96.
63. Kundu, M. and C.B.Thompson. 2008. Autophagy: Basic Principles and Relevance to Disease. *Annual Review of Pathology: Mechanisms of Disease* 3:427-455.
64. Kunkel, T.A. and K.Bebenek. 2000. DNA replication fidelity. *Annu. Rev Biochem* 69:497-529.
65. Lee, J.W., K.Beebe, L.A.Nangle, J.Jang, C.M.Longo-Guess, S.A.Cook, M.T.Davisson, J.P.Sundberg, P.Schimmel, and S.L.Ackerman. 2006. Editing-defective tRNA synthetase causes protein misfolding and neurodegeneration. *Nature* 443:50-55.
66. Levine, B. and G.Kroemer. 2008. Autophagy in the pathogenesis of disease. *Cell* 132:27-42.
67. Levine, R.L., L.Mosoni, B.S.Berlett, and E.R.Stadtman. 1996. Methionine residues as endogenous antioxidants in proteins. *Proc. Natl. Acad. Sci. U. S. A* 93:15036-15040.
68. Lindquist,SL. and G.Kim. Heat-shock protein 104 expression is sufficient for thermotolerance in yeast. Proc.Natl.Acad.Sci.USA 93[Microbiology], 5301-5306. 1996. Ling, J., N.Reynolds, and M.Ibba. 2009. Aminoacyl-tRNA Synthesis and Translational Quality Control. *Annu. Rev Microbiol.*
69. Luce, K., A.C.Weil, and H.D.Osiewacz. 2010. Mitochondrial protein quality control systems in aging and disease. *Adv. Exp. Med. Biol.* 694:108-125.
70. Lum, R., J.M.Tkach, E.Vierling, and J.R.Glover. 2004. Evidence for an Unfolding/Threading Mechanism for Protein Disaggregation by Saccharomyces cerevisiae Hsp104. *J. Biol. Chem.* 279:29139-29146.
71. Marquez, V., D.N.Wilson, W.P.Tate, F.Triana-Alonso, and K.H.Nierhaus. 2004. Maintaining the ribosomal reading frame: the influence of the E site during translational regulation of release factor 2. *Cell* 118:45-55.
72. Matsuda, T., K.Bebenek, C.Masutani, F.Hanaoka, and T.A.Kunkel. 2000. Low fidelity DNA synthesis by human DNA polymerase-eta. *Nature* 404:1011-1013.
73. McClellan, A.J. and J.Frydman. 2001. Molecular chaperones and the art of recognizing a lost cause. *Nat. Cell Biol.* 3:E51-E53.
74. Mijaljica, D., M.Prescott, and R.J.Devenish. 2006. Endoplasmic reticulum and Golgi complex: Contributions to, and turnover by, autophagy. *Traffic.* 7:1590-1595.
75. Miranda,I., R.Silva, and M.Santos. Evolution of the genetic code in yeasts. Yeast *Yeast* 2006[23], 203-213. 2006.
76. Miranda, I., R.Rocha, M.C.Santos, D.D.Mateus, G.R.Moura, L.Carreto, and M.A.Santos. 2007. A genetic code alteration is a phenotype diversity generator in the human pathogen Candida albicans. *PLoS. One.* 2:e996.
77. Mogk, A., T.Haslberger, P.Tessarz, and B.Bukau. 2008. Common and specific mechanisms of AAA+ proteins involved in protein quality control. *Biochem. Soc. Trans.* 36:120-125.
78. Mogk, A., C.Schlieker, K.L.Friedrich, H.J.Schonfeld, E.Vierling, and B.Bukau. 2003a. Refolding of substrates bound to small Hsps relies on a disaggregation reaction mediated most efficiently by ClpB/DnaK. *J. Biol. Chem.* 278:31033-31042.
79. Mogk, A., C.Schlieker, C.Strub, W.Rist, J.Weibezahn, and B.Bukau. 2003b. Roles of individual domains and conserved motifs of the AAA+ chaperone ClpB in oligomerization, ATP hydrolysis, and chaperone activity. *J. Biol. Chem.* 278:17615-17624.
80. Mosser, D.D. and R.I.Morimoto. 2004. Molecular chaperones and the stress of oncogenesis. *Oncogene* 23:2907-2918.
81. Moura, G.R., L.C.Carreto, and M.A.Santos. 2009. Genetic code ambiguity: an unexpected source of proteome innovation and phenotypic diversity. *Curr. Opin. Microbiol.* 12:631-637.
82. Namy, O., A.Galopier, C.Martini, S.Matsufuji, C.Fabret, and J.P.Rousset. 2008. Epigenetic control of polyamines by the prion [PSI(+)]. *Nat. Cell Biol.*
83. Nangle LA, Motta CM, and Schimmel P. 2007. Global effects of mistranslation from an editing defect in mammalian cells. *Chemistry & Biology* 13:1091-1100.
84. Navon, A. and A.Ciechanover. 2009. The 26 S proteasome: from basic mechanisms to drug targeting. *J. Biol. Chem.* 284:33713-33718.
85. Netzer, N., J.M.Goodenbour, A.David, K.A.Dittmar, R.B.Jones, J.R.Schneider, D.Boone, E.M.Eves, M.R.Rosner, J.S.Gibbs, A.Embry, B.Dolan, S.Das, H.D.Hickman, P.Berglund,

J.R.Bennink, J.W.Yewdell, and T.Pan. 2009. Innate immune and chemically triggered oxidative stress modifies translational fidelity. *Nature* 462:522-526.
86. Ninio, J. 1991. Connections between translation, transcription and replication error-rates. *Biochimie* 73:1517-1523.
87. Ogata, M., S.i.Hino, A.Saito, K.Morikawa, S.Kondo, S.Kanemoto, T.Murakami, M.Taniguchi, I.Tanii, K.Yoshinaga, S.Shiosaka, J.A.Hammarback, F.Urano, and K.Imaizumi. 2006. Autophagy Is Activated for Cell Survival after Endoplasmic Reticulum Stress. *Mol. Cell. Biol.* 26:9220-9231.
88. Parker, J. and J.Precup. 1986. Mistranslation during phenylalanine starvation. *Mol. Gen. Genet.* 204:70-74.
89. Parsell, D.A., A.S.Kowal, M.A.Singer, and S.Lindquist. 1994. Protein disaggregation mediated by heat-shock protein Hsp104. *Nature* 372:475-478.
90. Persson, B.C., C.Gustafsson, D.E.Berg, and G.R.Bjork. 1992. The gene for a tRNA modifying enzyme, m5U54-methyltransferase, is essential for viability in Escherichia coli. *Proc. Natl. Acad. Sci. U. S. A* 89:3995-3998.
91. Precup, J. and J.Parker. 1987. Missense misreading of asparagine codons as a function of codon identity and context. *J. Biol Chem* 262:11351-11355.
92. Priault, M., B.Salin, J.Schaeffer, F.M.Vallette, J.P.di Rago, and J.C.Martinou. 2005. Impairing the bioenergetic status and the biogenesis of mitochondria triggers mitophagy in yeast. *Cell Death. Differ.* 12:1613-1621.
93. Qin, S.L., A.G.Xie, M.C.Bonato, and C.S.McLaughlin. 1990. Sequence analysis of the translational elongation factor 3 from Saccharomyces cerevisiae. *J Biol Chem* 265:1903-1912.
94. Reynolds, N.M., B.A.Lazazzera, and M.Ibba. 2010. Cellular mechanisms that control mistranslation. *Nat Rev Microbiol.* 8:849-856.
95. Rocha, E.P. 2004. Codon usage bias from tRNA's point of view: redundancy, specialization, and efficient decoding for translation optimization. *Genome Res.* 14:2279-2286.
96. Rocha, E.P. and A.Danchin. 2004. An analysis of determinants of amino acids substitution rates in bacterial proteins. *Mol. Biol. Evol.* 21:108-116.
97. Rosenbaum, J.C., E.K.Fredrickson, M.L.Oeser, C.M.Garrett-Engele, M.N.Locke, L.A.Richardson, Z.W.Nelson, E.D.Hetrick, T.I.Milac, D.E.Gottschling, and R.G.Gardner. 2011. Disorder targets misorder in nuclear quality control degradation: a disordered ubiquitin ligase directly recognizes its misfolded substrates. *Mol. Cell* 41:93-106.
98. Rosenberger, R.F. and G.Foskett. 1981. An estimate of the frequency of in vivo transcriptional errors at a nonsense codon in Escherichia coli. *Mol Gen. Genet* 183:561-563.
99. Rossi, J.M. and S.Lindquist. 1989. The intracellular location of yeast heat-shock protein 26 varies with metabolism. *J. Cell Biol.* 108:425-439.
100. Santos, M.A., C.Cheesman, V.Costa, P.Moradas-Ferreira, and M.F.Tuite. 1999. Selective advantages created by codon ambiguity allowed for the evolution of an alternative genetic code in Candida spp. *Mol Microbiol.* 31:937-947.
101. Santos, M.A., V.M.Perreau, and M.F.Tuite. 1996. Transfer RNA structural change is a key element in the reassignment of the CUG codon in Candida albicans. *EMBO J* 15:5060-5068.
102. Schaupp, A., M.Marcinowski, V.Grimminger, B.Bosl, and S.Walter. 2007. Processing of proteins by the molecular chaperone Hsp104. *J. Mol. Biol.* 370:674-686.
103. Schneider-Poetsch, T., J.Ju, D.E.Eyler, Y.Dang, S.Bhat, W.C.Merrick, R.Green, B.Shen, and J.O.Liu. 2010. Inhibition of eukaryotic translation elongation by cycloheximide and lactimidomycin. *Nat Chem Biol* 6:209-217.
104. Shah, P. and M.A.Gilchrist. 2010. Effect of correlated tRNA abundances on translation errors and evolution of codon usage bias. *PLoS. Genet.* 6.
105. Shimozawa, N. 2007. Molecular and clinical aspects of peroxisomal diseases. *J. Inherit. Metab Dis.* 30:193-197.
106. Shoffner, J.M., M.T.Lott, A.M.Lezza, P.Seibel, S.W.Ballinger, and D.C.Wallace. 1990. Myoclonic epilepsy and ragged-red fiber disease (MERRF) is associated with a mitochondrial DNA tRNA(Lys) mutation. *Cell* 61:931-937.
107. Silva, R.M., J.A.Paredes, G.R.Moura, B.Manadas, T.Lima-Costa, R.Rocha, I.Miranda, A.C.Gomes, M.J.Koerkamp, M.Perrot, F.C.Holstege, H.Boucherie, and M.A.Santos. 2007. Critical roles for a genetic code alteration in the evolution of the genus Candida. *EMBO J.* 26:4555-4565.
108. Skogerson, L. and D.Engelhardt. 1977. Dissimilarity in protein chain elongation factor requirements between yeast and rat liver ribosomes. *J Biol Chem* 252:1471-1475.
109. Spiess, C., A.S.Meyer, S.Reissmann, and J.Frydman. 2004. Mechanism of the eukaryotic chaperonin: protein folding in the chamber of secrets. *Trends Cell Biol.* 14:598-604.
110. Stahl, G., S.N.Salem, L.Chen, B.Zhao, and P.J.Farabaugh. 2004. Translational accuracy during exponential, postdiauxic, and stationary growth phases in Saccharomyces cerevisiae. *Eukaryot. Cell* 3:331-338.
111. Stolz, A., R.S.Schweizer, A.Schafer, and D.H.Wolf. 2010. Dfm1 forms distinct complexes with Cdc48 and the ER ubiquitin ligases and is required for ERAD. *Traffic.* 11:1363-1369.
112. Stolz, A. and D.H.Wolf. 2010. Endoplasmic reticulum associated protein degradation: a chaperone assisted journey to hell. *Biochim. Biophys. Acta* 1803:694-705.

113. Taipale, M., D.F.Jarosz, and S.Lindquist. 2010. HSP90 at the hub of protein homeostasis: emerging mechanistic insights. *Nat. Rev. Mol. Cell Biol.* 11:515-528.
114. Tatsuta, T. 2009. Protein quality control in mitochondria. *J. Biochem.* 146:455-461.
115. Tatsuta, T. and T.Langer. 2008. Quality control of mitochondria: protection against neurodegeneration and ageing. *EMBO J.* 27:306-314.
116. Tatsuta, T. and T.Langer. 2009. AAA proteases in mitochondria: diverse functions of membrane-bound proteolytic machines. *Res. Microbiol.* 160:711-717.
117. Tomala, K. and R.Korona. 2008. Molecular chaperones and selection against mutations. *Biol. Direct.* 3:5.
118. Triana-Alonso, F.J., K.Chakraburtty, and K.H.Nierhaus. 1995. The elongation factor 3 unique in higher fungi and essential for protein biosynthesis is an E site factor. *J. Biol. Chem.* 270:20473-20478.
119. True, H.L., I.Berlin, and S.L.Lindquist. 2004. Epigenetic regulation of translation reveals hidden genetic variation to produce complex traits. *Nature* 431:184-187.
120. True, H.L. and S.L.Lindquist. 2000. A yeast prion provides a mechanism for genetic variation and phenotypic diversity. *Nature* 407:477-483.
121. Villarreal, F. and W.Y.W.Lew. 2010. Protein Quality Control in Heart Disease: Using Established Drugs to Target Novel Mechanisms. *J Am Coll Cardiol* 56:1427-1429.
122. Voges,D., P.Zwickl, and W.Baumeister.The 26S proteasome: a molecular machine designed for controlled proteolysis**.** Ann.Rev.Biochem 68, 1015-1068. 1999.
123. Wang, X. and J.Robbins. 2006. Heart failure and protein quality control. *Circ. Res.* 99:1315-1328.
124. Weibezahn, J., P.Tessarz, C.Schlieker, R.Zahn, Z.Maglica, S.Lee, H.Zentgraf, E.U.Weber-Ban, D.A.Dougan, F.T.Tsai, A.Mogk, and B.Bukau. 2004. Thermotolerance requires refolding of aggregated proteins by substrate translocation through the central pore of ClpB. *Cell* 119:653-665.
125. Wiedemann, N., A.E.Frazier, and N.Pfanner. 2004a. The protein import machinery of mitochondria. *J. Biol. Chem.* 279:14473-14476.
126. Wiedemann, N., K.N.Truscott, S.Pfannschmidt, B.Guiard, C.Meisinger, and N.Pfanner. 2004b. Biogenesis of the protein import channel Tom40 of the mitochondrial outer membrane: intermembrane space components are involved in an early stage of the assembly pathway. *J. Biol. Chem.* 279:18188-18194.
127. Wilhelm, B.T., S.Marguerat, S.Watt, F.Schubert, V.Wood, I.Goodhead, C.J.Penkett, J.Rogers, and J.Bahler. 2008. Dynamic repertoire of a eukaryotic transcriptome surveyed at single-nucleotide resolution. *Nature* 453:1239-1243.
128. Winklhofer, K.F., J.Tatzelt, and C.Haass. 2008. The two faces of protein misfolding: gain- and loss-of-function in neurodegenerative diseases. *EMBO J* 27:336-349.
129. Witt, S.N. 2010. Hsp70 molecular chaperones and Parkinson's disease. *Biopolymers* 93:218-228.
130. Wolf, D.H. and W.Hilt. 2004. The proteasome: a proteolytic nanomachine of cell regulation and waste disposal. *Biochim. Biophys. Acta* 1695:19-31.
131. Xie, W., L.A.Nangle, W.Zhang, P.Schimmel, and X.L.Yang. 2007. Long-range structural effects of a Charcot-Marie-Tooth disease-causing mutation in human glycyl-tRNA synthetase. *Proc. Natl. Acad. Sci. U. S. A* 104:9976-9981.
132. Yang, J.R., S.M.Zhuang, and J.Zhang. 2010. Impact of translational error-induced and error-free misfolding on the rate of protein evolution. *Mol Syst Biol* 6.
133. Yorimitsu, T., U.Nair, Z.Yang, and D.J.Klionsky. 2006. Endoplasmic reticulum stress triggers autophagy. *J Biol. Chem.* 281:30299-30304.
134. Zaher, H.S. and R.Green. 2009. Fidelity at the molecular level: lessons from protein synthesis. *Cell* 136:746-762.
135. Zhang, G., I.Fedyunin, O.Miekley, A.Valleriani, A.Moura, and Z.Ignatova. 2010. Global and local depletion of ternary complex limits translational elongation. *Nucleic Acids Res.* 38:4778-4787.
136. Zhu Y and Gao Q. Review on Patents for Ubiquitin-Proteasome Inhibitor as Medical Advance in Major Human Diseases. Recent Patents on Biomedical Engineering 2, 180-192. 2009. Bentham Science Publishers Ltd.

Chapter 2
Mistranslation induces protein aggregation and autophagy in yeast

Unpublished work, in preparation

Abstract

Mistranslation of mRNA can destabilize the proteome and cause disease, however, the molecular basis of cell degeneration induced by mistranslation remains unclear. In order clarify this question we have engineered yeast cells to express mutant serine tRNAs that misread leucine CUG codons as serine. We show here that such mistranslation results in accumulation of insoluble proteins, ultrastructural cellular alterations and in the formation of autophagosomes. Immuno-TEM analysis shows ubiquitin accumulation in the vacuole and functional and biochemical assays confirm the up-regulation of autophagic activity. Interestingly, the *PNC1* longevity gene, which regulates the activity of the Sir2p deacetylase, was strongly induced by such mistranslation and we show that both genes activate autophagy in mistranslating cells but do not participate in autophagy activated under starvation conditions.

Taken together, these data indicate that autophagy plays an important role in clearance of aberrant proteins and malformed organelles produced by genome translational errors. Since most of the basic cellular processes are mechanistically conserved between yeast and humans, this study suggests that translational errors may cause disease and cell degeneration through accumulation of aggregated proteins and organelle malfunction.

Introduction

To maintain cellular homeostasis and fitness, cells must guarantee that the information contained in the genome is properly translated into proteins. However, the informational steps from DNA replication to mRNA translation are not error free and may, in certain circumstances, lead to proteotoxic stress. Basal error rates range from 10^{-8}- 10^{-9} for DNA replication to 10^{-3} for tRNA selection by ribosomes (Roy H and Ibba M, 2006). At the translation level, several types of errors can occur. For instance, tRNAs are wrongly selected by the ribosome or incorrectly aminoacylated by aminoacyltRNA synthetases aaRS (i.e., missense errors) at frequencies of 10^{-3} to 10^{-5} (Loftfield and Vanderjagt, 1972; Jakubowski and Goldman, 1992; Stansfield et al., 1998). tRNA slippage during mRNA decoding (i.e., frameshifting) occurs at a frequency of 10^{-5} (Farabaugh and Bjork, 1999) and nonsense errors that result from read-through of stop codons and ribosome drop-off happen with a frequency of 10^{-3} and $4x10^{-4}$, respectively (Valente and Kinzy, 2003; Menninger, 1976).

In order to minimize the potential toxic effects of awry protein synthesis, cells possess a multiplicity of quality control check points, namely aaRS editing activity, ribosome proofreading and protein quality control systems, namely the *U*biquibiquitin-*P*roteasome *P*athway (UPS), *E*ndoplasmatic *R*eticulum *A*ssociated *D*egradation (ERAD) and molecular chaperones (Bukau et al., 2006). Most of the aberrantly synthesized proteins misfold and are degraded or may be refolded, but some aggregate into potentially toxic structures (Roy H and Ibba M, 2006). Protein misfolding/aggregation are features of many incurable

diseases, namely Alzheimer's, Parkinson's, Huntington's and several spinocerebellar ataxias, which may happen as a consequence of failure or overloading of the cellular quality control mechanisms (Kaganovich et al., 2008). For example, mischarging of alanine (Ala) tRNAs with serine (Ser), due to mutations in the editing domain of the mouse alanyl-tRNA synthetase, results in protein misfolding, aggregation and ubiquitination, activation of autophagy and UPR, loss of Purkinje cells and premature mouse death (Lee et al., 2006). Similar phenotypes occur in mammalian mistranslating cell lines, where miRNAs deregulation and apoptosis are also observed (Nangle LA et al., 2007; Geslain et al., 2010). Surprisingly, in fungi and bacteria, mistranslation can be advantageous. For instance, misincorporation of Ser at Leu CUG codons increases *S.cerevisiae* tolerance to a variety of toxic compounds (Silva RM et al., 2007; Santos et al., 1999), while in *C.albicans* mistranslation generates phenotypic diversity (Miranda et al., 2007; Gomes et al., 2007). On the other hand, mistranslation in *E.coli* induced by antibiotics and mutant tRNAs also generates genetic diversity and increase adaptation, while in *A. baylyi* misincoporation of isoleucine tRNAs with valine can be advantageous in situations where isoleucine is limiting for growth (Bacher et al., 2005; Balashov and Humayun, 2002).

Eukaryotes use autophagy and the UPS as the major protein degradation pathways (Kraft et al., 2008). The UPS contributes to cellular homeostasis by rapidly degrading short-lived and many regulatory proteins, is essential to maintain amino acid pools during starvation and contributes to degradation of defective proteins. Autophagy has been implicated in various human pathological and physiological conditions, such as neurodegeneration, immunity, cancer, development and differentiation, myopathies, heart diseases, liver

diseases and also longevity, and plays an important role in the clearance of ubiquitinated-protein aggregates induced by hyperglycemia (Kaniuk et al., 2007), and protein aggregation associated to various human diseases (Ravikumar and Rubinsztein, 2004; Iwata et al., 2005). A central issue in the discussion of the role of autophagy in disease is to clarify its role in adaptation to cellular stress versus its contribution to cell death. For instance, basal activity of autophagic processes is important in the turnover of long-lived proteins and in the removal of surplus or damaged organelles. This latter function may explain the role of autophagy in lifespan extension (Levine and Klionsky, 2004). In addition, autophagy can eliminate invasive pathogens, including viruses, parasites and bacteria and promote MHC class II presentation of microbial (and self) antigens. On the other hand, several studies indicate that, in the absence of apoptosis, autophagy may participate in a type of programmed cell death, termed type II programmed cell death, which is distinct from apoptosis, although its physiological relevance is not clear (Levine and Yuan, 2005).

In this work, we have engineered yeast strains to misincorporate serine at leucine CUG sites at low level (1.4%) and at high level (2.3%) (Silva RM et al., 2007). We have evaluated the role of mistranslation in protein aggregation and we then investigated how the aggregates were cleared by the cell.

Results

Mistranslation increases accumulation of insoluble proteins

Throughout the years, the majority of the studies on mistranslation were performed using mistranslation-inducing drugs, namely aminoglycosidic antibiotics (neomycin, streptomycin, ribostamycin and paromomycin) and nonsense and missense suppressor tRNAs (Grant et al., 1989; Grant and Tuite, 1994; Al Mamun et al., 2002; Al Mamun et al., 1999; Al Mamun et al., 2006; Kohanski et al., 2008; Nagel and Chan, 2006). The main goal of these initial studies was to shed new light on bactericidal and drug resistance mechanisms as well as to identify mutations affecting mRNA decoding efficiency and, therefore, the chronic effects of mistranslation on cellular physiology remained obscure (Santos et al., 1996a; Santos and Tuite, 1995; Yarus, 1982). Hence, our laboratory has developed a yeast model system that allows the study of chronic mistranslation and its effects on the cellular physiology. This system is based on a mutant serine tRNA that misreads leucine CUG codons as Ser ($tRNA_{CAG}^{Ser}$) (Silva RM et al., 2007; Silva, 2005). As the yeast genome has approximately 30 000 CUG codons than can be found on 88.8% of its genes, it means that the misincorporation of serine at leucine sites occurs at a proteome wide scale, affecting cell as a whole. Since mistranslation results in the synthesis of aberrant proteins that may misfold and/or aggregate, we have investigated whether protein aggregates could be detected in the mistranslating yeast cells. For this, insoluble fractions of proteins were isolated from total protein extracts using the protocol described by Holland with minor modifications (see methods) (Holland et al., 2007; Rand and Grant, 2006a). This protocol involves solubilization and separation of membrane

proteins, so reducing the background of insoluble proteins in aggregate fractions. Also, the term 'aggregated protein', in this context, refers to those fractions that include residual insoluble protein, separated from total protein and that are triton-X insoluble. The insoluble protein content was quantified by densitometry using an odyssey scanner. Two mutant yeast strains with diminished proteasome activity (rpn4Δ) and impaired autophagy (atg5Δ) were used as controls in these experiments. Similarly, the role of *SIR2* and *PNC1* genes in protein aggregation under increased mistranslation conditions was also investigated due to the strong up-regulation of *PNC1* expression and increased Sir2p activity detected previously in mistranslating cells (Silva et al., 2009).

Mistranslation increased the level of insoluble proteins relative to control cells (Figure 15, A). This was more significant in the sir2Δ mistranslating cells, but surprisingly a minor increase in protein aggregation was observed in pnc1Δ mistranslating cells. Similar levels of protein aggregation were expected in the sir2Δ and pnc1Δ mistranslating cells because Pnc1p regulates Sir2p activity. The phenotype observed in sir2Δ mistranslating cells is consistent, to some extent, with a scenario where there is increased expression of *HSP104* (Supp.Table 1) but diminished activity of the protein as consequence of protein carbonylation and oxidative stress (Erjavec and Nystrom, 2007; Erjavec et al., 2007). Additionally, we have also tested another genetic system (tRNA integrated in yeast's genome) and a slightly different quantification methodology, which confirmed the previously described results (Supp.Figure 1).

To further quantify protein aggregation, we used the *E.coli* β-galactosidase gene, which contains 54 CUG codons, as a reporter. For this, control mistranslating *S.cerevisiae* cells were co-transformed with the pGL-C1 vector, which contains a GST-β-galactosidase chimeric gene. Mistranslating cells showed to accumulated insoluble β-gal (Figure 15, B), which was consistent with the results described above. This result was further supported by the observation that ADH, which does not have CUG codons, did not accumulate in the insoluble fraction (Figure 15, B).

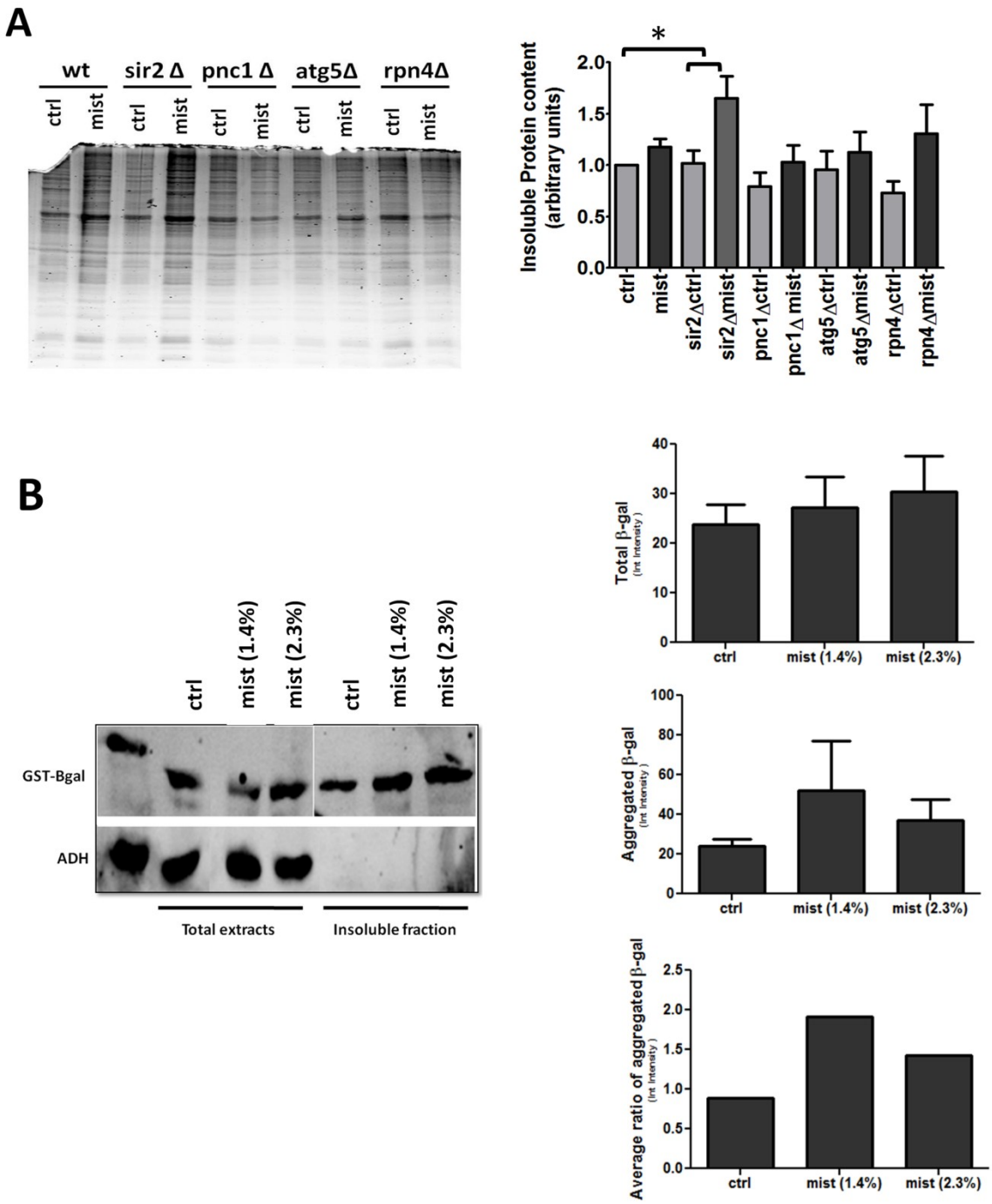

Figure 15- **Mistranslation results in the accumulation of insoluble proteins A)** To quantify insoluble proteins, cells were grown to mid exponential phase and the insoluble protein fraction was isolated from total protein extracts by centrifugation. Insoluble fraction extracts were resolved by SDS-PAGE electrophoresis (left) and quantified by densitometry using an Odyssey scanner. A

representative image of at least three independent experiments is shown. Error bars represent the standard error of the mean (right) **B)** β-gal was used as a reporter system for protein aggregation in mistranslating cells. Yeast cells co-transformed with both mistranslating tRNAs and a β-gal encoding vector, were grown to mid exponential phase and insoluble protein fractions were isolated from total protein extracts by centrifugation. Total and insoluble fraction extracts were resolved using SDS-PAGE and immunoblotted with an anti- β gal antibody. ADH was used both as loading and as negative controls. A representative image of at least three independent experiments with similar outcomes is shown (left). The upper and middle histograms on the right show the protein content in each fraction (total and insoluble), while below the average ratio between insoluble/total is shown. Protein bands were quantified by densitometry using an Odyssey scanner, the values were averaged and the ratio between the fractions was calculated for each strain.

A stronger increase in insoluble protein content was observed in Δrpn4 mistranslating cells relative to Δatg5 mistranslating cells (Figure 15). This suggested that most of the mistranslated proteins were eliminated by the proteasome and a smaller fraction was eliminated by autophagy. This is in line with previous results that showed a moderate increase proteasomal activity in mistranslating cells, that which we have also confirmed (Figure 16, Silva, 2005; Silva et al., 2009). These data are also consistent with our microarray data, which showed up-regulation of proteasome related genes (RPN4 1.7x fold increase; PRE8 1.4 fold up regulation) in the control mistranslating cells (data not shown).These expression values are apparently low, but the expression of proteasome subunit genes is regulated at the translational level meaning that, despite these mRNA expression values, higher proteasomal protein content , as well as activity (see below; Silva *et al* 2007), is expected in control mistranslating strains. We have extended the proteasome activity evaluation to the other knockout strains and, as expected, the RPN4 knockout strain had only 60% of the proteasome activity than the control strain in the absence of mistranslation (Figure 16), which was expected since previous reports showed

that deletion of this gene decreases proteasome activity by approximately 50% (London et al., 2004). When mistranslation was induced in this genetic background, proteasome activity increased slightly (74% relative to the control strain) (Figure 16). This strongly supports the idea that mistranslation indeed up-regulates proteasome activity but raises other questions, namely how the proteasome activity is regulated in this particular mistranslating background, as Rpn4p is a known proteasome regulator. Interestingly, proteasome activity was decreased by 35% and 17% in the Δsir2 and Δpnc1 strains respectively (Figure 16), which may anticipate that the PNC1/SIR2 pathway may control proteasome activity. Surprisingly, mistranslation in these genetic backgrounds did not increase proteasome activity. A tempting explanation for this unanticipated observation would be related to increased oxidative stress in mistranslating cells. Indeed, under mild oxidative stress conditions, oxidized proteins that resist to the cellular antioxidant defenses are re-directed to the proteasome for degradation leading to an increase in the proteasome activity but harsh oxidation levels have been reported to result in inhibited proteolytic degradation (Ding et al., 2006). Also, this impairment of proteasomal activity would be expected to result in up regulation of proteasome subunit expression (Meiners et al., 2003; Ju and Xie, 2004). Unexpectedly, proteasome activity in atg1Δ cells remained below that of control cells suggesting that inhibition of autophagy had a negative impact on proteasome activity. This could be explained by strong protein aggregation in atg1Δ cells but this was not observed (Figure 15,Figure 16).

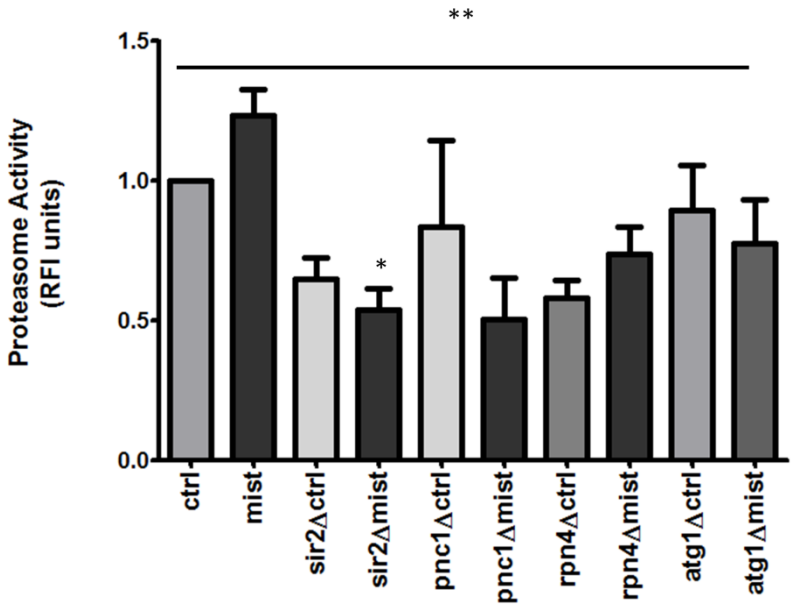

Figure 16- Proteasome activity in mistranslating yeast strains. Proteasome activity was assayed using the fluorogenic peptide s-LLVY-MCA as a substrate. Protein extracts (100 µg) were incubated at 37 ºC with 50 µM s-LLVY-MCA for 60 minutes and fluorescence emission was read at 435 nm. Wild-type control activity was set to 1 and the relative activity of the mutants was then calculated. The results are expressed as mean ± SEM of 5 to 14 determinations, corresponding to at least 3 independent experiments. * denotes statistical significance (1-way ANOVA, Dunnett's test, compared to control non deleted non mistranslating cells), while * plus line denotes statistical significance (1-way ANOVA, $p<0.05$).

Mistranslation induces ultrastructural alterations in yeast

Since aberrant proteins generated by mistranslation apparently form insoluble aggregates, we have used transmission electron microscopy (TEM) to further confirm the presence of such aggregates (Figure 17). Exponential growing mistranslating cells appeared highly heterogeneous at the ultrastructural level which was consistent with the morphological heterogeneity observed by light microscopy. For example, vacuoles appeared fragmented, had various morphologies and numerous vesicles spread through the cytoplasm were also visible (Figure 17 D, F; Supp.Figure 3). Long and thick membranar structures, which are consistent with expanded ER, were also detected

(Figure 17 E, F; Supp.Figure 3). Cells contained small round membranar structures that resembled autophagosomes (Figure 17C, E, F; Supp.Figure 3). Nuclei and cell walls showed typical morphologies while the cytoplasm of mistranslating cells had a uniform dense aspect, which complicated the observation of the protein aggregates. Overall, the ultrastuctural alterations observed in mistranslating cells were consistent with the hypothesis that aberrant protein synthesis up-regulated autophagy and increased ER stress.

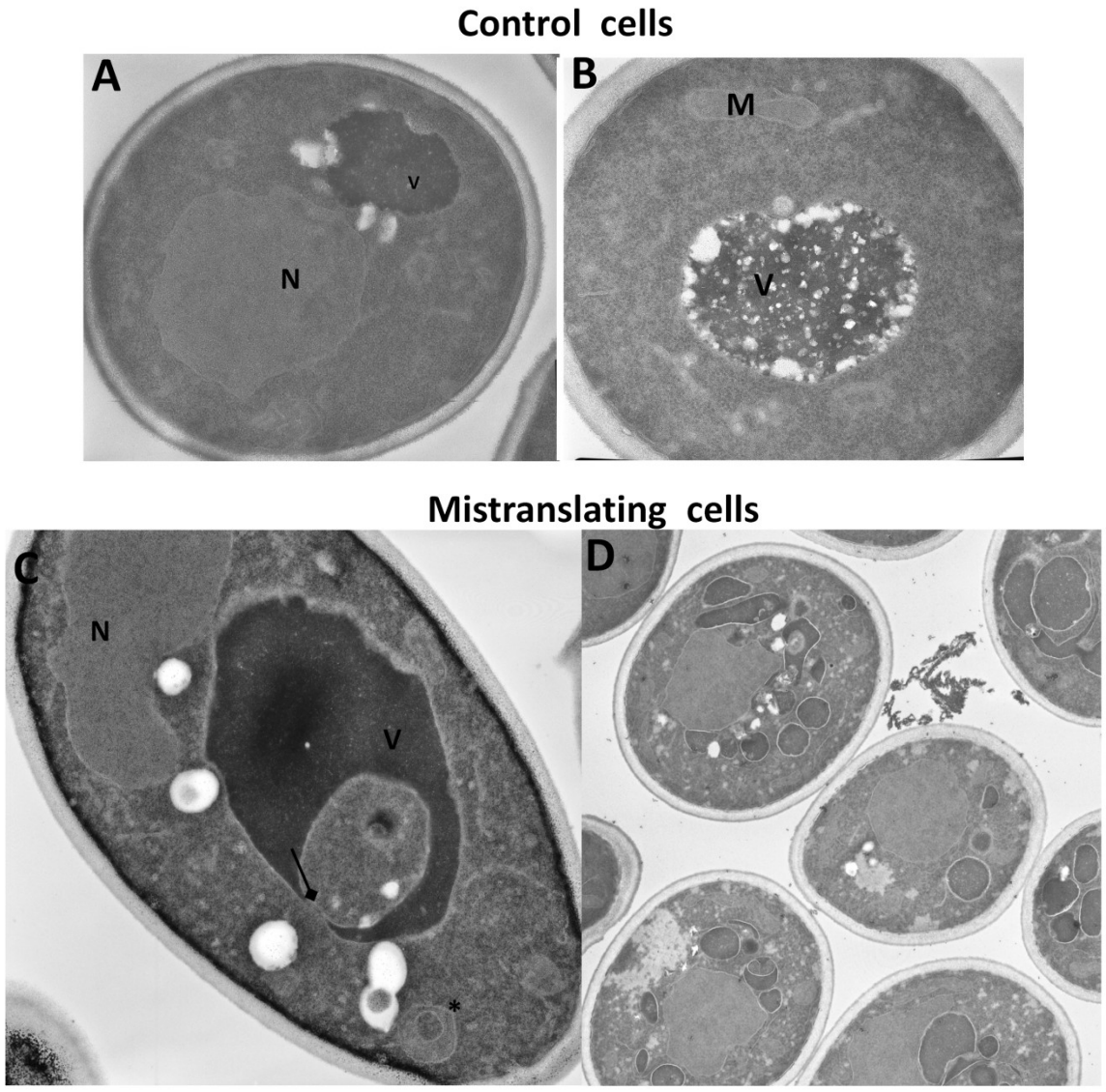

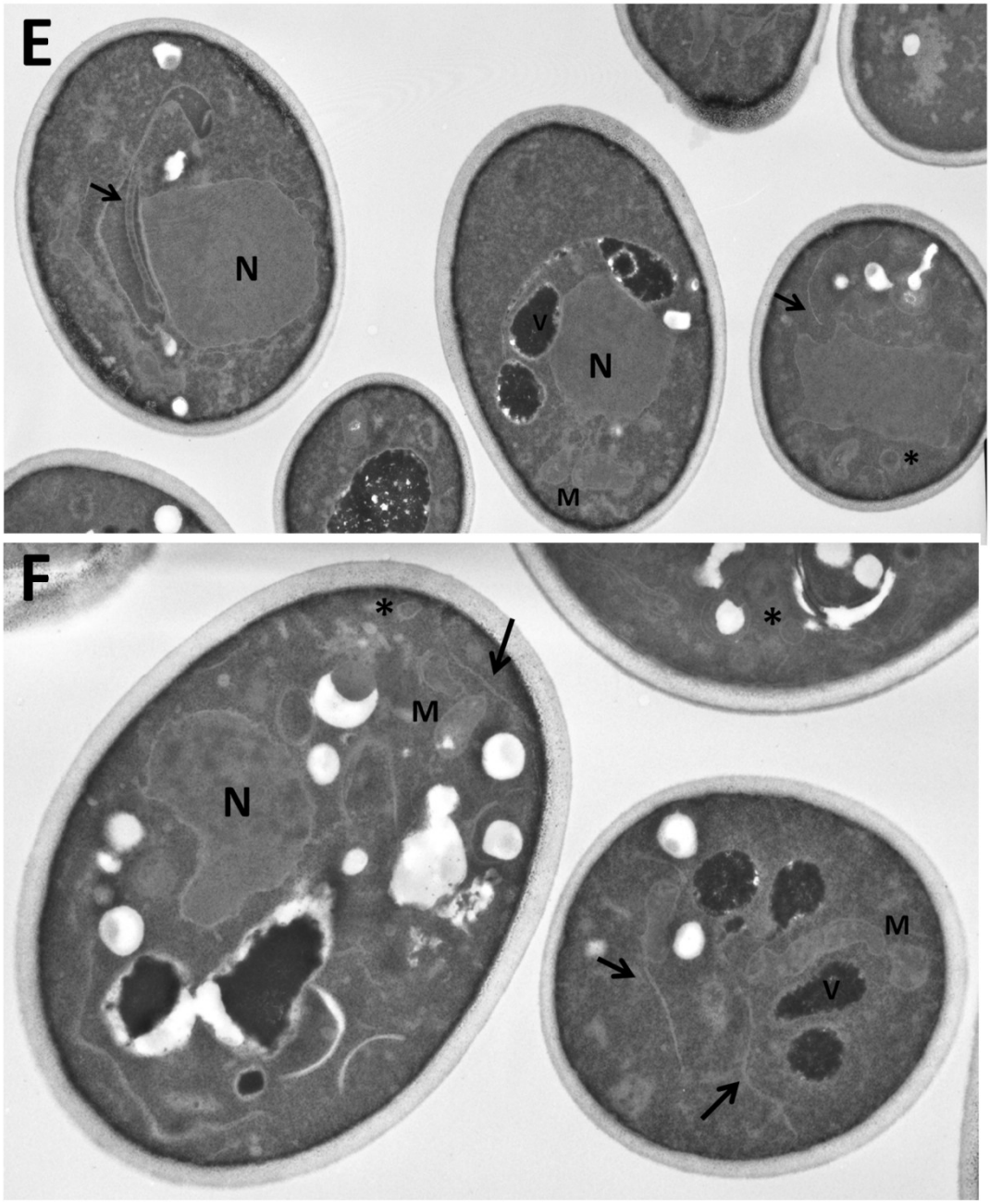

Figure 17- Electron microscopy of mistranslating cells showing expanded ERs and autophagosomes. Additionally, alterations in vacuolar morphology were also detected, namely vacuolar fragmentation. Control cells expressing no tRNA (A, B; **Supp.Figure 2**) and cells expressing the tRNA (C-F) were grown to exponential phase and were prepared for electron microscopy. Osmium staining was used to reveal cellular structures. Arrows indicate expanded ER; N stands for nucleus; M for mitochondrion; V for vacuole. Autophagosomes are marked with an *.Additional images are shown in **Supp.Figure 2** and **Supp.Figure 3** . A – 4x zoom; B – 31 000x amplification; C- 2x zoom; D, E and F- 4x zoom.

Stationary phase control cells contained a large vacuole and peripherical mitochondria, with some cristae (Figure 18, A, B and C), the cytoplasm of mistranslating cells contained

many membranar structures, and vacuoles contained highly heterogeneous content. Very few mitochondria were observed and those that could be observed showed abnormal morphologies (Figure 18, I).

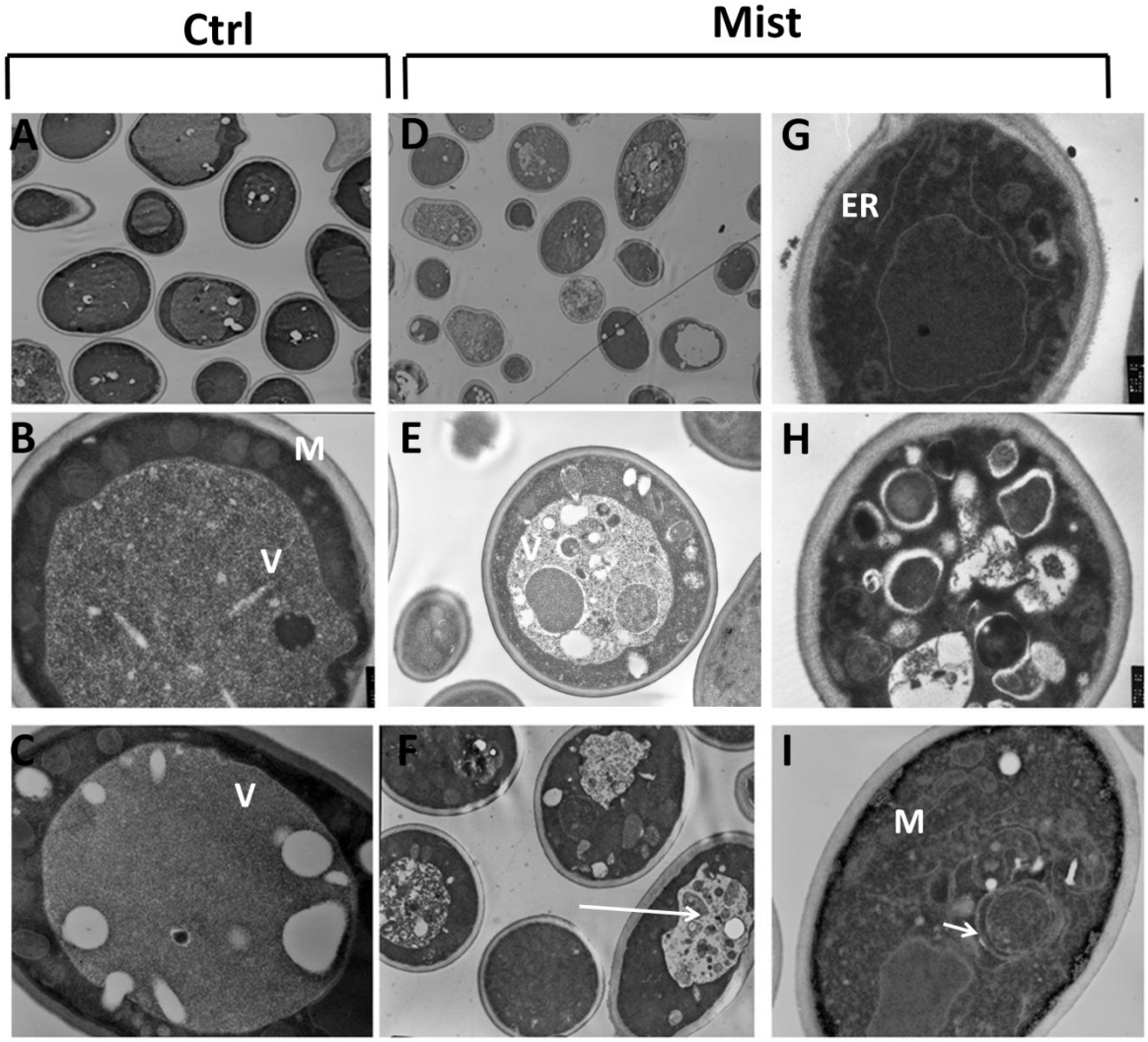

Figure 18 - Electron microscopy of stationary phase mistranslating cells on stationary phase. Alterations in vacuolar morphology, namely vacuolar fragmentation and absence of the typical peripherical mitochondrial distribution were observed. Control (A, B and C) or mistranslating cells (D to I) were grown to stationary phase and were prepared for electron microscopy. Osmium staining was used to reveal cellular structures. ER-stands for endoplasmatic reticulum; N stands for nucleus; M for mitochondrion; V for vacuole. Arrows indicate membranar structures and autophagic bodies inside the vacuoles. A and D images were acquired using 4400x amplification; B, F and G correspond to a 31 000x amplification; C, H and I to a 21 000x amplification and E to 7100x.

Mistranslation leads to ubiquitin accumulation in the vacuoles

In mammalian cells, mistranslation leads to accumulation of ubiquitinated protein aggregates in the cytoplasm (Lee et al., 2006). Therefore, we expected that similar protein ubiquitination could be detected in mistranslating yeast cells. To confirm this hypothesis, cells were analyzed by immuno-electron microscopy (Figure 19 A and 19 B, Supp.Figure 4) and by western blot (Figure 19, C). No significant differences in the content of ubiquitinated proteins were observed in the cytoplasm of control and mistranslating cells. However, immuno-TEM showed that the ubiquitin signal accumulated mainly in the vacuoles of mistranslating cells (Figure 19 A and 19B), supporting the hypothesis that autophagy, rather than the UPS, was the main degradation pathway of mistranslating cells. This is in line with recent studies which showed specific autophagic degradation of polyubiquitinated protein aggregates during neurodegenerative disease. In other words, it is likely that the mistranslated proteins that misfolded but did not aggregate were rapidly degraded by the proteasome, while mistranslated protein aggregates were polyubiquitinated and targeted to autophagy. In addition, western blot showed that indeed mistranslating cells did not seem to accumulate more ubiquitin than control cells (Figure 19,C) and that mistranslation increased ubiquitination in rpn4Δ strain (which has lower proteasome activity) (London et al., 2004) as well as in pnc1Δ strain (also with lower proteasome activity, see Figure 16). Surprisingly, *SIR2* deletion *per se* seemed to increase protein ubiquitination, which could be related to the lower proteasome activity previously detected (Figure 16), but mistranslation did not increased ubiquitin accumulation any further. Unexpectedly the mistranslating atg5Δ strain which has

impaired autophagy did not accumulate polyubiquitylated proteins suggesting that most of the mistranslated ubiquitinated proteins are degraded by the proteasome and not by autophagy. It is also possible that the specific fraction of polyubiquitinated proteins that accumulated in the vacuole of mistranslating cells was lost during the protein extraction procedure.

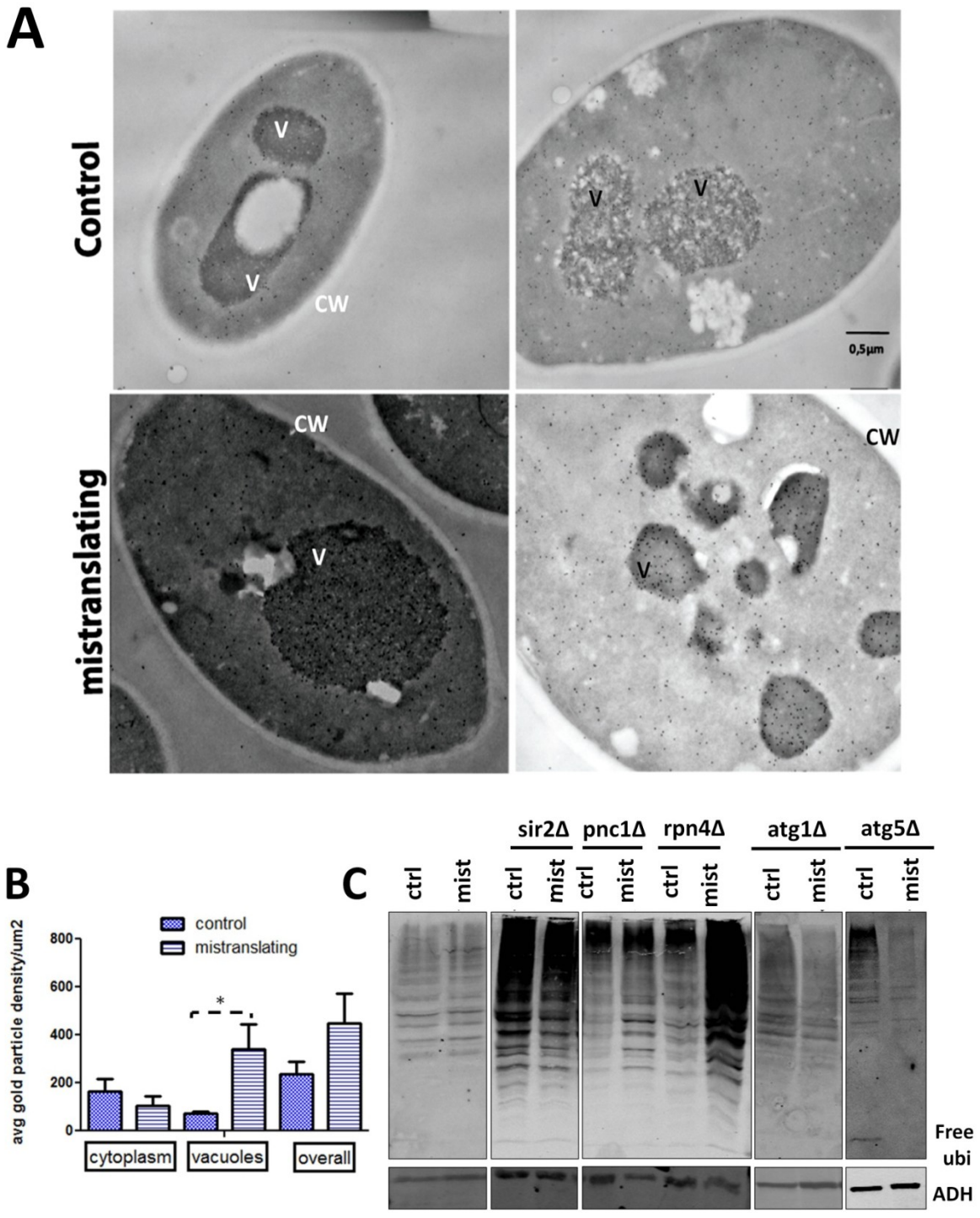

Figure 19- Protein ubiquitination in mistranslating cells A) Exponentially growing cells were analysed by immuno-TEM using ultrathin sections mounted on grids. Immuno-gold labeling was performed as described in methods. The primary antibody was a mouse anti-ubiquitin antibody diluted 1:100. The secondary antibody was a goat-anti-mouse antibody coupled to 10 nm gold

particles. The ubiquitin signal was detected both on control and mistranslating cells. V-vacuole; CW-cell wall. **B)** Histogram showing the number of immuno-gold beads in the indicated cellular compartments **C)** Anti-ubiquitin western blot analysis using 50 µg of total protein extracts prepared from exponentially growing cells which were fractioned by SDS-PAGE and incubated with an anti-ubiquitin rabbit polyclonal antibody. Signals were detected using an Odyssey scanner. Representative images of at least 3 independent experiments with similar outcome are shown. Additional images of mistranslating cells are shown in supplementary data (**Supp.Figure 4**)

Mistranslation induces autophagy

TEM and immuno-TEM data suggested that autophagy was likely up-regulated in mistranslating cells. In order confirm this hypothesis we have used a GFP-ATG8 chimeric gene as an autophagy marker. This reporter allows for detection of a dot-like organelle known as the phagophore assembly site or pre-autophagosomal structure (PAS). In yeast cells, a number of Atg proteins co-localize with the PAS which apparently functions as an assembly site from which nascent phagophores emanate in the form of membrane vesicles or cisternae equipped with autophagy-specific proteins and protein conjugates (Suzuki and Ohsumi, 2010). The PAS is easily detected using fluorescence microscopy as a perivacuolar dot (Meiling-Wesse et al., 2004). Cells were co-transformed with a plasmid encoding GFP-Atg8 (pRS316GFP-AUT7; *AUT7* is an alternative name for *ATG8*) and pRS315 (control plasmid) or pUCK715/pUKC716 (mistranslating tRNA). Cells were then grown in SMD medium until mid-log phase and were observed by epifluorescence microscopy (Figure 20 A, supp. Figure 5). Control cells grown under standard minimal media showed lower fluorescence levels than the mistranslating cells indicating up-regulation of autophagy in the latter. PAS were detected in 20% of the control cells and residual vacuolar fluorescence (≈2.5% of cells) was also observed while 30% of mistranslating cells

showed PAS and 8% had vacuolar fluorescence (Figure 20,Supp.Figure 5). Both phenotypes were, however, weaker when compared to cells grown under starvation conditions, where an almost complete shift of the GFP-Atg8 signal from the PAS to the vacuolar lumen was observed (Supp.Figure 5). In other words, up-regulation of autophagy in mistranslating cells is smaller than in starved cells.

Since an N-terminal GFP-Atg8 chimeric reporter allows for detection of intralysosomal degradation of Atg8p, due to GFP accumulation in the vacuolar lumen (Ma et al., 2007; Shintani and Klionsky, 2004; Suzuki and Ohsumi, 2007; Suzuki et al., 2007; Klionsky et al., 2007) we have tested whether mistranslation could induce GFP accumulation in the vacuole, an indication of autophagy induction. Free GFP was not detected in control cells unless they were starved (Figure 20), whereas mistranslating cells showed a small amount of free GFP under both standard growth conditions and starvation. The amount of free GFP was higher in cells that mistranslated at higher levels (2.3%) than in cells mistranslating at lower levels (1.4%). When cells were subjected to starvation the presence of free GFP in the vacuole was clear, showing that mistranslation works synergistically with starvation conditions in the up-regulation of autophagy.

The above data prompted us to further test induction autophagy by analyzing Atg8p lipidation. In order to attach to the phagophore membrane the Atg8 protein is proteolitically processed and is conjugated to PE by Atg7p (which is a E1-like activating enzyme) and Atg3p (which is an E2-like conjugating enzyme) (Tanida, Mizushima et al. 1999; Ichimura, Kirisako et al. 2000; Tanida, Tanida-Miyake et al. 2001; Tanida, Tanida

Miyake et al. 2002). The process is facilitated by a multimeric complex that may function as an E3-like enzyme and is composed of three proteins, Atg12p, Atg5p and Atg16p (Suzuki, Kirisako et al. 2001; Hanada, Noda et al. 2007). Since Atg8–PE can be resolved from Atg8p alone using SDS-PAGE gels containing urea we have used this method to confirm induction of autophagy (Kirisako, Ichimura et al. 2000). In this assay pep4Δ cells were used as controls since they are defective in intravacuolar vesicle breakdown leading to the accumulation of higher levels of Atg8-PE (Klionsky et al., 2007). As before, cells transformed with the mistranslation-inducing plasmids were allowed to grow to exponential phase and were subjected to immunoblot analysis. Surprisingly, under our growth conditions, we were unable to detect the increased Atg8-PE in cells mistranslating at low levels (1.4%) and trace amounts of Atg8-PE were detected in cells that mistranslated at 2.3% (Figure 20, D). However, starvation induced a considerable accumulation of both unconjugated and conjugated forms of Atg8 in mistranslating cells (Figure 20, C). Again, this accumulation was stronger in cells that mistranslated at high level. Additional microscopy experiments using mistranslation inducing drugs, like l-azetidine-carboxylic acid (AZC) also support the mistranslation-induced autophagy phenotype (Supp.Figure 6). We have also determined Pho8Δ60 activity which measures bulk autophagy, but we were not able to detect increased activity in mistranslating cells (data not shown). Pho8p is a vacuolar alkaline phosphatase which is delivered to the vacuole by the secretory pathway using the N-terminal transmembrane domain. The Pho8Δ60 mutant lacks the N-terminal and accumulates in the cytosol. Autophagy is the only form of delivering this protein to the vacuole, where it is converted to its mature form, allowing enzymatic determination of its activity (Klionsky et al., 2007). Therefore,

the lack of up-regulation of Pho8Δ60 activity suggests that this enzyme is not delivered to the vacuole, which contradicts our previous result showing accumulation of free GFP in the vacuole of mistranslating cells.

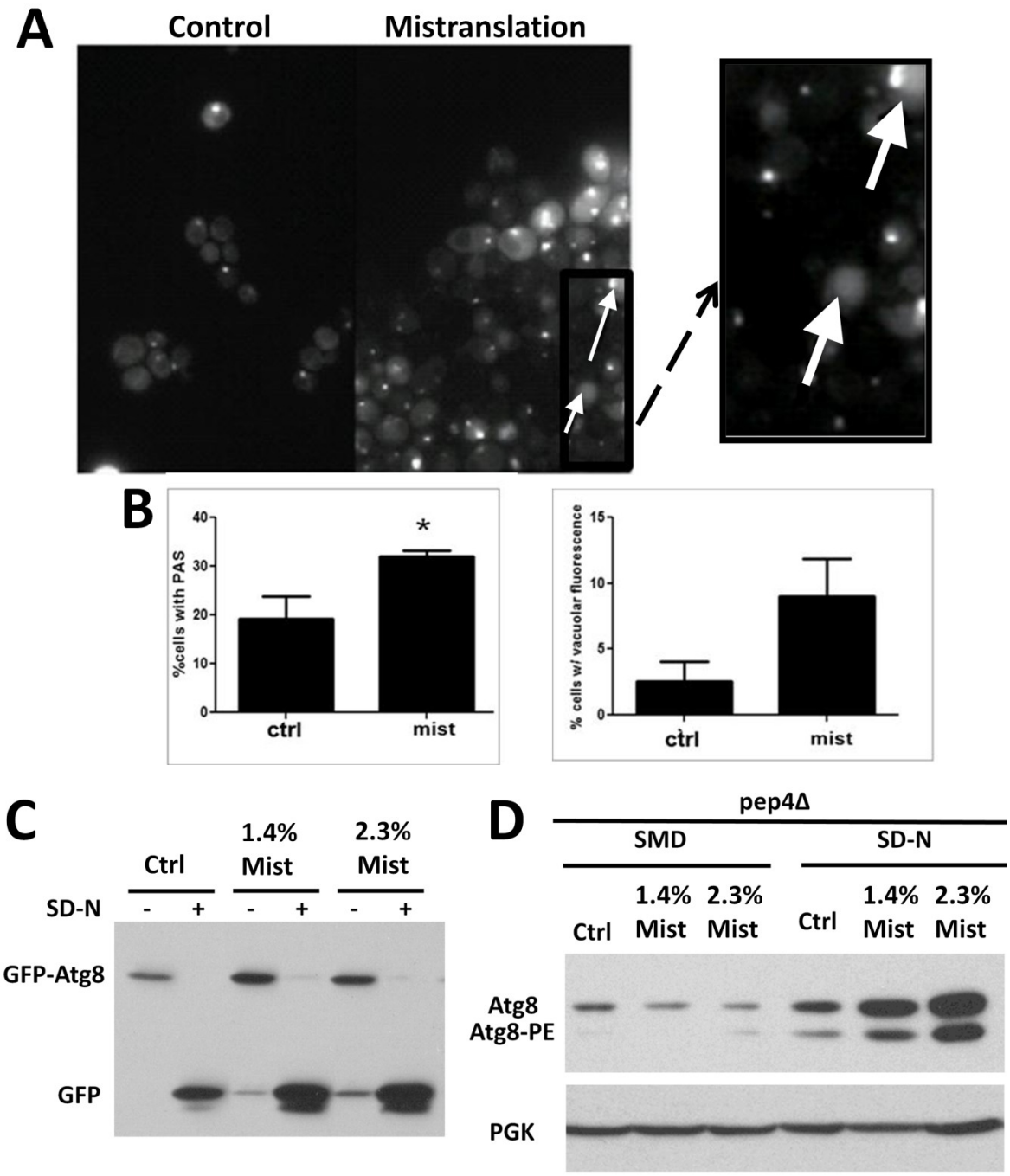

Figure 20- mRNA mistranslation induces autophagy A) The localization of GFP-Atg8 fusion protein was examined by fluorescence microscopy. Cells co-expressing the mutant misreading tRNA and GFP-Atg8 harboring plasmids were grown to mid log phase in SMD selective medium and were analyzed by epifluorescence. The right panel shows a detail of the left panel image. Arrows indicate PAS and vacuolar fluorescence. **B)** The number of cells with fluorescence signals on the PAS and cells that presented vacuolar fluorescence were determined. Left panel shows the quantification of cells with PAS while the histogram on the right shows the quantification of cells with vacuolar fluorescence. A clear increase in both parameters was detected, indicating that

mistranslation induces autophagy. The average of at least two independent experiments is shown and 150 cells for each strain and experiment were monitored. Error bars represent the standard error of the mean and * represents the significant results with $p<0.05$ for a student's two-tailed t-test **C)** Mistranslation induces GFP release in the vacuole**.** GFP-Atg8 processing was monitored by western blot analysis. Cells were co-transformed with both the mistranslating tRNA harboring plasmid and the GFP-Atg8 plasmid. As expected, free GFP was detected mistranslating cells **D)** mRNA mistranslation activates Atg8-PE formation. Mutant cells, defective in vacuolar degradation - pep4Δ, were transformed with the mistranslating tRNA gene harboring plasmids. Atg8–PE and Atg8p forms were resolved using 12% SDS PAGE in the presence of 6% Urea. Atg8-PE formation was not detected in cells that mistranslated at 1.4% and was hardly detected in cells mistranslating at 2.3%. However, when cells were subjected to starvation conditions clear differences could be detected between control and mistranslating cells. In both assays, cells were grown to early mid log phase in SMD medium or starved for 3 h in SD-N. Cells were collected, protein extracts were prepared and free GFP and Atg8 conjugated were detected using anti-GFP antibody or anti-Atg8 antiserum. Ctrl- control cells transformed with an empty plasmid.

Regulation of autophagy in mistranslating cells

We have previously shown that mistranslation strongly induces the expression of the *PNC1* longevity gene which is a regulator of the Sir2 deacetylase (Silva et al., 2009). A more recent study showed that the mammalian homolog of Sir2 (Sirt1) regulates autophagy in mice (Lee et al., 2008) by preventing acetylation of proteins required for autophagy in cultured cells and in embryonic and neonatal tissues. Knockdown of *SIRT1* expression blocks autophagy in these cells. These observations prompted us to determine whether Pnc1p and Sir2p could also regulate autophagy in mistranslating yeast cells. For this, we have induced mistranslation in cells harboring deletions in *PNC1* or *SIR2* genes and quantified autophagy using GFP-Atg8 punctua formation and GFP appearance in vacuoles. No accumulation of PAS or GFP fluorescence were detected in the vacuoles of the mutant mistranslating cells (Figure 21,A-C),suggesting that both Pnc1p and Sir2p are

required for induction of autophagy by mistranslation. Furthermore, the observed difference between control mistranslating cells and knockout mistranslating cells suggested that both Pnc1p and Sir2p are required for full induction of the PAS. Western blot analysis confirmed the microscopy observations as the GFP-Atg8 concentrations did not change and free GFP was not detected (Figure 21, D).

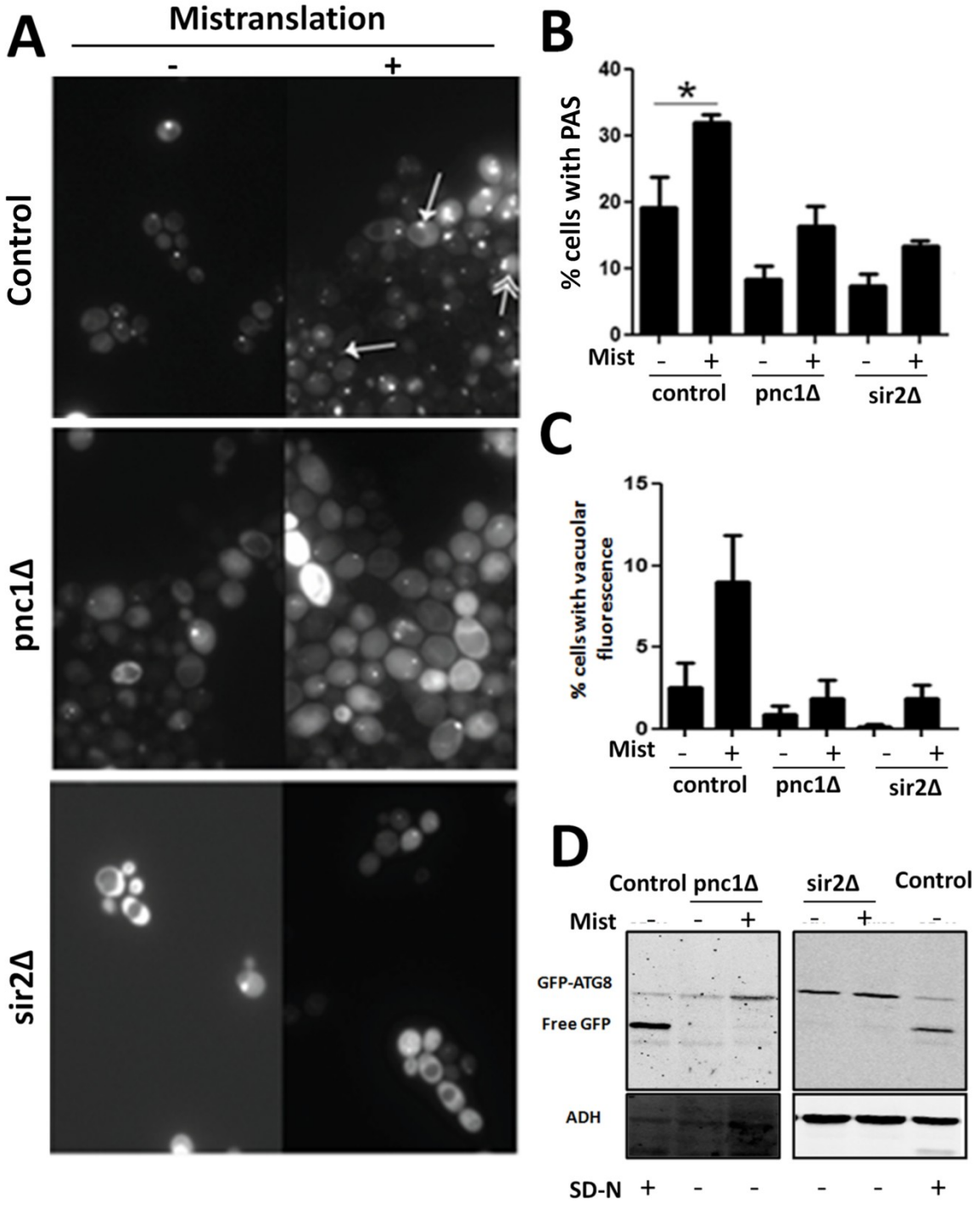

Figure 21 - *PNC1* and *SIR2* regulate autophagy in mistranslating yeast cells A) The localization of the GFP-Atg8 fusion protein was assessed by fluorescence microscopy. Mutant cells harboring deletions in the *PNC1* or *SIR2* genes were transformed with the mistranslating tRNA gene or with an empty vector and a vector containing the GFP-Atg8 chimeric gene. Cells were grown to mid log phase in SMD selective medium and were then analyzed by epifluorescence microscopy. Single headed arrows show PAS while double headed arrows show vacuolar

fluorescence. **B and C) Quantification** of PAS and vacuolar fluorescence**.** Cells with fluorescence signals on the PAS and in the vacuole were counted and the result was plotted in the histograms shown. Deletions of either gene lead to decrease in PAS or vacuolar fluorescence. The average of at least two independent experiments is shown and 150 cells for each strain and experiment were monitored. Error bars represent the standard error of the mean and * represents the significant results with $p<0.05$ for a student's two-tailed t-test D**)** Deletion of Pnc1 or Sir2 blocked GFP release in the vacuole. GFP-Atg8 processing was monitored by western blot analysis using an anti-GFP antibody. Cells were co-transformed with both the tRNA and the GFP-Atg8 plasmids. Free GFP was not detected in the pnc1Δ or sir2Δ strains**. "**Mist"- mistranslation; SD-N- starvation conditions.

DNA microarray data supported induction of autophagy in the control strains. Indeed, several ATG genes were significantly up-regulated in all strains tested, namely *ATG1* and *ATG8*. The expression of these genes was further confirmed by RT-PCR (Figure 22) and a good correlation was obtained between the two data sets. For wild-type strains a 2-3 fold up-regulation of the expression of both genes was detected. However, under starvation conditions, these two genes were up regulated by 6.5-fold and 20-fold respectively (data not shown). The qRT-PCR experiment showed stronger up-regulation of both *ATG1* and *ATG8* in the pnc1Δ background than in the other backgrounds. Sir2Δ mistranslating cells showed a small increase in the expression of *ATG1* and no increase *ATG8* expression of ATG8. Therefore, mistranslation up-regulates poorly autophagy compared to starvation and these results may also suggest that deletion of *PNC1* or *SIR2* abrogates the autophagic step at a yet unidentified step.

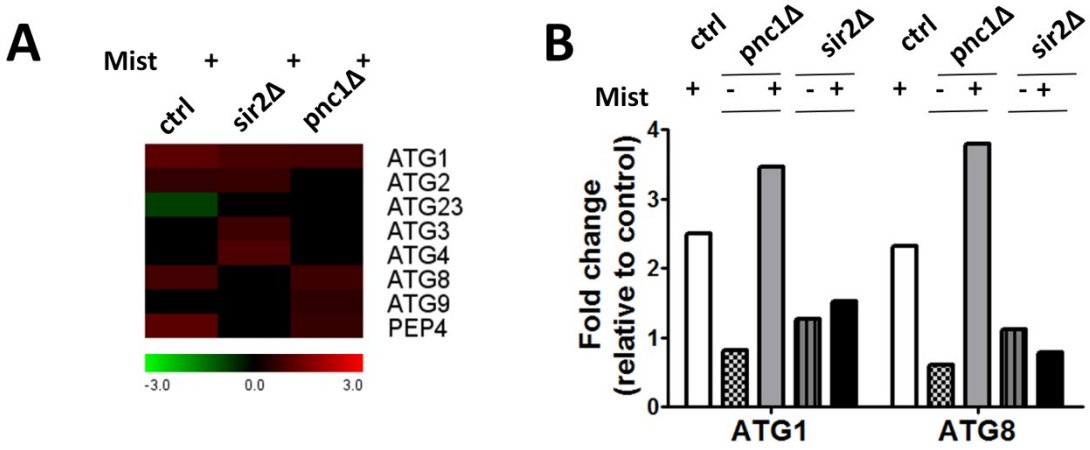

Figure 22- Mistranslation deregulates expression of ATG1 and ATG8. **A)** Partial mRNA profile highlighting expression patterns of ATG genes. Up-regulation of several ATG genes was observed in different mistranslating strains. Each expression data set was analyzed using 1-class SAM analysis as described in methods. **B)** qRT-PCR confirmation of microarray data. The levels of expression of *ATG1* and *ATG8* were quantified using real-time quantitative PCR. The expression values were normalized using the alcohol dehydrogenase (ADH) gene and were compared to the fold change values obtained in the microarray experiment. Each RT-PCR measurement was performed at least twice using independent samples.

The *PNC1* and *SIR2* genes do not regulated autophagy under starvation

Since the roles of the *PNC1* and *SIR2* genes in yeast autophagy are unknown, we also analyzed autophagy induction in the knockout strains grown under starvation conditions. For this cells in mid-exponential phase expressing GFP–Atg8 chimera and the misreading tRNA were starved in SD (−N) media and autophagy was monitored by epifuorescence microscopy or immunoblotting. Nitrogen deprivation for 3 h led to a strong induction of autophagy in all strains, as PAS and free vacuolar GFP were strongly detected (Figure 23 A-C; Supp.Figure 7; Supp.Figure 8). We have also used Ald6p (cytosolic acetaldehyde dehydrogenase) degradation to monitor autophagy under starvation conditions since this

protein is specifically targeted to the vacuole by autophagosomes under starvation conditions (Onodera and Ohsumi, 2004; Cebollero and Gonzalez, 2006). In all the tested strains a sharp decrease in the amount of Ald6p was observed under starvation (Figure 23 D), suggesting that, conversely to what was observed in mammalian cells and in mistranslating yeast cells the *PNC1* and *SIR2* genes are not needed for starvation induced autophagy.

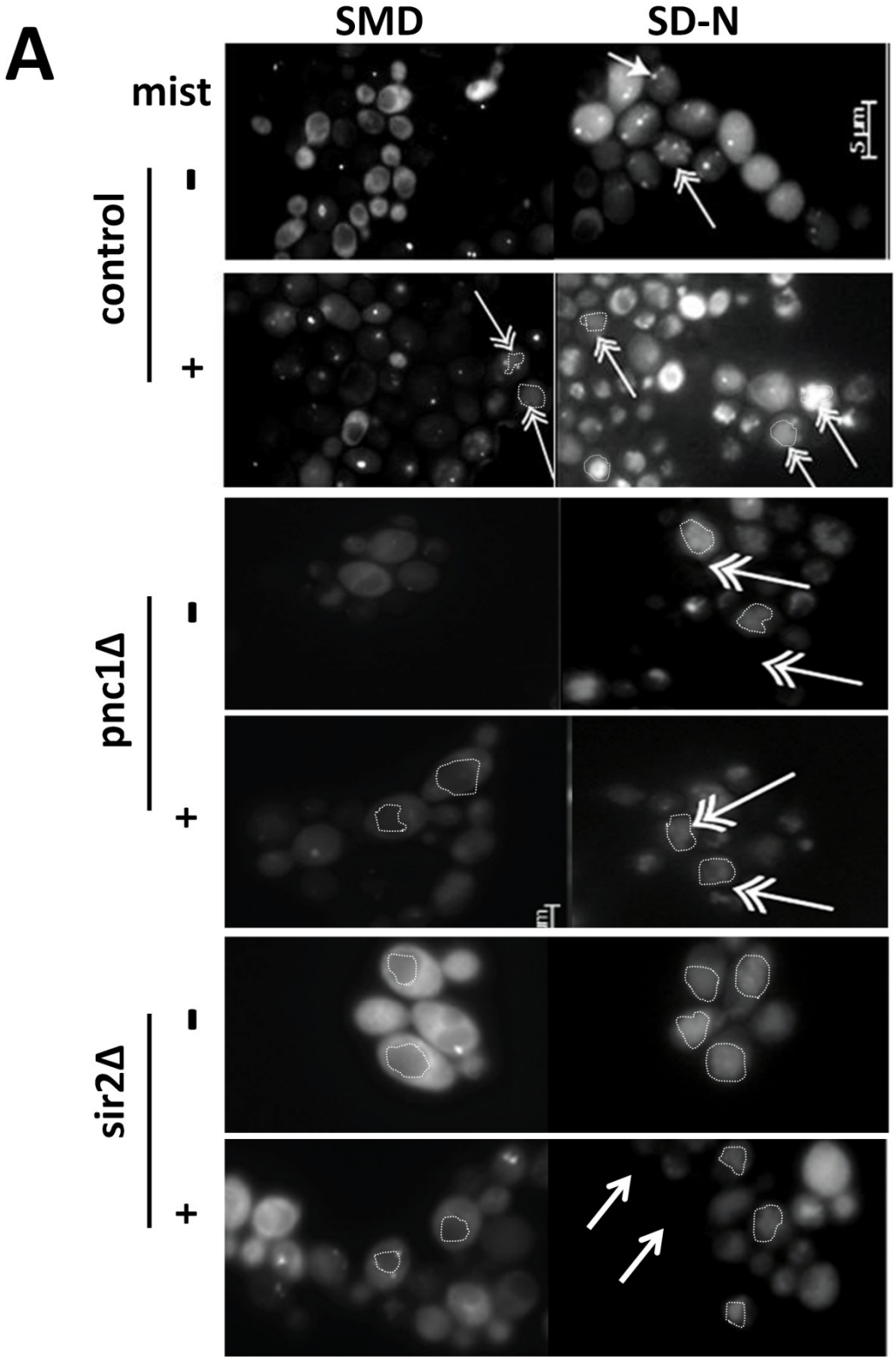
A
SMD
SD-N
mist
control
-
+
pnc1Δ
-
+
sir2Δ
-
+

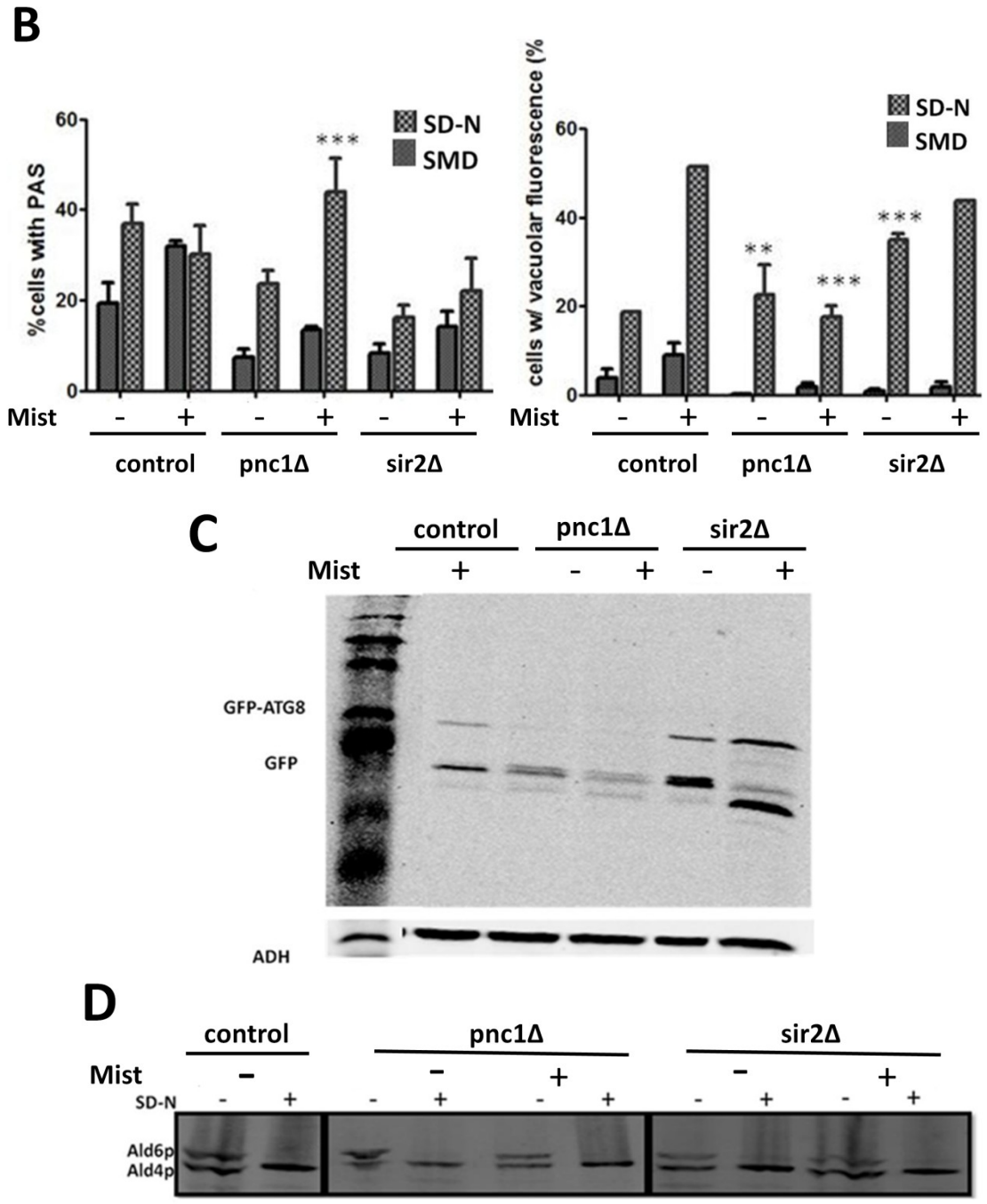

Figure 23- *Sir2* and *Pnc1* are not required for starvation induced autophagy A) Wild-type and knockout strains that mistranslate constitutively were observed by epifluorescence microscopy. Representative images are shown. Vacuoles are delimitated with dashed lines. It is clear that in non starved cells, vacuoles are well distinguished and darker than the rest of the cell, while under starvation conditions the dark vacuoles disappear to give place to fluorescence accumulation. **B)** Quantification of PAS and vacuolar fluorescence. Cells with PAS puncta and free GFP in the

vacuole were quantified for GFP-Atg8 either in growing conditions or after shifting to SD-N for 3 h. Approximately 150–250 cells of each strain were analyzed. Experiments were repeated at least twice, except where no error bar (SEM) is shown.* shows the statistical significance of the data using a student's unpaired two tailed t-test. **C)** GFP-Atg8 processing. Cell extracts of cells grown under starvation conditions were subjected to SDS–PAGE electrophoresis followed by immunoblot analysis using anti-GFP antibodies **D)** Ald6p degradation. Western blot analysis of protein extracts from wild-type or mutant mistranslating strains grown in SD-N or SMD at 30°C. Membranes were probed with a rabbit monoclonal anti-acetaldehyde dehydrogenase antibody. In all strains a strong decrease in Ald6p was observed.

Discussion

To date, very little effort has been devoted to understand the biology of mistranslation. The commonly accepted view is that it is a nuisance to the cell with little or no biological relevance. However, our data show that low levels of mistranslation, which are compatible with life, increase protein aggregation, lead to vacuolar ubiquitin accumulation up-regulate autophagy, likely through the *PNC1* and *SIR2* genes.

Protein aggregation induced by mistranslation supports our microarray data showing that mistranslation up regulates *HSP104* and other molecular chaperones (supp table 1; Silva, 2005) and increases proteasome activity (this study; Silva RM et al., 2007). Surprisingly, strains with impaired autophagy (atg5Δ) and diminished proteasome activity (rpn4Δ) did not show higher levels of insoluble proteins than the wild-type mistranslating cells. Our data does not clarify this puzzling result. However, a likely explanation is that inactivation of one of these proteome quality control systems up-regulates the others allowing cells to remove aberrant proteins. The effect of mistranslation on protein aggregation was

however more evident in the *SIR2* deleted mistranslating strain, suggesting a critical role of this gene in the cellular response to mistranslation. Previous studies show that cells lacking Sir2p also have reduced PQC mainly due to increased carbonylation of chaperones. This results in defective growth recovery after stress conditions that cause protein aggregation and also on retarded rate of aggregates break down. Therefore, in the sir2Δ background, although the expression of *HSP104* was up-regulated (Supp.Table 1), its activity and the activity of other chaperones may be strongly impaired. In this context, it would be interesting to evaluate the carbonylation levels of Hsp104p in mistranslating cells. Additionally, our data also indicate that sir2Δ mistranslating cells fail to up-regulate autophagy and have lower proteasome activity, which should also contribute to the accumulation of insoluble proteins. The lower proteasome activity of this mistranslating mutant is interesting as it suggests that these mistranslating cells are subjected to a higher oxidative stress than the wild-type mistranslating cells.

The vacuolar accumulation of ubiquitin in mistranslating cells provides evidence for increased autophagic activity and suggests that mistranslation overloads the ubiquitin-proteasome and the ERAD systems. Autophagy may work as a backup system to clear aggregated proteins. Alternatively, mistranslation may cause significant damage to mitochondria and other organelles and autophagy may be mainly up-regulated to eliminate such dysfunctional organelles.

Our data does not elucidate why mistranslating cells impaired in autophagy failed to accumulate ubiquitinated proteins (at least in the cytoplasm), which would indicate an

increase in protein aggregation, or why such cells did not have significantly increased proteasome activity (this work). Yet, a possible justification may reside in the molecular structure of the aggregates.

Recent studies show that protein aggregates localize in two different quality control compartments, depending on whether they can be recovered to the soluble form or terminally aggregated. The former accumulate in a juxta nuclear compartment (JUNQ), where there is a high number of proteasomes, while the latter accumulate in a perivacuolar compartment (IPOD) (Kaganovich et al., 2008). It has been suggested that spatial sequestration of the aggregates may facilitate their clearance either by autophagy or by dilution through retention in the mother cell. It is tempting to speculate that the accumulation of ubiquitins in the vacuoles of mistranslating cells is a consequence of the passage of aggregated proteins from IPOD to the vacuole for degradation, which would be in line with the idea that autophagy recycles aggregated proteins. This is an attractive hypothesis since *ATG8* and the PAS co-localize at the IPOD (Kaganovich et al., 2008). However, this is not consistent with the hypothesis that ubiquitination is necessary to maintain the solubility of misfolded proteins and their consequent sequestration to JUNQ and that only non-ubiquitinated proteins are sorted to IPODs (Kaganovich et al., 2008). Therefore, it would be interesting to carry out co-localization studies to determine whether mistranslated proteins co-localize to IPODs or JUNQs. This could be done using a fluorescent protein encoded by a gene with high CUG content or using GFP-HSP104 reporter genes, which would co-localize at the IPODs. In addition, GFP-tagged

proteasome could be used to verify whether or not these co-localize with ubiquitin rich regions, which could correspond to JUNQ.

Our data provides strong evidence for a pivotal role of Sir2p in the cellular response to mistranslation. Indeed, strong accumulation of protein aggregates was observed in the sir2Δ strain, likely due to lower proteasome activity and impaired autophagy. The longevity gene *PNC1* may also play an important role in the cellular response to mistranslation. A recent study showed that Pnc1p interacts physically with the proteasome subunits Rpn10p (a receptor of ubi-substrates) and Rpn11p (which recognizes the same substrates) (Guerrero et al., 2008). Therefore, it is possible that in the absence of Pnc1p these interactions are disrupted and ubi-substrates cannot be received by the proteasome for recycling. This could explain the strong up-regulation of the expression of *PNC1* by mistranslation (Silva, 2005; Silva et al., 2009) as the latter generates aberrant proteins which should be targeted to the proteasome. It remains unclear why proteasome activity did not increase in the sir2Δ strain. Recent studies show that the mouse homologue of Sir2p (Sir2α) is involved in ubi-proteasome dependent degradation of a specific histone variant (H2A.z) in cardiac myocytes (Chen et al., 2006), establishing a putative link between Sir2p, Pnc1p and the proteasome. Additionally, Sir2p also interacts with Slx5p, which works in complex with Slx8p promoting ubiquitination of sumoylated proteins for degradation by the proteasome. Although this interaction as been linked to transcriptional silencing, it is possible that it also affects proteasome activity (Darst et al., 2008). As Pnc1p regulates Sir2p it is also possible that an unknown SIR2-dependent pathway regulates the proteasome or that proteasome is inhibited by

the accumulation of toxic aggregates that clog the proteasome or inhibit it by other mechanisms, similarly to what happens in vertebrate models. Indeed, aggregated α-synuclein inhibits proteasomal activity strongly (Snyder et al., 2003; Snyder et al., 2005; Bennett et al., 2007). However, in this case, a sharp increase in protein aggregation should have been observed, which was not the case.

In any case, this study indicates that autophagy contributes to the cellular response to mistranslation, probably by clearing ubiquitinated protein aggregates, which is in line with previous work that highlight the role of this pathway in aggregate protein processing (Yao, 2010). Our study also shows that deletion of *PNC1* or *SIR2* genes decreased the basal level of autophagy, but the latter was restored by mistranslation, despite the fact that autophagosome fusion/degradation was not detected. These observations may indicate that pnc1Δ and sir2Δ are less sensitive to mistranslation and, therefore, no autophagy induction occurs. It may also imply that these genes are regulating some autophagy steps downstream PAS assembly or that, in a similar way to what happens in cells where UPR is induced by DTT or tunicamycin, no cleavage of the GFP-Atg8 chimera occurs (Bernales et al., 2006).

The other important cellular phenotypes induced by mistranslation were ER expansion and vesicle morphology alterations. These alterations reflect ER stress due to accumulation of aggregated proteins and possible induction of the UPR. The latter is strongly associated to ER expansion and proliferation (Bernales et al., 2006) and its main function is apparently to dilute unfolded proteins and minimize their aggregation.

Additionally, these morphological alterations also support the induction of autophagy, as the latter is strongly linked to the UPR, both in yeast (Bernales et al., 2006; Yorimitsu et al., 2006) and in mammalian cells (Ogata et al., 2006). Indeed, ER-stress caused by accumulation of misfolded proteins and the activation of UPR both stimulate the assembly of PAS and, consequently, induced autophagy.

In conclusion, our results envisage possible roles for IPOD and JUNQ in the cellular response to mistranslation. The former may reduce protein aggregation toxicity by condensing proteins that cannot be recovered while the latter contains ubiquitinated proteins and works as a recycling system for partially aggregated proteins. It also unveils a link between *SIR2*, *PNC1* autophagy and proteasome activity. In any case, mistranslation leads to proteotoxic stress, which is characterized by ER-stress and concomitant activation of UPR/ERAD and culminates in autophagy activation. This cascade of events allows cells to cope with proteotoxic stress.

Material and Methods

Yeast Strains and plasmids

Yeast strains and plasmids used in this study are listed in Table 1 and Table 2. Strains were transformed with the plasmids pRS315 (Control), pUKC715 or pUKC 716 (Santos et al., 1996b) according to Gietz (Gietz, 2002; Gietz and Schiestl, 2007b; Gietz and Schiestl, 2007a) with minor modifications. For the autophagy experiments cells were further co-

transformed with pRS316-GFP-AUT7 (Table 2) to visualize the localization of Atg8p and to measure GFP–Atg8 degradation (see below). Standard methods for yeast manipulation were used. Cells were grown in SMD-leu or SMD-leu-ura (0.67% yeast nitrogen base, 2% glucose or 2% galactose, 0.2% drop-out mix containing all amino acids except leucine or leucine and uracyl). For starvation experiments, cells were grown in SMD until early exponential phase (OD_{595} 0.3-0.5), washed once in SD-N (0.17% yeast nitrogen base without amino acids, 2% glucose) and then ressuspended in SD-N for 3-6 h.

Table 1- Strains used in this study

Strain	Genotype	Source	Description	Study
sUA4	Mat a/ α Trp1-289/trp1-289,leu2-13,/112/leu2-13,112,KanMX in LEU2	our laboratory	CEN.PK2 background;control strain	Electron Microscopy
sUA6	Mat a/ α Trp1-289/trp1-289,leu2-13,/112/leu2-13,112,KanMX+tRNA$^{ser}_{cag}T_{33}$ in LEU2	our laboratory	CEN.PK2 background;tRNA integrated in LEU2 locus	Electron Microscopy
CENPK2	*MAT a /α, ura3-52 / ura3-52, trp1-289 / trp1-289, leu2-3, 112 / leu2-3, 112, his31 / his31*	Euroscarf	Wild type strain	Electron Microscopy
BY4743	*MAT a /α,*	Euroscarf	Wild type strain	Autophagy analysis
rpn4Δ	BY4742; Mat a; his3D1; leu2D0; lys2D0; ura3D0; YDL020c::kanMX4	Euroscarf	BY4743 deleted for the rpn4 gene	aggregation studies
atg5Δ	BY4742; Mat a; his3D1; leu2D0; lys2D0; ura3D0; YPL149w::kanMX4	Euroscarf	BY4742 deleted for the atg5 gene	aggregation studies

Table 2- Plasmids used in this study

Plasmid	Description	Source
pRS315	Empty plasmid	our laboratory
pUKC715	**Low mistranslation**. Plasmid based on the single copy vector pRS315 .Contains the *Candida albicans* Ser-tRNA$_{CAG}$ G33 (Santos et al, 1996)	our laboratory
pUKC716	**High mistranslation.** Plasmid based on the single copy vector pRS315 contains the *Candida albicans* Ser-tRNA$_{CAG}$ T33 (Santos et al, 1996)	our laboratory
pRS316GFPAUT7	centromeric plasmid carrying a GFP–Atg8 fusion protein under control of the native *ATG*8 promoter	kind gift from Dr Ohsumi laboratory

Protein aggregation determination

Starter cultures were grown overnight in 5 ml SMD, at 30^{o}C and vigorous shaking. The following day, the initial cultures were used to inoculate 30 ml of sterile fresh medium and cells were grown in the same conditions to an OD_{595} of 0.3-0.5 (log phase) . Protein extraction (total and insoluble fractions) was performed as described in Rand and Grant (Rand and Grant;Rand and Grant, 2006b;Holland et al., 2007), with minor modifications .Briefly, equal amount of cells, as determined by the OD's (7.5 OD_{595} units) were harvested at 4000 rpm, RT, for 5 minutes and the pellet was kept overnight at -80^{o}C. Cells were ressuspended in 300µl of lysis buffer (PBS pH7 50 mM, EDTA 1 mM. Glycerol 5% v/v, PMSF 1mM , Protease Inhibitors ROCHE) and further incubated at 30°C for 30 minutes with 7.5 µl of lyticase (20mg/ml) .Cells were disrupted with glass beads using a

pre-cellys device for 3 X 45s at 4ºC. Each beating was followed by 1 minute cooling in ice. Intact cells were removed by centrifugation at 3000xg for 15 minutes (total fraction). The membrane and aggregated proteins were isolated from the supernatant by centrifugation at 15000xg for 20 minutes. The membrane proteins were removed by washing pellets with 320 µl of lysis buffer supplemented with 80 µl of 10% triton-X100, centrifuging at 15000 x g 20 minutes. The supernantant was removed and the final protein extract was ressuspended in 100ul of lysis buffer (aggregated proteins-insoluble fraction).Equal volumes of insoluble extract were resolved by SDS-PAGE. Gels were stained with comassie blue for 30 minutes, destained and digitalized in an Odyssey scanner after 24h (3-4 changes in the destaining solution in between).

Anti β-gal western blots

S.cerevisiae strains were co-transformed with pG1-C1 plasmid (Santos et al., 1996a), and pRS315 (ctrl), pUkc715 (G_{33}) or pUkc716 (T_{33}) (Table 2). Cells were grown to exponential phase in selective medium. Protein extraction was performed as described above (see protein aggregation determination). Proteins were transferred to nitrocellulose membrane (semi-dry transfer system, Biorad), blocked and incubated the primary antibody mix (anti-β-gal 1:5000, anti-ADH 1:1000, 3% low fat milk TBS-T), over night at 4^{o}C. Membranes were further incubated with the secondary antibodies mix (1:10000 anti-rabbit, IRDye680, Ly-cor Biosciences) during 3h. Blots were visualized in Odyssey and quantified using Odyssey software (default settings).

Transmission Electron Microscopy

Cells were grown to an OD_{595} of 0.3-0.5 (log phase). TEM samples were then prepared using a modified procedure of the Wright's protocol (Wright, 2000). Briefly, 5 ml of exponentially growing cells were poured to an equal volume of 2x fixative (0.2M sodium cacodylate pH 6.8; 0.8M sorbitol; 2mM $MgCl_2$; 2mM $CaCl_2$; 4% glutaraldehyde). The mixture was allowed to incubate at RT for 5 minutes and was gently centrifuged at 1500g for 5 minutes. Cells were resuspended in 1x fixative and were incubated overnight at 4^{o}C. At this point cells were kept at 4^{o}C until further use. Fixed cells were washed three times in sodium cacodylate 0.1M pH 7.3 and further incubated in 1% aqueous sodium metaperiodate for 45 minutes RT. Post-fixation in 1% OsO_4/1.5% Ferrocyanide for 1h was then applied to the cells. These were further washed with sodium cacodylate and sodium maleate 0.05M pH6.0 and in-block stained with 2% uranyl acetate overnight. Following this incubation, cells were washed in sodium maleate 0.05M pH6.0 and dehydrated with 25%, 50%, 75%, 95% and 100% ethanol. Cells were washed with propylene oxide, and infiltrated with EPON resin (Mecalab, Canada) for 72h. Ultrathin sections were cut with a diamond knife (Leica) and further stained with 2% uranyl acetate for 7 minutes and lead citrate for 10 minutes. Grids were examined using a Philips 410 electron microscope

Immuno-TEM

Cells were grown to an OD_{600} of 0.3-0.5 (log phase) and 5 ml of cell suspension were poured in an equal volume of 2x fixative (0.2M sodium cacodylate pH 6.8 ; 0.8M sorbitol; 2mM $MgCl_2$; 2mM $CaCl_2$; 4% glutaraldehyde). The mixtures were incubated at RT for 5 minutes and gently centrifuged at 1500 x g for 5 minutes. Cells were then resuspended in

1x fixative and were kept at 4℃ until further use. Fixed cells were washed three times in sodium cacodylate 0.1M pH 7.3 and further incubated in 1% aqueous sodium metaperiodate for 45 minutes at RT. Cells were then washed in sodium cacodylate, dehydrated and impregnated with Lowicryl K4M resin as follows: cells were incubated for 5 minutes at 0℃ in 30% methanol, followed by 5 minutes at the same temperature in 50% methanol and 5 minutes at -20℃ in 70% methanol. A final incubation in 90% methanol at -20℃ was carried out. Cells were transferred to a solution of K4M/methanol 90% (1:1) and incubated at -20℃ for 1h. An additional incubation of 1h was performed in a K4M/methanol 90% (2:1) solution and cells were then transferred to K4M lowicryl. Samples were polymerized for 10 days under UV light. Blocks were sectionated and grids were immunolabelled and stained as follows. Grids were incubated in PBS containing 1% ovalbumine at RT for 5 minutes and were incubated with the diluted antibody (1:100, FK1, Biomol). The incubation was carried out overnight at 4℃ and grids were rinsed with PBS at RT (3 times, 5 minutes each). A final 5 minutes incubation with PBS containing 1% ovalbumin was carried out and grids were passed to the secondary antibody solution (anti-mouse IgM 10nm gold conjugated in PBS 0.02% PEG) for 30 min at RT. Grids were again washed with PBS and double distilled water, stained with uranyl acetate for 10 min and examined in a Philips 410 electron microscope.

Epifluorescence Microscopy

Cells expressing the fluorescent protein-fusion GFP-Atg8 (Klionsky et al., 2007; Kabeya et al., 2000) were grown as described above. Briefly, cells were immobilized in a glass slide using an agarose bed (1% in water) and were observed using an Axiovision imager Z1

microscope (Zeiss). GFP tagged proteins were revealed and photographed with an AxioCam Hrc camera and Axiovision Software. For starvation conditions cells were grown as described elsewhere. Results from at least two independent experiments are expressed as the mean ± SEM, except where otherwise stated. Results were compared using t-test or ANOVA with $P<0.05$ considered statistically significant, as stated elsewhere. 150 cells were analyzed per sample.

Protein Extraction and Western Blotting

Cells harboring the green fluorescent protein gene (GFP) fused to the *ATG8* gene plus the hybrid tRNA or the control plasmid were grown at 30°C until exponential phase (OD_{595} 0.3-0.6) in SMD-leu-ura or SMD-ura (0.67% yeast nitrogen base, 2% glucose , 0.2% drop-out mix containing all amino acids except leucine and uracyl or just uracyl). 7.5 OD units of cells were collected and immediately frozen. For protein extraction, cells were resuspended in 300µl of lysis buffer (PBS pH7 50 mM, EDTA 1 mM, glycerol 5% v/v, PMSF 1mM , 1x Protease Inhibitors (Roche) and were disrupted with glass beads using a Precellys tissue homogenizer (Bertin Technologies) for 3 X 45'' at 4°C. Each beating was followed by 1 minute cooling on ice. Intact cells and debris were removed by centrifugation at 3000xg for 15 minute. Protein extracts were quantified using the BCA kit (Pierce) and equal amounts of protein were loaded per well (30-150 µg). Proteins were fractionated using standard SDS-PAGE and electroblotted into nitrocellulose membranes. GFP fusion proteins and free GFP were detected using antibodies against GFP (Clontech). Polyubiquitinated proteins were detected with a mouse monoclonal anti-ubiquitin antibody (P4D1, Covance). In order to avoid loading and experimental variation,

membranes were stripped and further incubated with rabbit anti-ADH antibody (Rockland) as internal control. For Ald6p detection a rabbit anti-acetaldehyde dehydrogenase monoclonal antibody (Rockland, Gilberstville, PA) was used. This antibody reacts with both Ald6p and Ald4p, providing an internal control for extract concentration and gel loading (Cebollero and Gonzalez, 2006). Detection of proteins was performed using an Odyssey Infrared Imaging system.

DNA microarrays

RNA preparation

Cells (25 OD_{600} units) were harvested by centrifugation at 4000 rpm for 5 minutes, immediately frozen in liquid nitrogen and stored at -80^{o}C until further use. Frozen pellets were resuspended in 500 µl Acidic Phenol-Chlorophorm (5:1, pH4.7; Sigma), heated at 65^{o}C prior to use. The same volume of hot TES buffer (10 mM Tris, pH 7.5; 10 mM EDTA, 0.5%SDS) was then added. Pellets were resuspended by vortexing for 20 seconds and were immediately incubated at 65°C for 1 hour with vortexing every 10 minutes, in order to maintain a homogeneous suspension. The extracts were then transferred to clean microfuge tubes and cells debris and organic phase were separated from upper aqueous phase by centrifugation at 14000 rpm for 20 minutes at 4°C. The upper phase was collected and extracted twice with 1 volume of Phenol:Chlorophorm (5:1, pH 4.7; Sigma) and once with Chlorophorm:Isoamyl-alcohol (25:1; Sigma). At each step, extracts were centrifuged at 14000 rpm for 10 minutes at 4°C. The RNA was precipitated by addition of 1 volume of 3M sodium acetate (pH 5.2) plus 3 volumes of ice-cold absolute ethanol,

followed by an overnight incubation at -20°C. The RNA was pelleted by centrifugation at 14000 rpm for 5 minutes at 4°C, washed once with 70% ethanol and again pelleted by centrifugation. The remaining alcohol was evaporated using a speed-vac (Savant) and the RNA pellets were dissolved in 50 µl of RNase-free water. RNA concentration was determined by OD_{260} in a Nanodrop 1000 (ThermoScientific) (van de et al., 2003).

Data Analysis and Statistical Analysis

Microarray were scanned using a Agilent G2565AA laser scanner, and images were processed using QuantArray® software package (Packard BioChip Technologies). Background was subtracted and bad spots were excluded after manual inspection. Slides were normalized using standard ratio-based methods (print-tip lowess normalization within arrays) as implemented in Biometric Research Branch BRB-Array Tools v3.4.0 software. Experiments were performed in two independent assays, corresponding to two different clones for each strain, with dye-swapping. Microarray data analyses were performed using MEV software (TM4 Microarray Software Suite, Saeed et al., 2006; Saeed et al., 2003). Data were analyzed based on $\log_2$ ratio (M) values. Genes included in the final dataset exhibited significance based on a FDR median< 0.05, in a SAM 1-class analysis (Salin 2008, Tusher 2001, Saeed 2003, van Helden 2003).

Real-Time PCR

Primer sequences used in real–time PCR are indicated in Table 3. Total RNA samples were treated with 10 units of DNase I (invitrogen) and were incubated at RT for 30 minutes, followed by addition of 10 µl of EDTA (25mM) and incubation at 65°C for 15 minutes. The treated RNA was further purified by extraction with equal volumes of

phenol/chloroform/isoamyl alcohol (25:24:1) and chloroform followed by ethanol precipitation. Dried RNA samples were resuspended in RNase free water. RNA quantity and quality were assessed using the Nanodrop 1000 (ThermoScientific) and Agilent 2100 Bioanalyzer systems, respectively. Samples were stored at -80°C until further use. 1 µg of RNA, prepared as described above, was used for cDNA synthesis *in vitro* using the Superscript II™ (Invitrogen). Briefly, the first cDNA strand was synthesized in a mixture containing 12 µl of mQH_2O, 0.1 mM dNTPs, 0.04 µg oligo (dT) 12-18 primers and 1 µg of total RNA as the starting material. The mixture was heated at 65°C for 5 minutes and then 4 µl of the 5× buffer, 1 µl of 0.1M DTT were added to the previous mixture. Finally, 200 U of SuperScript™ Reverse Transcriptase (Invitrogen) were added and the mix was incubated at 42°C for 1 h, followed by 1 minute at 70°C, to inactivate the enzyme. In order to remove any RNA complementary to the synthetic cDNA, 2 units of RNase H were added and the cDNA was incubated at 37°C for 20 additional minutes. All samples of each experiment were reverse transcribed simultaneously. The resulting cDNA was diluted 1:4 in RNase-free water before real-time PCR. Standard dilution curves were prepared for each primer set to ensure that they had similar amplification efficiencies, which were calculated using Equation 2. An ABI Prism 7500 Sequence Detection System (Applied Biosystems) was used for RT-PCR. Control reactions lacking reverse transcriptase (RT-minus) or template (NTCs) were performed for all samples. The real-time thermal cycler was programmed as follows: 95°C for 15'', 55°C for 30'', 72°C for 20'' for 40 PCR cycles. Melting curves were recorded from 60°C to 95°C. Duplicate reactions for each RNA sample were carried out and repeated at least in three independent cDNA samples. The $2^{-\Delta\Delta CT}$ method was used to calculate relative changes in gene expression (where C_t stands

for cycle threshold) (Livak and Schmittgen, 2001). The average C_T was calculated for both target genes and *ADH* and the ΔC_T was determined as defined by Equation 1. The $\Delta\Delta C_T$ represented the difference between the paired samples, as calculated by Equation 3. All analyses were performed using REST-MCS vs2 software. Fold change values were also calculated using Equation 4. Up-regulation was considered for fold change >1.5 and down-regulation for fold change values <0.6, with p-values <0.01.

Table 3- Primers used for RT-PCR

Target mRNA	Primers	Amplicon Size
ADH (reference gene)	Fw 5′-TCAACCAAGTCGTCAAGTC-3′ Rv 5′-TTCTGGCAAGGTAGACAAG-3′	140 bp
ATG1	Fw 5′-GCATGGCTAACTTTGAGAAC-3′ Rv 5′-CGTGGATAAGCAATCTTCC-3′	125 bp
ATG8	Fw 5′-TATGCTACCCCCTGAGAAG-3′ Rv 5′-AACCCGTCCTTATCCTTG-3′	204 bp
KAR2	Fw 5′-CGAATCTTTGTCCAAGGTC-3′ Rv 5′-GAAATAATCACCATCGTCATCT-3′	115 bp
MON1	Fw 5′-GCGATATACCAGCACCAATG-3′ Rv 5′-CTAGCCCCTGTGAAGAATCC-3′	120 bp
PNC1	Fw 5′-GCAAGAGGGTATTTTGTGG-3′ Rv 5′-AGGCGGAGTAGTATTCACG-3′	146 bp
RPN4	Fw 5′-TCGTGCCAAGAGTTCTAGTC-3′ Rv 5′-GTCCCCGTTCATCTAACAG-3′	107 bp
SIR2	Fw 5′-TCTTTTGGGGTACTGTGATGA-3′ Rv 5′-ACGCCCTTATCCTTCTCTTG-3′	126 bp

Equation 1- ΔC_T calculation. C_t- cycle threshold; avg- average

ΔC_T = avg C_T for target gene –avg C_T for ADH

Equation 2- Efficiency calculation

$$Eff = 10^{(-1/slope)} - 1$$

Equation 3 - $\Delta\Delta C_T$ calculation

$\Delta\Delta C_T$ = (ΔC_T of test - ΔC_T of control)

Equation 4- Fold change calculation

$$\text{Fold change} = 2^{\log_2 \text{ratio}}$$

Acknowledgements: The authors would like to thank to Dr. Oshumi and Dr. Kabeya for sending plasmids and to Dr Klionsky and Jiefei Geng for strains, help with the experiments (Atg8-PE blots, PhoΔ84 activity) and for the most helpful discussions and interest in my work. Also to Dr.Michel Desjardins, Christiane Rondeau, Diane Gingras for help with TEM and immuno-TEM experiments.

Supplementary *Data*

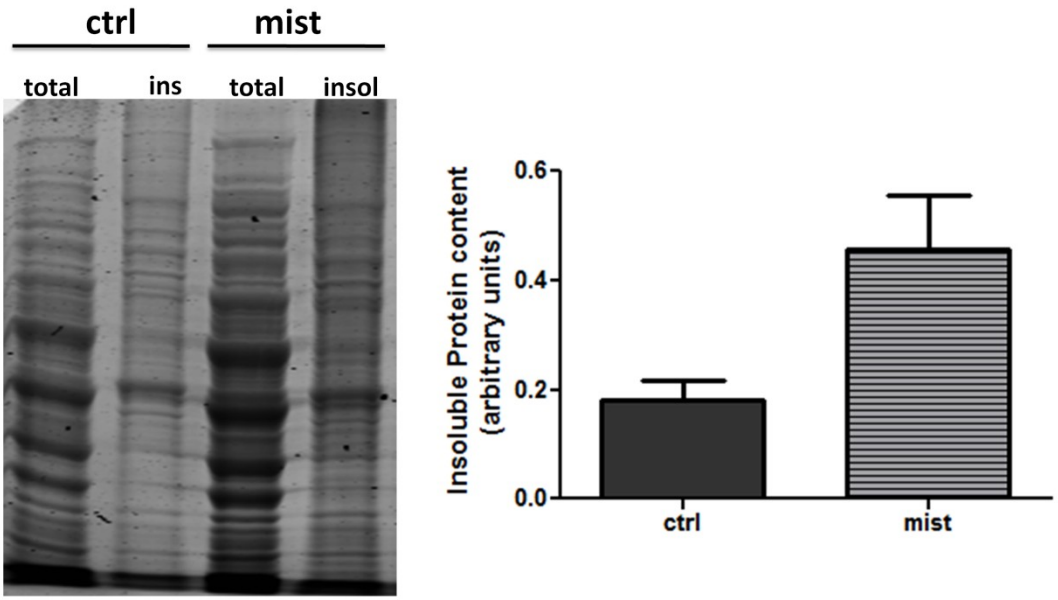

Supp.Figure 1- Protein Aggregation – *S.cerevisiae* strains sUA6 and sUA4 were used, that is, cells with the mistranslating tRNAs integrated in their genome, instead of the same being expressed through a plasmid. Starter cultures of were grown overnight in 5 ml YPD (2% glucose,1%peptone,1%yeast extract) plus geneticin, at 30 ºC and vigorous shaking. The following day, this initial culture were used to inoculate 30 ml of sterile YPD medium and cells were grown in the same conditions to an OD_{595} of 0.3-0.5 (log phase) . Protein extraction (soluble and aggregated –insoluble- fraction) was performed as described in methods. Protein quantity in each fraction was quantified with BCA assay (Pierce) accordingly to manufacturer's instructions. The ratio insoluble/soluble (Ins) protein amount was calculated for each strain. The gel on the right shows a representative image of 3 independent experiments. The data shows a clear trend for the accumulation of insoluble proteins in mistranslating cells, in accordance to what was previously described.

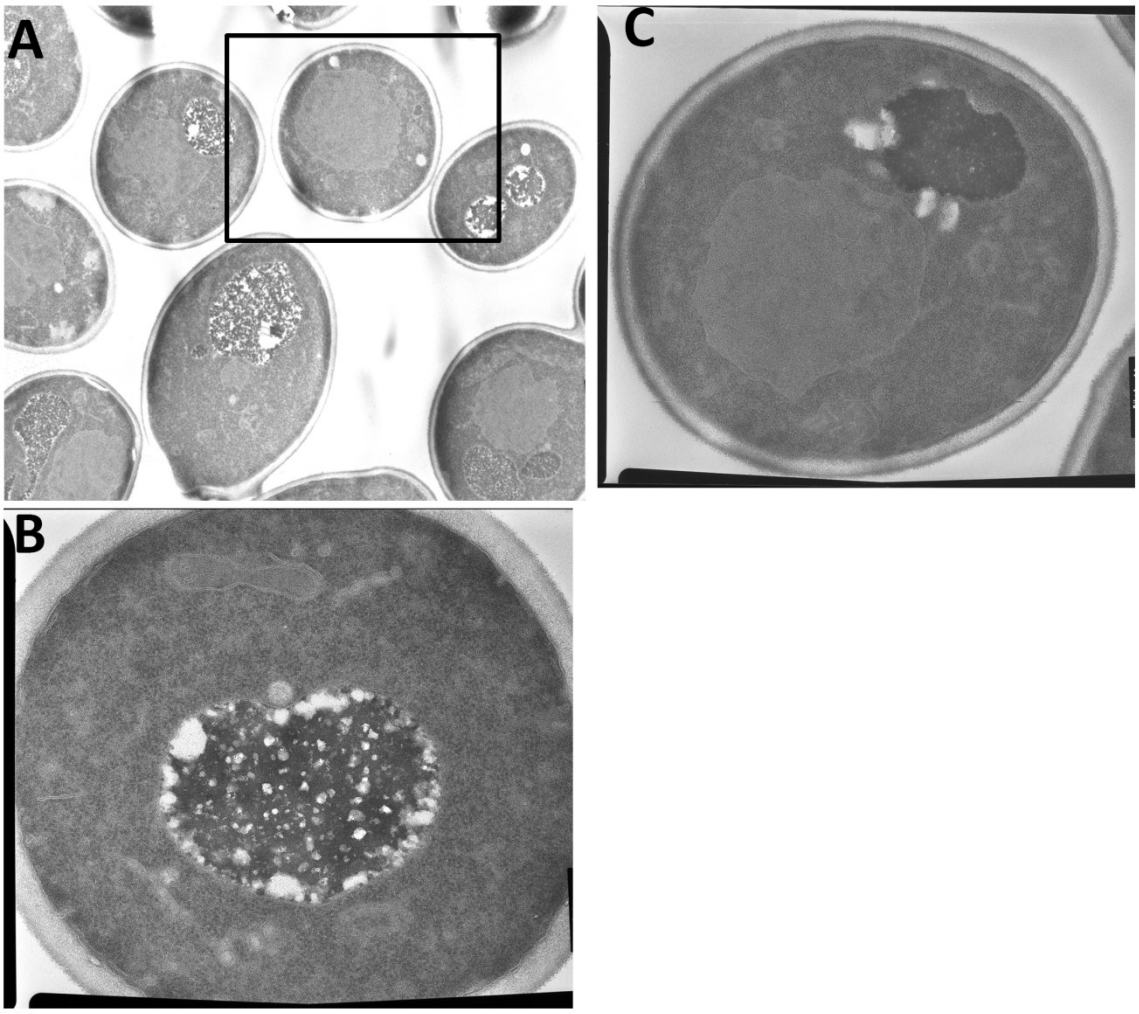

Supp.Figure 2- Electron microscopy of control cells showing normal morphology. Control cells expressing no tRNA were grown to exponential phase and were prepared for electron microscopy. Osmium staining was used to reveal cellular structures. The squares indicate the cells whose zoomed view is shown in Figure 3 and in E (zoomed 8x). A and B were originally acquired using a 4400x amplification, while C was obtained with 14 000x amplification (zoomed 2x in F). Image shown in A was originally acquired using 7100 x amplification, image shown in B was originally acquired using 31 000 x amplification and C was originally acquired using 21 000 x amplification.

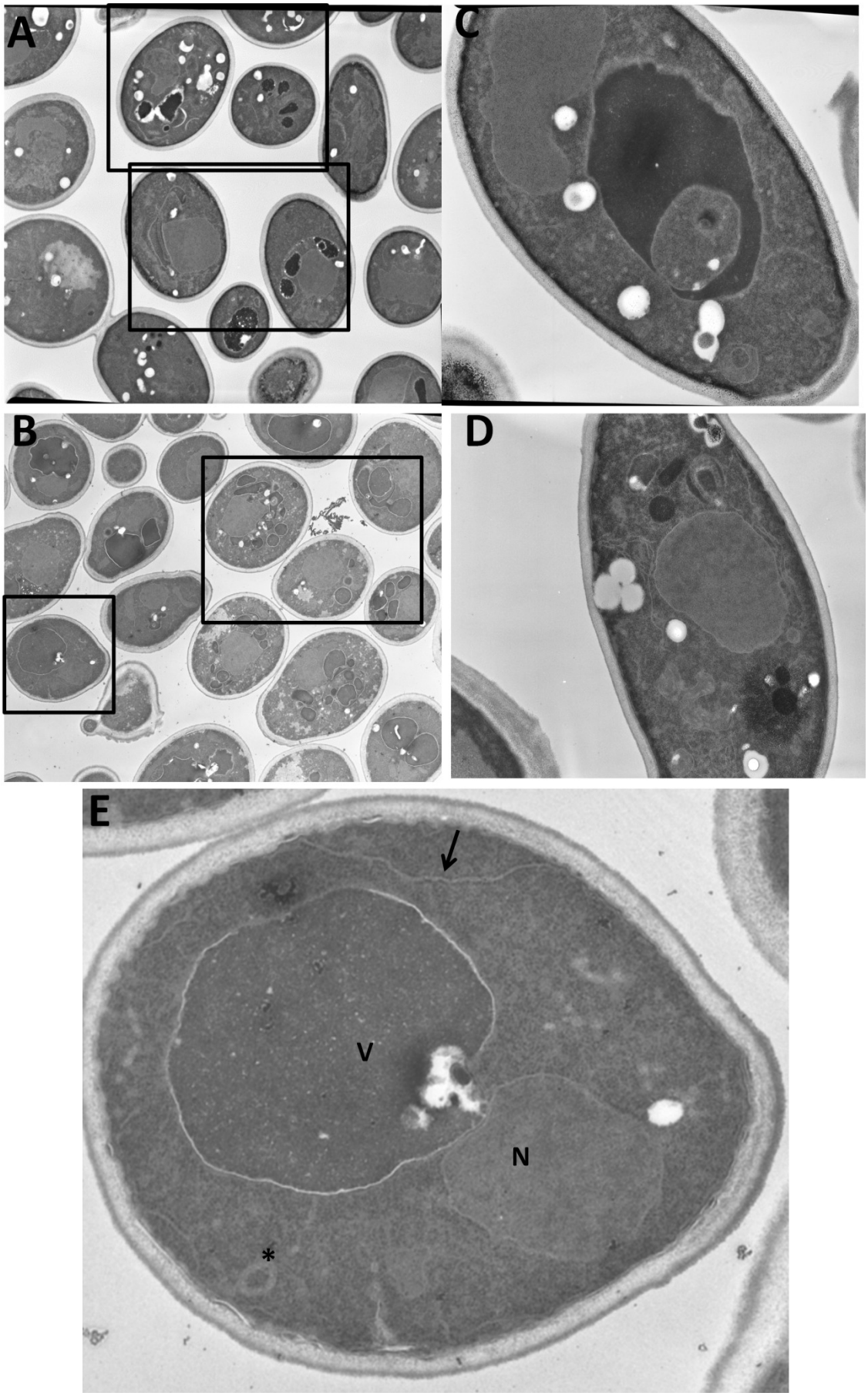
A
C
B
D
E
V
N
*

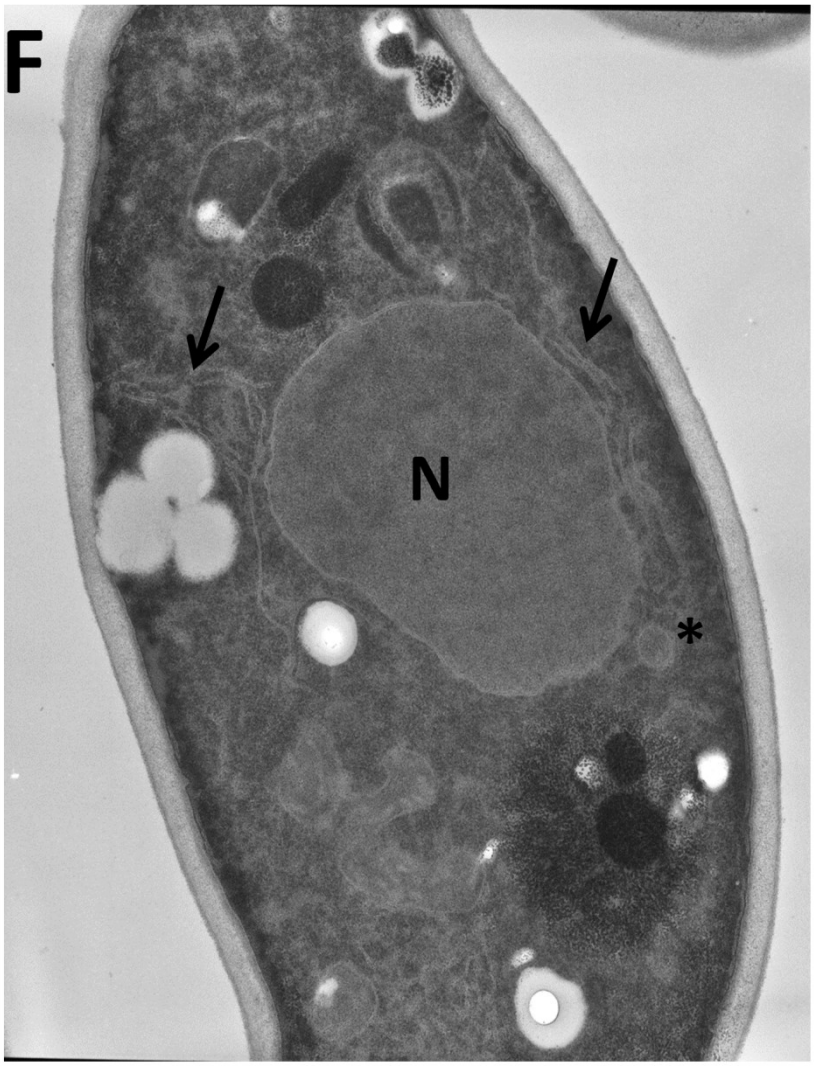

Supp.Figure 3- Electron microscopy of mistranslating cells showing expanded ERs and autophagosomes. Alterations in vacuolar morphology were detected, namely vacuolar fragmentation as well as ER-expansion and autophagosome formation. Cells expressing the tRNA (A-F) were grown to exponential phase and were prepared for electron microscopy. Osmium staining was used to reveal cellular structures. Arrows indicate expanded ER; N stands for nucleus; M for mitochondrion; V for vacuole. Autophagosomes are marked with an *. The squares indicate the cells whose zoomed view is shown in Figure 3 and in E (zoomed 8x). A and B were originally adquired using a 4400x amplification, while C was obtained with 14 000x amplification. D was originally obtained with a 4400x amplification (zoomed 2x in F).

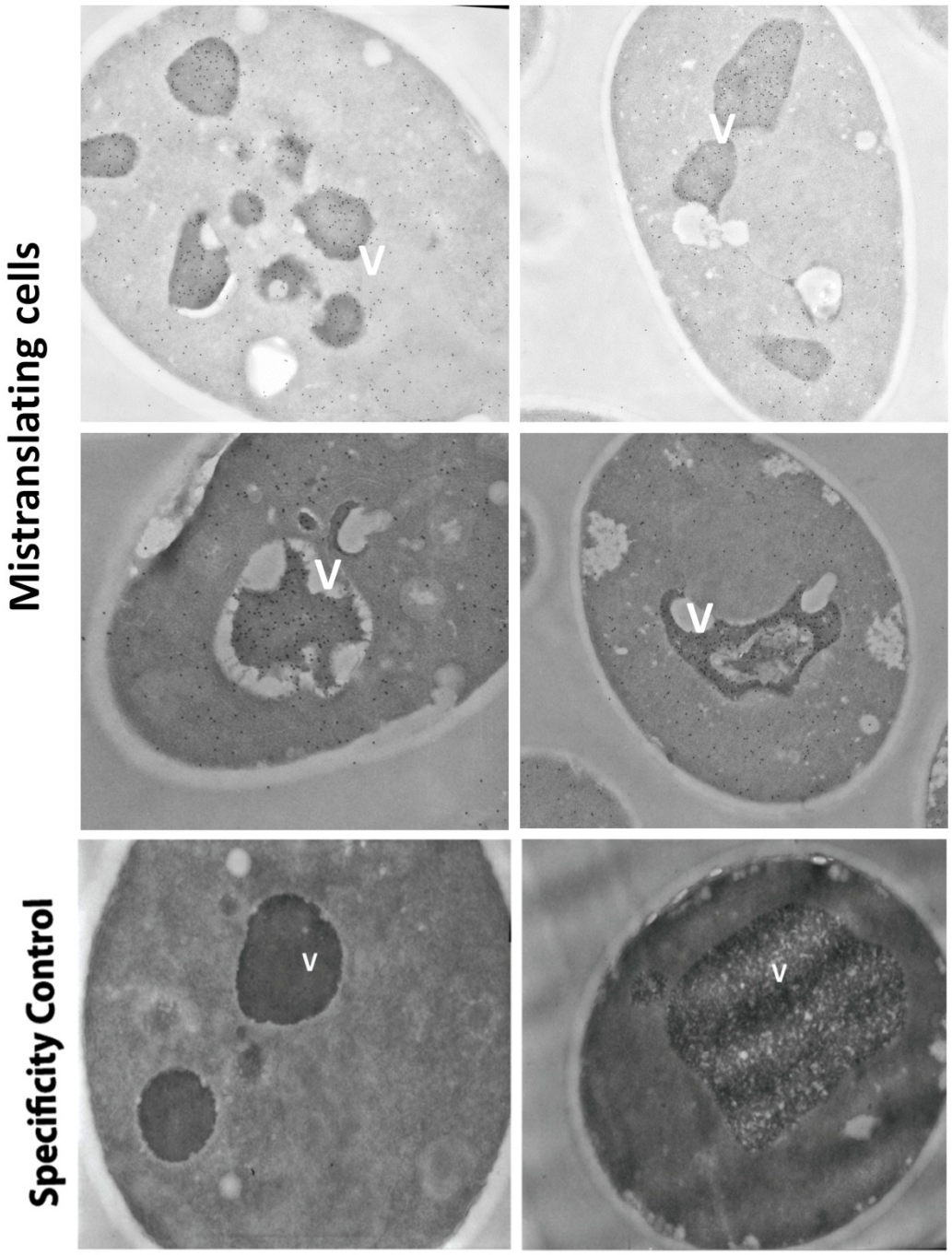

Supp.Figure 4 – Additional image of the Immuno TEM experiment.Only mistranslating cells are shown. A clear increase in the ubiquitin signal is cell's vacuoles is seen. Exponentially growing cells were analysed by immuno-TEM using ultrathin sections mounted on grids. Immuno-gold labeling was performed as described in methods. The primary antibody was a mouse anti-ubiquitin antibody diluted 1:100. The secondary antibody was a goat-anti-mouse antibody coupled to 10 nm gold particles. The ubiquitin signal was detected both on control and mistranslating cells. V-vacuole; CW-cell wall. Specificity control is also shown, that is, only IgM-gold was used (antibody step omission) to assess non specific adsorption of the probe to the sections .Original images taken using a 4400x amplification.

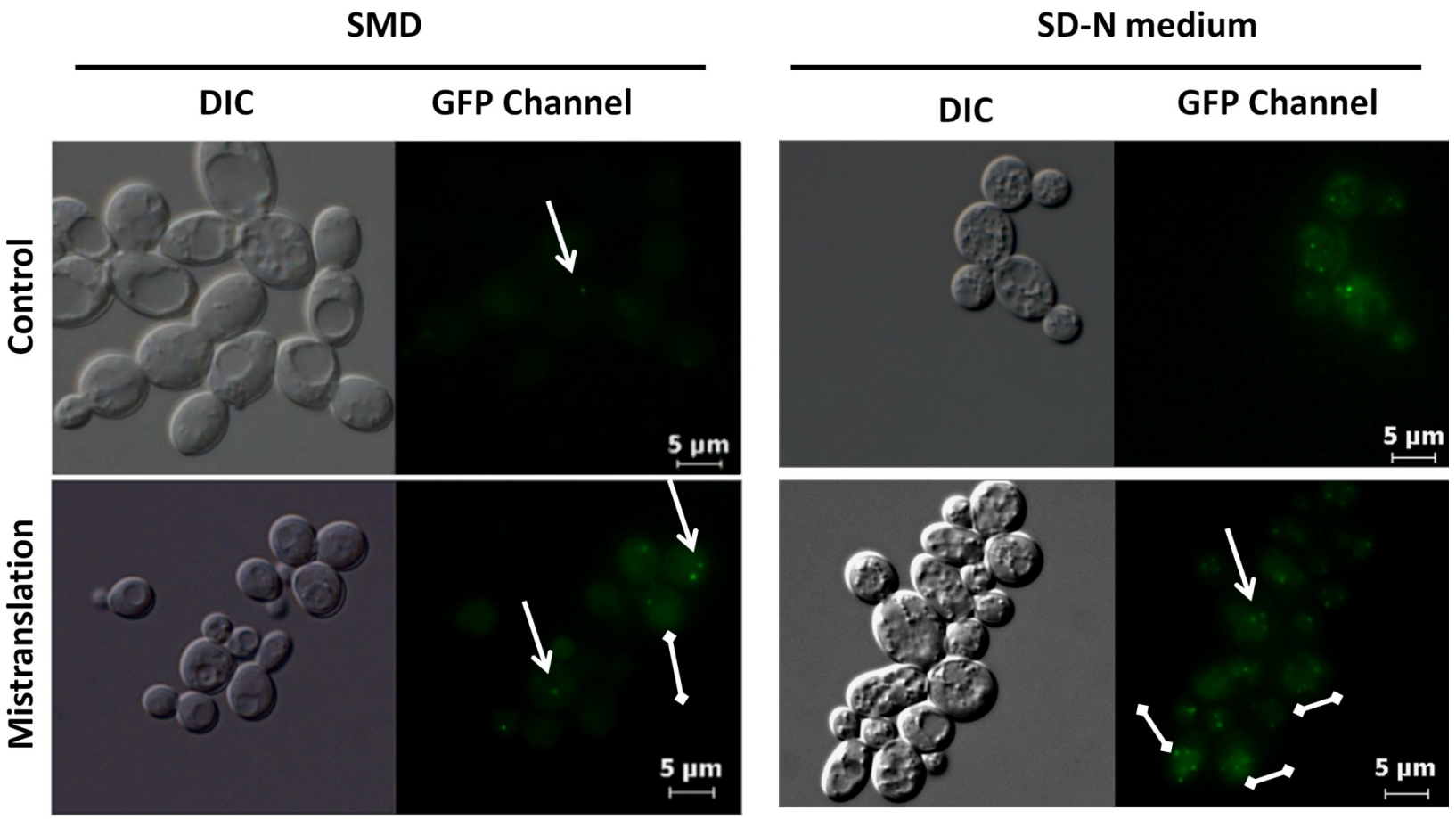

Supp.Figure 5- mistranslation induces autophagy –Additional images. The localization of GFP-Atg8 fusion protein was examined by fluorescence microscopy .Cells co-expressing the mutant misreading tRNA and GFP-ATG8 harboring plasmids were grown to mid log phase in SMD or in SD-N for 3 hours and were analyzed by epifluorescence. Arrows indicate PAS, Double square lines indicate vacuolar fluorescence.

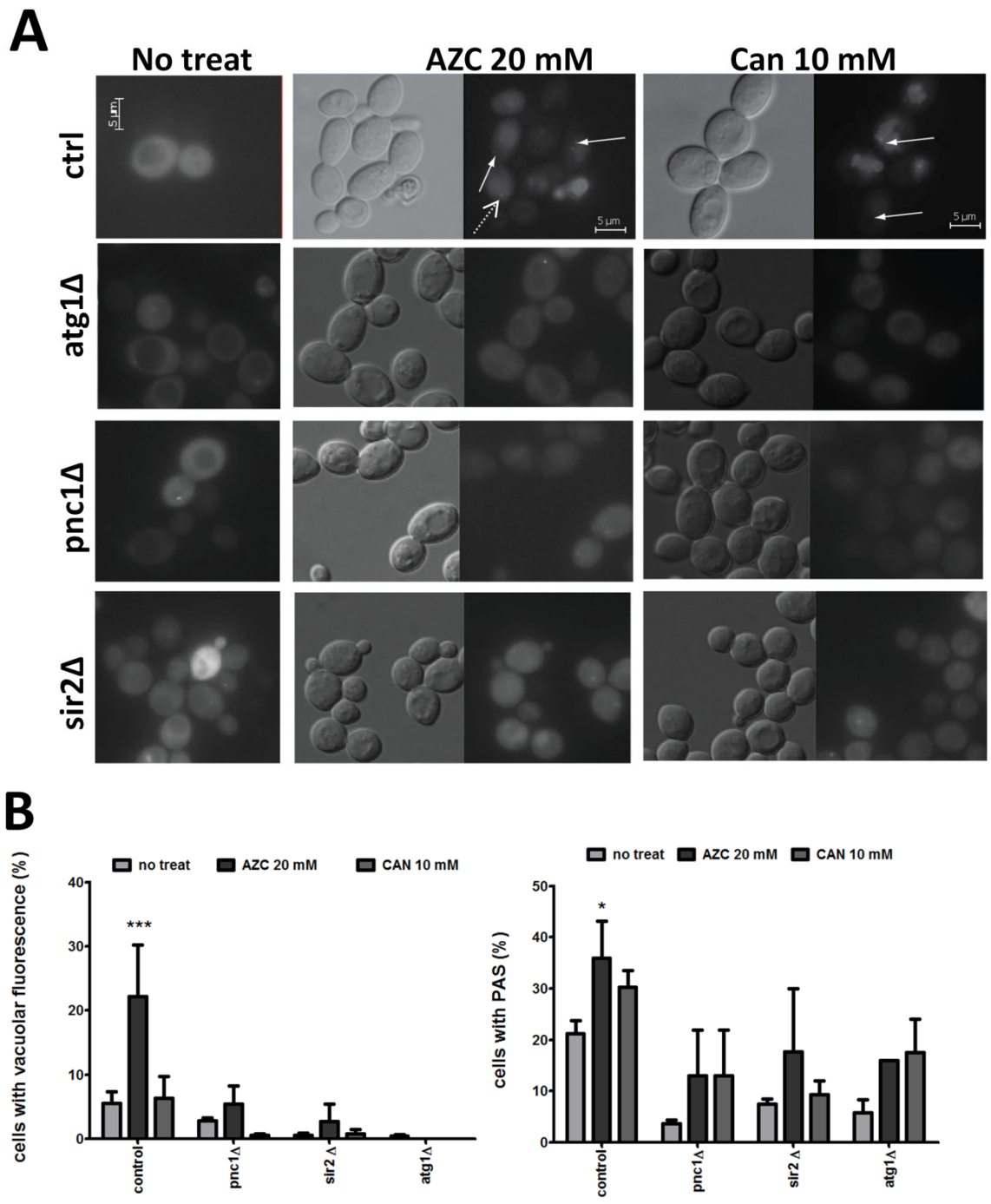

Supp.Figure 6 - mRNA mistranslation induces autophagy – Amino Acid analogues tests **A)** The localization of GFP-Atg8 fusion protein was examined by fluorescence microscopy in cells treated with the mistranslation inducing amino acid analogs l-azetidine-carboxylix acid (AZC) or canavanine (CAN). The right panel shows a detail of the left panel image. Arrows indicate PAS and vacuolar fluorescence. **B)** The number of cells with fluorescence signals on the PAS and cells that presented vacuolar fluorescence were determined. Left panel shows the quantification of cells with vacuolar fluorescence while the histogram on the right shows the

quantification of cells with PAS. A clear increase in both parameters was detected, especially when mistranslation was induced by AZC, providing further evidences that mistranslation induces autophagy. The average of at least two independent experiments is shown and 150 cells for each strain and experiment were monitored. As before, no autophagy was detected neither on pnc1Δ nor sir2Δ indicating a possible blockage of the process in these strains. Error bars represent the standard error of the mean and * represents the significant results with $p<0.05$ for a student's two-tailed t-test.

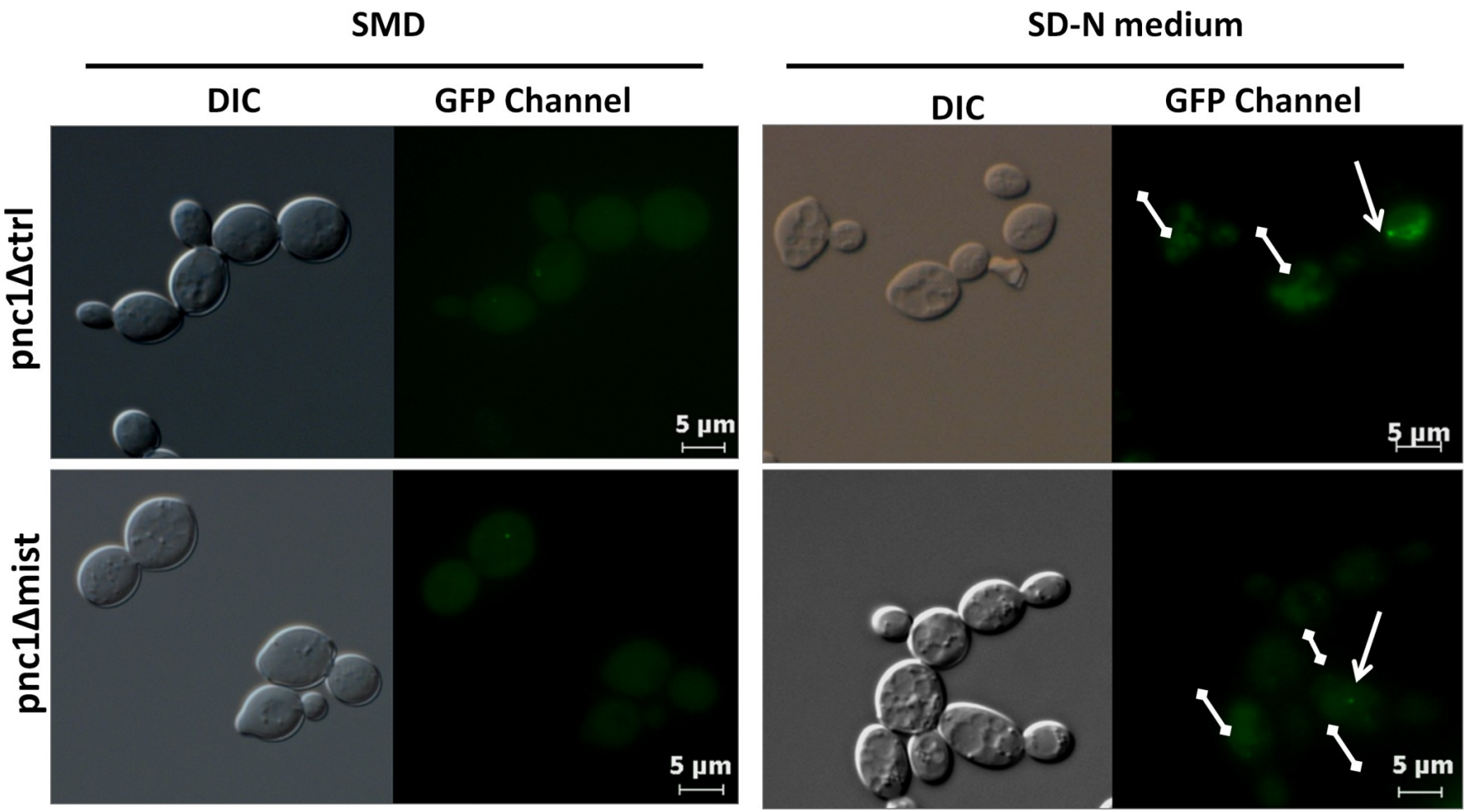

Supp.Figure 7- Pnc1p is involved in mistranslation induced autophagy but is is not required for starvation induced autophagy- Additional images .

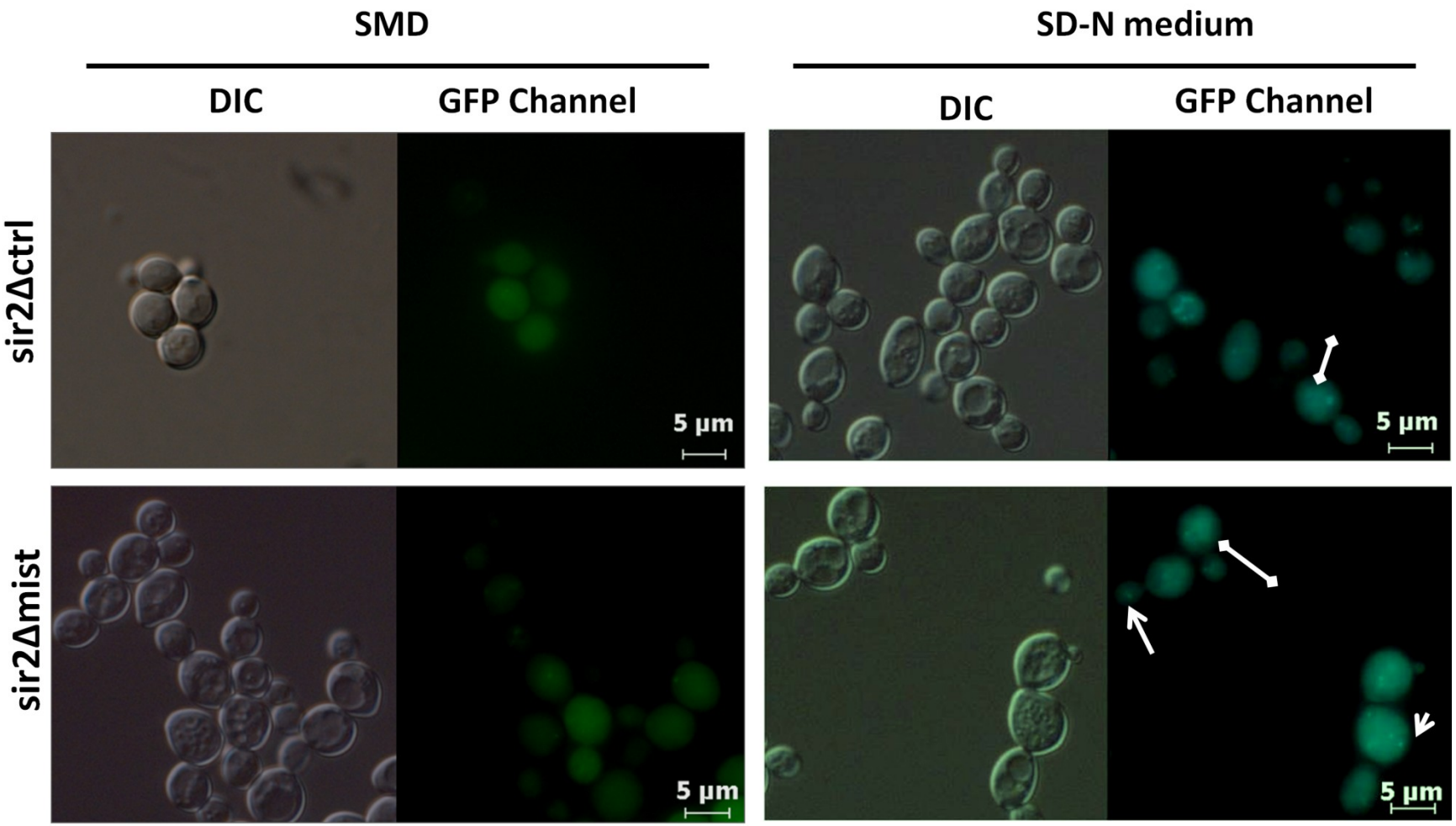

Supp.Figure 8- Sir2p is involved in mistranslation induced autophagy but is is not required for starvation induced autophagy- Additional images .

Supp.Table 1- Expression changes of genes encoding molecular chaperones (fold change values). Each expression data set was analyzed using 1-class SAM analysis as described in methods, based on a FDR median< 0.05.Each dataset was further analyzed in the on-line tool Genecodis(Nogales-Cadenas et al., 2009;Carmona-Saez et al., 2007)

Gene	GO term (BP)	ctrl mist	p-value	sir2Δmist	p-value	pnc1Δmist	p-value
HSP10		1,63					
HSP104		2,76		3,46		1,81	
HSP12		11,49				2,78	
HSP150		3,21					
HSP26	**response to stress**	11,88	3.0e-14		4.2e-06	4,20	9,871E-04
HSP30		2,14		6,51			
HSP42		3,07		4,31		2,16	
HSP60		1,85					
HSP78		4,48		2,80		2,53	

References

1. Al Mamun, A.A., S.Gautam, and M.Z.Humayun. 2006. Hypermutagenesis in mutA cells is mediated by mistranslational corruption of polymerase, and is accompanied by replication fork collapse. *Mol Microbiol.* 62:1752-1763.
2. Al Mamun, A.A., K.J.Marians, and M.Z.Humayun. 2002. DNA polymerase III from Escherichia coli cells expressing mutA mistranslator tRNA is error-prone. *J. Biol Chem* 277:46319-46327.
3. Al Mamun, A.A., M.S.Rahman, and M.Z.Humayun. 1999. Escherichia coli cells bearing mutA, a mutant glyV tRNA gene, express a recA-dependent error-prone DNA replication activity. *Mol Microbiol.* 33:732-740.
4. Bacher, J.M., V.de Crecy-Lagard, and P.R.Schimmel. 2005. Inhibited cell growth and protein functional changes from an editing-defective tRNA synthetase. *Proc. Natl. Acad. Sci. U. S. A* 102:1697-1701.
5. Balashov, S. and M.Z.Humayun. 2002. Mistranslation induced by streptomycin provokes a RecABC/RuvABC-dependent mutator phenotype in Escherichia coli cells. *J. Mol. Biol* 315:513-527.
6. Bennett, E.J., T.A.Shaler, B.Woodman, K.Y.Ryu, T.S.Zaitseva, C.H.Becker, G.P.Bates, H.Schulman, and R.R.Kopito. 2007. Global changes to the ubiquitin system in Huntington's disease. *Nature* 448:704-708.
7. Bernales, S., K.L.McDonald, and P.Walter. 2006. Autophagy counterbalances endoplasmic reticulum expansion during the unfolded protein response. *PLoS Biol* 4:e423.
8. Bukau, B., J.Weissman, and A.Horwich. 2006. Molecular chaperones and protein quality control. *Cell* 125:443-451.
9. Carmona-Saez, P., M.Chagoyen, F.Tirado, J.M.Carazo, and A.Pascual-Montano. 2007. GENECODIS: a web-based tool for finding significant concurrent annotations in gene lists. *Genome Biol* 8:R3.
10. Cebollero, E. and R.Gonzalez. 2006. Induction of Autophagy by Second-Fermentation Yeasts during Elaboration of Sparkling Wines. *Appl. Environ. Microbiol.* 72:4121-4127.
11. Chen, I.Y., J.Lypowy, J.Pain, D.Sayed, S.Grinberg, R.R.Alcendor, J.Sadoshima, and M.Abdellatif. 2006. Histone H2A.z is essential for cardiac myocyte hypertrophy but opposed by silent information regulator 2alpha. *J. Biol Chem* 281:19369-19377.
12. Darst, R.P., S.N.Garcia, M.R.Koch, and L.Pillus. 2008. Slx5 promotes transcriptional silencing and is required for robust growth in the absence of Sir2. *Mol. Cell Biol* 28:1361-1372.
13. Ding, Q., E.Dimayuga, and J.N.Keller. 2006. Proteasome regulation of oxidative stress in aging and age-related diseases of the CNS. *Antioxid. Redox. Signal.* 8:163-172.
14. Erjavec, N., L.Larsson, J.Grantham, and T.Nystrom. 2007. Accelerated aging and failure to segregate damaged proteins in Sir2 mutants can be suppressed by overproducing the protein aggregation-remodeling factor Hsp104p. *Genes & Development* 21:2410-2421.
15. Erjavec, N. and T.Nystrom. 2007. Sir2p-dependent protein segregation gives rise to a superior reactive oxygen species management in the progeny of Saccharomyces cerevisiae. *PNAS* 104:10877-10881.
16. Farabaugh, P.J. and G.R.Bjork. 1999. How translational accuracy influences reading frame maintenance. *EMBO J* 18:1427-1434.
17. Fry, K. and A.Spira. 1979. An ethanolic phosphotungstic Acid (EPTA) Analysis of photoreceptor and synaptic ultrstructure in the guines pig retina. *J. Histochem. Cytochem.* 28:142-148.
18. Geslain, R., L.Cubells, T.Bori-Sanz, R.varez-Medina, D.Rossell, E.Marti, and L.R.de Pouplana. 2010. Chimeric tRNAs as tools to induce proteome damage and identify components of stress responses. *Nucleic Acids Res.* 38:e30.
19. Gietz, R.D. and R.H.Schiestl. 2007a. High-efficiency yeast transformation using the LiAc/SS carrier DNA/PEG method. *Nat Protoc.* 2:31-34.
20. Gietz, R.D. and R.H.Schiestl. 2007b. Quick and easy yeast transformation using the LiAc/SS carrier DNA/PEG method. *Nat Protoc.* 2:35-37.
21. Gietz, R.a.W.R. 2002. Transformation of yeast by the Liac/SS carrier DNA/PPEG method. *Methods in Enzymology* 350:87-96.
22. Gomes, A.C., I.Miranda, R.M.Silva, G.R.Moura, B.Thomas, A.Akoulitchev, and M.A.Santos. 2007. A genetic code alteration generates a proteome of high diversity in the human pathogen Candida albicans. *Genome Biol* 8:R206.
23. Grant, C.M., M.Firoozan, and M.F.Tuite. 1989. Mistranslation induces the heat-shock response in the yeast Saccharomyces cerevisiae. *Mol Microbiol.* 3:215-220.
24. Grant, C.M. and M.F.Tuite. 1994. Mistranslation of human phosphoglycerate kinase in yeast in the presence of paromomycin. *Curr. Genet.* 26:95-99.
25. Guerrero, C., T.Milenkovic, N.Przulj, P.Kaiser, and L.Huang. 2008. Characterization of the proteasome interaction network using a QTAX-based tag-team strategy and protein interaction network analysis. *Proc. Natl. Acad. Sci. U. S. A* 105:13333-13338.

26. Holland, S., E.Lodwig, T.Sideri, T.Reader, I.Clarke, K.Gkargkas, D.C.Hoyle, D.Delneri, S.G.Oliver, and S.V.Avery. 2007. Application of the comprehensive set of heterozygous yeast deletion mutants to elucidate the molecular basis of cellular chromium toxicity. *Genome Biol* 8:R268.
27. Hu, B.R., S.Janelidze, M.D.Ginsberg, R.Busto, M.Perez-Pinzon, T.J.Sick, B.K.Siesjo, and C.L.Liu. 2001. Protein Aggregation After Focal Brain Ischemia and Reperfusion. *J Cereb Blood Flow Metab* 21:865-875.
28. Iwata, A., J.C.Christianson, M.Bucci, L.M.Ellerby, N.Nukina, L.S.Forno, and R.R.Kopito. 2005. Increased susceptibility of cytoplasmic over nuclear polyglutamine aggregates to autophagic degradation. *Proceedings of the National Academy of Sciences of the United States of America* 102:13135-13140.
29. Jakubowski, H. and E.Goldman. 1992. Editing of errors in selection of amino acids for protein synthesis. *Microbiol. Rev.* 56:412-429.
30. Ju, D. and Y.Xie. 2004. Proteasomal degradation of RPN4 via two distinct mechanisms, ubiquitin-dependent and -independent. *J Biol Chem* 279:23851-23854.
31. Kabeya, Y., N.Mizushima, T.Ueno, A.Yamamoto, T.Kirisako, T.Noda, E.Kominami, Y.Ohsumi, and T.Yoshimori. 2000. LC3, a mammalian homologue of yeast Apg8p, is localized in autophagosome membranes after processing. *EMBO J* 19:5720-5728.
32. Kaganovich, D., R.Kopito, and J.Frydman. 2008. Misfolded proteins partition between two distinct quality control compartments. *Nature* 454:1088-1095.
33. Kaniuk, N.A., M.Kiraly, H.Bates, M.Vranic, A.Volchuk, and J.H.Brumell. 2007. Ubiquitinated-Protein Aggregates Form in Pancreatic β-Cells During Diabetes-Induced Oxidative Stress and Are Regulated by Autophagy. *Diabetes* 56:930-939.
34. Klionsky, D.J., A.M.Cuervo, and P.O.Seglen. 2007. Methods for monitoring autophagy from yeast to human. *Autophagy.* 3:181-206.
35. Kohanski, M.A., D.J.Dwyer, J.Wierzbowski, G.Cottarel, and J.J.Collins. 2008. Mistranslation of membrane proteins and two-component system activation trigger antibiotic-mediated cell death. *Cell* 135:679-690.
36. Kraft, C., A.Deplazes, M.Sohrmann, and M.Peter. 2008. Mature ribosomes are selectively degraded upon starvation by an autophagy pathway requiring the Ubp3p/Bre5p ubiquitin protease. *Nat Cell Biol* Apr 6.
37. Lee, I.H., L.Cao, R.Mostoslavsky, D.B.Lombard, J.Liu, N.E.Bruns, M.Tsokos, F.W.Alt, and T.Finkel. 2008. A role for the NAD-dependent deacetylase Sirt1 in the regulation of autophagy. *PNAS* 105:3374-3379.
38. Lee,J., K.Beebe, L.Nangle, J.Jang, C.Longo-Guess, S.Cook, M.Davisson, J.Sundberg, P.Schimmel, and S.Ackerman. Editing-defective tRNA synthetase causes protein misfolding and neurodegeneration. Nature. 2006.
39. Levine, B. and D.J.Klionsky. 2004. Development by self-digestion: molecular mechanisms and biological functions of autophagy. *Dev. Cell* 6:463-477.
40. Levine, B. and J.Yuan. 2005. Autophagy in cell death: an innocent convict? *J. Clin. Invest* 115:2679-2688.
41. Livak, K.J. and T.D.Schmittgen. 2001. Analysis of relative gene expression data using real-time quantitative PCR and the 2(-Delta Delta C(T)) Method. *Methods* 25:402-408.
42. Loftfield, R.B. and D.Vanderjagt. 1972. The frequency of errors in protein biosynthesis. *Biochem. J.* 128:1353-1356.
43. London, M.K., B.I.Keck, P.C.Ramos, and R.J.Dohmen. 2004. Regulatory mechanisms controlling biogenesis of ubiquitin and the proteasome. *FEBS Lett.* 567:259-264.
44. Ma, J., R.Jin, C.J.Dobry, S.K.Lawson, and A.Kumar. 2007. Overexpression of autophagy-related genes inhibits yeast filamentous growth. *Autophagy.* 3:604-609.
45. Meiling-Wesse, K., H.Barth, C.Voss, E.L.Eskelinen, U.D.Epple, and M.Thumm. 2004. Atg21 Is Required for Effective Recruitment of Atg8 to the Preautophagosomal Structure during the Cvt Pathway. *J. Biol. Chem.* 279:37741-37750.
46. Meiners, S., D.Heyken, A.Weller, A.Ludwig, K.Stangl, P.M.Kloetzel, and E.Kruger. 2003. Inhibition of proteasome activity induces concerted expression of proteasome genes and de novo formation of Mammalian proteasomes. *J. Biol Chem* 278:21517-21525.
47. Menninger, J.R. 1976. Peptidyl transfer RNA dissociates during protein synthesis from ribosomes of Escherichia coli. *J. Biol Chem.* 251:3392-3398.
48. Miranda, I., R.Rocha, M.C.Santos, D.D.Mateus, G.R.Moura, L.Carreto, and M.A.S.Santos. 2007. A Genetic Code Alteration Is a Phenotype Diversity Generator in the Human Pathogen Candida albicans. *PLoS ONE* 2:e996.
49. Nagel, R. and A.Chan. 2006. Mistranslation and genetic variability: the effect of streptomycin. *Mutat. Res* 601:162-170.
50. Nangle LA, Motta CM, and Schimmel P. 2007. Global effects of mistranslation from an editing defect in mammalian cells. *Chemistry & Biology* 13:1091-1100.

51. Nogales-Cadenas, R., P.Carmona-Saez, M.Vazquez, C.Vicente, X.Yang, F.Tirado, J.M.Carazo, and A.Pascual-Montano. 2009. GeneCodis: interpreting gene lists through enrichment analysis and integration of diverse biological information. *Nucleic Acids Res* 37:W317-W322.
52. Ogata, M., S.i.Hino, A.Saito, K.Morikawa, S.Kondo, S.Kanemoto, T.Murakami, M.Taniguchi, I.Tanii, K.Yoshinaga, S.Shiosaka, J.A.Hammarback, F.Urano, and K.Imaizumi. 2006. Autophagy Is Activated for Cell Survival after Endoplasmic Reticulum Stress. *Mol. Cell. Biol.* 26:9220-9231.
53. Onodera, J. and Y.Ohsumi. 2004. Ald6p Is a Preferred Target for Autophagy in Yeast, Saccharomyces cerevisiae. *J. Biol. Chem.* 279:16071-16076.
54. Rand, J.D. and C.M.Grant. 2006a. The thioredoxin system protects ribosomes against stress-induced aggregation. *Mol. Biol Cell* 17:387-401.
55. Ravikumar, B. and D.C.Rubinsztein. 2004. Can autophagy protect against neurodegeneration caused by aggregate-prone proteins? *Neuroreport* 15:2443-2445.
56. Roy H and Ibba M. 2006. Molecular biology: sticky end in protein synthesis. *Nature* Sept.
57. Saeed, A.I., N.K.Bhagabati, J.C.Braisted, W.Liang, V.Sharov, E.A.Howe, J.Li, M.Thiagarajan, J.A.White, and J.Quackenbush. 2006. TM4 microarray software suite. *Methods Enzymol.* 411:134-193.
58. Saeed, A.I., V.Sharov, J.White, J.Li, W.Liang, N.Bhagabati, J.Braisted, M.Klapa, T.Currier, M.Thiagarajan, A.Sturn, M.Snuffin, A.Rezantsev, D.Popov, A.Ryltsov, E.Kostukovich, I.Borisovsky, Z.Liu, A.Vinsavich, V.Trush, and J.Quackenbush. 2003. TM4: a free, open-source system for microarray data management and analysis. *Biotechniques* 34:374-378.
59. Santos, M.A., C.Cheesman, V.Costa, P.Moradas-Ferreira, and M.F.Tuite. 1999. Selective advantages created by codon ambiguity allowed for the evolution of an alternative genetic code in Candida spp. *Mol Microbiol.* 31:937-947.
60. Santos, M.A., V.M.Perreau, and M.F.Tuite. 1996a. Transfer RNA structural change is a key element in the reassignment of the CUG codon in Candida albicans. *EMBO J* 15:5060-5068.
61. Santos, M.A. and M.F.Tuite. 1995. The CUG codon is decoded in vivo as serine and not leucine in Candida albicans. *Nucleic Acids Res* 23:1481-1486.
62. Shintani, T. and D.J.Klionsky. 2004. Cargo proteins facilitate the formation of transport vesicles in the cytoplasm to vacuole targeting pathway. *J Biol. Chem.* 279:29889-29894.
63. Silva, R.M., J.A.Paredes, G.R.Moura, B.Manadas, T.Lima-Costa, R.Rocha, I.Miranda, A.C.Gomes, M.J.Koerkamp, M.Perrot, F.C.Holstege, H.Boucherie, and M.A.Santos. 2007. Critical roles for a genetic code alteration in the evolution of the genus Candida. *EMBO J.* 26:4555-4565.
64. Silva, R.M., I.C.N.Duarte, J.A.Paredes, T.Lima-Costa, M.Perrot, H.Boucherie, B.J.Goodfellow, A.C.Gomes, D.D.Mateus, G.R.Moura, and M.A.S.Santos. 2009. The Yeast *PNC1* Longevity Gene Is Up-Regulated by mRNA Mistranslation. *PLoS ONE* 4:e5212.
65. Silva, R. Reconstrução molecular de uma alteração ao código genético / Molecular reconstruction of a genetic code alteration. 2005. Biologia Universidade de Aveiro.
66. Snyder, H., K.Mensah, C.Hsu, M.Hashimoto, I.G.Surgucheva, B.Festoff, A.Surguchov, E.Masliah, A.Matouschek, and B.Wolozin. 2005. β-Synuclein reduces proteasomal inhibition by alpha-synuclein but not gamma-synuclein. *J. Biol Chem* 280:7562-7569.
67. Snyder, H., K.Mensah, C.Theisler, J.Lee, A.Matouschek, and B.Wolozin. 2003. Aggregated and monomeric alpha-synuclein bind to the S6' proteasomal protein and inhibit proteasomal function. *J. Biol Chem* 278:11753-11759.
68. Stansfield, I., K.M.Jones, P.Herbert, A.Lewendon, W.V.Shaw, and M.F.Tuite. 1998. Missense translation errors in Saccharomyces cerevisiae. *J. Mol. Biol* 282:13-24.
69. Suzuki, K., Y.Kubota, T.Sekito, and Y.Ohsumi. 2007. Hierarchy of Atg proteins in pre-
70. Suzuki, K. and Y.Ohsumi. 2007. Molecular machinery of autophagosome formation in yeast, Saccharomyces cerevisiae. *FEBS Lett.* 581:2156-2161.
71. Suzuki, K. and Y.Ohsumi. 2010. Current knowledge of the pre-autophagosomal structure (PAS). *FEBS Letters* 584:1280-1286.
72. Valente, L. and T.G.Kinzy. 2003. Yeast as a sensor of factors affecting the accuracy of protein synthesis. *Cell Mol. Life Sci.* 60:2115-2130.
73. van de, P.J., P.Kemmeren, B.H.van, M.Radonjic, L.D.van, and F.C.Holstege. 2003. Monitoring global messenger RNA changes in externally controlled microarray experiments. *EMBO Rep.* 4:387-393.
74. Wright R. Transmission Electron Microscopy of Yeast. Microscopy Research and technique 51, 496-510. 2000.
75. Yarus, M. 1982. Translational efficiency of transfer RNA's: uses of an extended anticodon. *Science* 218:646-652.
76. Yorimitsu, T., U.Nair, Z.Yang, and D.J.Klionsky. 2006. Endoplasmic reticulum stress triggers autophagy. *J Biol. Chem.* 281:30299-3030

Chapter 3
mRNA mistranslation causes ROS accumulation and mitochondrial dysfunction

Unpublished work, in preparation

Abstract

Errors in mRNA translation (mistranslation) result in the production of abnormal proteins, which can misfold or aggregate and ultimately result on cell degeneration and disease phenotypes. Still, various phenotypes associated with mistranslation and the cellular protection mechanisms against such errors have been difficult to decipher. Recent work from our laboratory indicate that acute mistranslation leads to UPR induction and increases reactive oxygen species (ROS) production (Paredes JA, 2010). ROS diffuse into the cytosol, where they react with various molecules, including lipids, proteins, sugars and nucleotides contributing to increased oxidative stress. Enhanced oxidative stress occurs in a number of degenerative diseases and ROS are considered the main causes of aging-related diseases namely Parkinson's, Alzheimer's, vascular-damage-related brain diseases, cancer, artherioschlerosis and diabetes. In order to further clarify the possible link between mistranslation and ROS, we have engineered *Saccharomyces cerevisiae* cells to mistranslate leucine CUG codons as serine on a global scale. Using a combination of different biochemical techniques we show that chronic mistranslation leads to ROS accumulation and triggers the oxidative stress response. Our data also supports a role for PNC1p and Sir2p on ROS management and show that mistranslation affects mitochondrial morphology and leads to respiratory defects, but does not induce mitophagy. This study contributes to understand the molecular basis of human diseases caused by mistranslation and provides new insight on how mistranslation affects cellular physiology, unveiling new therapeutic targets for mistranslation associated diseases.

Introduction

The ability to express genetic information with minimal errors is essential for cellular homeostasis. Still, errors in transcription and translation (mRNA mistranslation) occur naturally at low level and cells possess several quality control mechanisms, namely proofreading activity at the amino-acyltRNA synthethase or at the ribosome level, or post-translational quality control systems to correct or destroy the erroneous translational products. Chaperones, ERAD, UPR, autophagy and the proteasome-ubiquitin systems form a multifunctional system of protein quality control. Despite this, small increases in translational errors are associated with cellular degeneration and disease phenotypes.

The translational fidelity of mRNA is affected by several factors, namely mutations in translational factors and environmental stress. For example, oxidative stress decreases translation initiation and protein synthesis rate in order to prevent deleterious effects that could arise from the error-prone conditions caused by such stress (Shenton et al., 2006), namely DNA and RNA damage (Macomber et al., 2007; Ott et al., 2007). Also, chromate, which is a redox-active metal, causes mRNA mistranslation in an oxygen-dependent manner. This is related to methionine and cystein depletion, which ultimately affect cognate and non-cognate amino acid competition, resulting in increased mistranslation (Holland et al., 2007; Holland et al., 2010). In human cell lines, eIF4E has been shown to be involved in the cellular toxicity of cadmium in a ROS-mediated way (Othumpangat et al., 2005). Finally, studies performed in *E.coli* have

shown that the Cys^{182} residue of threonyl-tRNA-synthetase is oxidised by H_2O_2, impairing the enzyme editing activity (Ling and Soll, 2010). Furthermore, recent work from our laboratory has shown that acute mistranslation leads to UPR induction and ROS accumulation (Paredes JA, 2010).

ROS are highly unstable molecules and represent different oxidation states of dioxygen (0_2), including the singlet oxygen ($^1 0_2$), the superoxide anion (0_2^-), hydrogen peroxide ($H_2 0_2$) and the highly reactive hydroxyl radical (OH^-) (Halliwell and Gutteridge, 1999). They are byproducts of normal cellular metabolism and are also generated by various cellular stresses, namely pro-oxidants, such as menadione and paraquat, by hyperoxia or re-oxygenation of hypoxic cells and by ultraviolet and ionizing radiation (Halliwell and Gutteridge, 1999). When in excess, ROS can damage cells by peroxidizing lipids and disrupting structural proteins, enzymes and nucleic acids or by perturbing the internal redox potential and thus preventing proper enzymatic activity (Halliwell and Gutteridge, 1999). The site of generation, rates of chemical reactivity, abundance and diffusion are factors that contribute to ROS toxicity. However, these negative effects of ROS has been challenged by recent data showing that $H_2 0_2$ and other ROS function as essential secondary messengers in several regulatory processes (Linnane et al., 2007). Indeed, elevated levels of $H_2 0_2$ are associated with extended chronological life span (CLS) as it activates superoxide dismutase activity that in turn inhibits 0_2^- accumulation (Mesquita et al., 2010).

Under normal conditions, antioxidant defences have limited capacity to protect cells from a sudden burst of oxidative stress – defined as an imbalance that favours ROS production over antioxidant defences. In order to survive, yeast cells sense oxidative stress and build a response that involves the up-regulation of both primary and secondary antioxidant defences. The adaptation to stress conditions requires early and late responses, to allow cells to return to non-stress conditions, in a rapid and ordered way.

At the transcriptional level, YAP1, SKN7, MSN2 and MSN4 are the main regulators of the oxidative stress response. SKN7 co-operates in the activation of at least 15 of the YAP1 target proteins in response to H_2O_2 and t-butyl hydroperoxide, but does not participate in the regulation of metabolic pathways that regenerate the main cellular reducing power, like glutathione and NADPH (de la Torre-Ruiz MA et al., 2010). MSN2 and MSN4 activate genes whose promoters contain the stress response element (STRE: CCCCT) including oxidative stress genes. Several proteins are regulated by YAP1 and the MSN2／4 regulon. However, the latter activates a small number of antioxidant enzymes. Their transcriptional activity is more dedicated to the activation of heat-shock proteins, metabolism enzymes, proteases, and is involved in activities of the ubiquitin and proteasome degradation pathways (de la Torre-Ruiz MA et al., 2010). Both MSN2 and MSN 4 are negatively regulated by the Ras-cAMP-protein kinase A (PKA) pathway, which has been suggested to down-regulate Yap1-regulated transcription. Yap1 is the best characterized member of the YAP family. It is known to

be involved both in oxidative stress response and arsenic stress response (Rodrigues-Pousada et al., 2004; Rodrigues-Pousada et al., 2010).

Early responses involve the post-translational activation of pre-existing defences and the activation of signal transduction pathways which initiate late responses, namely the *de novo* synthesis of stress and antioxidant proteins. These antioxidant defences operate at different levels and repair or remove the products of oxidative damages to cellular components. Primary defences neutralise ROS through electron transfer mechanisms, and involve cytoplasmic and mitochondrial superoxide dismutase (SOD1,SOD2), cytoplasmic catalase T (CTT1), catalase A (CTA1), glutathione synthetase (GSH1), the metallothionein (CUP1), cytoplasmic and mitochondrial thioredoxins (TRX1, TRX2), among others (Moradas-Ferreira et al., 1996). Secondary defences, on the other hand include molecules like mitochondrial 8-oxoguanine glycosylase/ lyase (OGG1), protein disulphide isomerise (PDI), glutathione synthetase (GSH1), cytomplasmatic thioredoxin (TRX2), glutathione reductase (GLR1), cytoplasmic or mitochondrial thioredoxin reductases (TRR1, TRR2) and glucose-6-phosphate dehydrogenase (ZWF1)(Moradas-Ferreira et al., 1996). In addition, recent studies have added other genes to this list, namely *SIR2*. Indeed the mammalian *SIRT1* (homologue of Sir2), was shown to play a role in oxidative stress response in mice heart, in an expression dependent way (high levels of Sirt1 increase oxidative stress while moderate expression of Sirt1 induces resistance to oxidative stress and apoptosis) (Alcendor et al., 2007). Also, deletion of the yeast *SIR2* has been shown to increase chronological lifespan (CLS) which is accompanied by an increase in oxidative stress. Despite this, it was suggested that Sir2p was not needed for promoting oxidative stress

resistance and that oxidative stress was not limiting replicative lifespan (RLS, growth on glucose low conditions) under normal conditions, as dietary restriction conditions that promoted RLS, which are SIR2 dependent, did not increase oxidative stress resistance. Notwithstanding, this sirtuin is implicated in the segregation of oxidatively damaged proteins during yeast budding (Erjavec and Nystrom, 2007) as well as in the reduction of the levels of ROS in daughter cells, which delays oxidative damage and gives cells a superior capacity to deal with external ROS (Erjavec and Nystrom, 2007) .

Besides contributing to cellular homeostasis by performing several crucial tasks like ATP production, heme production and Ca^{2+} regulation, mitochondria are a major source of ROS, but also one of the most susceptible organelles to ROS deleterious effects. If cellular energy demands are low mitochondria may produce excessive ROS and damaged or dysfunctional mitochondria can release ROS, cytochrome c and pro-apoptotic molecules. Recent studies in *S.pombe* show that cells lacking mitochondrial components accumulate ROS indicating that intrinsic oxidative stress can be a consequence of mitochondrial disruption and dysfunction (Zuin et al., 2008). Mitochondrial dynamics help keeping the mitochondrial population healthy by means of fusion and fission events and selective autophagy – mitophagy – is activated when superfluous or damage mitochondria are found in the cell.

The aims of the current study were to evaluate ROS accumulation in yeast cells affected by chronic mistranslation, determine the physiological effects of that

accumulation and identify the source of the ROS. We have also evaluated if the role of Sir2p on ROS management.

Results

mRNA mistranslation up-regulates antioxidant stress response

In order to characterize mistranslating cells using global approaches, we have carried out a detailed microarray analysis of their transcriptome. Several classes of genes were up-regulated, including genes involved in cell redox homeostasis (1.7%), cellular respiration (1.02%), response to oxidative stress (1.2%), mitochondrial electron transport, succinate to ubiquinone (0.9%), electron transport chain (3%), response to stress (8%) and oxidation-reduction (18%) (Table 4). A GO terms analysis showed that the up-regulated genes list was enriched in genes that are mainly related to mitochondria and mitochondrial function, namely amino acid biosynthesis, TCA cycle, etc (Table 4; Supp.Table 2). In addition, 27.3% of the genes (44 in total) are related to primary and secondary antioxidant defenses (Table 5). In other words, these lists show that mistranslation leads to oxidative stress response activation plus mitochondrial function deregulation. These data prompted us to analyze in detail the oxidative stress response in the mistranslating cells.

Table 4- Functional enrichment analysis of genes up-regulated in mistranslating cells. Microarray data analyses were performed using MEV software (TM4 Microarray Software Suite) (Saeed et al., 2006; Saeed et al., 2003d). Data were analyzed based on $\log_2$ ratio (M) values. Genes included in the final dataset exhibited significance based on a FDR median< 0.05, in a SAM 1-class analysis (Salin 2008, Tusher 2001, Saeed 2003, van Helden 2003). This dataset was further analyzed using the on-line tool Genecodis (Nogales-Cadenas et al., 2009; Carmona-Saez et al., 2007)

GO annotation (Biological Process)	corrected p-value	% of genes
GO:0055114 :oxidation reduction	5,10E-30	18,3
GO:0008152 :metabolic process	1,65E-20	16,8
GO:0034605 :cellular response to heat	9,58E-25	12,1
GO:0007039 :vacuolar protein catabolic process	1,64E-26	10,1
GO:0006807 :nitrogen compound metabolic process	3,29E-33	9,9
GO:0006082 :organic acid metabolic process	2,42E-37	9,7
GO:0006519 :cellular amino acid and derivative metabolic process	1,28E-31	8,5
GO:0006725 :cellular aromatic compound metabolic process	1,60E-31	8,4
GO:0006950 :response to stress	1,69E-09	8,0
GO:0008652 :cellular amino acid biosynthetic process	3,53E-17	7,7
GO:0044262 :cellular carbohydrate metabolic process	5,37E-05	4,3
GO:0009266 :response to temperature stimulus	1,48E-14	3,6
GO:0006096 :glycolysis	4,91E-07	3,2
GO:0022900 :electron transport chain	2,33E-01	3,1
GO:0051186 :cofactor metabolic process	9,14E+00	3,1
GO:0006099 :tricarboxylic acid cycle	5,56E-05	2,9
GO:0006066 :alcohol metabolic process	9,04E-01	2,9
GO:0008219 :cell death	4,85E-02	2,4
GO:0006112 :energy reserve metabolic process	2,59E-01	2,2
GO:0006094 :gluconeogenesis	1,39E-03	2,1
GO:0009086 :methionine biosynthetic process	5,07E-01	2,1
GO:0009082 :branched chain family amino acid biosynthetic process	5,06E+00	1,4
GO:0006526 :arginine biosynthetic process	6,13E+00	1,2
GO:0006979 :response to oxidative stress	1,02E-04	1,2
GO:0006121 :mitochondrial electron transport, succinate to ubiquinone	8,77E+00	0,9
GO:0034354 :de novo NAD biosynthetic process from tryptophan	8,77E+00	0,9
GO annotation (cellular component)		
GO:0005739 :mitochondrion (CC)	7,43E-10	28,4
GO:0001950 :plasma membrane enriched fraction (CC)	3,24E-10	6,0
GO:0009277 :fungal-type cell wall (CC)	1,60E+00	3,9
GO:0005759 :mitochondrial matrix (CC)	9,67E+00	4,3

Table 5-Genes related to antioxidant defenses that were up-regulated by mistranslation. RNA was extracted and microarray hybridizations were performed. Microarray data analyses were performed using MEV software (TM4 Microarray Software Suite) (Saeed et al., 2006;Saeed et al., 2003c). Data were analyzed based on $\log_2$ ratio (M) values. Genes included in the final dataset exhibited significance based on a FDR median< 0.05, in a SAM 1-class analysis (Salin 2008, Tusher 2001, Saeed 2003, van Helden 2003).

Gene Name	Fold change	type of antioxidant defence	Product	Function
AHP1	2,7	primary	cytoplasmic thioredoxin peroxidase III	
APN2	2,3	secondary	nuclear AP endonuclease	
CTA1*	*2,0*	*primary*	*catalase A, peroxisomal*	Decomposition of hydrogen peroxide
COQ3**	•	primary	ubiquinone	
CTT1	4,9	primary	cytoplasmic catalase T	Decomposition of hydrogen peroxide
GPX1	2,3	primary	glutathione peroxidases	Reduction of hydrogen peroxide and alkyl hydroperoxides
GRX1	2,1	secondary	glutaredoxin	
PDI 1	1,6	secondary	protein disulphide isomerase	
SOD2	1,5	primary	mitochondrial superoxide dismutase	
TRX2	1,7	primary	cytoplasmic thioredoxin	Reduction of hydrogen peroxide and alkyl hydroperoxides
TSA1	1,8	primary	cytoplasmic thioredoxin peroxidase I	
TSA2	2,2	primary	cytoplasmic thioredoxin peroxidase II	
ZWF1	2,6	secondary	glucose-6-phosphate dehydrogenase	
GND2	2,8		6-phosphogluconate dehydrogenase	

* down-regulated

** encodes 3,4-dihydroxy-5-hexaprenylbenzoate methyltransferase, which catalyzes different o-methylation steps in ubiquinone (Coenzime Q) biosynthesis; COQ4 and COQ5, from the same family, are upregulated in response to mistranslation

Yeast primary and secondary antioxidant defence gene list contained originaly 44 genes and was obtained from Marques M , 2004

Mistranslation increases ROS production

Our microarray data strongly suggested that mistranslation increased oxidative stress. In addition, other experiments from our laboratory which used inducible mistranslation showed that production and accumulation of ROS were the main cause of cell viability loss in mistranslating cells (Paredes JA, 2010). Therefore, we have decided to analyze ROS production in our strains. Although ROS include a number of molecular species derived from oxygen that are reactive, most of them are biologically originated from either superoxide and/or hydrogen peroxide (H_2O_2). Therefore, by principle, it should be sufficient to restrict our attention to these two compounds. For this, cells were stained either with the dyhydroethidium probe (DHE), which is a widely used to monitor superoxide (O_2^-), or with the dihydrorhodamine probe (DHR123) which reacts preferentially with H_2O_2. Stained cells were then analyzed either in exponential phase or at the beginning of stationary phase /post diauxic growth using flow cytometry and epifluorescence microscopy. In order to get a more detailed picture of the effect of mistranslation on oxidative stress we have also used strains harboring deletions in the *YAP1* and *YAP2* transcription factors. In exponential growth phase, elevated levels of both O_2^- and H_2O_2 were detected in our control mistranslating cells, but a stronger accumulation was observed in yap1Δ cells mistranslating cells, yap2Δ mistranslating cells did not show increased H_2O_2 production (Figure 24). In stationary phase, accumulation of H_2O_2 was observed in all mistranslating strains. Accumulation of the superoxide anion was observed in the yap2Δ and yap1Δyap2Δ mistranslating cells, but not in control or yap1Δ mistranslating cells. The evaluation of

membrane integrity with propidium iodide (Supp.Figure 14) excluded the hypothesis that DHR123 fluorescence be an artifact due to unspecific binding of the dye to dead cells (Wysocki and Kron, 2004; Poliakova et al., 2002). In addition, we also saw that mistranslation did not lead to apoptotic features (data not shown).

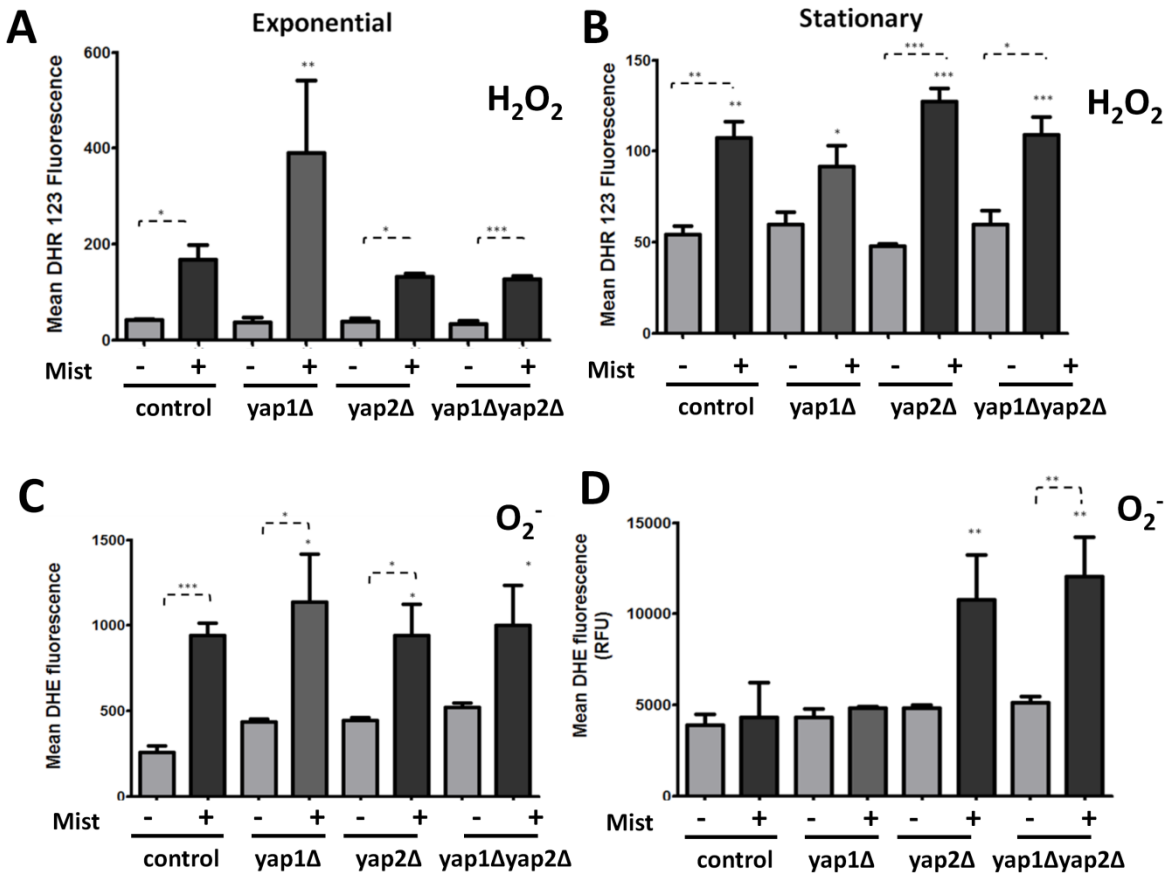

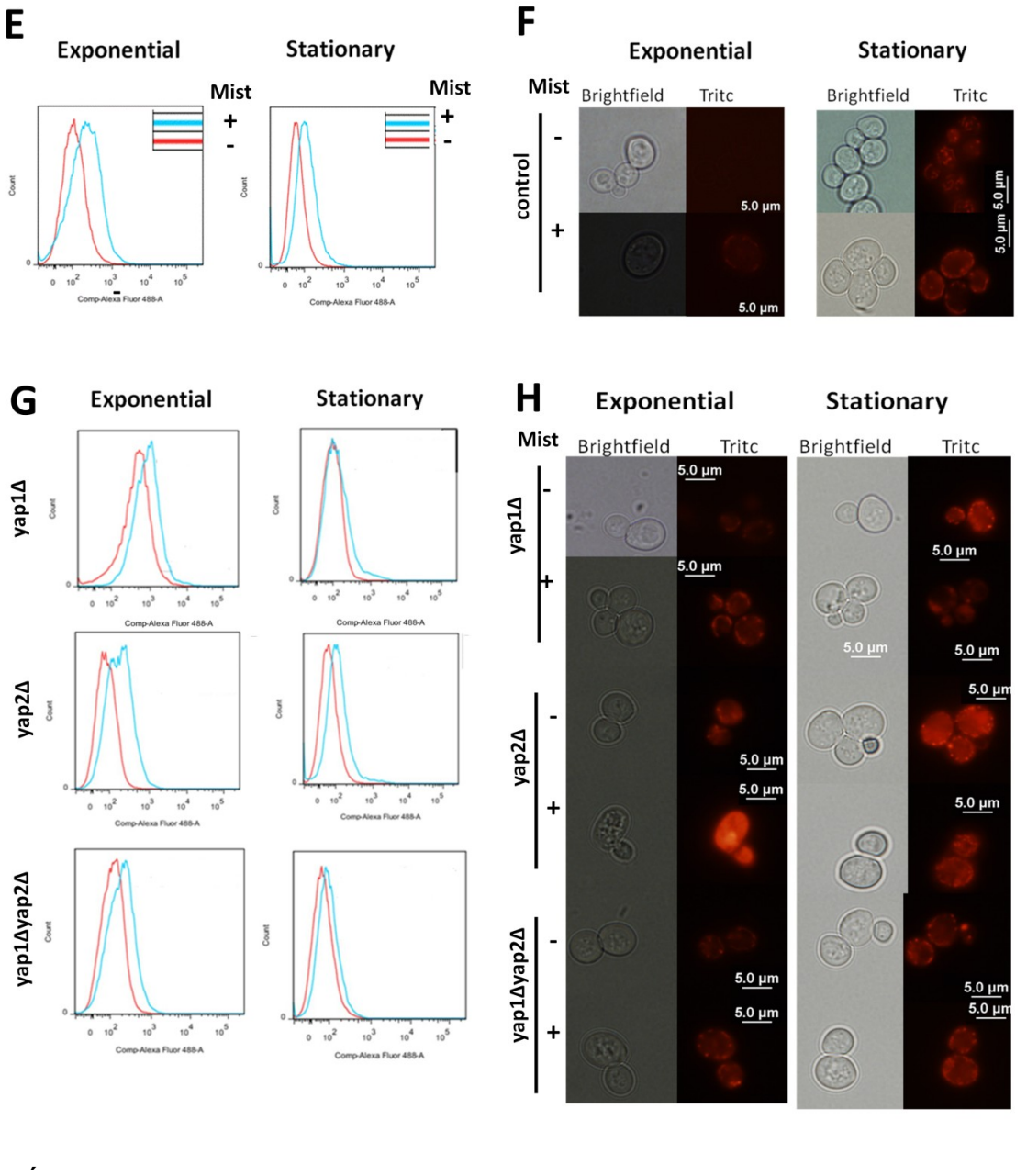

Figure 24-Mistranslation generates ROS. Intracellular ROS accumulation was monitored by flow cytometry in cells incubated with either dihydrorhodamine 123 (DHR123, probe for H_2O_2) (A, B, E, G) or dyhydroethidium (DHE, probe for O_2^-) (C, D, F, H) in both exponential and stationary phase. Cells were analyzed by FACS. Data analysis was performed using FlowJo® software. Histograms displayed in A-D show intracellular H_2O_2 accumulation, as indicated by DHR123 fluorescence and O^{2-} accumulation as quantified by DHE fluorescence. Dashed lines and * show significance levels for an unpaired student's t-test ($p<0.05$) * without lines indicate significance levels for 1-WAY ANOVA, all compared to ctrl (dunnet's test); dashed lines indicate significance levels for two-tailed t-test. Representative fluorescence profiles are also shown (E and G). Red lines indicate non mistranslating cells, while blue lines indicate mistranslating cells,

as seen in E. n= 2 to 6 independent cultures, corresponding to at least 2 different clones ($p<0.05$). Enlarged views of F and H are shown in Supp.Figure 9, Supp.Figure 10 and Supp.Figure 12.

Additional physiological characterization showed that mistranslation affected negatively growth rate and short term viability. Indeed, mistranslation decreased growth by 34.6% in the non deleted control and also of the yap1Δ strain by 21% . Additionaly, it had effects on both yap2Δ and yap1Δ yap2Δ strains (40-50% decrease). In short-term viability experiments, the mistranslation effects were identical independently of the strain background, with a marked viability loss (Figure 25, F). Similar results were obtained with other mistranslating mutant strains (Figure 29).

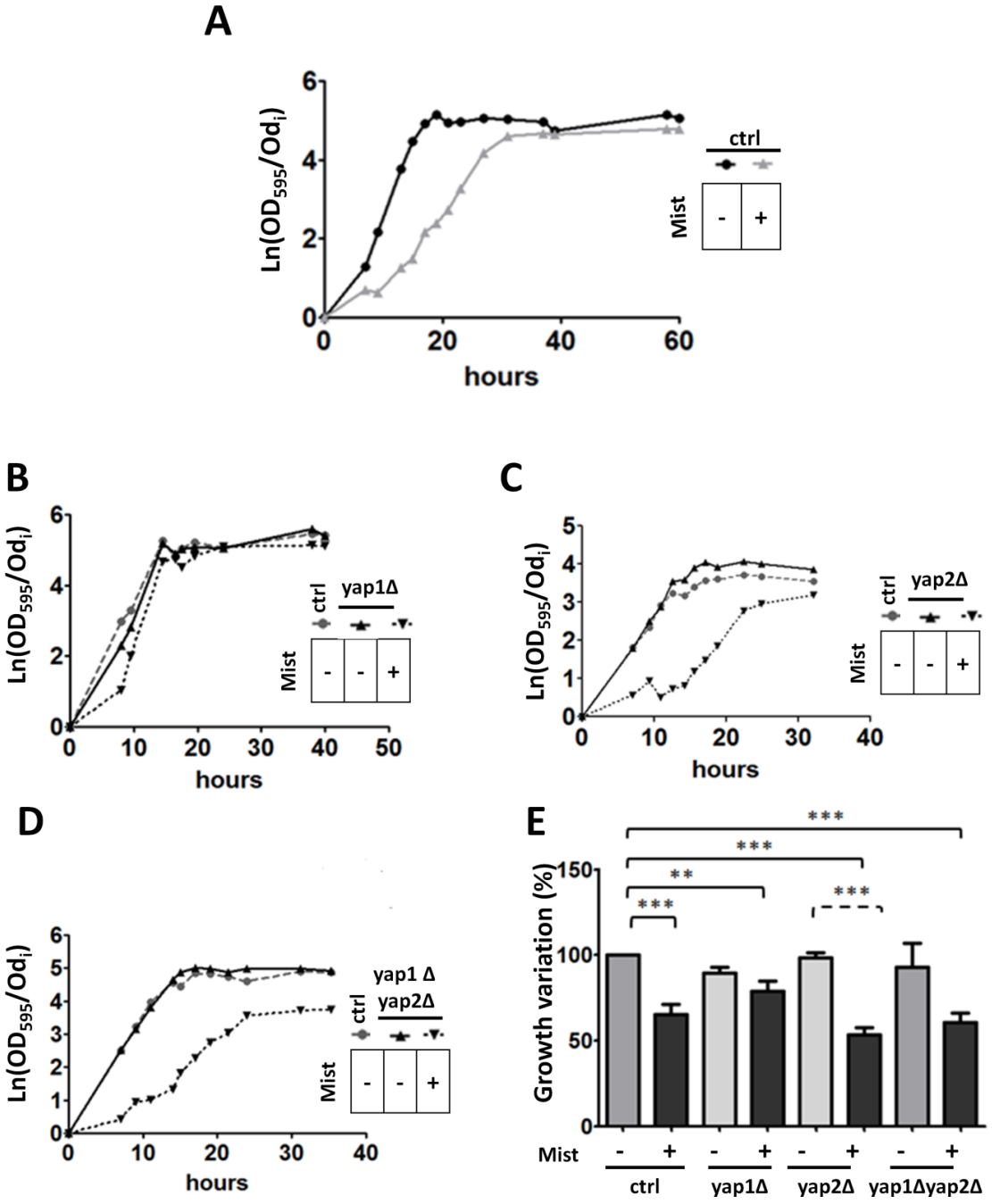
A
Ln(OD595/Odi)
hours
ctrl
Mist
B
yap1Δ
C
yap2Δ
D
yap1 Δ
yap2Δ
E
Growth variation (%)
ctrl
yap1Δ
yap2Δ
yap1Δyap2Δ

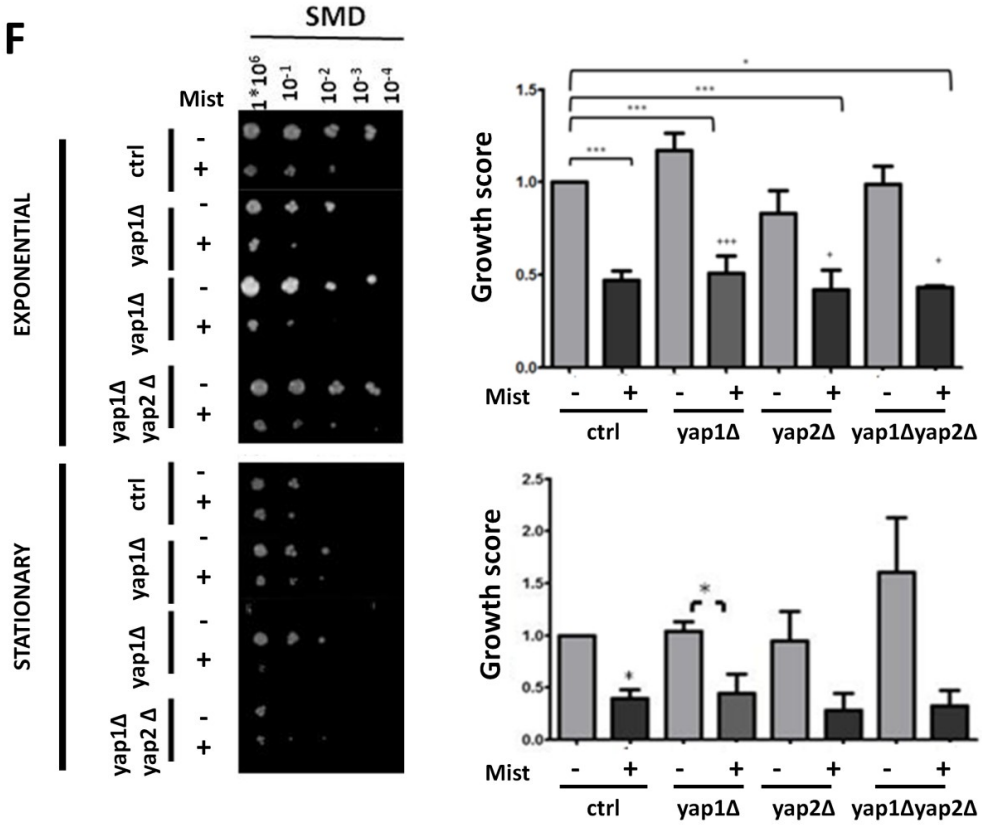

Figure 25- Mistranslation affects growth rate and short-term viability. A-E) Effects of mistranslation on growth rate were assessed in control (A) and in the *YAP* knockout strains (B-D). Cultures were grown in 50 ml flasks at 30°C and the OD_{595} was measured every 2 hours. The graph shows representative plots of at least 2 independent cultures corresponding to 2 different clones. OD_{595} values for each time point were transformed on Ln od/odi, as described by previously (Toussaint and Conconi, 2006). The relative decrease in growth rates of mistranslating yeast cells were determined from the specific growth rates of each clone. The values represent the growth rate in relation to control non mistranslating cells. The bars show the average results ± SEM for at least 2 independent experiments/biological replicates (clones) full lines and *,**,*** indicate the levels of statistical significance, 1-way ANOVA, dunnett's test (comparison to ctrl) , $p<0.05$ and dashed lines indicate statistical significance for a two tailed unpaired t-test , $p<0,05$. **F)** Yeast viability and growth variation in solid media- Viability and growth variability of exponentially and quiescent cells was determined by plating in solid media. For this, cells were initially grown in liquid media and were aliquoted at the indicated time points. Cell number was normalized, serial dilutions were prepared and cells were spotted into solid media with the help of a robot. Plates were incubated at 30ºC for 4 days. Growth scores are shown in the histograms.* indicates the significance levels for 1-way ANOVA with a dunnett's post-test (all compared to non mistranslating control cells). Dashed lines indicate the significance levels for an unpaired two-tailed t-test between each non-mistranslating mutant

strain and its counterpart mistranslating mutant. Histograms show mean ± SEM for three independent clones grown at least 3 times. Ctrl- control; Mist– mistranslation.

Since the accumulation of ROS would be a plausible explanation for the above described phenotypes we have evaluated growth/ viability on solid glucose-containing media in the presence of ROS scavengers (ascorbate and gluthathione). These scavengers improved growth/viability in the control mistranslating strains but this positive effect was neglectible in the *YAP* deleted strains, except for yap1Δ (Figure 26). Similar results were observed when stationary cells were plated in the presence of the same compounds (data not shown). The alleviation of the growth defect points to an intrinsic negative effect of oxidative stress on cellular viability.

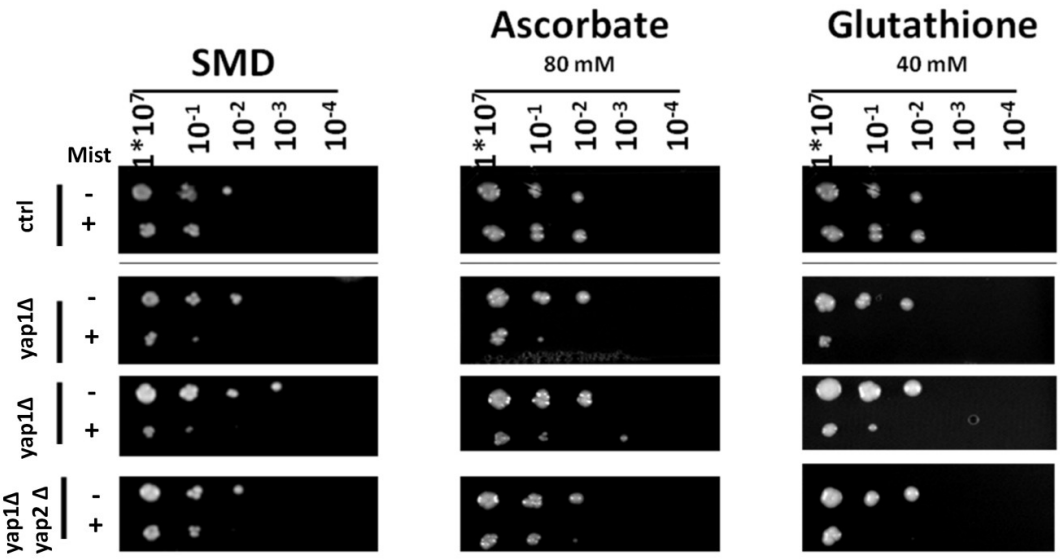

	Mist	SMD	ASC	GLU	statistical significance (1-way ANOVA)
ctrl	-	1,0	1,4	1,3	***
	+	0,5	1,5	1,3	***
yap1Δ	-	1,2	0,9	1,5	ns
	+	0,5	1,0	2,1	**
yap2Δ	-	0,8	1,0	1,3	ns
	+	0,4	2,0	4,0	ns
yap1Δyap2Δ	-	1,0	3,0	3,5	ns
	+	0,4	0,7	1,1	ns

Figure 26- Effect of ROS scavengers in cell's survival. Representative images of mistranslating cells grown on plates in the presence of different ROS scavengers. In the table below, growth scores are shown. Each strain was normalized to the control non-mistranslating strain in the respective plate and then the normalized scores for each condition were averaged and compared. The statistical analysis refers to 1-way ANOVA test between each condition and SMD condition, for each strain. The data refer to at least two independent experiments – 2 different clones). Ctrl- control; Mist- mistranslating.

SIR2 role on ROS management in response to mistranslation

Since mRNA mistranslation up-regulates *PNC1* and increases Sir2p activity (Silva et al., 2009) and the latter is involved in the reduction of ROS levels in yeast progeny, we have decided to investigate the role of these genes in the cellular response to mistranslation, in particular in ROS detoxification. Deletion of *PNC1* alone increased H_2O_2 accumulation as indicated by DHR123 fluorescence (Figure 27), which is in line with work published by others (Tahara et al., 2007). Deletion of *SIR2* did not result in H_2O_2 accumulation and the effect of mistranslation in this background was similar to that observed in the control mistranslating cells. In stationary phase, mistranslation increased notoriously the accumulation of H_2O_2 regardless of the strain background. Comparison of both phases of growth, showed that H_2O_2 accumulates in higher

amounts in exponential phase (Figure 27, A). When using DHE as ROS indicator (Figure 27, B), it was also clear that mistranslation increased ROS accumulation. *SIR2* or *PNC1* deletions contributed slightly to O_2^- accumulation in both stages of growth. However, and as stated above, in exponential growth phase, ROS accumulation, namely H_2O_2, was more notorious in the pnc1Δ background and it seems to be due to the deletion of *PNC1 per se*. Also interesting, was that pnc1Δ deleted cells had tendencially more O_2^- content and that mistranslation notorious increased this compound accumulation O_2^- in pnc1Δ cells (Figure 27 B, upper histogram).This strongly supports a role for Pnc1p in ROS detoxification. Conversely, the *SIR2* deletion led to a clear accumulation of O_2^- in stationary phase mistranslating cells, the latter being consistent with the role for *SIR2* in the control of oxidative damage (Erjavec and Nystrom, 2007), specially in O_2^- detoxification in non-dividing cells. Although H_2O_2 and O_2^- accumulate in mistranslating cells, they followed opposite trends in exponential and stationary phases, in the majority of the strains tested. While H_2O_2 accumulated in exponential phase, O_2^- accumulated mainly in stationary phase. As before, PI staining was used to evaluate DHR123 specificity that guaranteed that ROS results were faithful (Supp.Figure 15). Therefore our data indicate that *PNC1* and *SIR2* play active roles in ROS detoxification in both mistranslating and control cells but this role is dependent both on the oxidative compound and the phase of growth of the cells.

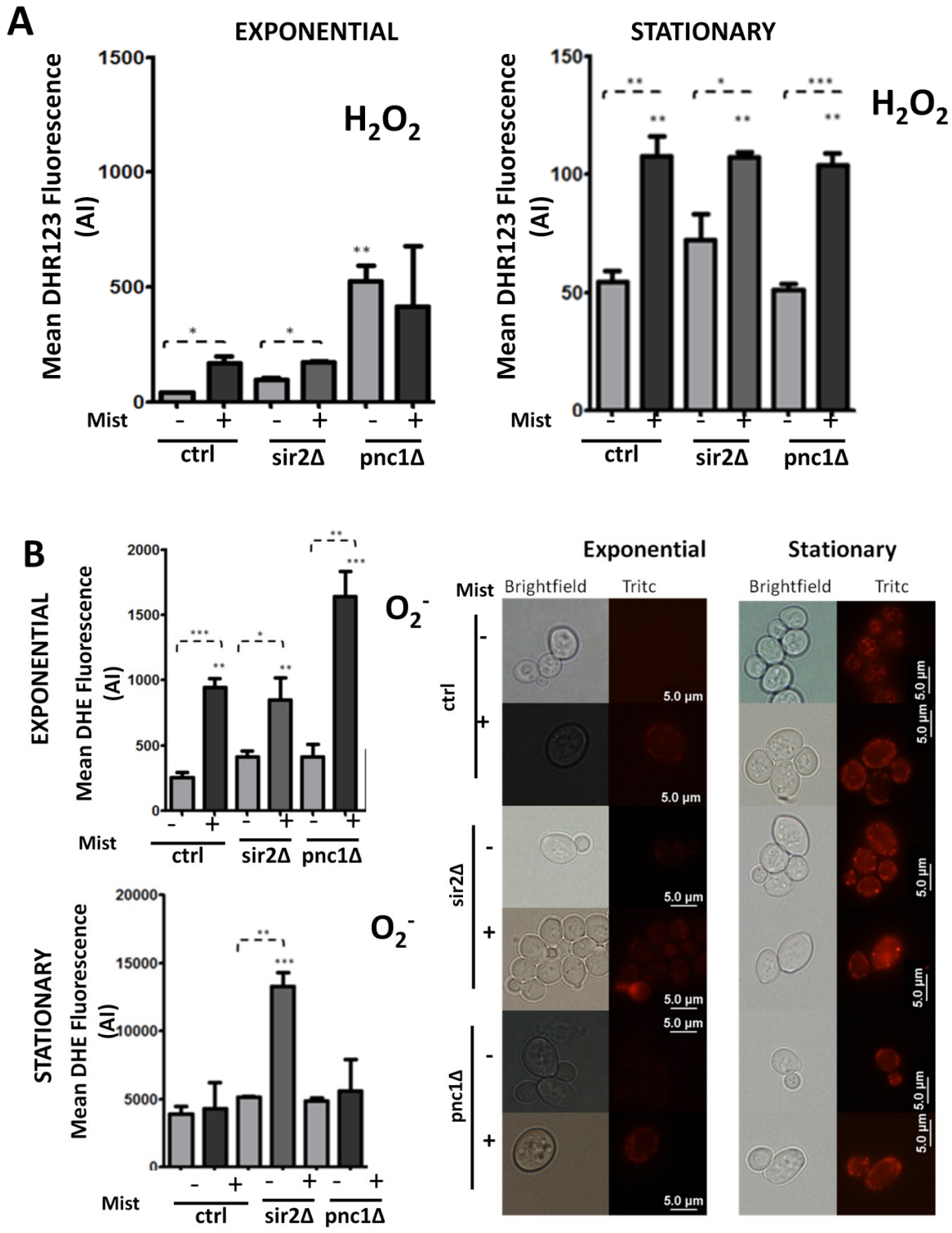

Figure 27- ROS accumulation in SIR2 and PNC1 deleted strains. A) H_2O_2 quantification, using dihydrorhodamine 123. **B)** O_2^- quantification, cells stained with DHE**.** Cells in exponential growth phase or in stationary phase were analyzed using FACS. Data analysis was performed with FlowJo ® software. Histograms show intracellular ROS levels, expressed as mean fluorescence intensities (RFU)**.** Epifluorescence and phase-contrast micrographs of control and mistranslating cells stained with dyhydroethidium (DHE) are also shown. * with no line indicate significance levels for 1-WAY ANOVA, all

compared to ctrl (dunnet's test); dashed lines indicate significance levels for two-tailed t-test. n= 2 to 4 independent cultures, corresponding to at least 2 different clones ($p<0.05$)

Recently, a role for PNC1p in the response to oxidative stress has been proposed (Minard and ister-Henn, 2010), which would be consistent with the H_2O_2 accumulation reported above for the pnc1Δ mutant and also would justify the increased expression of this gene observed in mistranslating cells. Indeed, the authors of that study showed that the function of Pnc1p is related to its function on the NAD^+ regulation levels. In fact, Pnc1p is a key enzyme in the NAD^+ salvage pathway. NAD^+ is used to produce NADP by NAD-kinase action which is then converted to NADPH in the pentose phosphate pathway. The latter is an essential cofactor for antioxidant systems involving glutathione and thioredoxin. This means that cells with high ROS content and that have active antioxidant defense mechanisms have higher NAD^+ needs. Therefore, to test the hypothesis that Pnc1p up-regulation in mistranslating cells could be due to the need of increasing the cellular levels of NAD^+, we decided to quantify the levels of both NAD (H) and NADP (H) in mistranslating cells. Our control cells had 3.3 ± 1.7 mM of NAD^+ content which is consistent with values reported by others for yeast cells grown under standard conditions (Lin et al., 2004; Sporty et al., 2008; Anderson et al., 2002; Evans et al., 2010). The NAD^+ concentration almost duplicates in the control cells exposed to mistranslation (Figure 28, A). This supports the previously observed content of H_2O_2 as it is consistent with data reported by others that showed an 3 fold increase in NAD^+ content in cells exposed to H_2O_2 (Castegna et al., 2010). Additionally, in the pnc1Δ background, a sharp decrease in NAD^+ was detected, fact that is consistent with the abrogation of the NAD salvage pathway and indicates that the

assay was working properly. Deletion of *SIR2* increased NAD^+ levels, which can be in part explained by the fact that, in the absence of Sir2p, NAD^+ is not used in NAD-dependent deacetylation reactions carried out by this deacetylase. However, this is arguable as other authors have observed that sir2Δ had similar NAD^+ levels as wild-type controls, indicating that Sir2p was is not a major consumer of NAD^+ (Anderson et al., 2002). On the other hand it should be noticed that *SIR2* deletion does not necessarily abrogate the salvage pathway as other sirtuins, namely Hst1, Hst2 and Hst3 can replace Sir2p (Anderson et al., 2002). In the light of these results it is plausible to speculate that the NAD^+ salvage pathway may be the primary mechanism for the increase in the levels of NAD(H) in mistranslating cells, when the cellular needs excess the normal physiological levels. NADH levels of control cells were within the limits reported by Sporty and co-workers (Evans et al., 2010). Mistranslation decreased NADH levels by 50%. Decrease in NADH concentration has been described before for cells under calorie resriction conditions (CR) (Evans et al., 2010; Sporty et al., 2008). The knockouts studied decreased intracellular NADH levels, however in the sir2Δ, NADH increased relative to the non-mistranslating cells. Mistranslation increased the NAD/NADH ratio in all strains. This increase was more notorious in control mistranslating cells. The increase in the ratio of oxidized (NAD^+) to reduced (NADH) metabolite is consistent with an increase in oxidative metabolism and rapid delivery of NADH to the respiratory chain. However, given the altered mitochondrial morphology and the respiration defective phenotype observed (see below) one would expect a decrease rather than an increase in NAD^+/NADH ratios, because NADH should not be efficiently oxidized to NAD in the mithocondrial respiratory chain. Also increased

NAD^+/NADH ratios have been reported to be related to enhanced respiratory rate and Sir2p activation (Lin et al., 2004). Still, one must notice that these experiments were performed in actively growing yeast cells that rely mainly on fermentation rather than on respiration. Additionally, the difference found in NAD^+/NADH ration supports a redox imbalance provoked by mistranslation, which was previously antecipated by the increased ROS levels. Regarding the intracellular concentration of NADP in control non mistranslating strain, it was in line with the 10 nmol/mg protein reported by Hector and co-workers (Hector et al., 2009).Mistranslation in control background decreased NADP (H) levels slightly but no major changes were noticed on the other strains tested. The fact that steady states of NADPH do not vary significantly does not exclude the hypothesis that this cofactor is being rapidly used/recycled, that is, all the systems (NAD(H)/NADP(H) sources, antioxidant defenses, etc) are working in a dynamic equilibrium that allows for mistranslating cell survival. Still, given the dynamics of these compounds and the numerous pathways that drive their biosynthesis/consume/recycling conclusions should be cautious.

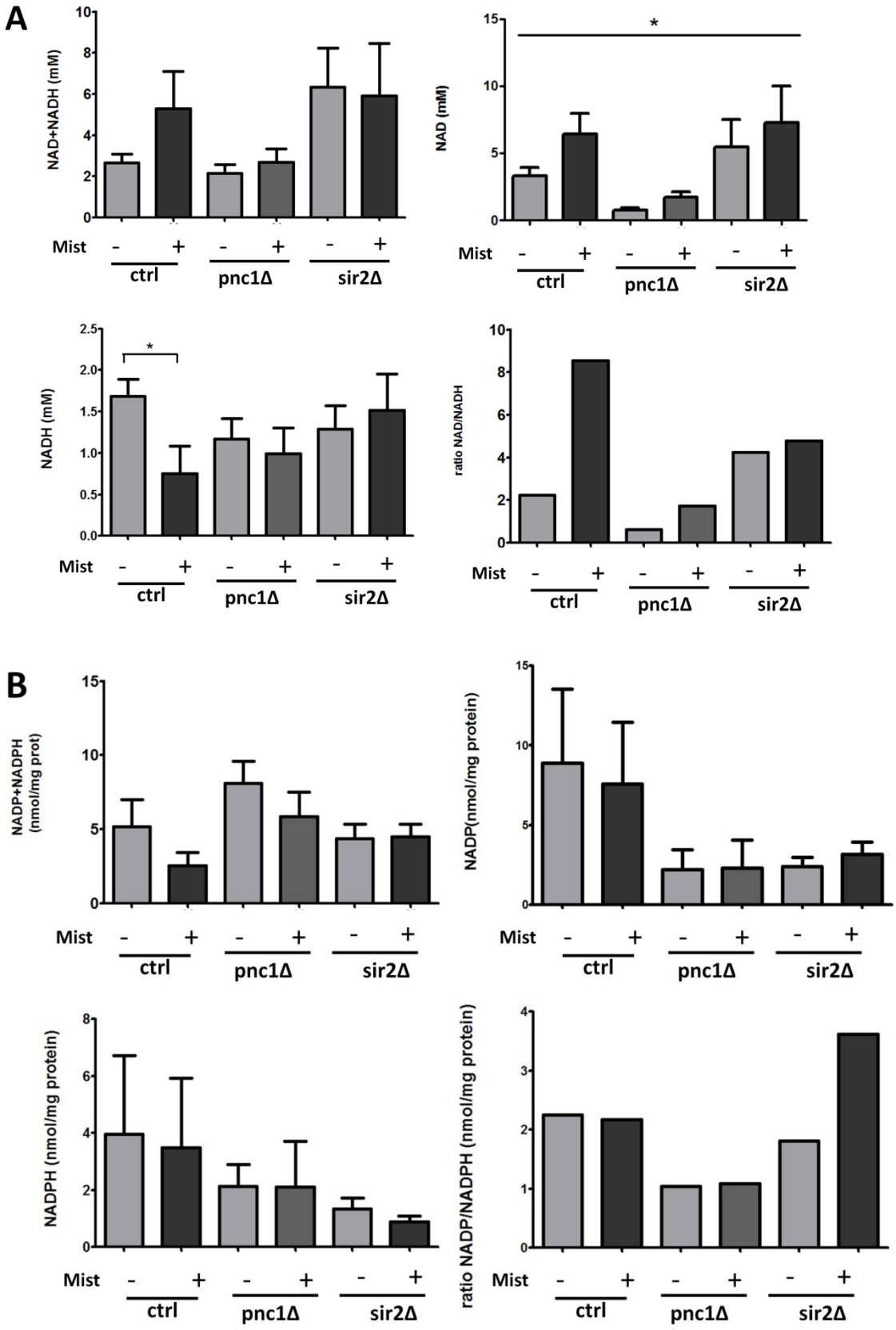

Figure 28- Metabolomics of mistranslating cells- NAD(H)/NADP(H) quantification Cells were grown in selective media (SMD-leu, 20% glucose) to mid-exponential phase and metabolites were extracted has

described in methods. Metabolite concentrations were determined using the Amplite colorimetric NAD/NADH or Amplite colorimetric NADP/NADPH kit. **A) Mistranslation affects NAD/NADH biosynthesis.** NAD^+ and NADH levels are shown as NAD^+, NADH or NAD+ NADH concentration (in micro molar) normalized to the number of cells present in the reaction. **B) Effect of mistranslation on NADP and NADPH metabolism.** NADP, NADPH or NADP+ NADPH levels are shown concentration (in nanomolar) normalized to total protein amount in whole cell extracts. Data are represented as mean ± SEM of at least 2 independent cultures (corresponding to 2 different clones. * with full line represents statistical significance for 1-way ANOVA, Dunnett's post test, all compared to non deleted non mistranslating control, $p<0.05$; * with [square bracket] represents statistical significance for an unpaired student's t-test, $p<0.05$.

As before, additional physiological characterization of these strains was performed but the knockout strains showed in similar phenotypes to the control strains (Figure 29) In other words, ROS scavengers alleviated slightly the growth defects caused by mistranslation, showing that ROS contribute to short term cellular degeneration.

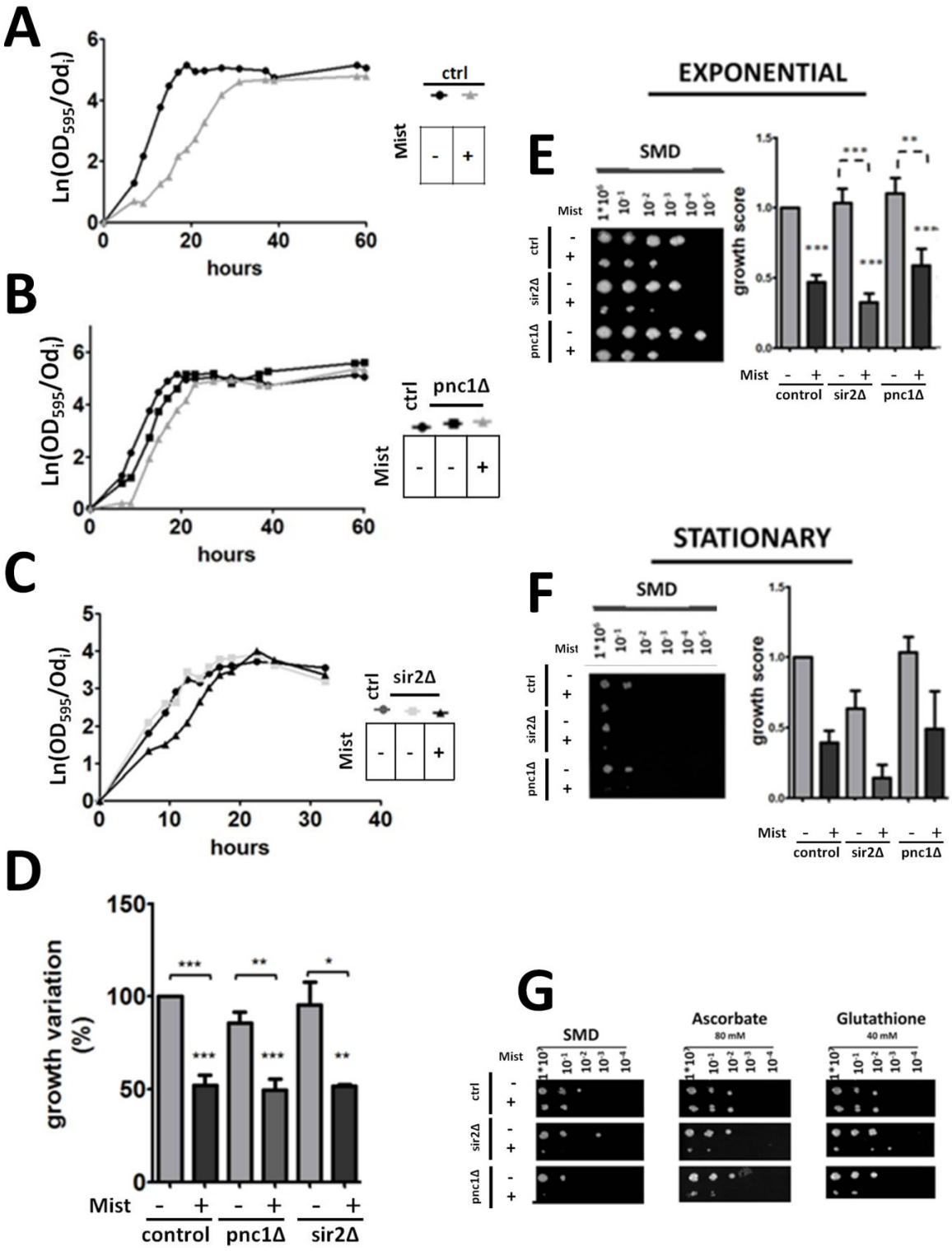

Figure 29- Characterization of pnc1Δ and sir2Δ mistranslating strains. A-D) Mistranslation affects growth in different genetic backgrounds – Growth profiles of mistranslating yeast strains harboring knockouts in the *PNC1* and *SIR2* genes. Cultures were grown in 50 ml flasks at 30°C and growth was monitored at OD_{595} nm. Representative plots of at least 3 independent cultures corresponding to 2 different clones are shown. OD_{595}nm values were normalized using OD_{595}nm

values at T0, to compensate for possible differences in the initial inocula. For each time point, the normalized OD values were transformed to a Ln scale (Toussaint and Conconi, 2006). In D) the histogram shows relative growth variation determined using the specific growth rate values of each clone, which were calculated using the slope of the regression line. The values represent the growth variation relative to control cells transformed with the pRS315 vector alone. The histogram shows the average results ± SEM for at least 3 independent experiments/biological replicates (clones) and * indicates the levels of statistical significance for 1-way ANOVA, dunnett's test (comparison to control, non mistranslating cells), $p<0.05$. Dashed lines indicate statistical significance for an unpaired two-tailed t-test between the each of the mutant control and its mistranslating counterpart. **E) Viability and growth variability of exponentially and quiescent cells in solid media.** Cells were initially grown in liquid media and were then aliquoted at the indicated time points. Cell number was normalized, serial dilutions were prepared and cells were spotted into solid media with the help of a robot. Plates were incubated at 30ºC for 4 days. Growth scores are shown in the histograms.* indicates the significance levels for 1-way ANOVA with a dunnett's post-test (all compared to non mistranslating control cells). Dashed lines indicate the significance levels for an unpaired two-tailed t-test between each non-mistranslating mutant strain and its counterpart mistranslating mutant. Histograms show mean ± SEM and scores are the result of the analysis of three independent clones grown at least 3 times Control cells, both mistranslating and non mistranslating, grew similarly in both liquid and solid media showing good consistency between both tests. The decrease in viability was confirmed for both time points. As for sir2Δ cells the results of both tests were more consistent in exponential phase than in stationary phase. Interestingly, the pnc1Δ strain, grew better than the control strain in the same conditions but showed poor growth consistency between solid and liquid media.**F) Effect of ROS scavengers on cell's growth.** Representative images of mistranslating cells growing on plates containing different ROS scavengers are shown. Both ROS scavengers had a positive effect on the growth of sir2Δ and pnc1 Δ mistranslating strains.

Since previous data showed that mistranslation increases tolerance to oxidative agents (Miranda et al., 2007; Santos et al., 1999; Silva RM et al., 2007), we have evaluated whether our mutant cells were tolerant to oxidative stress. For this, yeast cells were grown in solid media containing menadione, which is a known O_2^- generator, or H_2O_2. Mistranslation increased sensitivity to menadione and increased resistance to H_2O_2, which is in line with previous result from our laboratory (Silva RM et al., 2007). The *SIR2* deletion *per se* did not increased H_2O_2 sensitivity, which is also in line with the previous studies (Fabrizio et al., 2005), but mistranslation in this genetic background severely affected resistance to both stressors. Interestingly, in the pnc1Δ background

mistranslation increased resistance to menadione but not to H_2O_2 (Figure 30), which is also in line with other reports (Tahara et al., 2007).

We have further tested the ability of quiescent mistranslating cells (stationary phase cells) to survive in the presence of additional oxidative stress, as in general quiescent cells tend to be more resistant than rapidly dividing ones. For this, cells were grown for 36h (d1 stationary phase), 7 or 14 days in liquid culture and then plated in medium containing the additional stressor. Both control and knockout mistranslating strains were highly sensitive to menadione (Figure 30 B). Similar results were obtained for the non-mistranslating cells, although these cells were still able to grow slowly. In SMD (no stress besides mistranslation) there was a clear difference in stress sensitivity between mistranslating and non-mistranslating cells (Figure 30, B). Hydrogen peroxide affected the survival of both control and mistranslating cells, but the latter showed a stronger loss of viability. In general, control and mistranslating cells grown for 7 days showed decreased survival in both presence and absence of mistranslation (Figure 30, B). Similar analysis of the *YAP* deleted mutants showed that mistranslating cells had either severe or augmented sensibility to the oxidative stressors (Supp.Figure 16). As expected the *YAP1* deletion increased sensitivity to all oxidative stressors and this effect that was clearer when mistranslation was induced in this genetic background.

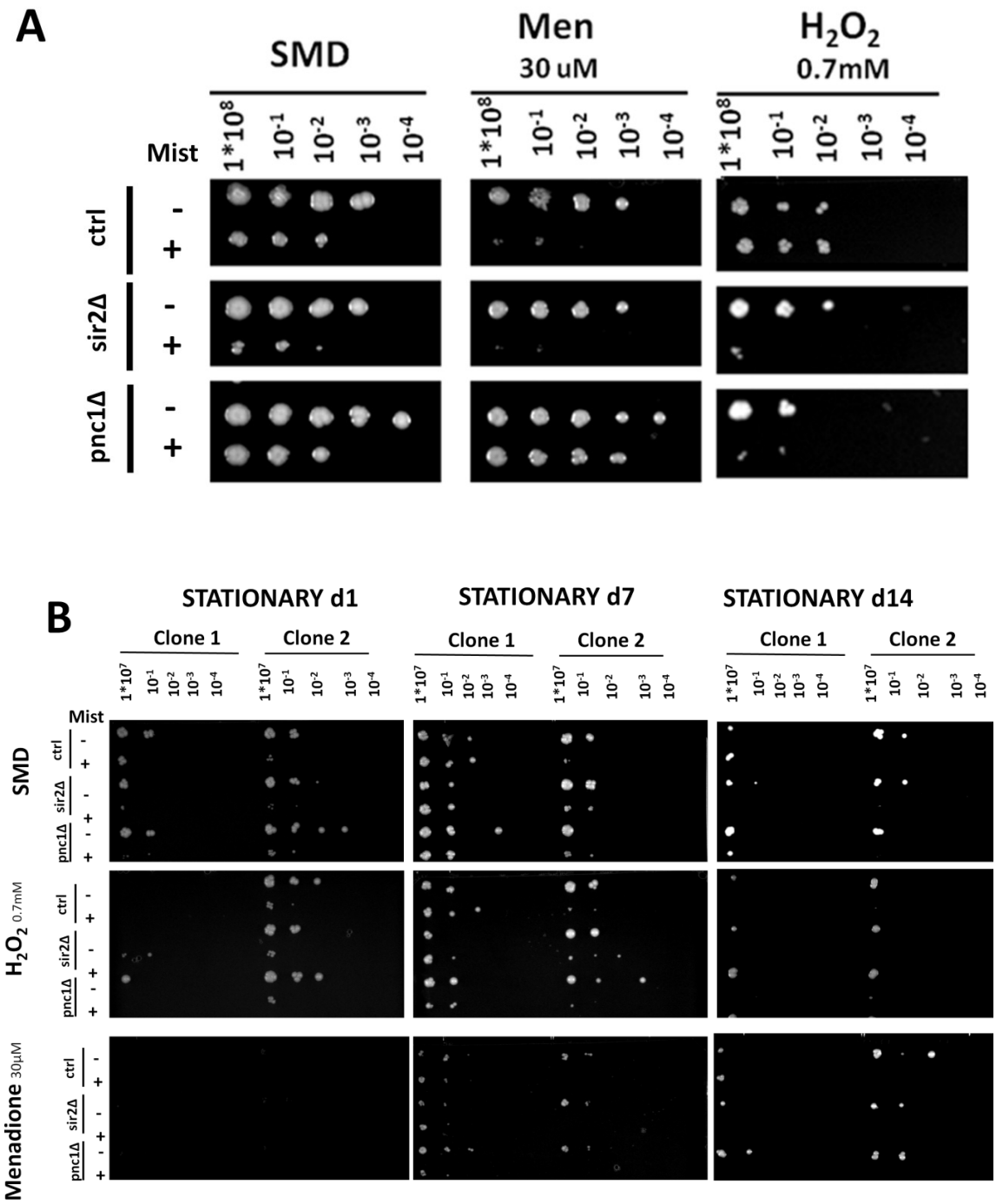

Figure 30- Resistance of mistranslating cells to exogenous oxidative stressors – A) Exponential phase cells. B) Stationary phase cells. Cells were grown to exponential phase **(**A) or left in culture for longer periods. At each time point, an aliquot was removed and cells were counted. Identical number of cells was used to prepare serial dilutions ($1x10^7$cells) for inoculation on solid media supplemented with different stressors. Inoculations were performed using a robot. A non mistranslating control and a mistranslating control strain were always

included on each plate to correct small differences in the batch of media. Representative images from at least two independent experiments are shown, corresponding to at least two different clones. Ctrl –control cells; Mist- mistranslation; + or – refer to mistranslation or no mistranslation respectively.

Mistranslation induces alterations on mitochondrial morphology

As shown above, mistranslation up-regulated oxidative stress response genes which are involved in reduction of hydroperoxide and superoxide-radicals and in maintaining the redox state of target cytoplasmic, ER and mitochondrial resident proteins and in protecting cells from lipids peroxidation (Table 4). Besides, other up-regulated genes are related to mitochondrial function (Supp.Table 2). This is consistent with increased production of ROS by the mistranslating cells, also shown above.

These observations prompted us to investigate whether mistranslation caused mitochondrial dysfunction and, consequently, higher rate of mitochondria turnover. For this, we have used the Om45-GFP assay, which has been developed to quantify mitophagy (Kanki et al., 2009a) as well as the concentration of the mitochondrial outer membrane protein Om45p. The Om45p tagged with the green fluorescent protein (Om45-GFP) localizes to the mitochondrial outer membrane and accumulates in the vacuole when mitophagy is induced (Kanki et al., 2009a). The fused protein is degraded in the vacuole while GFP is stable allowing for monitoring mitophagy through immune-blotting or epifluorescence microscopy (Kanki et al., 2009a). Interestingly, morphological changes in the mitochondrial network were observed. Control cells

exhibited a clearly differentiated mitochondrial network while mistranslating cells showed mitochondrial network fragmentation and disappearance in both exponential and stationary phase cells (Figure 31). In mistranslating cells these changes in mitochondrial morphology were accompanied by a negligible delivery of GFP into vacuoles (1.18% in exponential cells, 4.97% in stationary phase cells). This indicates that 1) mistranslating cells have a low fusion-to-fission ratio and, therefore, have numerous mitochondria, by opposition to control cells, that have high fusion-to-fission ratio, and have low number of mitochondria, which are highly interconnected (Bleazard et al., 1999; Chen et al., 2005; Chen and Chan, 2005; Chen et al., 2003; Sesaki and Jensen, 2001; Jensen et al., 2000) and 2) mitophagy was not activated. Despite these dramatic changes in mitochondrial morphology, no differences were found in the expression of genes known to be crucial for mitochondria morphology regulation (Supp.Table 3) suggesting that mistranslation effects on this organelles morphology is not due to alterations at the gene expression level. Stationary phase control cells showed patches of mitochondria localized on the cell periphery rather than the mitochondrial network or vacuolar fluorescence. Late stationary phase cells (5 and 7 days) (Supp.Figure 18) showed low level of vacuolar fluorescence. Disruption of the mitochondrial network was still observed in mistranslating cells and the differences between control and mistranslating cells was attenuated as the former had more mitochondrial fragmentation in stationary phase (Supp.Figure 19). This was in line with published data showing that 48h yeast cultures start showing mitochondrial fragmentation and tubules tend to be shorter (Bossy-Wetzel and Lipton,2003; Bossy-Wetzel et al., 2003; Palermo et al, 2010).

In order to confirm our phenotype we have tested the capacity of acetyl-L-carnitine (ALC) to attenuate mitochondrial fission (Palermo et al., 2010). Indeed, ALC addition to the medium tended to attenuate both mitochondrial fission induced by mistranslation (91.3% untreated vs 88.7% treated) and natural occurring mitochondrial fission (16.7% untreated vs 7.4% treated) (data not shown), indicating that control cells are apparently more responsive to ALC than mistranslating cells. This is similar to the phenotype observed in aging cells, where the protective effects of ALC were higher in respiratory competent cells rather than in respiration defective cells (rho^0) (Palermo et al., 2010).

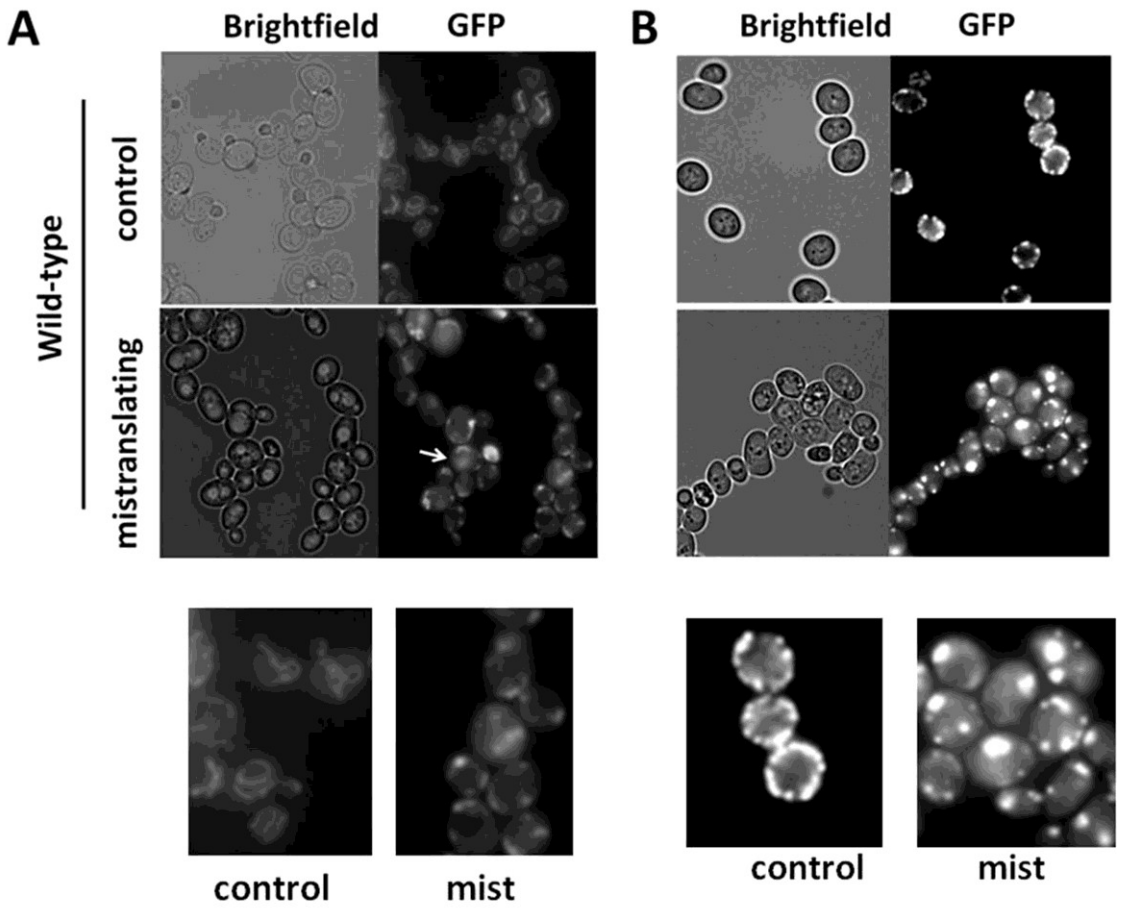

Figure 31- Mistranslation alters mitochondrial morphology. Cells expressing an Om45-GFP fusion were grown in YPD until mid-exponential phase (A) or to stationary phase (B) and were

observed by fluorescence microscopy in order to access mitochondrial morphology and activation of mitophagy. In the squares below, details are shown. Control - non mistranslating cells; mist- mistranslating cells. Enlarged view shown in supp.figure 18.

Western blot analysis confirmed the absence of free GFP in either growth phase indicating that mitophagy is not a major feature of the cellular response to mistranslation (Figure 32). Given our microarray data, that showed a 3.3 fold up-regulation of the *OM45* gene (Supp.Table 2) we were expecting to detect increased cellular content of this protein in mistranslating cells. However, this was not the case, suggesting a delay in translation of the *OM45* mRNA, which may be indicative of post-translational regulation. Also, we cannot completely exclude the possibility of mitochondrial autophagy in the mistranslating cells, because mitophagy has only been described in cells growing in lactate, and we were not able to perform this assay in lactate containing medium, as the mistranslating were not capable of growing on respiratory substrates (see below).

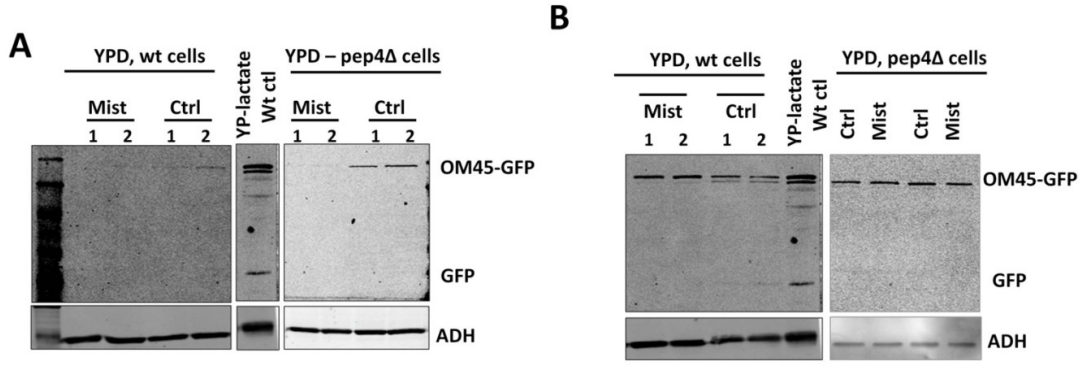

Figure 32 –Mistranslation does not induce mitophagy. Mitophagy was additionally verified by western blotting against GFP. A pep4Δ strain was included in the analysis, as a negative control, since this strains is mitophagy defective (Kanki et al., 2009a). As a positive control, control cells grown in YP-lactate were used. Control and mistranslating cells were grown in YPD until exponential phase (A) or stationary phase (B), collected and protein extracts were

prepared. Total extracts were fractionated by SDS-PAGE, transferred to nitrocellulose membranes and probed against GFP. ADH was used as a loading control. Two different clones for each strain are shown (indicated by 1 and 2). Ctrl-control cells; mist-mistranslating cells.

Mistranslation generates a respiratory deficiency phenotype

The alterations in mitochondrial morphology described above prompted us to investigate whether mistranslating cells were respiration defective. Surprisingly, mistranslating cells were completely unable to grow on respiratory substrates (Figure 33, A) namely lactate, acetate, glycerol and ethanol, supporting our hypothesis that mistranslation strongly affects mitochondrial function. Interestingly, ROS scavengers were not capable to rescue this growth deficiency phenotype demonstrating a strong impairment of mitochondrial function (Figure 33, B).

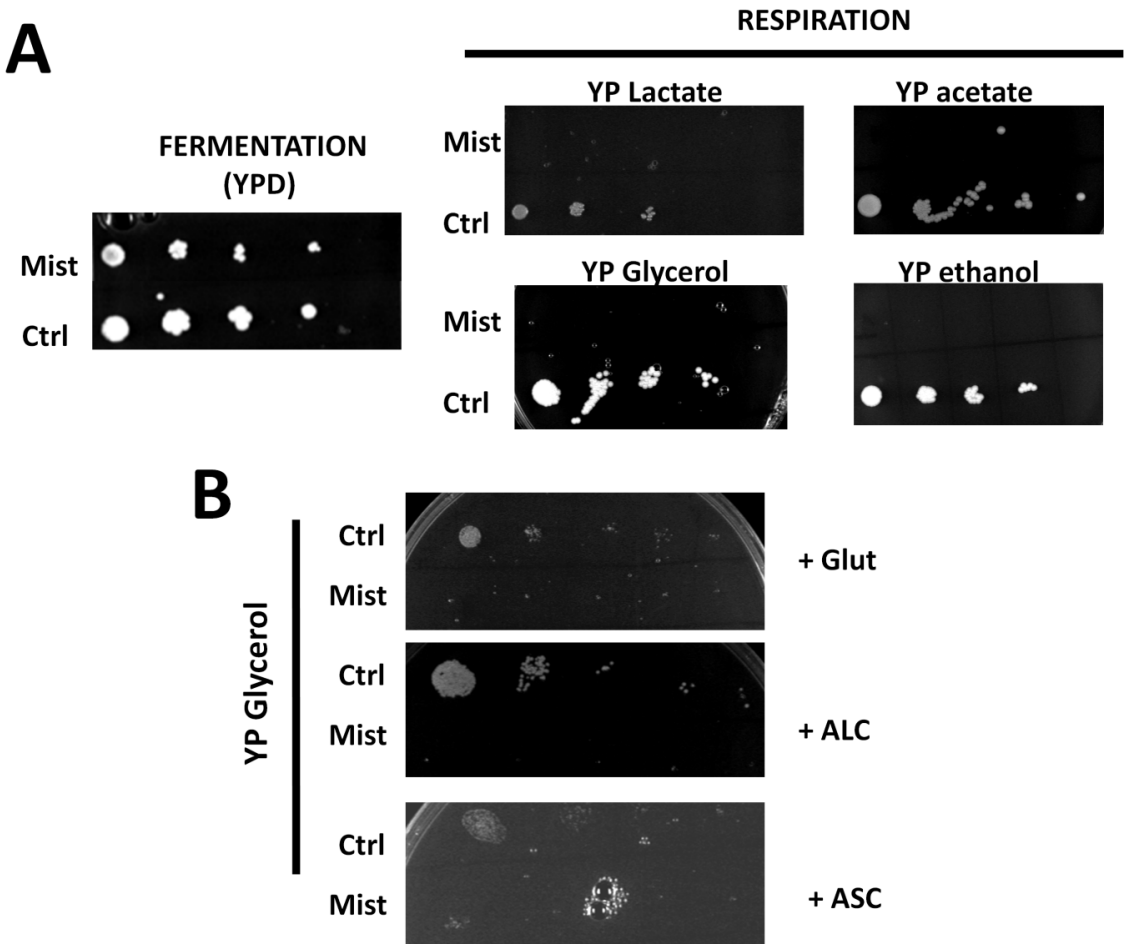

Figure 33-Mistranslation induces a strong respiratory deficiency – A) Cells were grown for 36h in liquid media and spotted on YPD (fermentative medium) or YPlactate, YPglycerol, YPethanol or YPacetate (respiratory media), in dilution series (starting on 1 x 10^7 cells). Proliferation of mistranslating cells was low on YPD and was abolished under respiration conditions (n= 2, different clones). Similar results were obtained when cells were plated on the same conditions, using exponential growing cultures as inocula. B) Cells were spotted in a respiratory substrate containing media supplemented with ROS scavengers' compounds. Similar results were obtained with other respiratory substrates and also when the same experiment was done in exponentially growing cells (data not shown). Ctrl- control non mistranslating cells; mist- mistranslating cells; Glut- glutathione 40mM; Asc- ascorbate 80mM; ALC- l-acetyl-carnitine 1mM.

In order to further validate this hypothesis, the transcriptomic profile of mistranslating cells was compared to that of respiratory incompetent rho^0 cells (ρ^0). These petite cells up-regulated the expression of genes related to peroxisomal activities, small molecule

transport systems and lipid, sugar, and amino acid turnover in order to increase the availability of OAA, acetyl-CoA, and propionyl-CoA for biosynthetic reactions (namely to overcome the block in the TCA cycle) (Epstein et al., 2001). We have found that 40% of the 43 genes of ρ^0 cells accepted as a fingerprint for respiratory deficiency (Epstein et al., 2001), were also deregulated in the mistranslating cells (Figure 34). Therefore, these data provide strong evidence for the respiratory deficiency phenotype.

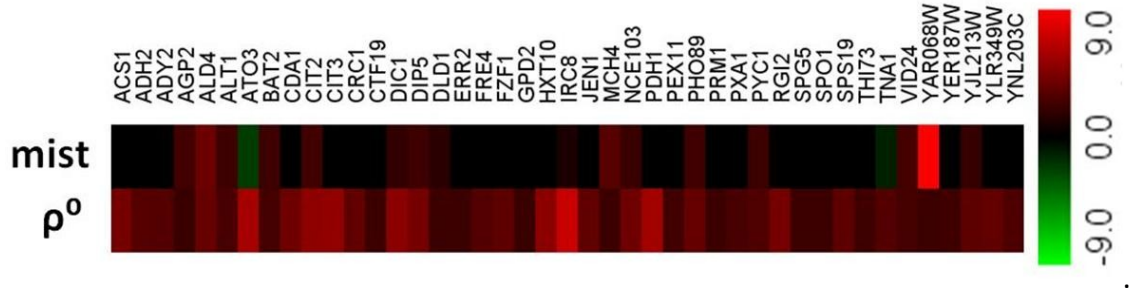

Figure 34- Comparison between the transcriptome profiles of mistranslating and petite (ρ^0) cells. mRNA expression profiles of mistranslating and ρ^0 cells were compared using the subset of 43 genes defined to be up-regulated in respiratory incompetent ρ^0 cells (Epstein et al., 2001).

Since the retrograde regulation pathway (RTG), which is an interorganelle communication pathway that regulates the expression of nuclear genes, is involved in mitochondrial function (Parikh et al., 1987), we have also compared the transcriptome profiles mistranslating cells and RTG mutants (Epstein et al., 2001). As before, a good overlap between deregulated genes (36 % - 50%) was observed, further confirming that mistranslation affects mitochondrial function (Table 6). Still, mistranslation did not altered the mRNA expression of the majority of RTG pathway positive (*RTG1, RTG2, RTG3, GRR1*) or negative regulators (*MKS1, LST8, BMH2*) with the exception on *BMH1*,

which was found to be up-regulated (data not shown). The relevance of the latter is not clear because the regulatory mechanism known involve (de)phosphorilation, ubiquitination and translocation reactions rather than just expression changes.

Table 6- Genes whose expression is altered in mistranslating cells compared to the expression profiles of ρ^0 and RTG mutant cells. 43.8% of the genes whose induction is dependent on RTG genes and are up-regulated in ρ^0 cells showed the same trend in mistranslating cells. On the other hand, 50% of the genes that are repressed by RTG genes (and, therefore, show induced expression on RTG mutants when compared to ρ^0 cells have the same behavior in mistranslating cells. A similar situation is observed for genes whose expression is independent on RTG genes (show induced expression on ρ^0 cells as well as in mistranslating ones,36.4% overlap) (Epstein et al., 2001).

genes up regulated in ρ^o cells (induction dependent on RTG genes)

Gene Name	expression in mist cells
REE1	unchanged
SUC2	unchanged
PHO84	UP
PDH1	unchanged
CIT2	UP
CIT3	unchanged
SLZ1	unchanged
SPL2	UP
ACO1	UP
IRC14	unchanged
BIO2	unchanged
IZH4	unchanged
IDH2	UP
LEU1	UP
CIT1	UP
YBL042C	unchanged

genes up-regulated in RTG mutants (relatively to ρ^o, i.e expression repressed by RTG)

Gene Name	expression in mist cells
YOR107	unchanged
YER158C	UP
AGP1	UP
TIS11	unchanged
PUT2	UP
PUT1	UP
CAR1	UP
YKR075C	unchanged
LEE1	unchanged
HMS1	UP
GAP1	unchanged
MCH5	unchanged
PDR15	UP
YLR346C	unchanged
PIG2	UP
NGR1	unchanged

genes up-regulated in ρ^o cells, but whose expression is independent of RTG

Gene Name	expression on mist cells
YGR259c	unchanged
YDR384C	unchanged
DIP5	UP
PHO89	UP
HXT2	UP
CRC1	unchanged
TNA1	down
JEN1	unchanged
DIC1	UP
ACS1	unchanged
YCR010C	unchanged

Mistranslation does not affect yeast chronological aging

Given the strong respiratory deficiency phenotype, described above one would expect a decrease in longevity of the mistranslating cells because yeast activate respiratory capacity at the beginning of stationary phase, when glucose is exhausted. Therefore, we have tested cell viability of aged cultures using both methylene blue and standard CFU counting assays. As before, we included the *YAP* knockout strains in this analysis. Surprisingly, mistranslation had a minor effect on long-term viability (Figure 35). Similar results were obtained in mistranslating strains harboring deletions in *PNC1* and *SIR2* genes (Supp.Figure 17). Quantitative assessment of cell viability using the CFU assay showed, however, that PNC1 deletion increased yeast viability in the presence or absence of mistranslation (Supp.Figure 17). Interestingly, we have found that 50% of the 32 genes that were previously identified as stationary phase essential genes (SP-essential) (Martinez et al., 2004), were up-regulated in our control mistranslating cells (Table 7). If up-regulation of these genes explains the lack of a viability loss phenotype of the mistranslating, it remains unclear why these cells are not able to grow on nonfermentable carbon sources, since deletion (and not overexpression) of those SP-essential genes is associated with growth defects on nonfermentable carbon sources.

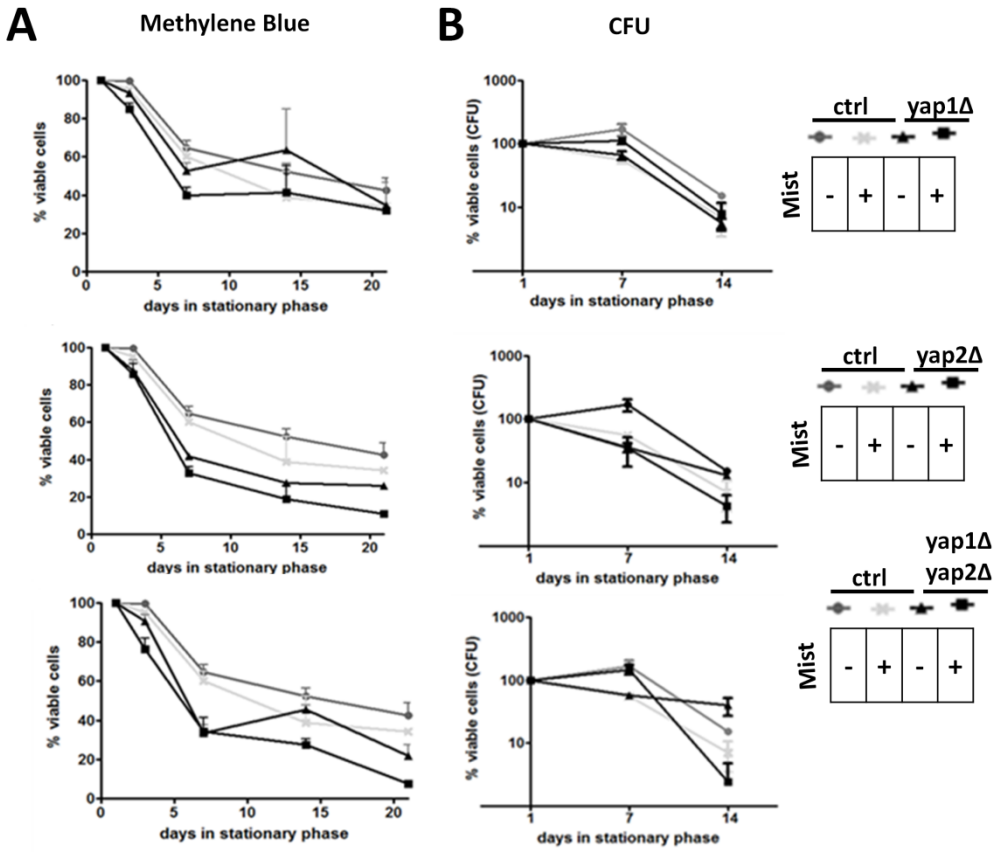

Figure 35- Mistranslation does not significantly affect yeast longevity. Cell Viability was accessed for each mistranslating strain using methylene blue staining **(A)** and CFU formation **(B).** The same cultures were used in both experiments. Cells grown at 30°C in selective medium were either stained with methylene blue or counted and plated on solid medium at the indicated time points. In the case of the methylene blue assay the number of stained (dead) and unstained (viable) cells was assessed by microscopy. A minimum of 300 cells (viable [unstained] and dead [stained] cells) were counted for each time point. Viability at day 1 of stationary phase (post diauxic growth) was considered as 100%. Results shown refer to at least two independent determinations, corresponding to 2 different clones analyzed. Error bar represent SEM. Points with no error bar refer to a single determination.

Table 7- Analysis of the expression profile of SP-essential genes in mistranslating cells. Microarray data analyses were performed using MEV software (TM4 Microarray Software Suite) (Saeed et al., 2006; Saeed et al., 2003b). Data were analyzed based on $\log_2$ ratio (M) values. Genes included in the final dataset exhibited significance based on a FDR median< 0.05, in a SAM 1-class analysis (Salin 2008, Tusher 2001, Saeed 2003, van Helden 2003) . The data was compared to the genes identified as SP-essential by Martinez and co-workers (Martinez et al., 2004).

gene name	fold change	gene name	fold change
ADY2	•	MOH1	2,4
ATP1	1,6	OM45	3,3
ATP2	•	PNC1	2,7
ATP3	•	POR1	1,6
CIT1	1,6	PST2	1,6
COX6	•	QCR7	•
COX7	1,4	RIP1	1,8
CTA1	•	SDH2	1,8
ETR1	1,5	SDH4	1,9
FAA1	•	SOD2	•
FMP45	•	SPG4	•
GLK1	3,2	SPG5	•
GTT1	1,8	SPG3	•
HBT1	•	SPG1	•
KGD1	•	NGR1	2,3
MDH1	1,8		

Discussion

Recent studies show that the biology of mistranslation is relevant to disease, evolution of genetic code alterations and phenotypic diversity (Reynolds et al., 2010; Silva RM et al., 2007; Gomes et al., 2007; Miranda et al., 2007; Moura et al., 2009). Here, we show that mistranslation activates the antioxidant stress response, leads to ROS

accumulation and has a negative impact on the mitochondrial network and mitochondrial function.

mRNA mistranslation, ROS accumulation and antioxidant stress response

Our DNA microarray data show that mistranslation induces the oxidative stress response due to increased ROS production. This did not pre-adapt cells to oxidative stress, rather increase sensitivity and lead to slow growth and decreased short term viability. ROS accumulation may potentiate proteome disruption because protein oxidation reduces or abrogates protein function (Reverter-Branch et al., 2004) and may even trigger the formation of potentially toxic aggregates (Grune et al., 2004), which occurs in mistranslating cells (this study, chapter 2).

Our data suggest that, together with the antioxidant stress response, Sir2p and Pnc1p play a role in minimizing the effects of ROS in mistranslating cells. In fact, sir2Δ mistranslating cells accumulated O_2^-, especially in stationary phase. It is known that Sir2p protects daughter cells by reducing ROS levels and by preventing ROS inheritance from the mother cells. Erjavec and Nystrom (2007) have shown that daughters have less ROS than mothers and that ROS levels are dependent on Sir2p since sir2Δ daughter cells accumulated superoxide and had impaired hydrogen peroxide scavenging (Erjavec and Nystrom, 2007). However, the mRNA levels of *CTT1*, *SOD1* or *TRX2* genes are identical between mother and daughter cells in control and sir2Δ strains and the latter have lower activity of Ctt1p and Sod1p independently of protein concentration. Conversely, mistranslating cells showed increased levels of the *CTT1*

mRNA, both in the sir2Δ background (4.5 fold, data not shown) and in the wild type background (4.9 fold). On the other hand, *PNC1* also proved to be important for ROS detoxification in actively growing mistranslating cells, as we have detected a major accumulation of O_2^- in mistranslating pnc1Δ cells, as well as H_2O_2 accumulation. We propose that this role is related to the primary role of Pnc1p in the NAD^+ salvage pathway which ultimately affects the mistranslating cells antioxidant response. Indeed, *PNC1* encodes a nicotinamidase for the NAD salvage pathway that, when absent, decreases intracellular levels of NAD^+. NAD^+ is used by NAD kinases to produce NADP, which in turn is converted into NADPH in the pentose phosphate pathway. The latter is essential to the antioxidant defenses to work properly. Therefore, deleting *PNC1* significantly decrease the NAD^+ available for convertion into NADPH, leading to accumulation of ROS species. In other words, in mistranslation conditions the up-regulation of the longevity gene *PNC1* seems to be related to oxidative stress response rather than longevity *per se*.

ROS origin in mistranslating cells

Our data do not allow one to identify the source of ROS as they can be produced in the ER, peroxisomes, mitochondria, cytoplasm and cell membrane and the contribution of each of these organelles to ROS accumulation is variable, depending on several different conditionings like the ROS species, the cell type (strain in this case) and physiological conditions (Brown and Borutaite, 2011). For instance, it has been reported that the formation of disulfide bounds leads to production of ER localized H_2O_2 and that high levels of this ROS occur under ER stress (Starkov, 2010) making this

organelle a good candidate for ROS production in mistranslating cells. The ER-derived ROS production is not yet fully understood, but one hypothesis is that maintenance of the oxidative folding capacity of the ER lumen is the main source of ROS since the ER oxidation potential derives from molecular oxygen (Rutkowski and Kaufman, 2007; Tu and Weissman, 2004).

Mitochondria are assumed to be the main source of ROS, but also the target and sink of ROS. They are highly dynamic organelles which vary in number and shape and are capable of undergoing structural alterations through fusion and fission events. In addition, their internal structure can also change in response to physiology which affects mitochondrial function, namely respiratory capacity (Detmer and Chan, 2007). Our data show that mistranslating cells have numerous fragmented mitochondria, accumulate ROS and have marked respiratory deficiency. A possible explanation for the elevated levels of ROS in mistranslating cells could be related to higher number of mitochondria per cell and consequent increased respiratory capacity, because the respiratory chain is responsible for consumption of 90% of the cellular oxygen, 4-5% of which is converted to superoxide radicals (Spitz et al., 2000). However, our data show that mistranslating cells have dysfunctional mitochondria and compromised respiratory capacity as they are unable to grow in respiratory substrates and have gene expression profiles similar those of ρ^0 cells. Therefore, mistranslating cells accumulate dysfunctional mitochondria which may also contribute to ROS accumulation, as decreased mitochondrial respiration may increase ROS production (Hipkiss, 2010) due to leakage of electrons to molecular oxygen, leading to superoxide production (Kwong

and Sohal, 1998; Andreyev et al., 2005). This may also increase mutations in mtDNA. Such higher ROS content could also contribute to increased mitochondria dysfunction creating a positive feedback loop. Moreover, mutant cells defective in mitochondrial energy metabolism or mitochondria biogenesis have twice as much ROS as wild-type cells (Pastor et al., 2009), further supporting the hypothesis that dysfunctional mitochondria are a likely source of ROS in mistranslating cells.

Mistranslation and mitochondrial physiology

The fragmented mitochondrial network is very interesting since fusion and fission events control shape, size and number of mitochondria (Nunnari et al., 1997). This phenotype suggests disruption of the fusion and/or fission machinery. However, our DNA microarray data indicate that mistranslation does not affect expression of genes involved in mitochondrial morphogenesis, suggesting that the observed phenotype is likely a consequence of protein loss-of-function or arises due to ER stress. Indeed, it is known that ER and mitochondria exhibit tightly coupled dynamics, metabolism and extensive contacts. These contacts increase under ER stress (Bravo et al., 2011), are microtubule dependent and facilitate Ca^{2+} transfer from ER to mitochondria, enhancing mitochondrial respiration, reductive power and ATP production. One type of ER-mitochondria contacts is known as the ERMES (Endoplasmatic reticulum – mitochondrial encounter structure) protein complex, which is composed both by ER and mitochondrial proteins. ERMES is located at the interface of both organelles and serves to zipper them together. Mutations in ERMES proteins lead to mitochondrial morphology defects and inability of cells to grow on non fermentable carbon sources.

As ERMES mutants show frequently loss of mtDNA it is also plausible that mutations in proteins of this complex can be involved in the fusion/fission phenotype observed in mistranslating cells. Furthermore, mitochondrial fission occurs at regions of contact between mitochondria and ER that are characterized by ER tubules crossing and enwrapping mitochondria (Friedman et al., 2011) suggesting that ER-stress affects ER structure, tubule structure and mitochondrial fission.

Whatever the mechanism involved, mitochondrial fission and fusion events in mistranslating cells deserve further attention because fusion allows exchange of lipid and intramitochondrial contents, which is crucial for maintaining a healthy population of mitochondria (Chen et al., 2005; Detmer and Chan, 2007). That is, lower rate of lipid and intramitocondrial content interchanges in mistranslating cells may result in lack of dilution of damaged mitochondria, because dysfunctional mitochondria normally fuse to normal ones allowing the former to regain the essential mitochondrial components. This may not happen in mistranslating cells. Moreover, mtDNA, which encodes essential subunits of the respiratory complexes that are essential for oxidative phosphorylation, is organized in structures named nucleoids. When mitochondrial fusion is abolished a large fraction of the mitochondrial population loses mtDNA nucleoids, leading to reduced respiratory capacity (Chen and Chan, 2010; Gorsich and Shaw, 2004). Indeed, yeast strains that have lost their mtDNA are unable to grow on non-fermentable carbon sources (Goldring et al., 1971; Goldring et al., 1970). Therefore, it is likely that the defects observed at the respiratory level, could be explained by defects on mitochondrial fusion. On the other hand, mitochondrial fission

has been associated to apoptosis, although it is not a pre-requisite for it to happen (Detmer and Chan, 2007). Indeed, during early phase of cell death, mitochondria become fragmented due to an increase in fission activity. Mitochondrial outer membrane permeabilization (MOMP) and release of mitochondrial inner components, namely cytochrome c, to the cytoplasm occur. Cytochrome c release activates a cascade of caspases that propagate and execute apoptotic program (Arnoult, 2007; Youle and Karbowski, 2005). This leads to the question of why mistranslating cells do not have an apoptotic phenotype? A likely explanation is that, in mistranslating cells, there is no MOMP, which could indicate that the fragmentation of the mitochondrial network is not due to mitochondrial dysfunction.

We were unable to detect increased mitophagy in mistranslating cells, which suggests that they may not have damaged mitochondria, but rather normal mitochondria lacking the typical organization of the macromolecular network. In general, dysfunctional mitochondria have a reduced fusion capacity and become spatially separated from the intact network which makes them more prone to degradation by mitophagy, but a recent yeast study showed that mitochondrial fission is not a prerequisite for selective degradation of mitochondria (Mendl et al., 2011). On the other hand, mitophagy can be blocked by strong macroautophagy induction (Kanki et al., 2009b) or by N-acetylcysteine (NAC) under nitrogen starvation conditions or rapamycin treatment, because of the cellular redox imbalance, as NAC increases the pool of cellular reduced glutathione (Deffieu et al., 2009; Okamoto et al., 2009a; Okamoto et al., 2009b; Kissova and Camougrand, 2009). Accordingly, an increase in

gluthatione levels in mistranslating cells could also explain the lack of mitophagy. Finally one cannot exclude the possibility that mistranslating cells may degrade mitochondria by a non-selective pathway or rely on the activity of intrinsic mitochondrial proteases like Oma1p or Yme1p (Oma1p is activated upon mitochondrial dysfunction in mammalian cells), or ubiquitin-proteasome dependent degradation of mitochondrial proteins.

Mistranslation and metabolism

The negative impact of mistranslation on mitochondrial biology respiratory capacity can also be evaluated from another perspective. Increased respiration rates are correlated with highly interconnected mitochondrial networks (increased fusion), while decreased oxidative phosphorylation and increased glycolysis are linked to fragmentation of the mitochondrial network (fission) and mitochondrial matrix expansion (Alirol and Martinou, 2006). Therefore, it is possible that mistranslation leads to decreased oxidative phosphorylation and increased glycolysis similarly to the Warburg effect described in cancer cells, which is characterized by intense glycolysis and decreased respiration even in the presence of oxygen. It is well documented but remains unexplored at the mechanistic level, although it is assumed that it originates from increased glucose uptake and glycolysis and/or down regulation of mitochondrial metabolism. In this way oxidative stress is reduced, because one of the by-products of glycolysis is pyruvate, a known scavenger of hydroperoxide. In addition, glucose is also used in the pentose phosphate pathway, which produces NADPH a co-factor of glutathione reductase that reduces free-radicals (Spitz et al., 2000). This dependence

on glycolysis could be explained by the need to produce ATP in cells with defective mitochondria. Otto Warburg proposed a similar effect in cancer cells (Warburg et al., 1927), but this idea was later rejected as it became clear that the majority of the cancer cells had fully functional mitochondria (Vander Heiden et al., 2009; Gatenby and Gillies, 2004). Finally, it is also possible that although glycolysis produces ATP less efficiently than respiration, but faster, may be advantageous when energy sources are scarce (Pfeiffer et al., 2001; Bartrons and Caro, 2007). To our knowledge a true Warburg effect (also known as aerobic glycolysis) has not been described in yeasts. *S.cerevisiae* is crabtree-effect and therefore increased glycolysis vs decreased respiration applies more in stationary than in exponential phase cells. Indeed, in aerobic glucose rich conditions, due to the Crabtree effect glucose suppresses respiration and oxidative phosphorylation (Diaz-Ruiz, 2011, Rodrigues et al, 2005). Therefore, it would be interesting to evaluate glycolysis, oxygen consumption, ATP production and the pentose phosphate pathway in mistranslating cells. Preliminary data indicate that ATP content in mistranslating and control cells are similar (data not shown).

In respiratory deficient cells part of the TCA cycle cannot occur and oxaloacetate is not regenerated, which leads to remodeling of metabolism. Therefore, it is likely that mistranslating cells, like p^0 cells, remodel their metabolism, for instance through anaplerotic pathways, in order to get the intermediates required for the TCA cycle. For instance, peroxisome increased and activation of the glyoxylate cycle, would contribute with citrate and acetyl-coA production, respectively (Liu and Butow, 2006;

Liu et al., 2005). This hypothesis suggests that peroxisomes can be an interesting organelle to study in mistranslating cells, in particular because they can also be contribute to ROS production. Mistranslating cells up-regulated genes related to the TCA cycle, suggesting increased mitochondrial activity, which is somewhat puzzling given the respiratory deficiency observed in these cells. However, the TCA cycle intermediates are used as substrates for de novo synthesis of lipids and non essential amino acids (DeBerardinis et al., 2008). Also, TCA can be divided into two independent mini cycles: the first from oxaloacetate to α-ketoglutarate and another from α-ketoglutarate to oxaloacetate, suggesting that the up regulation observed can reflect the activation of only one of the mini cycles and not the all TCA cycle *per se,* for example for amino acid biosynthesis.

The above metabolic reconfiguration, and the similarities between the transcriptomic profile of mistranslating and p^0 cells, together with the mitochondrial dysfunction phenotype, suggest that, as in the case of the latter, the RTG pathway may also play a role in the response to mistranslation. This pathway enables communication between mitochondria and the nucleus, leading to changes in gene expression, which ultimately result in metabolic reconfigurations that allow cells to cope with mitochondrial defcets (Titorenko and Terlecky, 2011). Indeed, mitochondrial defects at mitochondrial level activate a cassete of nuclear genes (RTG genes) that lead to a downstream regulation of carbohydrate and nitrogen metabolism, activates peroxisome proliferation, promote peroxysomal fatty acid β-oxidation (which is a big energy producing process)

and anaplerotic reactions, stimulate stress responses and other effects that compensate for mitochondrial dysfunction.

Mistranslation effects on yeast longevity

Surprisingly, mistranslating cells did not show decreased longevity despite being respiratory deficient. This may be explained by the stationary-phase essential genes (SP-essential). Yeast encodes32 genes which are essential for survival in stationary phase at 37^{o}C (SP-essential) (Martinez et al., 2004a) and our data showed that 50% of these genes are up-regulated by mistranslation (Figure 35). An alternative explanation may be that mistranslating cells rely on glycolysis/fermentation in stationary phase, but this raises the question of how do these cells get glucose from? A likely possibility is the mobilization of trehalose and glycogen for glucose production.Indeed, previous studies from our laboratory have shown that mistranslating cells accumulate trehalose and glycogen at high level (Silva RM et al., 2007). Those data also showed a puzzling simultaneous activation of both trehalose synthesis and degradation genes which may explain the continuous need to produce glucose (Silva RM et al., 2007). In addition, our data also indicate that stationary phase mistranslating cells tend to accumulate H_20_2 when compared to control cells but the levels of 0_2^- remain similar to those of control cells. This is in line with the recent finding that elevated levels of H_20_2 are associated with extended chronological life span (CLS) as it activates superoxide dismutase activity that, in turn, inhibits 0_2^- accumulation (Mesquita et al., 2010).

In conclusion, mistranslation induces ROS accumulation, increases antioxidant responses and strongly affects mitochondrial function. In exponential phase, mistranslating yeast cells rely on fermentation and therefore the mitochondrial dysfunction phenotype is not phenotypically relevant in media containing glucose. Since mistranslating cells have lower respiratory rates, mitochondria should not be the major source of ROS, hinting on possible roles for ER and peroxisomes in ROS production. ROS accumulation up-regulates antioxidant defences and, therefore, higher levels of NADPH are needed. This is consistent with the up-regulation of *PNC1*, which contributes to increased NAD^+ production that will be converted in the pentose phosphate pathway into NADPH. In stationary phase, the mitochondrial dysfunction induced by mistranslation prevents respiration and, therefore, cells rely on glycolysis to survive. This is possible, because trehalose accumulated during exponential growth can be mobilized to produce glucose. The dysfunctional mitochondria can still contribute to ROS accumulation in stationary phase and and Sir2p may play an important role on ROS detoxification, especially in O_2^- detoxification. The Pnc1p role in stationary phase is apparently not much relevant for ROS detoxification for reasons that are still unclear.

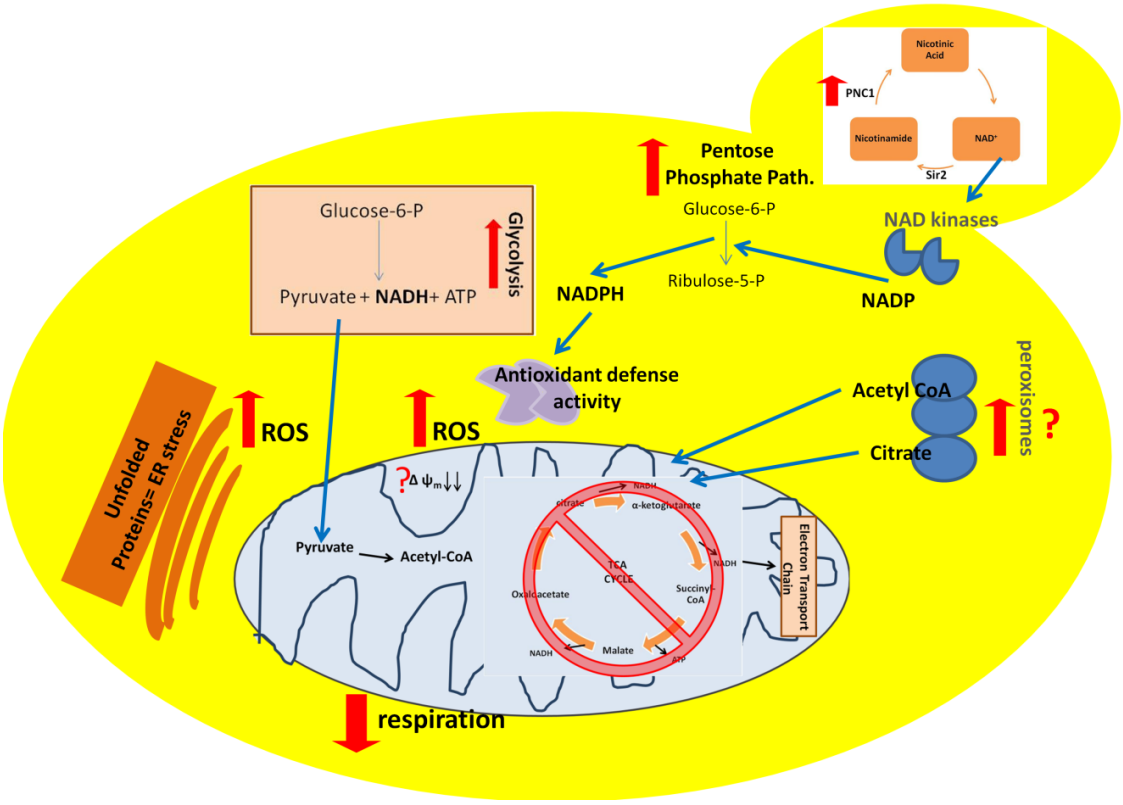

Figure 36- Integrative model for mistranslation consequences – Mistranslation leads to ROS accumulation and has a negative impact on the mitochondrial network and mitochondrial function probably culminating in metabolic reconfiguration towards glycolysis. In exponential phase, mistranslating yeast cells, due to the Crabtree effect, rely on fermentation. Indeed, cells have a low respiratory rate and most likely, mitochondria are not the major ROS source, hinting at the ER or peroxisomes as the major ROS sources. ROS accumulation up-regulates antioxidant defences increasing the cellular needs for NADPH. *PNC1* up-regulation leads to production of NAD^+ which will be used in the pentose phosphate pathway to produce NADPH. When cells are in stationary phase, mitochondrial defects and dysfunction become more problematic as the glucose levels in the medium are limiting leading to a metabolic shift towards respiration. However, mistranslating cells cannot rely on respiration and, therefore, still use glycolysis to survive by mobilizing glucose production via trehalose catabolism.

Materials and methods

Yeast Strains and manipulation

Yeast strains and plasmids used in this study are listed in Table 8 and Table 9. Strains were transformed with the plasmids pRS315 (Control) or pUKC715 (Santos et al., 1996) according to Gietz (Gietz, 2002; Gietz and Schiestl, 2007b; Gietz and Schiestl, 2007a) with minor modifications. Standard methods for yeast manipulation were used. Cells were grown in SMD-leu or SMD-leu-ura (0.67% yeast nitrogen base, 2% glucose or 2% galactose, 0.2% drop-out mix containing all amino acids except leucine or leucine and uracyl), unless otherwise stated.

Table 8- strains used in this study

Strain	Genotype	Source	Description
BY4742	*MAT α,his3Δ1/his3Δ1 leu2Δ0/leu2Δ0 LYS2/lys2Δ0 met15Δ0/MET15 ura3Δ0/ura3Δ0*	Euroscarf	Wild type strain
yap1Δ	BY4741 MAT a; his3Δ 1; leu2Δ 0; met15 Δ0; ura3Δ0 ;YML007w::kanMX4	Euroscarf, kind gift from C.Rodrigues-Pousada	BY4742 deleted for yap1 gene
yap2Δ	*BY4741; Mat a; his3∆1; leu2∆0; met15 ∆0; ura3∆0; YDR423c::kanMX4*	Euroscarf, kind gift from C.Rodrigues-Pousada	*BY4742 deleted for yap2 gene*
yap1Δyap2Δ	BY4742; Mat a; his3∆1; leu2∆0; lys2∆0; ura3∆0; YDR423c::kanMX4;YML007w::his	kind gift from C.Rodrigues- Pousada	*BY4742 deleted for yap1 and yap2 genes*
TKYM22	SEY6210 OM45-GFP::TRP1	kind gift from Dr.Daniel J. Klionsky (Kanki and Klionsky, 2008)	*SEY6210 , Om45-GFP integrated*
TKYM29	SEY6210 pep4∆::LEU2 OM45-GFP::TRP1	kind gift from Dr.Daniel J. Klionsky(Kanki and Klionsky, 2008)	*SEY6210 , Om45-GFP integrated, deleted for pep4 gene*
pnc1Δ	Mat a/ α; his3∆1; leu2∆0; lys2∆0; ura3∆0; YGL037c::kanMX4	Euroscarf	BY4743 deleted for pnc1 gene
sir2Δ	*Mat α; his3 ∆1; leu2 ∆0; lys2 ∆0; ura3 ∆0; YDL042c::kanMX4*	Euroscarf	*BY4742 deleted for sir2 gene*

Table 9-plasmids used in this study

Plasmid	Description	Source
pSR315	Empty plasmid	our laboratory
pUK715	Plasmid based on the single copy vector pRS315 .Contains the *Candida albicans* Ser-tRNA$_{CAG}$ G$_{33}$ (Santos *et al* , 1996)	our laboratory

DNA microarrays

RNA preparation

Cells (25 OD_{600} units) were harvested by centrifugation at 4000 rpm for 5 minutes, immediately frozen in liquid nitrogen and stored at -80ºC until further use. Frozen pellets were resuspended in 500 µl Acidic Phenol-Chlorophorm (5:1, pH4.7; Sigma) and heated at 65ºC prior use. The same volume of hot TES buffer (10 mM Tris, pH 7.5; 10 mM EDTA, 0.5%SDS) was added. Pellets were resuspended by vortexing for 20 seconds and were immediately incubated at 65°C for 1 hour with vortexing every 10 min, in order to maintain a homogeneous suspension. The extracts were then transferred to clean microfuge tubes and cells debris and organic phase were separated from upper aqueous phase by centrifugation at 14000 rpm for 20 minutes at 4°C. The upper phase was collected and extracted twice with 1 volume of Phenol: Chlorophorm (5:1, pH 4.7; Sigma) and once with Chlorophorm: Isoamyl-alcohol (25:1; Sigma). At each step, extracts were centrifuged at 14000 rpm for 10 minutes at 4°C. The RNA was precipitated by addition of 1 volume of 3M sodium acetate (pH 5.2) plus 3 volumes of ice-cold absolute ethanol, followed by an overnight incubation at -20°C. The RNA was

pelleted by centrifugation at 14000 rpm for 5 minutes at 4°C, washed once with 70% ethanol and again pelleted by centrifugation. The remaining alcohol was evaporated using a speed-vac (Savant) and the RNA pellets were dissolved in 50 µl of RNase-free water. RNA concentration was determined by OD_{260} in a Nanodrop 1000 (ThermoScientific)(van de et al., 2003) .

Data Analysis and Statistical Analysis

DNA microarrays were scanned using an Agilent G2565AA laser scanner, and images were processed using QuantArray® software package (Packard BioChip Technologies). Background noise was subtracted and bad spots were excluded after manual inspection. Slides were normalized using standard ratio-based methods (print-tip lowess normalization within arrays) as implemented in Biometric Research Branch BRB-Array Tools v3.4.0 software. Experiments were performed in two independent assays, corresponding to two different clones for each strain, with dye-swapping. Microarray data analyses were performed using MEV software (TM4 Microarray Software Suite, (Saeed et al., 2006; Saeed et al., 2003a). Data were analyzed based on $\log_2$ ratio (M) values. Genes included in the final dataset exhibited significance based on a FDR median< 0.05, in a SAM 1-class analysis (Salin 2008, Tusher 2001, Saeed 2003, van Helden 2003).

Assessment of intracellular reactive oxygen species (ROS)

Free intracellular reactive oxygen species (ROS) were detected either with dihydrorhodamine 123 (DHR123) (Molecular Probes, Eugene, OR, U.S.A.) or

dihydroethidium (DHE). DHR123 was added from a 1 mg/ml stock solution in ethanol to $5x10^6$ cells/ml suspended in PBS to a final concentration of 15 µg/ml. Cells were incubated during 90 minutes at 26°C in the dark, washed in PBS and then analyzed by flow cytometry. DHE was added to 1 x 10^6 cells/ml at a final concentration of 10 µg/ml. Cells were incubated at 30°C in the dark for 10 minutes. Analysis was carried out using a flow cytometer (BD LSRII). Twenty thousand cells per sample were analyzed. ROS production was expressed as mean fluorescence intensity calculated using FlowJo® software (Tree Star, Inc., Ashland, OR).

Plasma membrane Integrity

Cell viability was assessed simultaneously with ROS determination. 70 minutes after DRH123 addition, 5 µl of propidium iodide (0.5mg/ml stock solution, PI, Molecular Probes, Eugene, OR, U.S.A) were added to the cell suspension and stained cells were analyzed using a flow cytometer (BD LSRII). Twenty thousand cells per sample were analyzed. Data analysis was performed using FlowJo® software (Tree Star, Inc., Ashland, OR). Cells displaying values above a defined threshold of red fluorescence were considered as having compromised plasma membrane integrity.

Quantification of intracellular concentration of NAD /NADH

NAD/NADH procedure was adapted from Sporty et al (Sporty et al., 2008). Briefly, yeast cells were grown in liquid SMD-leu medium until mid log phase (OD_{595}=0.5) at 30°C with shaking. 25 OD units of cells were harvested at 4000 rpm for 3 minutes and immediately frozen in liquid-nitrogen. Cells were then resuspended in 300 µl of 50mM ammonium acetate buffer and the same amount of glass beads were added to all

samples. Yeast cells were bead blasted at 5000 rpm for 30'' using a Precellys tissue homogenizer (Bertin Technologies), followed by 2 minutes incubation on ice and another 30'' disruption. During the ice incubation period, a single 10'' vortexing to redistribute the heated-glass beads was performed. Tubes were centrifuged at 2000 rpm for 3 minutes at 4°C to separate cell lysates from glass beads. Cell lysates were transferred to new eppendorf tubes and were kept on ice. Glass beads were washed twice with 300 µl of ammonium acetate buffer, vortexed and centrifuged at 2000 rpm for 3 additional min. The supernatant was added to the previous cell lysate. Combined lysates were kept on ice during the entire procedure and extracts were never stored at -80°C for more than 12h. The concentrations of NAD_{total} and NADH were determined using the Amplite Colorimetric NAD+/NADH Assay Kit (ABD Bioquest). Briefly, 50 µl of supernatant was mixed with 50 µl of the enzymes. The colorimetric assay was conducted in a 96-well microplates and the absorbance was measured at 575 nm using a X-mark Biorad spectrophotometer. A NADH standard curve was used and the abundance of metabolites was calculated as a function of pmol per cell. This value was converted to into a cellular concentration value (mM) using 7×10^{-14} as the intracellular volume of a haploid yeast cell (Sherman, 2002). Metabolite measurements are presented as means of at least 2 independent yeast cultures.

Quantification of the intracellular concentration of NADP /NADPH

Yeast cells were grown in liquid SD-leu medium at 30°C with shaking until mid log phase (OD_{595}=0.5). 15 OD units (1.5×10^8 cells) of cells were harvested at 4000 rpm for 3 minutes and immediately frozen in liquid-nitrogen. Cells were resuspended in 300 µl of PBS buffer and disruption was performed as described above. The concentrations of

$NADP_{total}$ and NADPH in the supernatant were measured by Amplite Colorimetric $NADP^+$/NADPH Assay Kit (ABD Bioquest). Briefly, 50 µl of supernatant were mixed with 50 µl of the NAD cycling Enzyme Mix. The colorimetric assays were conducted in a 96-well microplates and the absorbance was measured at 575 nm in a X-mark biorad spectrophotometer. A NADPH standard curve was used and protein amounts for each lysate were determined using BCA protein assay (Thermo Scientific Pierce). Metabolite amounts were normalized to the protein present in the cell lysate (per reaction) and are reported as nanomoles per milligram of protein. Metabolite measurements were made using at least 2 independent yeast cultures, unless stated otherwise, and results are reported as means ± SEM.

Viability and long-term survival

In order to determine cell growth and viability in exponential phase and at the beginning of post-diauxic shift (referred as stationary phase day 1 - d1), which corresponds to 36h±5h post-inoculation), serial dilutions were plated on selective agar plates. Briefly, cells were cultured at 30°C with aeration in 100 ml flasks containing 20 ml of selective medium. When cultures reached an OD_{595} of 0.4-0.7, the number of cells was counted using a Vi-cell device (Beckman Coulter). The number of cells was normalized to $1x10^7$ cells/ml and serial dilutions were prepared using 96 well plates. Cells were spotted onto the agar plates with the help of a liquid handling robot (Caliper Life Sciences). Plates were then incubated at 30°C for 4 days and photographed. Images were analyzed using the ImageJ software (http://imagej.nih.gov/ij/index.html). When quantitative analysis was performed, images were analyzed using a custom software macro designed to automate spots identification and measurement. Images

were manually inspected and misidentified or contaminated spots were flagged for exclusion in subsequent analysis. Growth scores were calculated using the mean area of each spot. Briefly, spot size of the tested strains was normalized using the values for the corresponding spot of the wild-type control grown in the same plate. In some cases, normalization was mathematically impossible, for instance when the control strain grew while the tested strain did not, or vice-versa. In these cases, an arbitrary value of 1 (no growth when compared to the control strain) or 100 (no growth on the control strain) was attributed to the missing value. Normalized values (3-5 values, matching each of the serial dilutions) were then averaged to obtain the final relative fitness values that were used on the statistical analysis. Each strain was assayed using 3 different clones and at least 3 independent experiments were carried out for each case.

Long term cell survival was determined using vital staining (methylene blue staining) and colony formation assays. For this yeast cultures were grown in 100 ml flasks containing 20 ml of selective media, at 30°C with aeration. In methylene blue test, cells were assayed for viability at 1, 3 (post-diauxic growth), 7, 14 and 21 days after inoculation (stationary phase). At each of the points, small aliquots of the cell cultures were removed and the cell suspensions were mixed (v/v) with methylene blue solution (0.1 g/L of methylene blue in PBS buffer). Stained and non-stained cells were counted using a Newbauer chamber. At least 300 cells were counted for each aliquot. The percentage of viable cells was calculated as indicated in Equation 5. The percentage of viable cells at day 1 was considered as 100%. The viability at subsequent time points

was calculated in relation to the viability at day 1 for each strain. In the CFU test, cells were assayed at days 1, 7 and 14. Briefly, cell density in liquid culture was determined by counting the number of cells using the Vi-cell device (Beckman Coulter). Cells were plated in appropriate dilutions to obtain approximately 50 to 100 colonies per plate in selective medium and were incubated at 30°C for 4 days. Colonies were calculated as a percentage of the cells plated. As before, viability at d1 was considered 100%. Strains were assayed using 3 different clones and at least 3 independent experiments were carried out.

Equation 5- Viable cell calculation (methylene blue method)

$$\% \text{ viable cells} = \frac{Number\ of\ viable\ cells}{number\ of\ total\ cells}\ x\ 100$$

Mitochondrial morphology assessment

Cells expressing the OM45-GFP fusion were grown in YPD to mid log phase (OD_{595} 0.4-0.6), for 36h, 5 days or 7 days and then collected for microscopy and immunobloting. Cells were immobilized on glass slides using an agarose bed (1% in water) and were observed as fully growing cells. Observations were made using an Axiovision imager Z1 microscope (Zeiss). GFP tagged proteins were revealed and photographed with an AxioCam Hrc camera and Axiovision Software. Results from at least two independent experiments are expressed as the means± S.E.M, except where otherwise stated. Results were compared using t-test or ANOVA, with $P<0.05$ considered to be statistically significant, as stated elsewhere. 150 cells were analysed per experiment.

Analysis of respiratory deficiency and ROS scavenger effect

Cultures were grown for 36h in YPD media supplemented with Geneticin and plated on YPD (geneticin) plates or YP (geneticin) plates containing: i) 2%lactate ; ii) 3% glycerol; iii) 2% acetate or iv) 2% ethanol. Cultures were spotted on agar plates using 10-fold dilutions, starting with $1x10^7$ cells. Plates were incubated at 30°C for 4 days and photographed. Quantifications were performed as described above.

Acknowledgments: The author would like to thanks to Alexandra Silva and Professor Paula Ludovico for help in the ROS detection experiments and flow cytometry expertise. Also to thank to Dr Mathias Petter and Dr. Claudine Kraft for kindly sending plasmids.

Supplementary data

Supp.Table 2- Subset of genes that belong to GO term "mitochondrion" (associated p-value = 7.42^{-10}, as shown in Table 1), whose expression was found to be de-regulated in mistranslating cells. mRNA was extracted, cDNA synthesized and hybridized onto home-made arrays. Each expression data set was analyzed using 1-class SAM analysis as described in methods, based on a FDR median< 0.05.Each dataset was further analyzed in the on-line tool Genecodis(Nogales-Cadenas et al., 2009; Carmona-Saez et al., 2007)

Gene Name	Fold Change	Gene Name	Fold Change	Gene Name	Fold Change	Gene Name	Fold Change	Gene Name	Fold Change	Gene Name	Fold Change
ACH1	1,6	**ENO1**	2,0	**LAP3**	1,5	**PEP4**	2,1	**TPI1**	1,6	**YLR001C**	2,0
ADH4	1,7	**ENO2**	2,6	**LEU4**	3,7	**PET9**	1,5	**UIP4**	2,0	**YLR089C**	2,3
AI5_ALPHA	1,9	**ETR1**	1,5	**LSC1**	1,5	**PGI1**	1,5	**VPS13**	1,5	**YLR164W**	1,9
ALD4	3,9	**FBA1**	2,0	**LSC2**	1,8	**PGK1**	2,2	**WWM1**	1,9	**YLR193C**	1,5
ALD5	2,1	**FMT1**	2,7	**LSP1**	1,6	**PMA2**	1,8	**YAH1**	1,6	**YLR290C**	2,0
ARG5	2,6	**GCV1**	4,0	**LYS20**	2,5	**POR1**	1,6	**YBR047W**	4,0	**YLR327C**	5,2
ARO3	1,9	**GCV2**	2,9	**LYS21**	1,8	**POS5**	1,6	**YBR147W**	3,1	**YLR356W**	1,8
ATP1	1,6	**GCV3**	2,4	**MAE1**	2,5	**PRX1**	2,3	**YBR230C**	1,9	**YMR110C**	1,6
ATP7	1,5	**GDB1**	3,0	**MBR1**	1,9	**PST2**	1,6	**YBR262C**	1,8	**YMR118C**	5,7
BAT1	2,2	**GDH2**	2,0	**MCR1**	2,1	**PUT1**	2,5	**YBR269C**	1,7	**YMR31**	1,8
BI3	2,1	**GPA2**	1,4	**MCT1**	1,8	**PUT2**	1,5	**YDL222C**	2,4	**YNK1**	1,5
BNA4	2,6	**GPM1**	1,9	**MDH1**	1,8	**QCR10**	1,7	**YDR031W**	1,5	**YNL195C**	2,7
CEM1	1,6	**GTT1**	1,8	**MDJ1**	1,7	**QCR6**	1,5	**YDR070C**	6,9	**YNL200C**	1,9
CIT1	1,6	**GUT2**	2,7	**MDJ2**	2,1	**QCR9**	1,5	**YER053C**	1,8	**YNL208W**	1,9
CIT2	2,3	**HSP10**	1,6	**MDM34**	1,5	**RIP1**	1,8	**YFL030W**	2,2	**YNL274C**	2,0
COQ4	1,6	**HSP60**	1,9	**MET13**	1,8	**SDH1**	1,7	**YGL059W**	2,1	**YOR215C**	1,5
COS7	1,7	**HSP78**	4,5	**MIR1**	1,9	**SDH2**	1,8	**YGR110W**	2,8	**YPL159C**	1,5
COX12	1,4	**HXK1**	3,1	**MPM1**	1,5	**SDH3**	1,5	**YGR207C**	1,6	**YPR151C**	1,9
COX3	2,4	**HXT6**	1,5	**MRPS18**	1,9	**SDH4**	1,9	**YHL021C**	2,5	**YRO2**	1,7
COX5A	1,7	**IDH1**	1,7	**MSC1**	3,7	**SED1**	3,2	**YHR116W**	1,6		
COX5B	2,0	**IDH2**	1,7	**MTO1**	1,5	**SLS1**	1,5	**YHR162W**	2,1		
COX7	1,4	**IDP1**	1,8	**NCE102**	1,9	**SSA2**	1,8	**YHR198C**	1,6		
CYB2	1,8	**ILV2**	2,8	**NDI1**	1,6	**STF1**	2,9	**YIL087C**	2,0		
CYT1	1,6	**ILV3**	2,2	**NTH2**	1,9	**STF2**	3,1	**YJL045W**	1,8		
DCS1	2,2	**ILV5**	1,5	**OAC1**	2,6	**TDH1**	2,7	**YJL070C**	2,2		
DIC1	1,8	**ILV6**	2,5	**OM45**	3,3	**TDH2**	2,3	**YJL161W**	2,6		
DLD1	1,6	**INH1**	1,4	**ORT1**	1,9	**TDH3**	2,4	**YJR111C**	1,8		
ECM19	1,6	**IRA1**	1,5	**PDA1**	1,5	**TGL2**	1,7	**YKL037W**	1,7		
EMI5	1,7	**ISU1**	2,0	**PDR5**	1,8	**TPC1**	1,6	**YKR049C**	1,8		

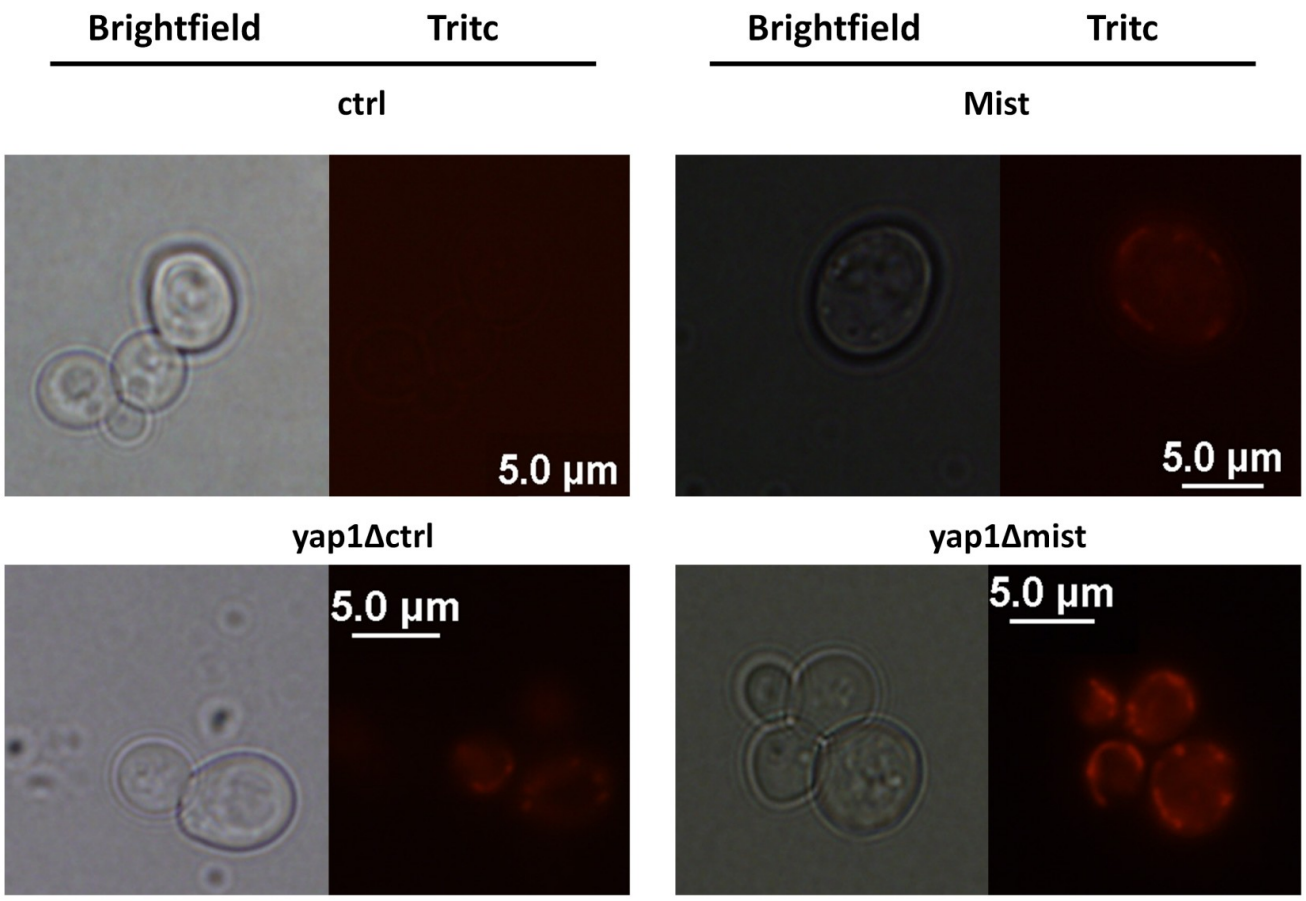

Supp.Figure 9- Enlarged view of images shown in Figure 24 F and H (upper image- exponential phase).

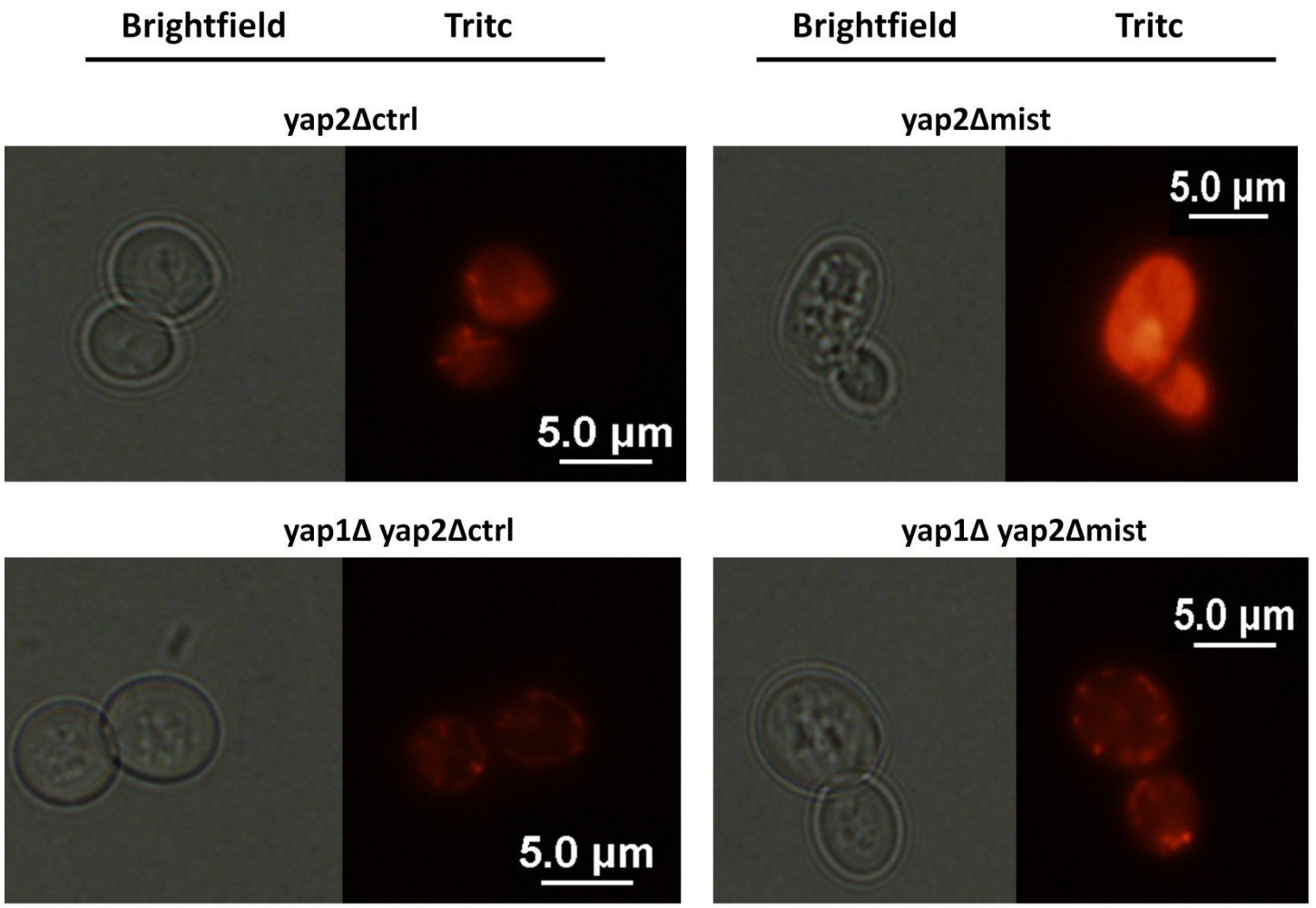

Supp.Figure 10- Enlarged view of images shown in Figure 24 H (middle and lower panels – exponential phase cells).

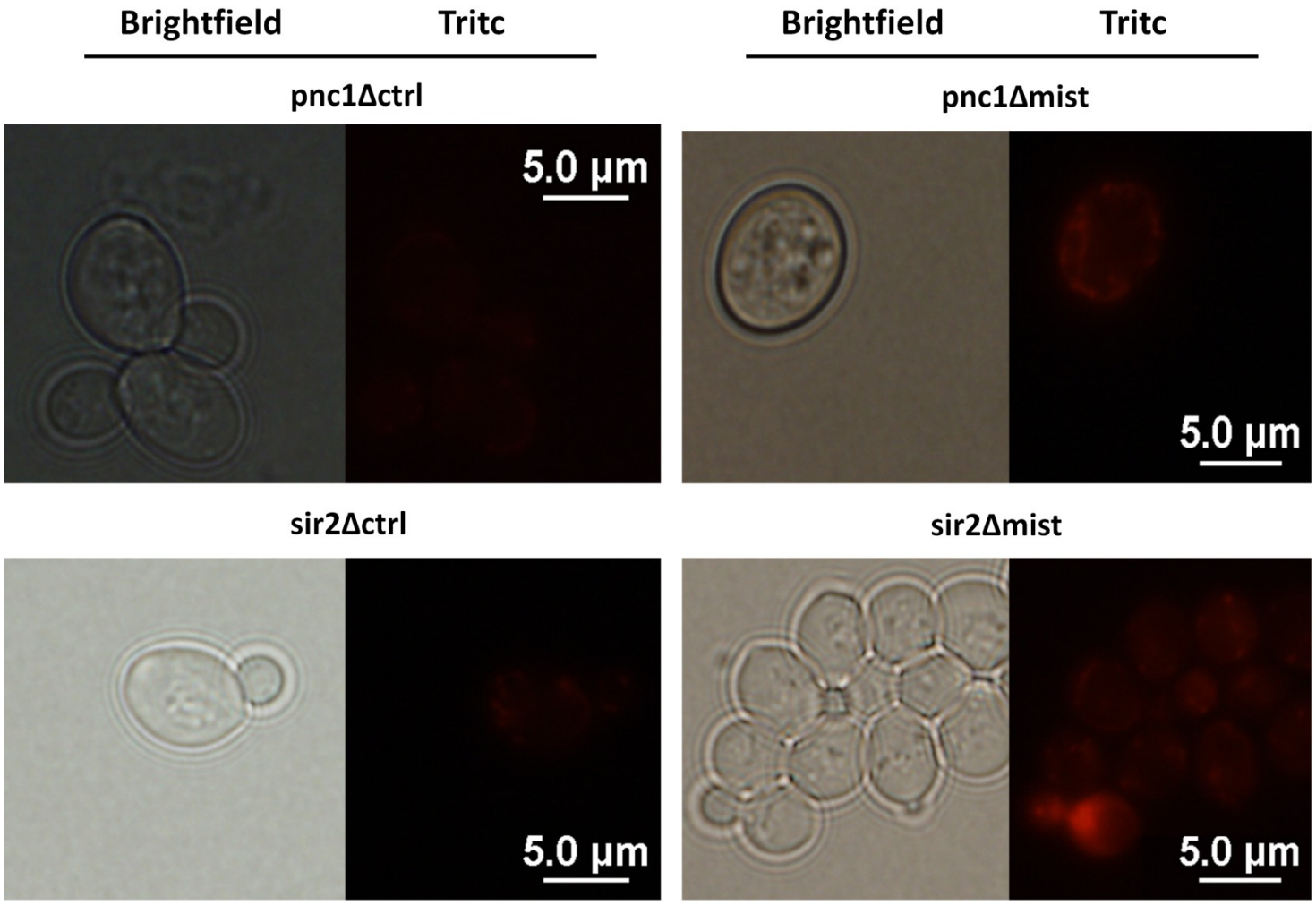

Supp.Figure 11- Enlarged view of images shown in Figure 27(exponential phase).

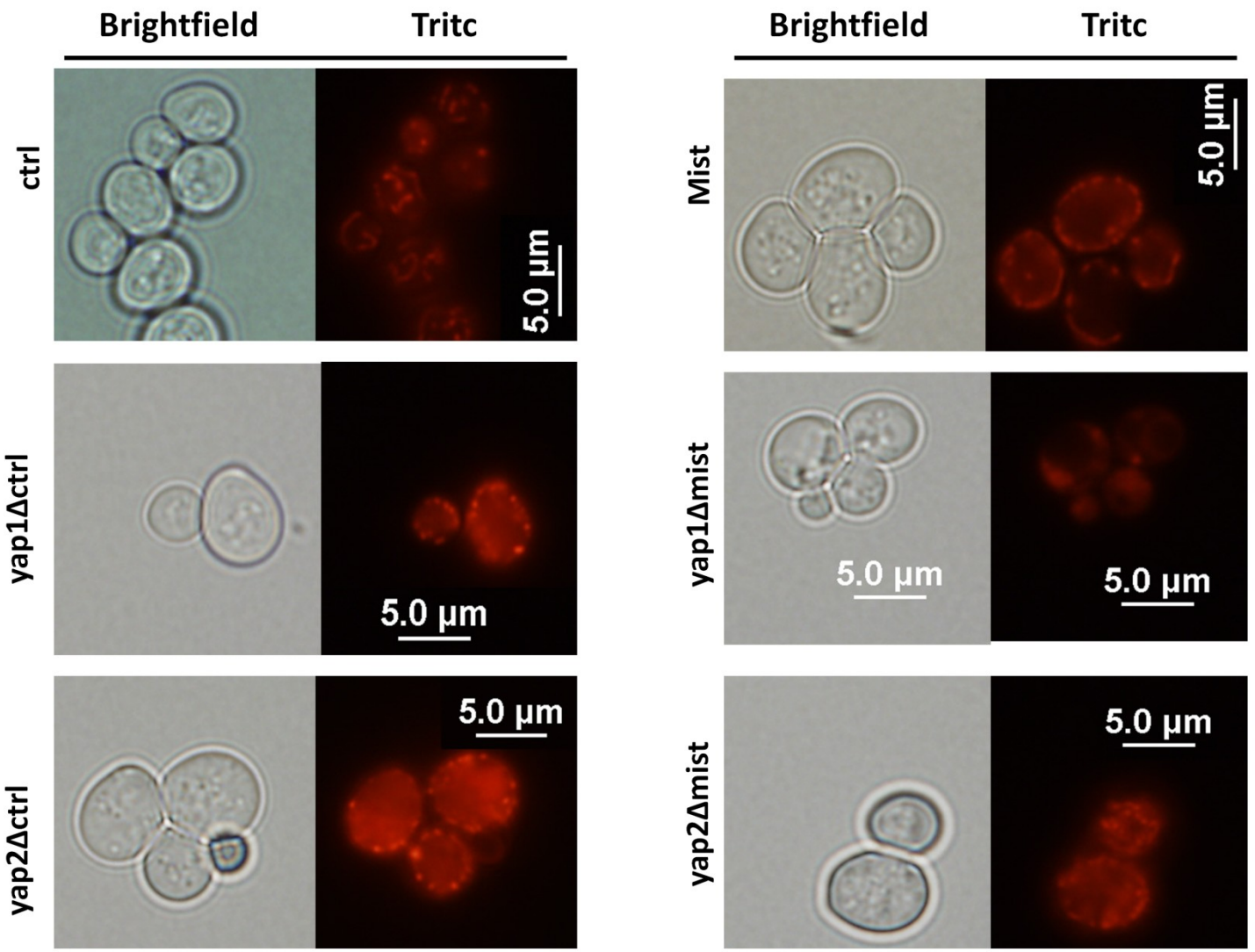
Brightfield
Tritc
ctrl
5.0 µm
yap1Δctrl
5.0 µm
yap2Δctrl
5.0 µm
Brightfield
Tritc
Mist
5.0 µm
yap1Δmist
5.0 µm
5.0 µm
yap2Δmist
5.0 µm

(CONT.)

(CONT.)

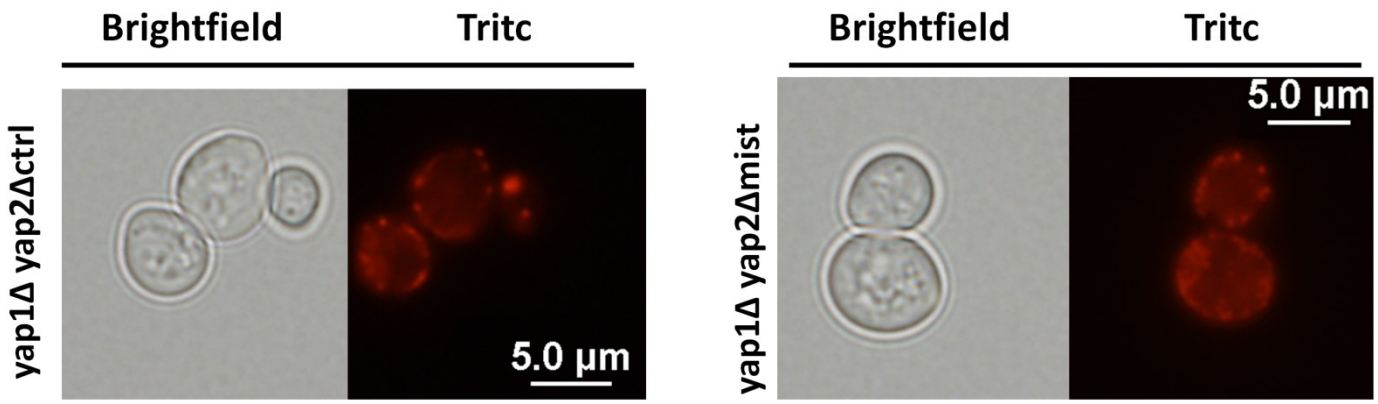

Supp.Figure 12- Enlarged view of images shown in Figure 24 (stationary phase cells).

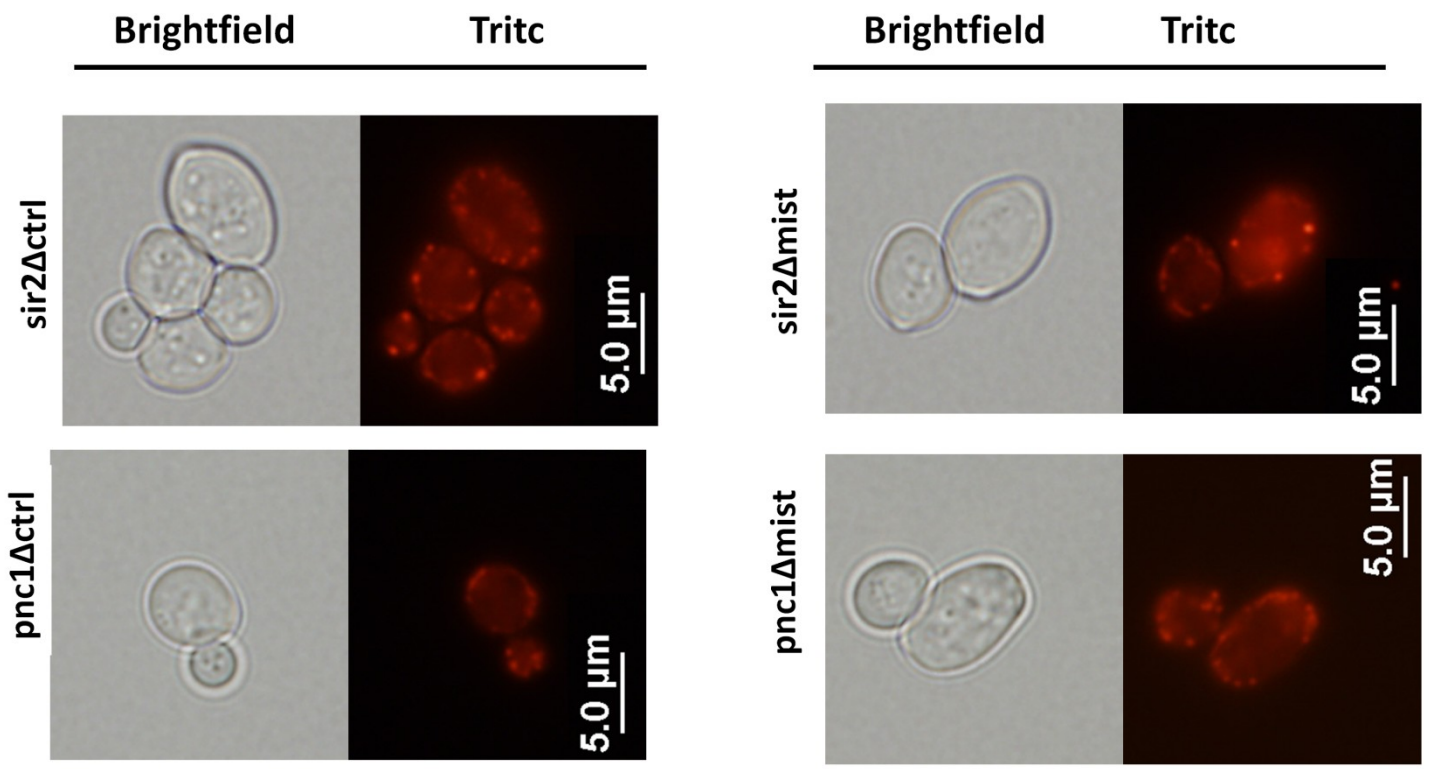

Supp.Figure 13- Enlarged view of images shown in **Figure 27** (stationary phase cells)

Supp.Table 3- Genes involved in mitochondrial morphology changes

	fold change	reference
ARG82	•	(Dimmer et al., 2002)
CAF4	•	(Griffin et al., 2005)
DNM1	•	(Bhar et al., 2006;Bleazard et al., 1999)
FIS1	•	(Mozdy et al., 2000)
FZO1	•	(Hermann et al., 1998)
GEM1	•	(Frederick et al., 2004)
MDM10	•	(Sogo and Yaffe, 1994)
MDM12	•	(Dimmer et al., 2005)
MDM30	•	Dimmer et al., 2002
MDM31	•	Dimmer et al., 2002
MDM32	•	Dimmer et al., 2002
MDM33	•	Dimmer et al., 2002
MDM34	1,5	Dimmer et al., 2002
MDM35	•	Dimmer et al., 2002
MDM36	•	Dimmer et al., 2002
MDM37	•	Dimmer et al., 2002
MDM38	•	Dimmer et al., 2002
MDM39	•	Dimmer et al., 2002
MDV1	•	(Herlan et al., 2003)
MGM1	•	(Wong et al., 2000)
MMM1	•	(Burgess et al., 1994)
MOT2	•	Dimmer et al., 2002
NUM1	•	Dimmer et al., 2002
REF2	•	Dimmer et al., 2002
TOM7	•	Dimmer et al., 2002

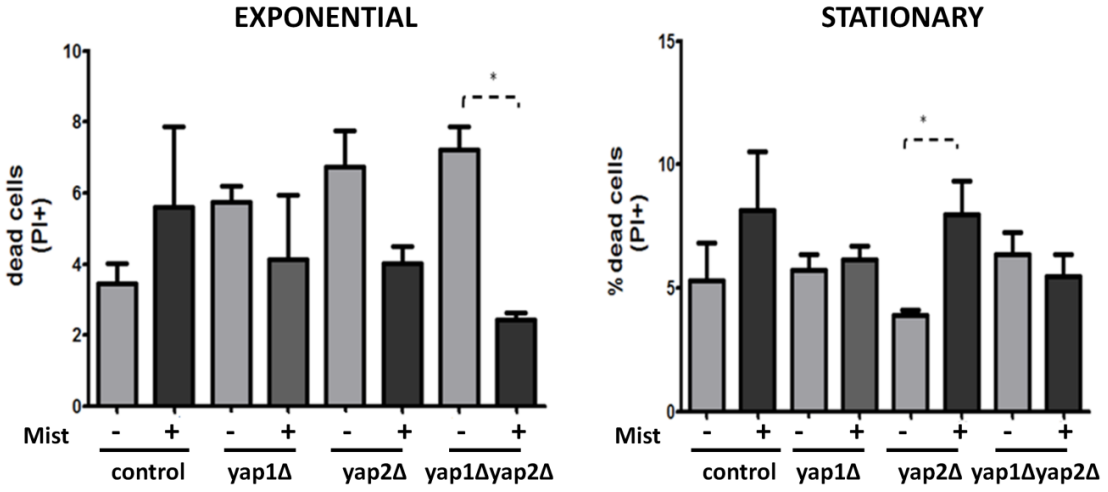

Supp.Figure 14 - Quantification of yeast membrane integrity. The unspecific binding of DHR123 to dead cells can be tested using a double staining procedure with a membrane integrity reporter. For this, cells were grown to exponential or stationary phase (36h post inoculation) and were stained with PI. The cells were analyzed using a flow cytometer and the data were analyzed using FlowJo® software. A fluorescence threshold was defined and cells displaying red fluorescence signal higher than that threshold were considered as being PI+ (dead or with compromised membrane). The data shows the average ± SEM of 2-4 independent experiments (different clones). The number of PI positive cells was low in both growth phases and no major differences were found between controls and mistranslating cells. Deletion of the *YAP* genes affected membrane integrity slightly in both phases of growth. Yap1Δ mistranslating cells showed no membrane damage problems, while yap2Δ and yap1Δyap2Δ mistranslating cells showed diminished number of cells with membrane damages in exponential phase. In stationary phase, the double mutant showed no effect and the yap2Δ mistranslating strain showed increased membranes damage. However, the percentage of PI positive cells was always below 10% and therefore, one could exclude a secondary effect when interpreting ROS results.

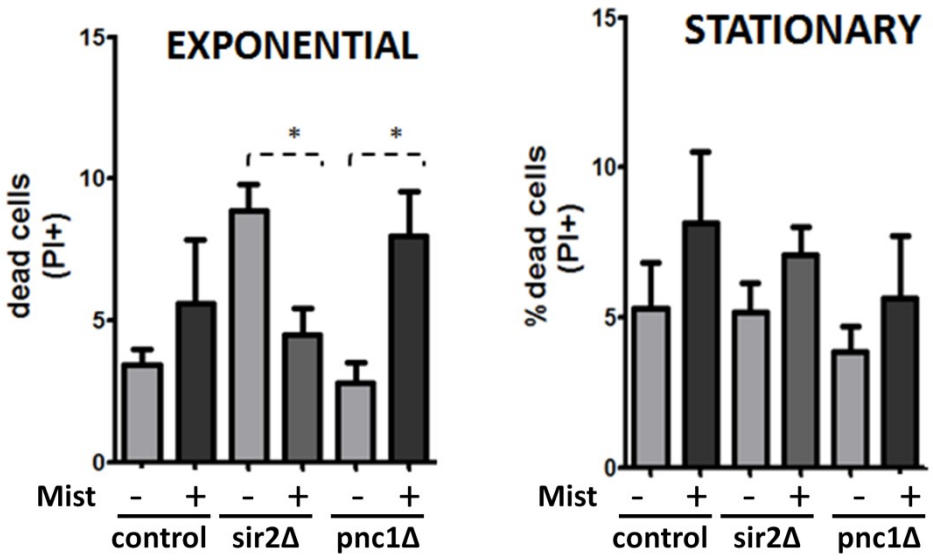

Supp.Figure 15 - Mistranslation does not affect membrane integrity of pnc1Δ and sir2Δ strains. Cells were grown to exponential (left) or post-diauxic phase (36h post inoculation) (right), were stained with PI and were analyzed using flow cytometry. The data were analyzed with FlowJo® software. A fluorescence threshold was defined and cells displaying red fluorescence higher than that threshold were considered as being PI+ (dead or with compromised membranes). The data represent the average ± SEM of 2-4 independent cultures, corresponding to different clones. The percentage of PI positive cells was always below 10% indicating that one could exclude a secondary effect when interpreting ROS results

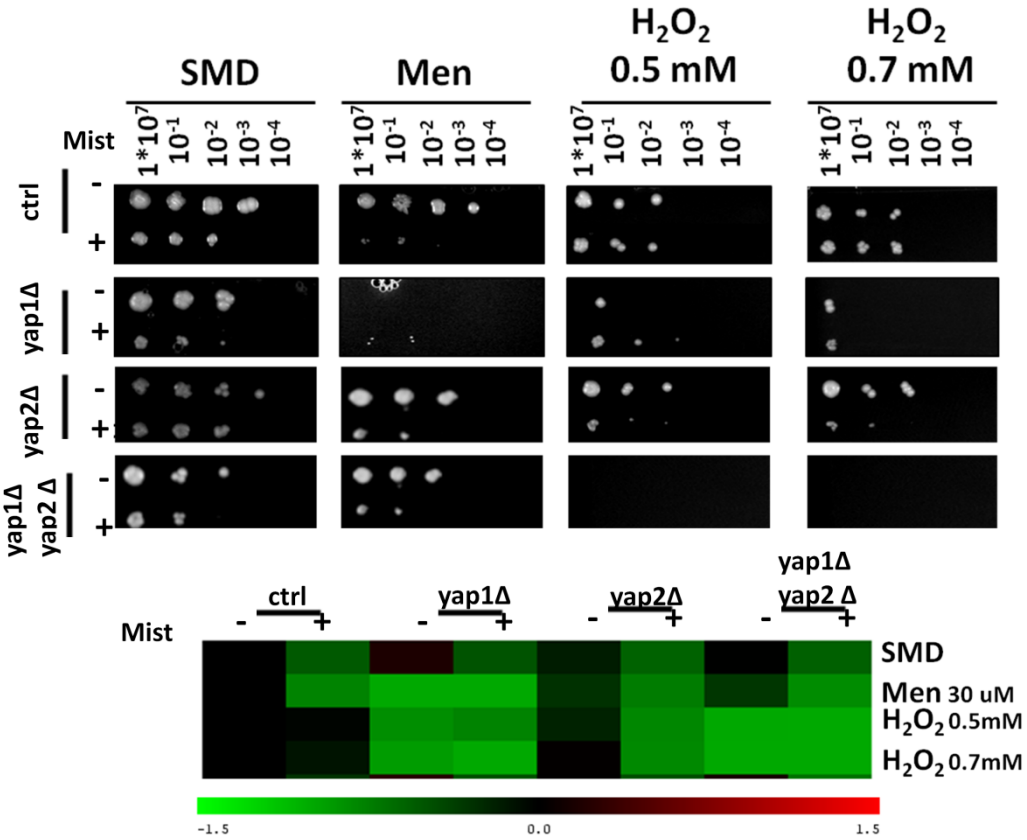

Supp.Figure 16- Effect of mistranslation on oxidative stress tolerance. Representative images of mistranslating cells growing on plates in the presence of different stress agents. In general, in exponentially growing cells, mistranslation increased sensitivity to the stressors and yap1Δ strains were the most sensitive. Deletion of each of the *YAP* genes had generally a deleterious effect on cell survival, even without mistranslation. As expected, from the *YAP* gene deletions studied, yap2Δ was the one that although sensitive, showed more resistance to the stressors, either in mistranslation situations or the deletion alone. yap1Δyap2Δ was the most sensitive strain to oxidative stress. However, and in an opposite trend to yap1Δ, the double mutant was resistant to menadione to some extend but was completely unable to grow in the presence of H_2O_2. Mistranslation in this genetic background did not restore growth.

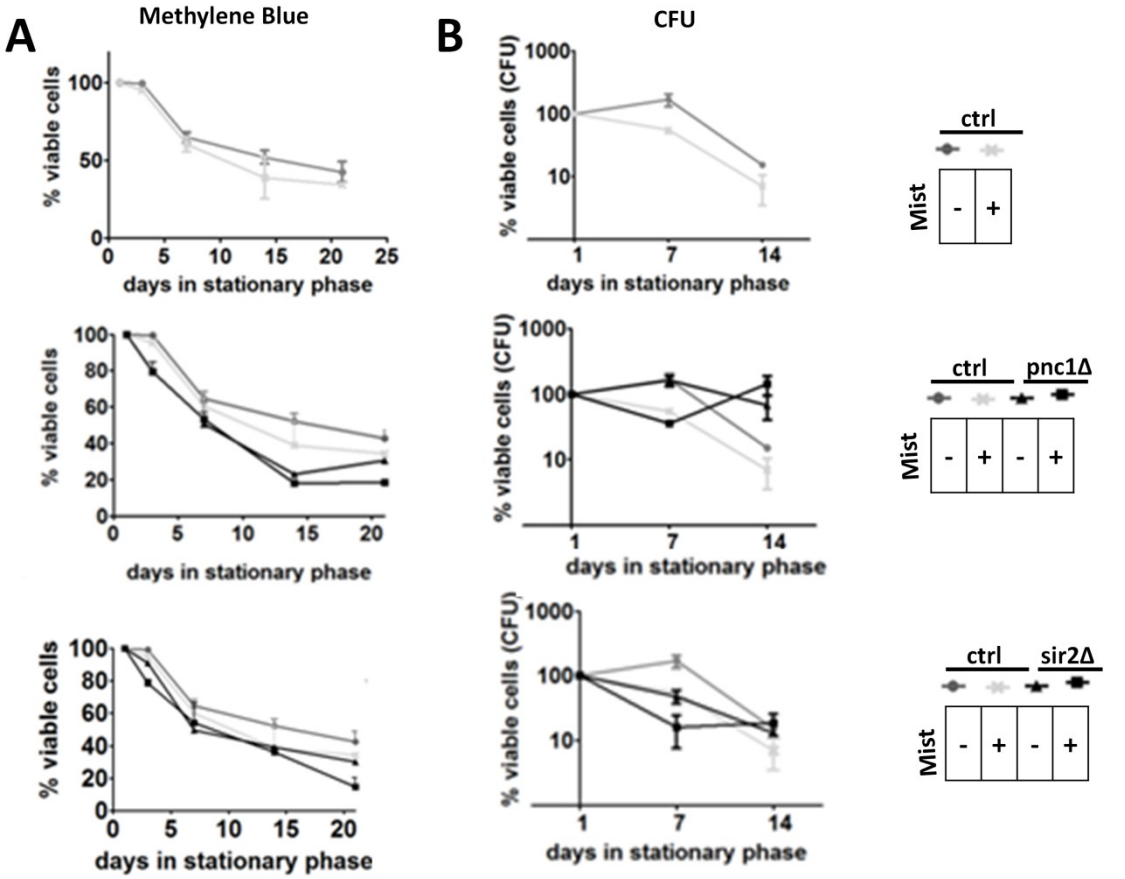

Supp.Figure 17- Long term viability of pnc1Δ and sir2Δ mistranslating cells. Cell viability was assessed using 2 different methodologies, namely methylene blue staining (A) and CFU formation (B). The same cultures were used in both experiments. Cells were grown at 30°C in selective minimal media. At the indicated time points, cells were either stained with methylene blue or plated on solid media. In the case of the methylene blue assays the number of stained (dead) and unstained (viable) cells was assessed using light microscopy. A minimum of 300 cells (viable [unstained] and dead [stained] cells) were counted for each time point. Viability at day 1 of stationary phase was considered as being 100%. Results shown refer to at least two independent determinations, corresponding to 2 different clones analyzed. Error bars represent SEM. Points with no error bar refer to a single determination.

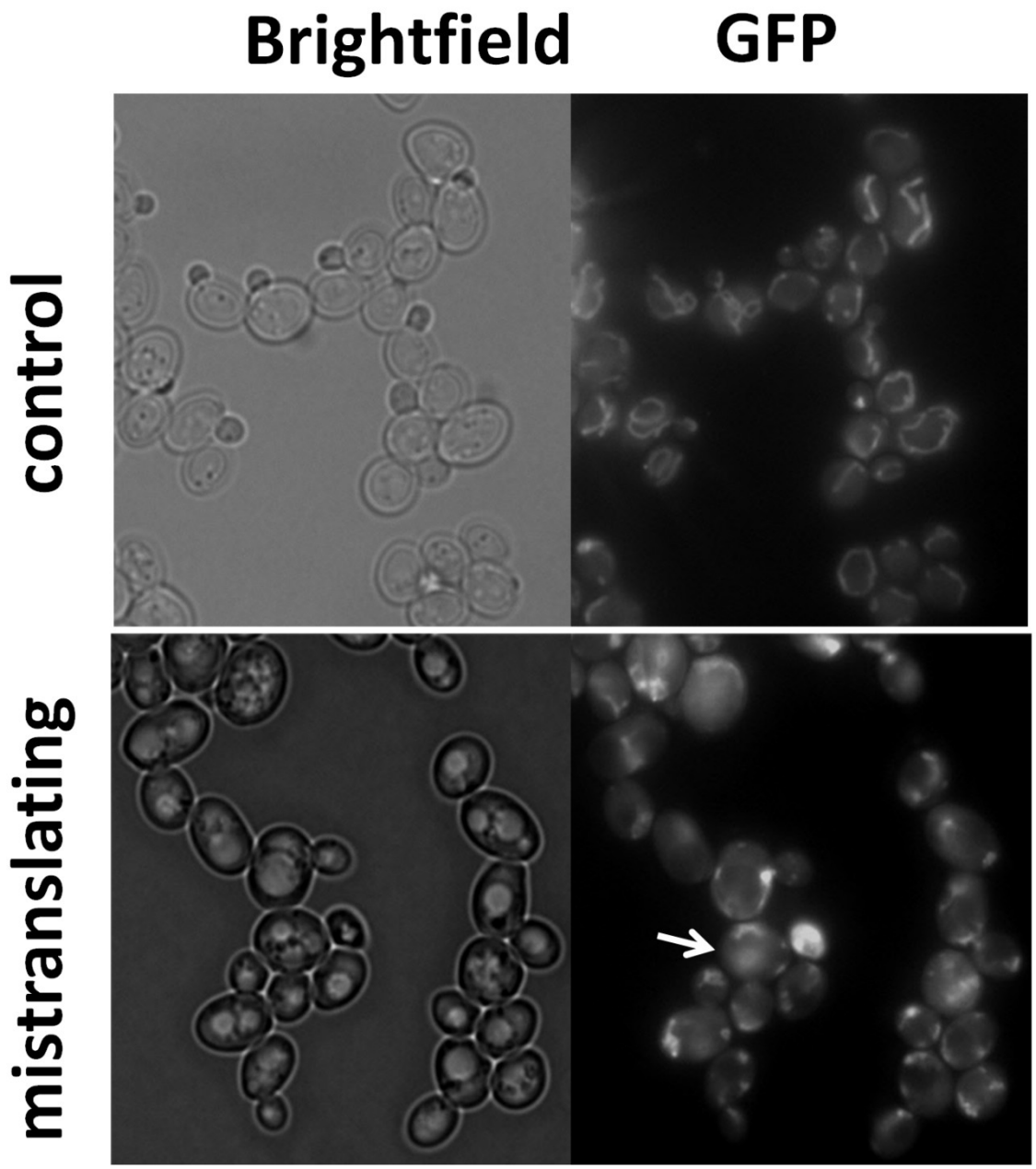

Supp.Figure 18- Enlarged view of images shown in figure 31.

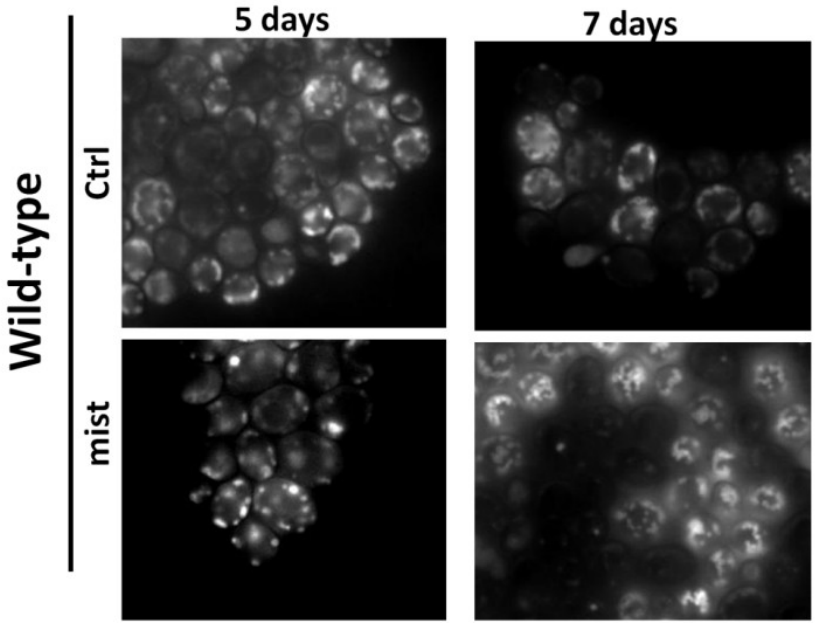

Supp.Figure 19- Mitochondrial morphology accessement in aged cells. Cells were left in culture for several days, with aeration. At the indicated time points, an aliquote was removed and cells were observed using a fluorescence microscope. Some vacuolar fluorescence was detected but at low levels. Mitochondrial network disruption was still present in mistranslating cells and the differences between control and mistranslating cells seemed to be attenuated, with increased number of mitochondrial fission seen in control cells

References

1. Alcendor, R.R., S.Gao, P.Zhai, D.Zablocki, E.Holle, X.Yu, B.Tian, T.Wagner, S.F.Vatner, and J.Sadoshima. 2007. Sirt1 Regulates Aging and Resistance to Oxidative Stress in the Heart. *Circ Res* 100:1512-1521.
2. Alirol, E. and J.C.Martinou. 2006. Mitochondria and cancer: is there a morphological connection? *Oncogene* 25:4706-4716.
3. Anderson, R.M., K.J.Bitterman, J.G.Wood, O.Medvedik, H.Cohen, S.S.Lin, J.K.Manchester, J.I.Gordon, and D.A.Sinclair. 2002. Manipulation of a nuclear NAD+ salvage pathway delays aging without altering steady-state NAD+ levels. *J Biol Chem.* 277:18881-18890.
4. Andreyev, A.Y., Y.E.Kushnareva, and A.A.Starkov. 2005. Mitochondrial metabolism of reactive oxygen species. *Biochemistry (Mosc.)* 70:200-214.
5. Arnoult, D. 2007. Mitochondrial fragmentation in apoptosis. *Trends Cell Biol* 17:6-12.
6. Bartrons, R. and J.Caro. 2007. Hypoxia, glucose metabolism and the Warburg's effect. *J. Bioenerg. Biomembr.* 39:223-229.
7. Bleazard, W., J.M.McCaffery, E.J.King, S.Bale, A.Mozdy, Q.Tieu, J.Nunnari, and J.M.Shaw. 1999. The dynamin-related GTPase Dnm1 regulates mitochondrial fission in yeast. *Nat Cell Biol* 1:298-304.
8. Bossy-Wetzel, E., M.J.Barsoum, A.Godzik, R.Schwarzenbacher, and S.A.Lipton. 2003. Mitochondrial fission in apoptosis, neurodegeneration and aging. *Curr. Opin. Cell Biol* 15:706-716.
9. Bossy-Wetzel, E. and S.A.Lipton. 2003. Nitric oxide signaling regulates mitochondrial number and function. *Cell Death. Differ.* 10:757-760.
10. Bravo, R., J.M.Vicencio, V.Parra, R.Troncoso, J.P.Munoz, M.Bui, C.Quiroga, A.E.Rodriguez, H.E.Verdejo, J.Ferreira, M.Iglewski, M.Chiong, T.Simmen, A.Zorzano, J.A.Hill, B.A.Rothermel, G.Szabadkai, and S.Lavandero. 2011. Increased ER-mitochondrial coupling promotes mitochondrial respiration and bioenergetics during early phases of ER stress. *J. Cell Sci.* 124:2143-2152.
11. Brown, G.C. and V.Borutaite. 2011. There is no evidence that mitochondria are the main source of reactive oxygen species in mammalian cells. *Mitochondrion.*
12. Carmona-Saez, P., M.Chagoyen, F.Tirado, J.M.Carazo, and A.Pascual-Montano. 2007. GENECODIS: a web-based tool for finding significant concurrent annotations in gene lists. *Genome Biol* 8:R3.
13. Castegna, A., P.Scarcia, G.Agrimi, L.Palmieri, H.Rottensteiner, I.Spera, L.Germinario, and F.Palmieri. 2010. Identification and functional characterization of a novel mitochondrial carrier for citrate and oxoglutarate in Saccharomyces cerevisiae. *J. Biol Chem* 285:17359-17370.
14. Chen, H. and D.C.Chan. 2005. Emerging functions of mammalian mitochondrial fusion and fission. *Hum. Mol. Genet.* 14 Spec No. 2:R283-R289.
15. Chen, H. and D.C.Chan. 2009. Mitochondrial dynamics--fusion, fission, movement, and mitophagy--in neurodegenerative diseases. *Hum. Mol. Genet.* 18:R169-R176.
16. Chen, H. and D.C.Chan. 2010. Physiological functions of mitochondrial fusion. *Ann. N. Y. Acad. Sci.* 1201:21-25.
17. Chen, H., A.Chomyn, and D.C.Chan. 2005. Disruption of fusion results in mitochondrial heterogeneity and dysfunction. *J. Biol Chem* 280:26185-26192.
18. Chen, H., S.A.Detmer, A.J.Ewald, E.E.Griffin, S.E.Fraser, and D.C.Chan. 2003. Mitofusins Mfn1 and Mfn2 coordinately regulate mitochondrial fusion and are essential for embryonic development. *J. Cell Biol* 160:189-200.
19. de la Torre-Ruiz MA, A.Mozo-Villarias, N.Pujol, and M.I.Petkova. 2010. How budding yeast sense and transduce the oxidative stress signal and the impact in cell growth and morphogenesis. *Curr. Protein Pept. Sci.* 11:669-679.
20. DeBerardinis, R.J., J.J.Lum, G.Hatzivassiliou, and C.B.Thompson. 2008. The biology of cancer: metabolic reprogramming fuels cell growth and proliferation. *Cell Metab* 7:11-20.
21. Deffieu, M., I.Bhatia-Kissova, B.Salin, A.Galinier, S.Manon, and N.Camougrand. 2009. Glutathione participates in the regulation of mitophagy in yeast. *J. Biol Chem.* 284:14828-14837.
22. Detmer, S.A. and D.C.Chan. 2007. Functions and dysfunctions of mitochondrial dynamics. *Nat Rev. Mol. Cell Biol* 8:870-879.
23. Dimmer, K.S., S.Fritz, F.Fuchs, M.Messerschmitt, N.Weinbach, W.Neupert, and B.Westermann. 2002. Genetic basis of mitochondrial function and morphology in Saccharomyces cerevisiae. *Mol. Biol Cell* 13:847-853.
24. Epstein, C.B., J.A.Waddle, W.Hale, IV, V.Dave, J.Thornton, T.L.Macatee, H.R.Garner, and R.A.Butow. 2001. Genome-wide Responses to Mitochondrial Dysfunction. *Mol. Biol. Cell* 12:297-308.

25. Erjavec, N. and T.Nystrom. 2007. Sir2p-dependent protein segregation gives rise to a superior reactive oxygen species management in the progeny of Saccharomyces cerevisiae. *PNAS* 104:10877-10881.
26. Evans, C., K.L.Bogan, P.Song, C.F.Burant, R.T.Kennedy, and C.Brenner. 2010. NAD+ metabolite levels as a function of vitamins and calorie restriction: evidence for different mechanisms of longevity. *BMC. Chem. Biol* 10:2.
27. Fabrizio, P., C.Gattazzo, L.Battistella, M.Wei, C.Cheng, K.McGrew, and V.D.Longo. 2005. Sir2 blocks extreme life-span extension. *Cell* 123:655-667.
28. Friedman, J.R., L.L.Lackner, M.West, J.R.DiBenedetto, J.Nunnari, and G.K.Voeltz. 2011. ER tubules mark sites of mitochondrial division. *Science* 334:358-362.
29. Gatenby, R.A. and R.J.Gillies. 2004. Why do cancers have high aerobic glycolysis? *Nat Rev. Cancer* 4:891-899.
30. Gietz, R.D. and R.H.Schiestl. 2007a. High-efficiency yeast transformation using the LiAc/SS carrier DNA/PEG method. *Nat Protoc.* 2:31-34.
31. Gietz, R.D. and R.H.Schiestl. 2007b. Quick and easy yeast transformation using the LiAc/SS carrier DNA/PEG method. *Nat Protoc.* 2:35-37.
32. Gietz, R.a.W.R. 2002. Transformation of yeast by the LiAc/SS carrier DNA/PEG method .*Methods in Enzymology* 350:87-96.
33. Goldring, E.S., L.I.Grossman, D.Krupnick, D.R.Cryer, and J.Marmur. 1970. The petite mutation in yeast. Loss of mitochondrial deoxyribonucleic acid during induction of petites with ethidium bromide. *J. Mol Biol* 52:323-335.
34. Goldring, E.S., L.I.Grossman, and J.Marmur. 1971. Petite mutation in yeast. II. Isolation of mutants containing mitochondrial deoxyribonucleic acid of reduced size. *J. Bacteriol.* 107:377-381.
35. Gomes, A.C., I.Miranda, R.M.Silva, G.R.Moura, B.Thomas, A.Akoulitchev, and M.A.Santos. 2007. A genetic code alteration generates a proteome of high diversity in the human pathogen Candida albicans. *Genome Biol* 8:R206.
36. Gorsich, S.W. and J.M.Shaw. 2004. Importance of mitochondrial dynamics during meiosis and sporulation. *Mol. Biol Cell* 15:4369-4381.
37. Grune, T., T.Jung, K.Merker, and K.J.Davies. 2004. Decreased proteolysis caused by protein aggregates, inclusion bodies, plaques, lipofuscin, ceroid, and 'aggresomes' during oxidative stress, aging, and disease. *Int. J. Biochem. Cell Biol* 36:2519-2530.
38. Halliwell, B. and J.Gutteridge. 1999. Free Radicals in Biology and Medicine. Oxford University Press, London.
39. Hector, R.E., M.J.Bowman, C.D.Skory, and M.A.Cotta. 2009. The Saccharomyces cerevisiae YMR315W gene encodes an NADP(H)-specific oxidoreductase regulated by the transcription factor Stb5p in response to NADPH limitation. *N. Biotechnol.* 26:171-180.
40. Hipkiss, A.R. 2010. Mitochondrial dysfunction, proteotoxicity, and aging: causes or effects, and the possible impact of NAD+-controlled protein glycation. *Adv. Clin. Chem* 50:123-150.
41. Holland, S., E.Lodwig, T.Sideri, T.Reader, I.Clarke, K.Gkargkas, D.C.Hoyle, D.Delneri, S.G.Oliver, and S.V.Avery. 2007. Application of the comprehensive set of heterozygous yeast deletion mutants to elucidate the molecular basis of cellular chromium toxicity. *Genome Biol* 8:R268.
42. Holland, S.L., E.Ghosh, and S.V.Avery. 2010. Chromate-induced sulfur starvation and mRNA mistranslation in yeast are linked in a common mechanism of Cr toxicity. *Toxicol. In Vitro* 24:1764-1767.
43. Jensen, R.E., A.E.Hobbs, K.L.Cerveny, and H.Sesaki. 2000. Yeast mitochondrial dynamics: fusion, division, segregation, and shape. *Microsc. Res Tech.* 51:573-583.
44. Kanki, T., D.Kang, and D.J.Klionsky. 2009a. Monitoring mitophagy in yeast: the Om45-GFP processing assay. *Autophagy.* 5:1186-1189.
45. Kanki, T., K.Wang, Y.Cao, M.Baba, and D.J.Klionsky. 2009b. Atg32 is a mitochondrial protein that confers selectivity during mitophagy. *Dev. Cell* 17:98-109.
46. Kissova, I.B. and N.Camougrand. 2009. Glutathione participates in the regulation of mitophagy in yeast. *Autophagy.* 5:872-873.
47. Kwong, L.K. and R.S.Sohal. 1998. Substrate and site specificity of hydrogen peroxide generation in mouse mitochondria. *Arch. Biochem. Biophys.* 350:118-126.
48. Lin, S.J., E.Ford, M.Haigis, G.Liszt, and L.Guarente. 2004. Calorie restriction extends yeast life span by lowering the level of NADH. *Genes Dev.* 18:12-16.
49. Ling, J. and D.Soll. 2010. Severe oxidative stress induces protein mistranslation through impairment of an aminoacyl-tRNA synthetase editing site. *Proc. Natl. Acad. Sci. U. S. A* 107:4028-4033.
50. Linnane, A.W., M.Kios, and L.Vitetta. 2007. Healthy aging: regulation of the metabolome by cellular redox modulation and prooxidant signaling systems: the essential roles of superoxide anion and hydrogen peroxide. *Biogerontology.* 8:445-467.
51. Liu, Z. and R.A.Butow. 2006. Mitochondrial retrograde signaling. *Annu. Rev. Genet.* 40:159-185.

52. Liu, Z., M.Spirek, J.Thornton, and R.A.Butow. 2005. A novel degron-mediated degradation of the RTG pathway regulator, Mks1p, by SCFGrr1. *Mol. Biol Cell* 16:4893-4904.
53. Macomber, L., C.Rensing, and J.A.Imlay. 2007. Intracellular copper does not catalyze the formation of oxidative DNA damage in Escherichia coli. *J. Bacteriol.* 189:1616-1626.
54. Martinez, M.J., S.Roy, A.B.Archuletta, P.D.Wentzell, S.S.nna-Arriola, A.L.Rodriguez, A.D.Aragon, G.A.Quinones, C.Allen, and M.Werner-Washburne. 2004a. Genomic analysis of stationary-phase and exit in Saccharomyces cerevisiae: gene expression and identification of novel essential genes. *Mol. Biol. Cell* 15:5295-5305.
55. Mendl, N., A.Occhipinti, M.Muller, P.Wild, I.Dikic, and A.S.Reichert. 2011. Mitophagy in yeast is independent of mitochondrial fission and requires the stress response gene WHI2. *J. Cell Sci.* 124:1339-1350.
56. Mesquita, A., M.Weinberger, A.Silva, B.Sampaio-Marques, B.Almeida, C.Leao, V.Costa, F.Rodrigues, W.C.Burhans, and P.Ludovico. 2010. Caloric restriction or catalase inactivation extends yeast chronological lifespan by inducing H2O2 and superoxide dismutase activity. *Proc. Natl. Acad. Sci. U. S. A* 107:15123-15128.
57. Minard, K.I. and L.ister-Henn. 2010. Pnc1p supports increases in cellular NAD(H) levels in response to internal or external oxidative stress. *Biochemistry* 49:6299-6301.
58. Miranda, I., R.Rocha, M.C.Santos, D.D.Mateus, G.R.Moura, L.Carreto, and M.A.S.Santos. 2007. A Genetic Code Alteration Is a Phenotype Diversity Generator in the Human Pathogen Candida albicans. *PLoS ONE* 2:e996.
59. Moradas-Ferreira, P., V.Costa, P.Piper, and W.Mager. 1996. The molecular defences against reactive oxygen species in yeast. *Mol. Microbiol.* 19:651-658.
60. Moura, G.R., L.C.Carreto, and M.A.Santos. 2009. Genetic code ambiguity: an unexpected source of proteome innovation and phenotypic diversity. *Curr. Opin. Microbiol.* 12:631-637.
61. Nogales-Cadenas, R., P.Carmona-Saez, M.Vazquez, C.Vicente, X.Yang, F.Tirado, J.M.Carazo, and A.Pascual-Montano. 2009. GeneCodis: interpreting gene lists through enrichment analysis and integration of diverse biological information. *Nucleic Acids Res* 37:W317-W322.
62. Nunnari, J., W.F.Marshall, A.Straight, A.Murray, J.W.Sedat, and P.Walter. 1997. Mitochondrial transmission during mating in Saccharomyces cerevisiae is determined by mitochondrial fusion and fission and the intramitochondrial segregation of mitochondrial DNA. *Mol. Biol Cell* 8:1233-1242.
63. Okamoto, K., N.Kondo-Okamoto, and Y.Ohsumi. 2009a. A landmark protein essential for mitophagy: Atg32 recruits the autophagic machinery to mitochondria. *Autophagy.* 5:1203-1205.
64. Okamoto, K., N.Kondo-Okamoto, and Y.Ohsumi. 2009b. Mitochondria-anchored receptor Atg32 mediates degradation of mitochondria via selective autophagy. *Dev. Cell* 17:87-97.
65. Othumpangat, S., M.Kashon, and P.Joseph. 2005. Eukaryotic translation initiation factor 4E is a cellular target for toxicity and death due to exposure to cadmium chloride. *J. Biol Chem* 280:25162-25169.
66. Ott, M., V.Gogvadze, S.Orrenius, and B.Zhivotovsky. 2007. Mitochondria, oxidative stress and cell death. *Apoptosis.* 12:913-922.
67. Palermo, V., C.Falcone, M.Calvani, and C.Mazzoni. 2010. Acetyl-L-carnitine protects yeast cells from apoptosis and aging and inhibits mitochondrial fission. *Aging Cell* 9:570-579.
68. Paredes JA. Estudo molecular da degeneração e evolução celular induzidas por erros na tradução do mRNA / Molecular study of cell degeneration and evolution induced by mRNA mistranslation. 2010. University of Aveiro.
Parikh, V.S., M.M.Morgan, R.Scott, L.S.Clements, and R.A.Butow. 1987. The mitochondrial genotype can influence nuclear gene expression in yeast. *Science* 235:576-580.
69. Pastor, M.M., M.Proft, and A.Pascual-Ahuir. 2009. Mitochondrial function is an inducible determinant of osmotic stress adaptation in yeast. *J. Biol Chem.* 284:30307-30317.
70. Pfeiffer, T., S.Schuster, and S.Bonhoeffer. 2001. Cooperation and competition in the evolution of ATP-producing pathways. *Science* 292:504-507.
71. Poliakova, D., B.Sokolikova, J.Kolarov, and L.Sabova. 2002. The antiapoptotic protein Bcl-x(L) prevents the cytotoxic effect of Bax, but not Bax-induced formation of reactive oxygen species, in Kluyveromyces lactis. *Microbiology* 148:2789-2795.
72. Reverter-Branch, E.Cabiscol, J.Tamarit, and J.Ros. 2004. Oxidative damage to specific proteins in replicative and chronological-aged Saccharomyces cerevisiae: common targets and prevention by calorie restriction. *J. Biol Chem.* 279:31983-31989.
73. Reynolds, N.M., B.A.Lazazzera, and M.Ibba. 2010. Cellular mechanisms that control mistranslation. *Nat Rev Microbiol.* 8:849-856.
74. Rodrigues-Pousada, C., R.A.Menezes, and C.Pimentel. 2010. The Yap family and its role in stress response. *Yeast* 27:245-258.
75. Rodrigues-Pousada, C.A., T.Nevitt, R.Menezes, D.Azevedo, J.Pereira, and C.Amaral. 2004. Yeast activator proteins and stress response: an overview. *FEBS Lett.* 567:80-85.
76. Rutkowski, D.T. and R.J.Kaufman. 2007. That which does not kill me makes me stronger: adapting to

77. Saeed, A.I., N.K.Bhagabati, J.C.Braisted, W.Liang, V.Sharov, E.A.Howe, J.Li, M.Thiagarajan, J.A.White, and J.Quackenbush. 2006. TM4 microarray software suite. *Methods Enzymol.* 411:134-193.
78. Saeed, A.I., V.Sharov, J.White, J.Li, W.Liang, N.Bhagabati, J.Braisted, M.Klapa, T.Currier, M.Thiagarajan, A.Sturn, M.Snuffin, A.Rezantsev, D.Popov, A.Ryltsov, E.Kostukovich, I.Borisovsky, Z.Liu, A.Vinsavich, V.Trush, and J.Quackenbush. 2003a. TM4: a free, open-source system for microarray data management and analysis. *Biotechniques* 34:374-378.
79. Santel, A. and S.Frank. 2008. Shaping mitochondria: The complex posttranslational regulation of the mitochondrial fission protein DRP1. *IUBMB. Life* 60:448-455.
80. Santos, M.A., C.Cheesman, V.Costa, P.Moradas-Ferreira, and M.F.Tuite. 1999. Selective advantages created by codon ambiguity allowed for the evolution of an alternative genetic code in Candida spp. *Mol Microbiol.* 31:937-947.
81. Santos, M.A.S., V.M.Perreau, and M.F.Tuite. 1996. Transfer RNA structural change is a key element in the reassignment of the CUG codon in Candida albicans. *EMBO J.* 15:5060-5068.
82. Sesaki, H. and R.E.Jensen. 2001. UGO1 encodes an outer membrane protein required for mitochondrial fusion. *J. Cell Biol* 152:1123-1134.
83. Shenton, D., J.B.Smirnova, J.N.Selley, K.Carroll, S.J.Hubbard, G.D.Pavitt, M.P.Ashe, and C.M.Grant. 2006. Global translational responses to oxidative stress impact upon multiple levels of protein synthesis. *J. Biol Chem* 281:29011-29021.
84. Sherman, F. 2002. Getting started with yeast. *Methods Enzymol.* 350:3-41.
85. Silva RM, Paredes JA, Moura GR, C.Vacher, Manadas B, Lima-Costa T, Rocha R, Miranda I, Gomes AC, Koerkamp MJ, Perrot M, Holstege FC, Boucherie H, and Santos MA. 2007. Critical roles for a genetic code alteration in the evolution of the genus Candida. *EMBO JOURNAL* oct 11 2007.
86. Silva, R.M., I.C.N.Duarte, J.A.Paredes, T.Lima-Costa, M.Perrot, H.+.Boucherie, B.J.Goodfellow, A.C.Gomes, D.D.Mateus, G.R.Moura, and M.A.S.Santos. 2009. The Yeast PNC1Longevity Gene Is Up-Regulated by mRNA Mistranslation. *PLoS ONE* 4:e5212.
87. Spitz, D.R., J.E.Sim, L.A.Ridnour, S.S.Galoforo, and Y.J.Lee. 2000. Glucose deprivation-induced oxidative stress in human tumor cells. A fundamental defect in metabolism? *Ann. N. Y. Acad. Sci.* 899:349-362.
88. Sporty, J.L., M.M.Kabir, K.W.Turteltaub, T.Ognibene, S.J.Lin, and G.Bench. 2008. Single sample extraction protocol for the quantification of NAD and NADH redox states in Saccharomyces cerevisiae. *J Sep. Sci* 31:3202-3211.
89. Starkov, A.A. 2010. Measurement of mitochondrial ROS production. *Methods Mol Biol* 648:245-255.
90. Tahara, E.B., M.H.Barros, G.A.Oliveira, L.E.Netto, and A.J.Kowaltowski. 2007. Dihydrolipoyl dehydrogenase as a source of reactive oxygen species inhibited by caloric restriction and involved in Saccharomyces cerevisiae aging. *FASEB J.* 21:274-283.
91. Titorenko, V.I. and S.R.Terlecky. 2011. Peroxisome metabolism and cellular aging. *Traffic.* 12:252-259.
92. Toussaint, M. and A.Conconi. 2006. High-throughput and sensitive assay to measure yeast cell growth: a bench protocol for testing genotoxic agents. *Nat Protoc.* 1:1922-1928.
93. Tu, B.P. and J.S.Weissman. 2004. Oxidative protein folding in eukaryotes: mechanisms and consequences. *J. Cell Biol* 164:341-346.
94. van de, P.J., P.Kemmeren, B.H.van, M.Radonjic, L.D.van, and F.C.Holstege. 2003. Monitoring global messenger RNA changes in externally controlled microarray experiments. *EMBO Rep.* 4:387-393.
95. Vander Heiden, M.G., L.C.Cantley, and C.B.Thompson. 2009. Understanding the Warburg effect: the metabolic requirements of cell proliferation. *Science* 324:1029-1033.
96. Warburg, O., F.Wind, and E.Negelein. 1927. The metabolism of tumors in the body. *J. Gen. Physiol* 8:519-530.
97. Wysocki, R. and S.J.Kron. 2004. Yeast cell death during DNA damage arrest is independent of caspase or reactive oxygen species. *J Cell Biol* 166:311-316.
98. 103. Youle, R.J. and M.Karbowski. 2005. Mitochondrial fission in apoptosis. *Nat Rev. Mol. Cell Biol* 6:657-663.
99. 104. Zuin, A., N.Gabrielli, I.A.Calvo, S.Garcia-Santamarina, K.L.Hoe, D.U.Kim, H.O.Park, J.Hayles, J.Ayte, and E.Hidalgo. 2008. Mitochondrial dysfunction increases oxidative stress and decreases chronological life span in fission yeast. *PLoS One.* 3:e2842.

Chapter 4
Mistranslation induces formation of p-bodies in yeast

Unpublished work, in preparation

Abstract

Gene mistranslation imposes permanent stress on the cell, due to increased synthesis of aberrant proteins. It is known that cells exposed to environmental, nutritional or chemical stressors down-regulate translation and sequester mRNAs bound to proteins (ribonucleoprotein complexes) in granules, namely in processing bodies (P-bodies) and stress granules (SG). P-bodies contain non-translating mRNAs complexed with translation repressors, decapping enzymes and an exonuclease and are sites of mRNA storage and/or degradation. On the other hand, stress granules contain untranslated mRNAs, translation initiation factors, the 40S ribosomal subunit and the poly-A binding protein (Pabp). These granules have been linked to viral infection, cancer, inflammatory and neurodegenerative diseases, and are necessary for optimal translation and for stress responses. In here, we have used epifluorescence microscopy to test whether the stress imposed by gene mistranslation also induces the formation of cytoplasmatic granules. Our data show that gene mistranslation promotes P-body formation but stress granules were not detected. We further show that mistranslation down-regulates the expression of ribosomal protein genes and decreases ribosomal proteins. These results show that post-transcriptional regulation of gene expression plays an important role in the cellular responses to accumulation of aberrant proteins.

Introduction

Post-transcriptional regulation of gene expression is extensive in eukaryotic cells (McCarthy, 1998; Lackner and Bεhler, 2008). Indeed, mRNAs are assembled into mRNPs (messenger ribonucleoproteins complexes) by RNA binding proteins and are exported to the cytoplasm for immediate or delayed translation. The fate of mRNAs depends on their *cis* elements and transacting proteins, which are responsive to cell cycle, cell type, developmental timing and environmental stressors. mRNAs programmed for delayed translation are transported and stored in cytoplasmatic foci until a particular stimuli determine their translation. Germ granules, neuronal granules, P-bodies and stress granules are some examples of these cytoplasmatic foci. Germ granules and neuronal granules play important roles in the localization and control of mRNAs in embryos and neurons, respectively, and are related to the two foci type mentioned above. Stress granules (SG) were originally thought to exist in mammalian cells only but granules with similar composition and assembly mechanism have been observed in yeast (Brengues and Parker, 2007; Hoyle et al., 2007; Hoyle and Ashe, 2008). These structures are dynamic and form when translation initiation is impaired, namely under stress - where translation is down-regulated, in the presence of drugs that block translation and by knockdown of specific initiation factors. The SGs composition can vary depending on the stress applied (Buchan and Parker, 2009; Buchan et al., 2011). Also, besides mRNAs, 40S ribosomal subunits, several initiation factors, poly (A) binding protein, RNA helicases, translation and stability regulators and factors involved in signaling are normally found in these granules. SG associate with P-

bodies (Buchan and Parker, 2009) which are specialized and evolutionary conserved structures, which exist in various organisms namely *S.cerevisiae* (Teixeira et al., 2005), *D.melanogaster* (Lin et al., 2006; Lin et al., 2008b), *T. brucei* (Cassola et al., 2007) and mammalian cells (van Dijk et al., 2002). They contain non-translated mRNAs, enzymes related to deccaping and degradation of mRNAs, namely Dcp2p, Dhh1p, Dcp1p, Xrn1p, the deadenylase hCcr4, the GW182 RNA-binding protein (mammals), the Lsm1-7 proteins, argonaute family proteins, the latter being involved in miRNA (micro-RNAs) and siRNA (small interference RNAs) mediated regulation of gene expression in mammals. Still, they do not contain ribosomes or translation factors, with the exception of eIF4E which has been found in mammalian P-bodies (Andrei et al., 2005).

Several roles have been proposed for P-bodies, namely mRNA decay and mRNA storage. When mRNA decay is trapped, either by inserting a strong secondary structure (polyG) in its 3'untranslated region (3'UTR) or by deletion of the 5' to 3' exonuclease Xrn1p, the decay intermediate localizes to P-bodies. Also, when the flux of the decay pathway is perturbed, P-bodies change in size: when mRNA entry into the foci is inhibited their size decreases (Teixeira et al., 2005; Franks and Lykke-Andersen, 2008) but when the deccaping or the 5'-3' degradation pathway are inhibited, foci size increases. In other words, if mRNAs are not degraded they accumulate in the cytoplasm. However, the aggregation of mRNPs into P-bodies is not required for mRNA decay (Buchan and Parker, 2009). Interestingly, when mRNAs are trapped into the translational pool using cycloheximide, which inhibits translation elongation, P-bodies decline (Teixeira et al., 2005) but, when translation initiation is inhibited using a

temperature sensitive allele of eIF3 or eIF4, the foci increase in size. Also, P-bodies increase in size and number in response to a variety of stresses, namely glucose starvation, osmotic stress or ultraviolet radiation (Teixeira et al., 2005; Teixeira and Parker, 2007). Furthermore, sorting of house-keeping messages to P-bodies has been proposed to play an important role in stress adaptive translational reprogramming by both repressing translation of growth related genes and by rapidly increasing the pool of translation factors available to bind to low abundace messages required for the appropriate stress response.

Several observations suggest that mRNAs can circulate between polysomes, P-bodies and stress granules. Indeed, the mRNAs present in P-bodies and stress granules increase in abundance while decreasing in polysomes when translation is inhibited (Teixeira et al., 2005; Kedersha et al., 2005). However, when mRNAs are trapped in polysome due to a translation elongation blockage, their relative abundance in P-bodies and stress granules decreases (Teixeira et al., 2005). Moreover, the two types of granules interact physically. For example, in mammalian cells they frequently dock together under stress and, in yeast, they partially overlap (Kedersha et al., 2005). Finally, mRNAs contained in P-bodies in mammalian and yeast cells, return to translation (Brengues et al., 2005; Bhattacharyya et al., 2006b). Together, these observations suggest a working model known as the mRNA cycle (Buchan and Parker, 2009; Balagopal and Parker, 2009), where mRNAs exist in 2 predominant mRNP states, namely translating or repressed and the later can accumulate in P-bodies and stress granules. Translation, deanylation and mRNA decay occur at different rates and in

different biochemical states and compartments and P-bodies may regulate mRNA transport and its localization throught discrete mechanisms, involving several proteins that move mRNA between compartments. Accordingly, the mRNAs in polysomes can undergo several rounds of translation. The mRNAs located in polysomes can interact with Dhh1p/Rckp and Pat1p, which repress translation initiation. This interaction facilitates trapping of the mRNAs into a non-translating state which may lead to run-off of elongating ribosomes, recruitment of what is left of the decapping machinery, decapping followed by degradation of the transcript and aggregation of an individual mRNP into a P-body. When mRNAs are complexed with the decapping machinery they can be degraded, aggregated into P-bodies or undergo mRNP rearrangement, the degradation machinery can be exchanged with translation initiation factors, which allow those mRNAs to re-enter translation. If translation initiation factors are limiting, these mRNAs can simply accumulate in a stress granule. This step can also define the composition of the stress granules which may explain the variable composition of this structure between different organisms and in response to different stressors. Specific mRNAs may preferentially accumulate in stress granules, P-bodies or polysomes depending on their relative transition rate between these different biochemical states. Such transitions can affect translation, degradation and even mRNA localization.

As stated above, P-bodies and stress granules are intrinsically connected to mRNA translation and control of this event is fundamental to regulate cellular homeostasis. Another factor that can control translation is the ribosome. This implies controlling its biogenesis as well as its degradation. The former involves the fine tuning of three nuclear RNA polymerases to produce equimolar amounts of four ribosomal RNAs

(rRNAs) and 80S ribosomal proteins (RPs). Interestingly, the mRNA expression profiles of the 137 RP genes and RiBi genes are very similar to profiles in response to starvation or environmental stresses (Jorgensen et al., 2004a;Gasch et al., 2000).Transcription coordination of ribosome biogenesis is controlled by several factors, namely c-Myc (multicellular eukaryotes) and Maf1p (Pluta et al., 2001; Eilers and Eisenman, 2008). Also, autoregulatory loops have been described to control ribosome biogenesis and provided links between the latter and cell cycle control (Bernstein et al., 2007; Lin et al., 2008a). In what degradation is concerned, recently reports have showed that ribosomes are selectively degraded by autophagy in a process denominated ribophagy, which is dependent on ubiquitination. Interestingly RP nuclear degradation has also been shown to depend on ubiquitination, in HeLa cells. A deeper analysis of ribosome biogenesis has allowed drawing links between it and several diseases, namely anemia and cancer, as well as aging. For instance, RP genes are haploinsuffiency tumor suppressors in the zebrafish model and deletion of several RPs lead to increased lifespan in *C.elegans* and yeast (Ruggero and Pandolfi, 2003; Steffen et al., 2008b; Amsterdam et al., 2004; Hamilton et al., 2005). Also, increased ribosomal biogenesis is a characteristic of aggressive human breast cancer (Belin et al., 2009).

Since mistranslation is a stressor, we endeavored to evaluate if it affects P-body and stress granule formation or remodels the translational machinery, namely the ribosome in yeast. Our data indicates that mRNA mistranslation induces P-body formation without affecting SG biogenesis and negatively affects ribosomal gene and protein expression, providing for the first time a link between errors in the translation process and cytoplasmatic granule formation.

RESULTS

Mistranslation induces P-Body assembly and does not affect stress granules dynamics

Genes are normally translated with high accuracy (10^{-4} to 10^{-5} errors *per* codon). However, under specific environmental conditions and in certain pathologies such errors can increase, thus destabilizing the proteome and imposing strong stress on the cell. This prompted us to investigate whether such stress (proteotoxic stress) would interfere with P-body and/or stress granule formation. For this, we have induced mistranslation in yeast using mutant serine tRNAs that can decode leucine CUG codons as serine (Silva, 2005; Silva et al., 2009; Santos et al., 1996). P-body formation was then monitored during both exponential and stationary growth phases using epifluorescence microscopy and two P-body fluorescent markers, namely the GFP-tagged Dcp2p (Figure 37) and the m-Cherry-tagged Edc3 protein (Figure 38). The former is a subunit of the decapping enzyme and is easily observed in P-bodies under all conditions (Teixeira et al., 2005) while the later is a decapping activator (Buchan et al., 2010).

In actively growing cells, mistranslation increased P-body size and number per cell (Figure 37). The average number of P-bodies per cell increased from 50% in mistranslating cells. Interestingly, the number of cells containing P-bodies increased 20% (from 18% to 38%) (Figure 37, C, control cell analysis). Additionally, the P-bodies

of mistranslating cells appeared to be bigger and brighter than those of the control cells.

In order confirm that the above alterations in P-body formation was due to mistranslation, P-body assembly was also accessed after treatment with drugs that induce mistranslation, namely the aminoglycosidic antibiotic paromomycin or the protein misfolding inducing drugs L-azetidine-2-carboxylic-acid (AZC) and canavanine (Figure 37). The aminoglicosidic antibiotics interact with the highly conserved decoding site of the ribosome where pairing between the codon of the mRNA and the corresponding anticodon of a cognate transfer-RNA occurs. When aminoglycosic antibiotics bind to the ribosome near-cognate tRNAs are able to decode erroneous codons, thus allowing for introduction of the wrong amino acid into the growing polypeptide chain. AZC is a L-proline analogue, which is recognized by the prolyl-tRNAsynthetase (ProRS) and is accepted by the ribosome and incorporated into proteins inducing misfolding. Canavanine is a naturally occurring analog of arginine that is also incorporated into proteins by the ribosome. When control cells were challenged with these drugs, we observed that AZC and paromomycin increased the P-body formation by 1.5 fold and 2.3 fold respectively while canavanine did not have visible effect on the number of P-bodies per cell (Figure 37, A and B).However, all mistranslation inducing drugs had a clear effect on the number of cells that presented P-bodies (20-30% increase) (Figure 37 A and C). Brightness and size of the granules did not change significantly between the different drug treatments, however addition of these drugs to mistranslating cells increased in the number of P-bodies per cell (1.5x

for AZC treatment and 1.2x for canavanine, Figure 37 A and B) was observed. The same effect was observed for the percentage of cells containing P-bodies, where only AZC had a clear positive effect. Both control and mistranslating cells were further challenged with oxidative stress and were also observed in stationary phase (Figure 37, C and D, respectively). Previous studies showed that oxidative stress does not affect P-body assembly (Teixeira et al., 2005), and our data confirmed those studies as oxidative stress did not lead to P-body accumulation. During diauxic shift the P-bodies increase in signal intensity and number, while in stationary phase they increase in size and a decrease in number (Teixeira et al., 2005). Our data support these findings for both control and mistranslating cells (Figure 37, D and data not shown).

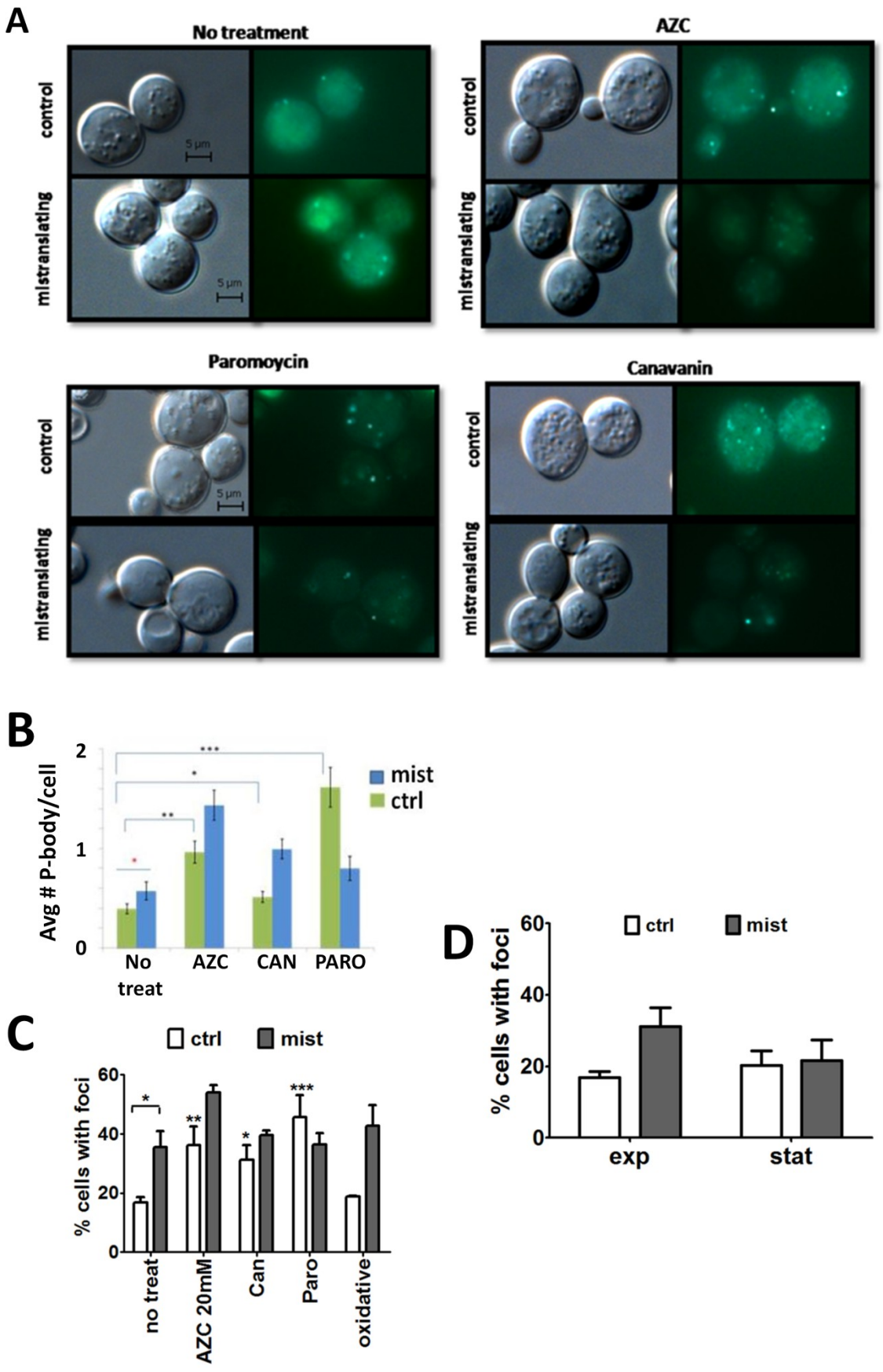
A
No treatment
AZC
Paromoycin
Canavanin
control
mistranslating
5 µm
B
Avg # P-body/cell
mist
ctrl
No treat
AZC
CAN
PARO
C
ctrl
mist
% cells with foci
no treat
AZC 20mM
Can
Paro
oxidative
D
ctrl
mist
% cells with foci
exp
stat

Figure 37- **P-body assembly in mistranslating yeast cells.** Cells were co-transformed with plasmids harboring mistranslation inducing tRNAs or an empty control plasmid plus a plasmid containing a Dcp2-GFP fusion. P-body formation was monitored during exponential growth phase by epifluorescence microscopy A) P-body formation induced by mRNA mistranslation in yeast. A misreading tRNA and the proline analogue L-azetidine-2-carboxylic-acid (AZC), the arginine analogue canavanine (CAN) or the aminoglycosidic antibiotic paromomycin were used. Pictures shown are collapsed stacks of Z-series of yeast photographs. B) Quantification of the number of P-bodies per cell. C) Quantification values (%) of cells with visible P-bodies, depending on the treatment are shown. Oxidative stress was tested, but no representative images are shown. D) Comparison between exponential and stationary phase. At least 2 independent experiments were analyzed and >150 cells for each condition and experiment were monitored. Error bars represent the standard error of the mean In C) * and full lines represents the significant results with $p<0.05$ for a t-test for independent samples and * alone represents significance levels for a 1-way ANOVA, followed by a Dunnetts test (comparison to no treatment condition, for each strain).

P-body assembly was also monitored using an Edc3-mCherry fusion, which confirmed the previously described observations (Figure 38). In this assay, we have also used glucose deprivation as a positive control for P-body formation, which is known to have a strong effect on P-body and SG formation (Buchan et al., 2010). Our results confirmed our previous observations (Figure 38). We were also able to quantify SG formation as the plasmid used also harbored a Pab1-GFP fusion. Yeast SG are usually not visible and only form when translation initiation is impaired, likely due to decreased function of eIF2 or eIF4 (Buchan et al., 2010). Mistranslation did not increase the number of SG positive cells (Figure 38). This result was somewhat surprising as SG formation is known to depend on P-body assembly (Buchan et al., 2008). That is, P-body accumulation should have resulted in increased SG formation. Interestingly, when cells were grown in the absence of glucose, the number of SG positive cells increased both in control and mistranslating cells, however the former

contained more SGs than the latter indicating that mistranslation has little or no effect on SG formation.

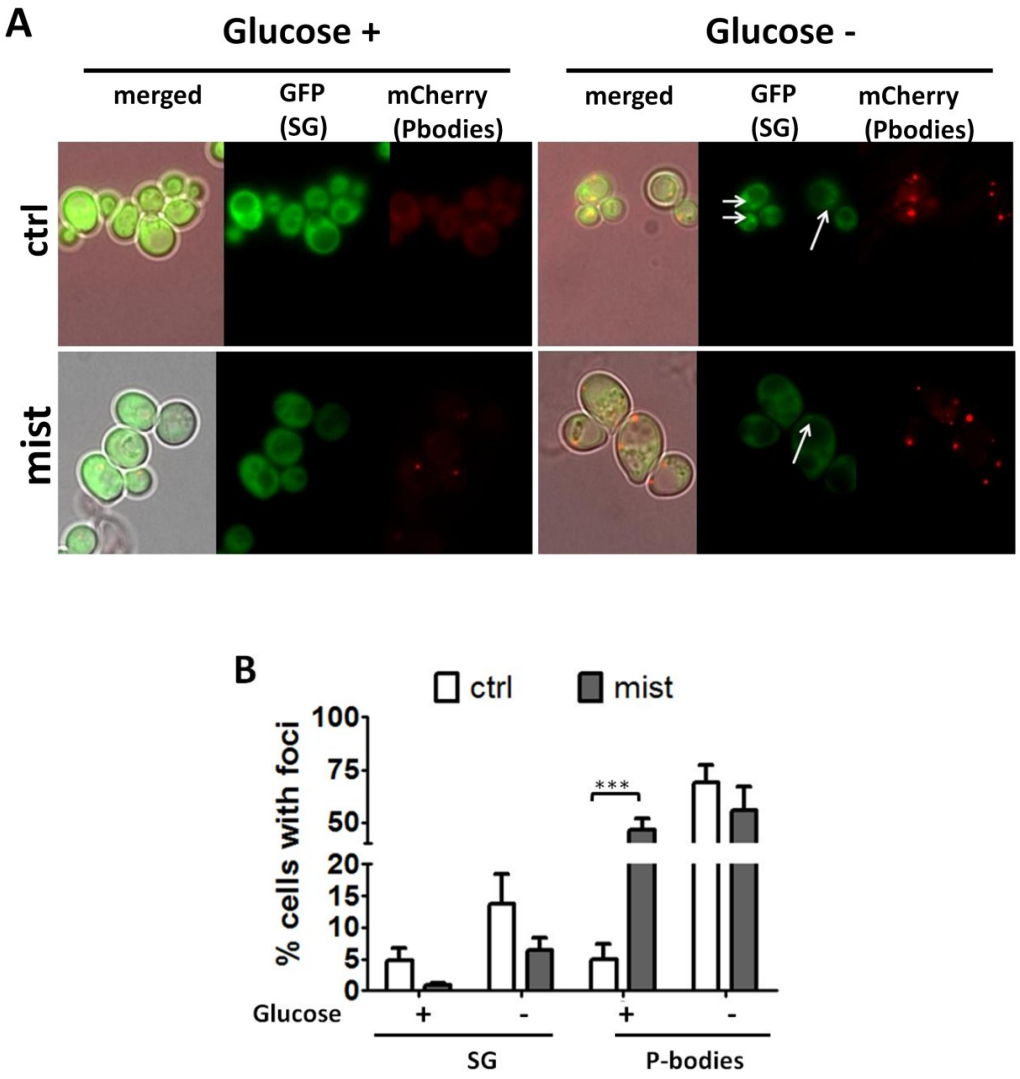

Figure 38- P-body and stress granules assembly in mistranslating yeast. P-body and stress granule formation was monitored in yeast during exponential growth phase using epifluorescence microscopy. An Edc3-mCherry fusion was used to monitor to P-bodies and a Pab1-GFP fusion was used to monitor stress granules. A) Epifluorescence images of mistranslating yeast cells where fluorescent foci represent P-bodies or SG. RNA granules formation was analyzed either in glucose rich (glucose +) and in glucose starvation conditions (glucose-, positive control) B) Fluorescent foci were quantified in at least 3 independent experiments where >150 cells were analyzed for each condition and experiment. Error bars represent the standard error of the mean and * represents the significant results with $p<0.05$ for a t-test for independent samples. ctrl- stands for control cells; mist- stands for mistranslating cells; SG- stands for stress granules. Enlarged view of cells grown in glucose rich medium is shown in supp.fig 20.

In stationary phase, the mistranslating cells presented increased SG formation (4.7% of cells were SG positive) which was similar to the increase observed in glucose starvation conditions (6.3%). These observations seem to indicate that SG accumulation is not a hallmark of mistranslation.

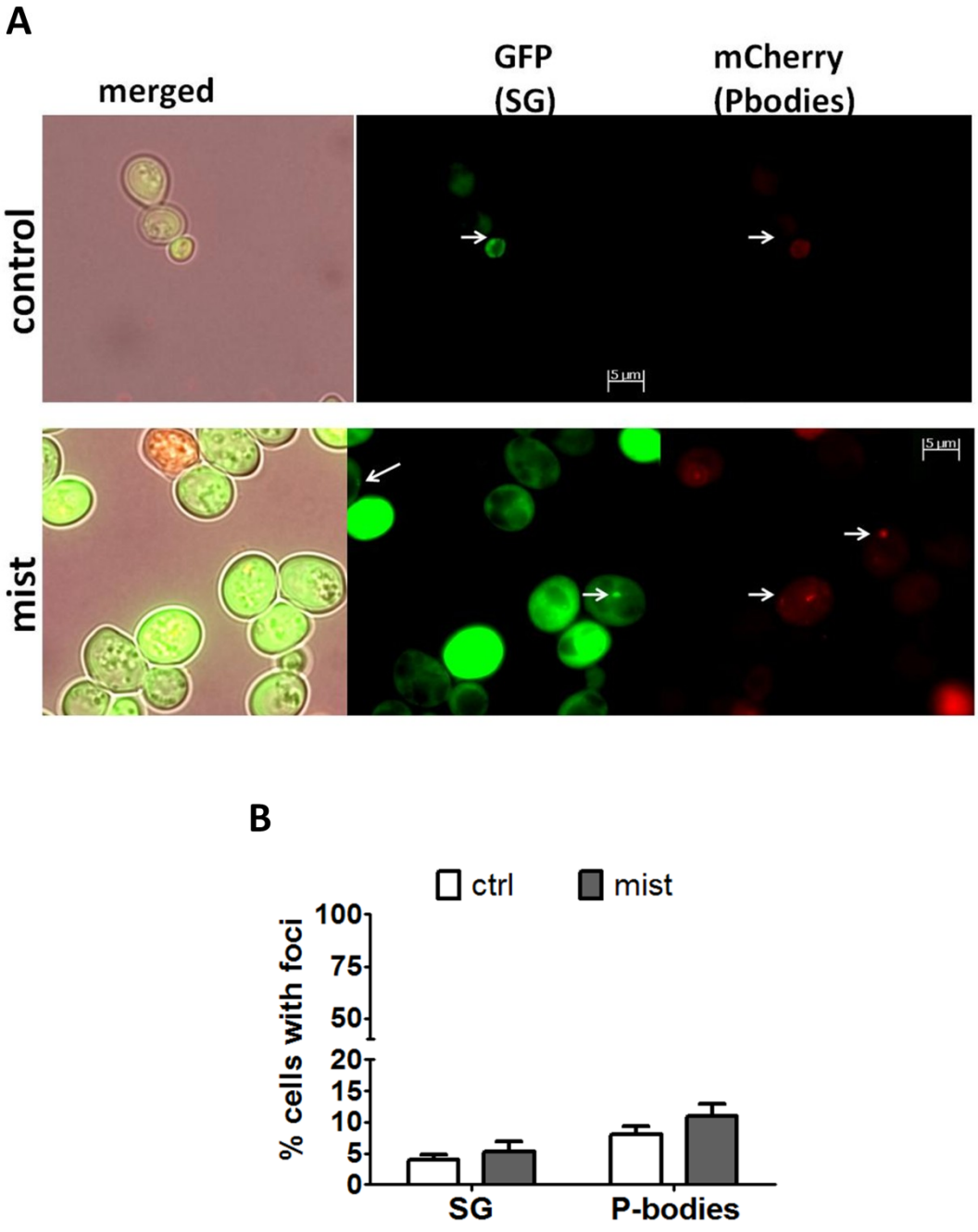

Figure 39- P-body and stress granule assembly in stationary phase cells. P-body and stress granule formation was monitored in yeast cultures growing for 36 ± 5h by epifluorescence microscopy using GFP-tagged proteins (Edc3-mCherry to monitor P-bodies and Pab1-GFP to

monitor stress granules). A) Epifluorescence images of mistranslating cells where fluorescent foci represent P-bodies or SG. B) Fluorescent foci were quantified in at least 3 independent experiments and >150 cells for each condition and experiment were analyzed. Error bars represent the standard error of the mean and * represents the significant results with $p<0.05$ for a t-test for independent samples.

Since P-bodies form under stress conditions where protein synthesis rate is decreased, we decided to investigate whether mistranslation affected protein synthesis machinery. Transcriptome profiling of the mistranslating cells showed down-regulation of genes encoding components of the protein synthesis machinery, namely RIBI regulon genes, translational factors, ribosome subunits, ribosome biogenesis factors and ribosomal RNA (rRNA) metabolism genes (Figure 40, A, Table 10, Table 11). This down-regulation was also reflected at the ribosomal protein level as a Rpl25-GFP fluorescent ribosomal protein showed a strong decrease in fluorescence (Figure 40, B) and a western blot of various ribosomal proteins further confirmed this result (Figure 40, C).

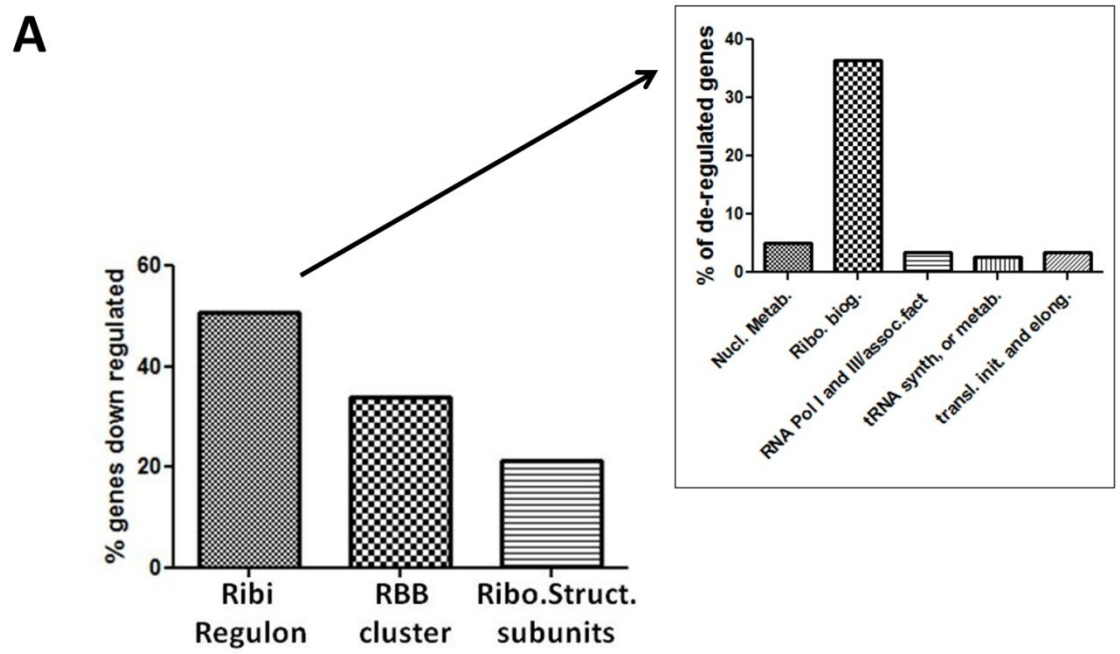

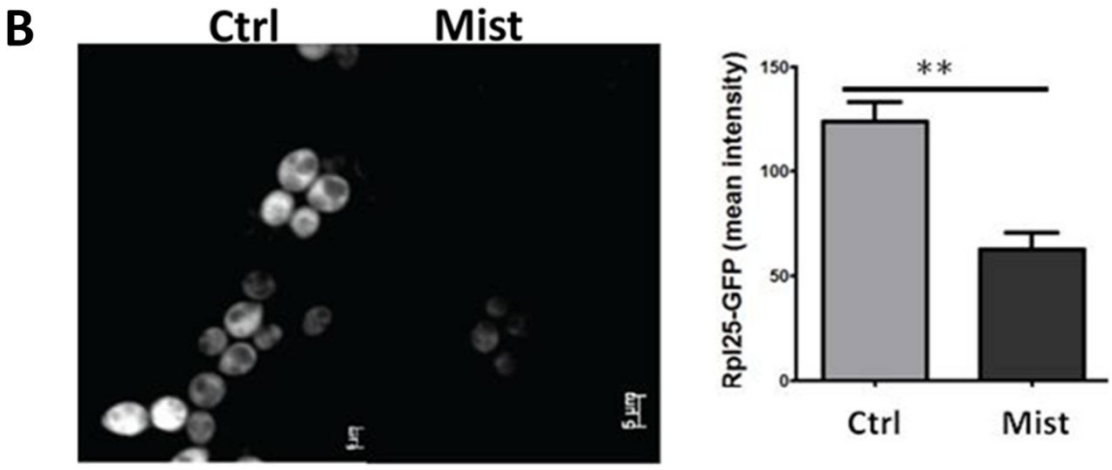

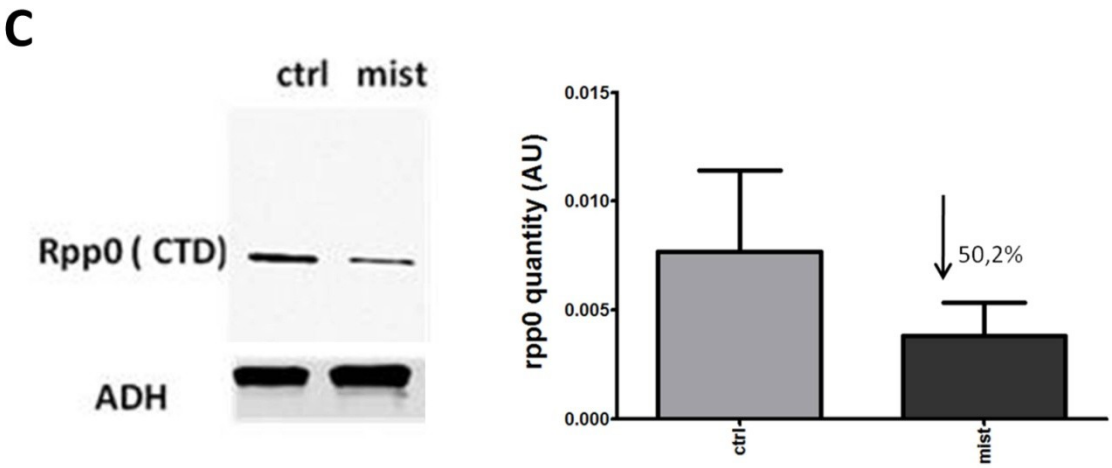

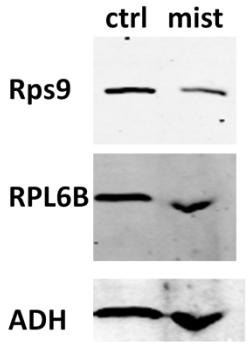

	log2 ratio	Fold change
RPL6B	-0,66	− 1,6
RPP0	-0,64	− 1,6
RPS9	unchanged	

Figure 40- Mistranslation down-regulates ribosome biogenesis A) Gene expression profiling of mistranslating cells showed strong down-regulation of genes involved in ribosome biogenesis, as determined by filtering the global gene expression profiles of mistranslating cells B) Ribosome number was determined by epifluorescence microscopy using the ribosomal protein RPL25 fused to GFP (Rpl25-GFP). Images shown were captured at identical exposure time frames for control and mistranslating cells. The histogram shows the level of GFP fluorescence determined using the ImageJ software package. At least two randomly chosen microscope fields were analyzed and 250-500 cells per clone/experiment were counted. **

indicates significant results for $p<0.05$, two tailed t-test. C) (Upper panel) The ribosomal protein Rpp0 was detected by western blot whose signals were quantified using infrared imaging (Odyssey scanner). (lower panel) Levels of ribosomal proteins Rps9 and Rpl6B that were also quantified using western blotting. The table shows the fold variation of the ribosomal proteins. Cells were grown to exponential phase and protein extracts were performed as described elsewhere. Proteins were fractioned by SDS-PAGE electrophoresis, transferred to nitrocellulose membranes blotted using anti-Rpl6 and anti-Rps9 antibodies. Membranes were scanned using an Odyssey scanner. The data refer to single experiments. Antibodies were a kind gift of Professor JPG Ballestra, Professor Sabine Rospert and Dr. Mathias Seedorf. Ctrl- control non mistranslating cells, Mist- mistranslating cells. *Note: ADH shown refers only to the RPL6 membrane.*

Table 10-Functional Enrichment Analysis of mistranslating cells (down-regulated genes)

GO TERM (Biological Process)	% of genes	corrected p value
GO:0042254 :ribosome biogenesis (BP)	22,3	1.41701e-53
GO:0006364 :rRNA processing (BP)	22,6	1.03116e-47
GO:0042273 :ribosomal large subunit biogenesis (BP)	6,6	2.08877e-17
GO:0009451 :RNA modification (BP)	7,5	6.9216e-15
GO:0000027 :ribosomal large subunit assembly (BP)	5,7	1.49034e-13
GO:0000462 :maturation of SSU-rRNA from tricistronic rRNA transcript (SSU-rRNA, 5.8S rRNA, LSU-rRNA) (BP)	6,3	2.06898e-11
GO:0018193 :peptidyl-amino acid modification (BP)	6,6	1.12245e-09
GO:0000447 :endonucleolytic cleavage in ITS1 to separate SSU-rRNA from 5.8S rRNA and LSU-rRNA from tricistronic rRNA transcript (SSU-rRNA, 5.8S rRNA, LSU-rRNA) (BP)	4,8	1.65733e-09
GO:0000480 :endonucleolytic cleavage in 5'-ETS of tricistronic rRNA transcript (SSU-rRNA, 5.8S rRNA, LSU-rRNA) (BP)	3,9	6.71497e-09
GO:0042274 :ribosomal small subunit biogenesis (BP)	4,2	1.81167e-08
GO:0000472 :endonucleolytic cleavage to generate mature 5'-end of SSU-rRNA from (SSU-rRNA, 5.8S rRNA, LSU-rRNA) (BP)	3,9	2.47484e-08
GO:0000463 :maturation of LSU-rRNA from tricistronic rRNA transcript (SSU-rRNA, 5.8S rRNA, LSU-rRNA) (BP)	2,7	1.35437e-07
GO:0042255 :ribosome assembly (BP)	3,0	1.77251e-07
GO:0006412 :translation (BP)	12,0	4.38331e-07
GO:0006417 :regulation of translation (BP)	7,2	6.50151e-06
GO:0006633 :fatty acid biosynthetic process (BP)	2,4	6.79095e-05
GO:0000750 :pheromone-dependent signal transduction involved in conjugation with cellular fusion (BP)	2,7	0.00010675
GO:0000466 :maturation of 5.8S rRNA from tricistronic rRNA transcript (SSU-rRNA, 5.8S rRNA, LSU-rRNA) (BP)	1,8	0.000175299
GO:0030488 :tRNA methylation (BP)	2,1	0.000213382
GO:0000054 :ribosomal subunit export from nucleus (BP)	2,4	0.000244909
GO:0019236 :response to pheromone (BP)	3,0	0.00034749
GO TERM (Cellular Component)	**% of genes**	**corrected p value**
GO:0005730 :nucleolus (CC)	30,7	1.40215e-58
GO:0030687 :preribosome, large subunit precursor (CC)	7,8	2.27163e-23
GO:0005634 :nucleus (CC)	50,3	3.46843e-17
GO:0030686 :90S preribosome (CC)	7,8	2.89798e-15
GO:0032040 :small-subunit processome (CC)	6,0	1.95891e-13
GO:0030529 :ribonucleoprotein complex (CC)	13,6	4.71376e-11
GO:0005840 :ribosome (CC)	11,4	5.6807e-07
GO:0005622 :intracellular (CC)	13,3	1.01348e-06
GO:0005654 :nucleoplasm (CC)	4,2	2.09703e-06
GO:0022627 :cytosolic small ribosomal subunit (CC)	3,6	0.000445873
GO:0005736 :DNA-directed RNA polymerase I complex (CC)	1,8	0.000667369
GO:0005737 :cytoplasm (CC)	39,2	0.000640694
GO:0070545 :PeBoW complex (CC)	0,9	0.000990674
GO:0005834 :heterotrimeric G-protein complex (CC)	0,9	0.000990674

Table 11-Composition of the Ribi regulon and respective expression variation in mistranslating cells(Jorgensen et al., 2004b)

ORF name	Gene Name	log2ratio
Nucleotide Metabolism		
YML056C	IMD4	-
YHR216W	IMD2	-
YLR432W	IMD3	-
YAR073W	IMD1	-
YHL011C	PRS3	-0,7
YMR217W	GUA1	-1
YKL181W	PRS1	-0,8
YKR099W	BAS1	-
YOL061W	PRS5	-
YBL039C	URA7	-1,4
YML106W	URA5	-0,7
YKL216W	URA1	-2
YNL141W	AAH1	-1,7
YDR399W	HPT1	-
YER056C	FCY2	-
YPR035W	GLN1	-
YML022W	APT1	-1,2
YER060W	FCY21	-0,8
YHR128W	FUR1	-0,7
YBR021W	FUR4	-
YBL042C	FUI1	-0,9
YNR012W	URK1	-
YOR095C	RKI1	-1,3
YPR074C	TKL1	-
Ribosome biogenesis		
YHR169W	DBP8	-
YDL153C	SAS10	-1,1
YKL078W	DHR2	-1,1
YPL193W	RSA1	-
YDR021W	FAL1	-
YOL144W	NOP8	-
YIR012W	SQT1	-
YGR095C	RRP46	-
YHR069C	RRP4	-0,9
YGR195W	SKI6	-
YHR065C	RRP3	-
YPR112C	MRD1	-1,0
YHR062C	RPP1	-
YOR001W	RRP6	-
YHR085W	IPI1	-
YCL031C	RRP7	-1,0
YAL025C	MAK16	-1,0
YNL112W	DBP2	-1,9
YGR245C	SDA1	-1,2
YLR175W	CBF5	-
YDR060W	MAK21	-
YER006W	NUG1	-1,2
YLR009W	RLP24	-0,8
YBR267W		-
YHR089C	GAR1	-
YPL012W	RRP12	-
YGR103W	NOP7	-1,4
YOR056C	NOB1	-0,8
YKL009W	MRT4	-1,2
YPL093W	NOG1	-
YHR052W	CIC1	-0,9
YNL061W	NOP2	-1,0
YNL075W	IMP4	-
YGL120C	PRP43	-1,1
YDR324C	UTP4	-
YDR101C	ARX1	-1,1
YDL014W	NOP1	-1,0
YMR049C	ERB1	-1,0
YER126C	NSA2	-0,8
YGR145W	ENP2	-
YHR196W	UTP9	-0,6
YPR144C	NOC4	-0,8

ORF name	Gene Name	log2ratio
Ribosome biogenesis (cont.)		
YNL182C	IPI3	-1,5
YOR145C	PNO1	-
YLR196W	PWP1	-
YMR229C	RRP5	-1,0
YGR162W	TIF4631	-0,9
YMR290C	HAS1	-1,3
YLR276C	DBP9	-0,7
YLL008W	DRS1	-
YLR449W	FPR4	-1,5
YKL082C	RRP14	-
YOR206W	NOC2	-0,8
YCL059C	KRR1	-1,2
YMR093W	UTP15	-1,5
YJL109C	UTP10	-
YEL026W	SNU13	-0,8
YDR496C	PUF6	-0,9
YPL043W	NOP4	-1
YDR299W	BFR2	-0,7
YPL217C	BMS1	-0,8
YKR081C	RPF2	-1
YCR072C		-
YML093W	UTP14	-0,8
YBR247C	ENP1	-
YOL077C	BRX1	-1
YPR016C	TIF6	-
YCR057C	PWP2	-0,8
YDR091C	RLI1	-
YLR002C	NOC3	-
YOL010W	RCL1	-
YKL143W	LTV1	-
YLL011W	SOF1	-
YNL002C	RLP7	-0,9
YPR137W	RRP9	-
YJR002W	MPP10	-0,9
YPL126W	NAN1	-
YKL172W	EBP2	-1
YER082C	UTP7	-0,8
YNL175C	NOP13	-1,2
YHR066W	SSF1	-0,8
YMR116C	ASC1	-
YHR170W	NMD3	-1,1
YKL014C		-
YGR081C		-
YOR078W	BUD21	-1,2
YHR088W	RPF1	-0,9
YCL054W	SPB1	-0,8
YOR272W	YTM1	-0,8
YDL148C	NOP14	-
YDR398W	UTP5	-0,8
YNL308C	KRI1	-0,7
YJL069C	UTP18	-0,8
YKL099C	UTP11	-0,8
YOR361C	PRT1	-0,7
YDR449C	UTP6	-0,8
YDR312W	SSF2	-
YNL110C	NOP15	-0,9
YGR155W	CYS4	-1
YPL211W	NIP7	-1,2
YKR024C	DBP7	-
YER002W	NOP16	-1,4
YER127W	LCP5	-
YFR001W	LOC1	-
YLR222C	UTP13	-
YMR128W	ECM16	-1
YDR432W	NPL3	-
YDL060W	TSR1	-1
YGL111W	NSA1	-0,7

ORF name	Gene Nan	log2ratio
Ribosome biogenesis (cont.)		
YAL035W	FUN12	-
YLR074C	BUD20	-0,8
YDL031W	DBP10	-0,9
YJL033W	HCA4	-
YCL037C	SRO9	-
YML074C	FPR3	-
YLR409C	UTP21	-
YBL004W	UTP20	-
YDL213C	NOP6	-1,0
YPL266W	DIM1	-0,7
YMR310C		-0,8
YDR087C	RRP1	-1,1
YLR197W	SIK1	-
YHR148W	IMP3	-0,8
YOL041C	NOP12	-0,8
YLR129W	DIP2	-
YNL132W	KRE33	-1,0
YGL171W	ROK1	-
YNR053C	NOG2	-
YGR159C	NSR1	-1,3
YMR131C	RRB1	-0,8
YGR211W	ZPR1	-0,8
YIL104C	SHQ1	-0,9
YHR197W	IPI2	-
YDR083W	RRP8	-1,1
YGL029W	CGR1	-1,0
YNR038W	DBP6	-0,8
YJL050W	MTR4	-
YJL010C		-0,8
YDL208W	NHP2	-0,9
YPR169W	JIP5	-
YLR336C	SGD1	-
YOR004W		-0,9
YNR054C		-
YMR239C	RNT1	-
YLR051C		-0,8
YKR092C	SRP40	-0,8
YIL091C		-0,8
RNA Polymerases I and III and		
YBR154C	RPB5	-0,6
YPR110C	RPC40	-0,9
YPR187W	RPO26	-0,8
YOR224C	RPB8	-
YNL113W	RPC19	-
YHR143W-A	RPC10	-
YOR207C	RET1	-
YOR116C	RPO31	-
YDL150W	RPC53	-1,0
YNR003C	RPC34	-
YOR341W	RPA190	-1,0
YNL248C	RPA49	-0,9
YPR010C	RPA135	-1,0
YJL148W	RPA34	-1,0
YOR340C	RPA43	-
YJR063W	RPA12	-
YDR156W	RPA14	-
YKL125W	RRN3	-
tRNA synthetases or metabolism		
YOR168W	GLN4	-0,9
YGR264C	MES1	-0,6
YOL097C	WRS1	-0,7
YDR037W	KRS1	-
YLR060W	FRS1	-
YBR121C	GRS1	-
YLL018C	DPS1	-
YGR094W	VAS1	-
YBL076C	ILS1	-

ORF name	Gene Nan	log2ratio
tRNA synthetases or metabolism		
YPL160W	CDC60	-
YDR023W	SES1	-
YHR019C	DED81	-
YPL212C	PUS1	-
YDR165W	TRM82	-0,8
YKL205W	LOS1	-
YDL048C	STP4	-
YHR070W	TRM5	-
YGL105W	ARC1	-
YBR061C	TRM7	-0,7
YDL201W	TRM8	-0,8
YDR341C	RRS1	-
YGR169C	PUS6	-
YPR033C	HTS1	-
translation initiation and elongation factors		
YAL003W	EFB1	-0,8
YOR133W	EFT1	-
YDR385W	EFT2	-
YOR260W	GCD1	
YNL062C	GCD10	
YER025W	GCD11	-0,7
YJL125C	GCD14	-
YDR211W	GCD6	-
YFR009W	GCN20	-
YKR026C	GCN3	-
YNL014W	HEF3	-
YKL081W	TEF4	-1,0
YDR460W	TFB3	
YKR059W	TIF1	-
YMR260C	TIF11	-1,4
YJL138C	TIF2	-
YPR163C	TIF3	-0,9
YMR146C	TIF34	-
YDR429C	TIF35	-0,8
YPR041W	TIF5	-0,8
YOR276W	CAF20	-0,6
YJR007W	SUI2	-
YLR249W	YEF3	-
YJR047C	ANB1	-

In order to evaluate if the lower fluorescence levels and amount of ribosomal proteins was due to lower gene expression or ribosome degradation, we took advantage of the above GFP chimera used in the epifluorescence assays to quantify ribophagy. Ribophagy, which is the selective degradation of ribosomes by autophagy, was detected but at very low levels. Indeed, the number of cells that presented vacuolar fluorescence and free GFP in the western blots was low, indicating that mistranslation affected ribosomal protein gene expression rather than ribosome degradation.

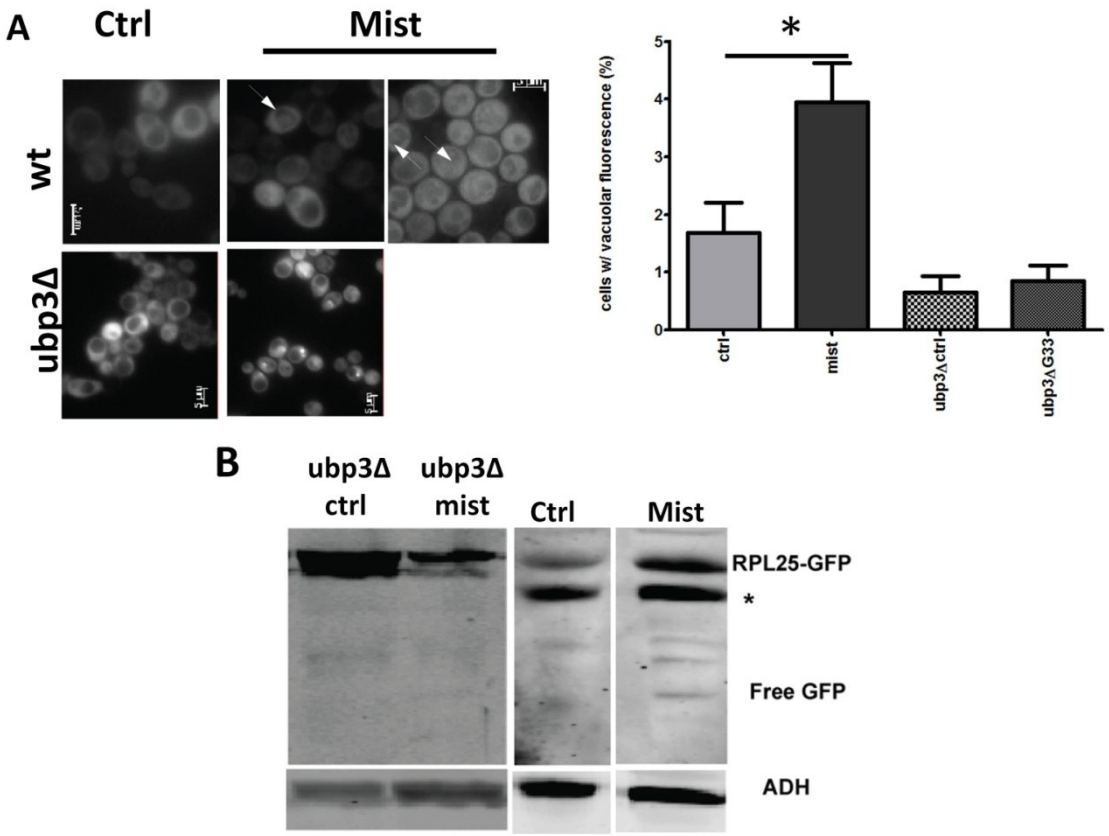

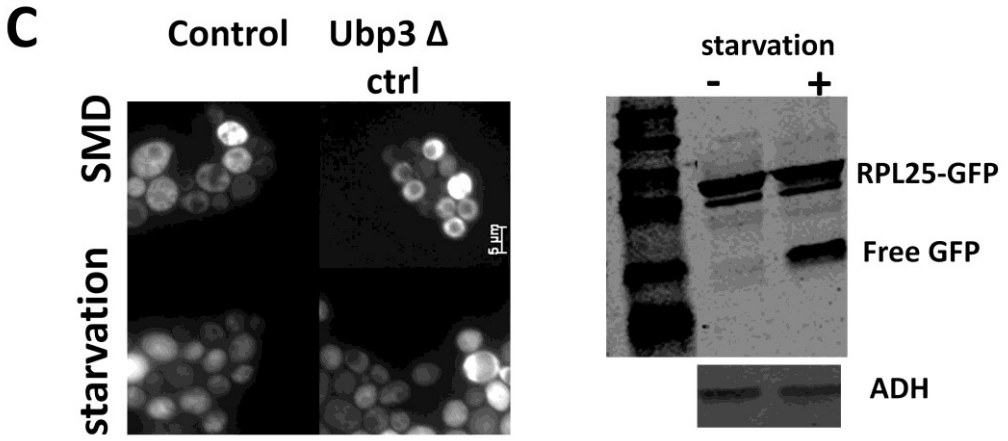

Figure 41- Ribosome degradation through selective autophagy A) Ribophagy was monitored by transforming mistranslating cells with a plasmid harbouring a fusion of the ribosomal protein RPL25 with GFP (Rpl25-GFP). Images shown were captured using epifluorescence microscopy and identical exposure time frames for control and mistranslating cells. The histogram shows the number of cells displaying vacuolar fluorescence. B) Ribophagy was also monitored by Western blotting using an antibody against GFP (lower panel, right inset) and confirmed the release of free GFP into the vacuole. C) the negative control of the above experiments was performed using ubp3Δcells, which are ribophagy defective, and positive controls were carried out by submitting cells to starvation. The blot on the right refers to wild-type control cells submitted to starvation. A significant increase in free GFP is seen. At least two randomly chosen microscopic fields were analyzed and 250-500 cells per clone/experiment were counted. ** indicates significant results, $p<0.05$, two tailed t-test. Ctrl indicates control cells; mist indicates mistranslating cells.

We have also tested induction of ribophagy in the presence of mistranslation inducing drugs. For this, cells were grown at 30^{o}C but the presence of AZC or canavanine for 24h. These drugs and the mistranslation tRNAs produced similar effects (Figure 42). In other words, total re-localization of GFP fluorescence in the vacuoles was not observed, rather a faint fluorescence signal or dotted fluorescence likely associated to autophagic bodies containing ribosomes as cargo (Kanki and Klionsky, 2008). This dotted phenotype was not observed before with the misreading tRNAs. A dotted pattern of ribosomal fluorescence in cells treated with canavanine was observed,

which contrasted with the evenly distribution of cytoplasmatic fluorescence of control untreated cells or cells treated with AZC.

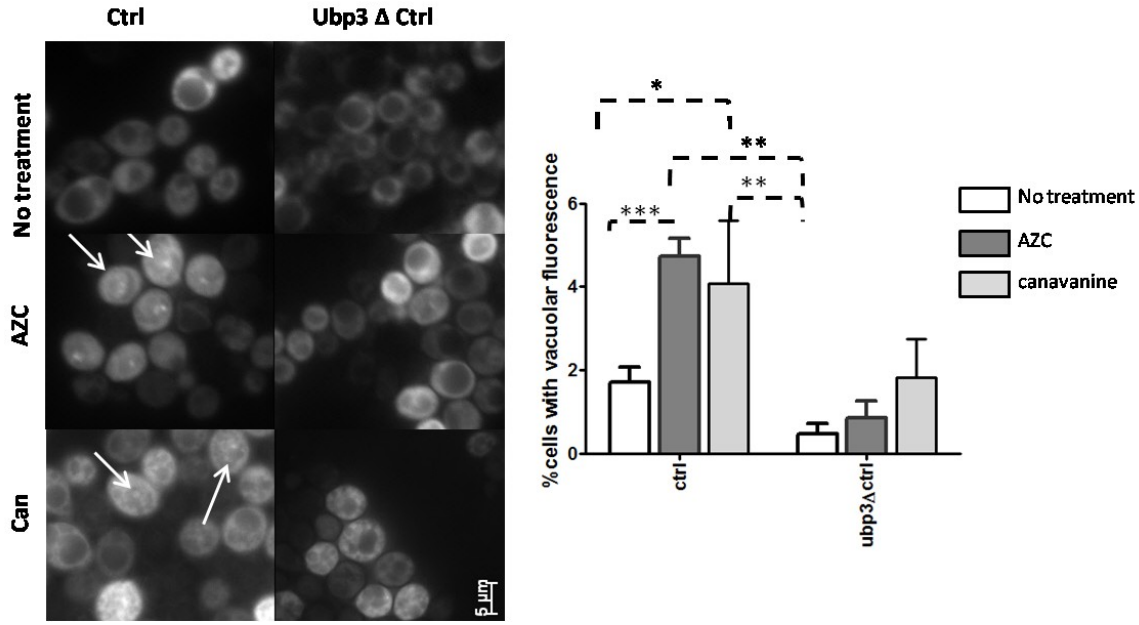

Figure 42- Effect of mistranslation inducing drugs on selective ribosome degradation (A) Control cells were transformed with a plasmid harboring Rpl25-GFP fusion. Cells were grown to mid-log phase and were treated with mistranslation inducing drugs for 24 h. Cells were further analyzed by epifluorescence microscopy. Cells with vacuolar fluorescence were manually counted. At least 2 randomly chosen microscopic fields were counted and 250-500 cells per clone/experiment were counted. Dashed lines and * indicate significative results for two tailed t-test. Data relative to 2 biological replicates and 3 independent experiments.

DISCUSSION

During the last few years it became clear that the control of mRNA translation and degradation can involve P-bodies and stress granules (Balagopal and Parker, 2009). We have analyzed the impact of gene mistranslation on the formation of P-bodies and SG in yeast and we were able to demonstrate that cells respond to mistranslation by

deregulating protein synthesis and increasing formation of p-bodies. However, mistranslation did not affect SG formation. In addition, we have clearly demonstrated that mistranslation down-regulates ribosomal gene expression and that this down-regulation is also reflected at the protein level, but ribophagy contributes poorly to the lower cellular ribosomal content observed.

Decreased P-body formation is usually associated with increased polysome size, due to slower translation elongation rate, enhanced translation or decreased translation repression. Previous work from our laboratory showed that mRNA mistranslation decreases the polysomal fraction and also protein synthesis rate, which is in line with increased P-body formation.

P-bodies and SG store mRNAs, in different ways. P-bodies are sites where mRNA degradation may take place while SG are mainly sites of mRNA storage that permit reinitiation of translation of the stored mRNAs once environmental conditions become favorable. Therefore, one possible explanation for the lack of a positive effect of mistranslation on SG formation is that mistranslation triggers mRNA degradation through recruitment to P-bodies. However, the set of target mRNAs that are recruited to P-bodies in mistranslating cells needs to be identified. That p-body assembly contributes to increase the local concentration or/and depletion of translational factors in the cytosol, may facilitate or limit protein interactions involved in the regulation of apoptosis, in a similar way to what has been suggested for MAPK sequestration to stress granules (Arimoto et al., 2008). It is also possible that p-body

assembly may contribute to transcription repression due to an unbalance in the mRNA pool. Finally, because mRNAs within P-bodies can return to translation, p-bodies can simply store transcripts that will be released upon additional stress or in certain environmental conditions, in order to respond rapidly to the new condition (Aragon et al., 2006; Brengues et al., 2005; Bhattacharyya et al., 2006a). If so, mRNA release and reentry in the translational cycle will be independent of SG formation in mistranslating cells. As mRNA mistranslation has a negative impact in protein synthesis in mammalian cells (Geslain et al., 2010) the same likely happens in yeast. The lack of SG in mistranslating cells does not, however, imply that translation initiation is not blocked, because SG formation occurs when mRNAs are stalled in specific translation time frames or is dependent upon specific initiation factors.

The isolation of the mRNAs present in p-body aggregates by sucrose gradient centrifugation and the use of this mRNA fraction in DNA-microarray profiling would help to identify the mRNAs trapped in P-bodies. Comparison of the transcriptome profiles of p-bodies, polysome and total mRNA fractions would allow for identification of genes whose expression is regulated at the translational level in mistranslating cells. The use of marked target RNAs - for instance the PGK1 reporter mRNA containing multiple U1A-specific binding sites in its 3'UTR to which the U1A-GFP fusion binds, as described by Brengues and Teixeira (Brengues et al., 2005; Teixeira et al., 2005), - would allow one to follow their fate in the cell and could provide some hints on the destiny of those mRNAs. In order to gain further insight on the physiological relevance of p-body formation in mistranslating cells, mistranslation should be induced in

mutants with impaired P-body assembly to evaluate their viability. Additionally, it would be important to determine whether different cell types respond similarly to mistranslation, in terms of both SG and P-body formation. For example, comparison of SG and p-body formation in various types of mammalian cells exposed to mistranslation.

Translation of mRNA is, in general, repressed in response to various cellular perturbations, mainly due to down-regulation of ribosomal proteins, which can contribute to modification of the ribosome itself. Modifications of ribosome structure/composition have recently been associated with adjustments of the affinity of the ribosomes for particular classes of mRNAs which is another level of mRNA translational control (Baker and Coller, 2005). For instance, deletion of large subunit ribosomal genes, or genes involved in 60S processing or maturation have been shown to result in increased lifespan (Steffen et al., 2008a). In mistranslating cells, rather than contributing to increasing life span, the down-regulation of ribosome related genes is likely relevant to viability and cell survival. Ribosome biogenesis and protein translation are among the cellular process that consume the highest level of energy, explaining the tight control of ribosome production. Down-regulation of ribosomal gene expression and ribosomal protein production may, therefore, represent an "energy-saving" strategy, or allow for its utilization in protein folding.

During the last few years, several autoregulatory mechanisms and connections between ribosomes, cell cycle and cell growth have been discovered. Some studies

have shown that limiting ribosome biogenesis results in small cell volume (Jorgensen and Tyers, 1999;Jorgensen et al., 2002), while others showed that decreasing ribosome biogenesis by Pwp2 depletion, results in increased cell size (Bernstein et al., 2007) . Our data are in line with the second hypothesis as we have observed that mistranslating cell populations are highly heterogeneous, and large cells appear often in the population (data not shown). *PWP2* is also down-regulated in mistranslating yeast. These observations establish a relationship between mRNA mistranslation and cell cycle progression and we have observed that mistranslation arrests the cell cycle in the G0/G1 phase and leads to increased ploidy (data not shown). Therefore, ribosome biogenesis may be important for mistranslating cells to "sense" size for cell cycle progression. In addition, our observation that mistranslation up-regulates autophagy correlates well with ribosome biogenesis defect and Pwp2 decrease (Bernstein et al., 2007). These observations suggest that it would be of interest to evaluate the expression of the *WHI5* gene, the yeast homologue of the Rb mammalian tumor suppressor gene, as it is involved in the coordination of adequate ribosome biogenesis to G1 cell cycle progression and which might provide a link between mistranslation, ribosome biogenesis and cell cycle in yeast.

The degradation of ribosomes poses a much bigger problem to the cell than the degradation of tRNAs or mRNAs, since the rRNAs are protected by the ribosomal proteins and are not directly available to RNases. Our work shows that selective degradation of ribosomes is not a major contributor to the lower ribosomal content observed in mistranslating cells. Still, one cannot disregard the prevalence of other

ribosomal degradation pathways in mistranslating cells, namely non-functional rRNA decay (NRD) (Fujii et al., 2009) or even autophagy, which is up-regulated in mistranslating cells. Degradation of ribosomes is important to rapidly shut down translation and to remove non-functional or misassembled organelles.

In conclusion, we discovered that mistranslation induces P-body assembly in yeast cells, but it does not seem to have any impact on SG formation. This is in line with down-regulation of ribosomal proteins and an expected down-regulation of translation (Figure 43). These observations further highlight the previously described dynamics and variability of the RNP granules and adds mistranslation to the list of stressors involved in p-body formation. The present study also highlights the importance of remodeling of protein synthesis in mistranslating cells and further exposes the relevance of cycling of mRNAs between translating and nontranslating cytoplasmatic pools and the important role of post-transcriptional regulation in mistranslation contexts.

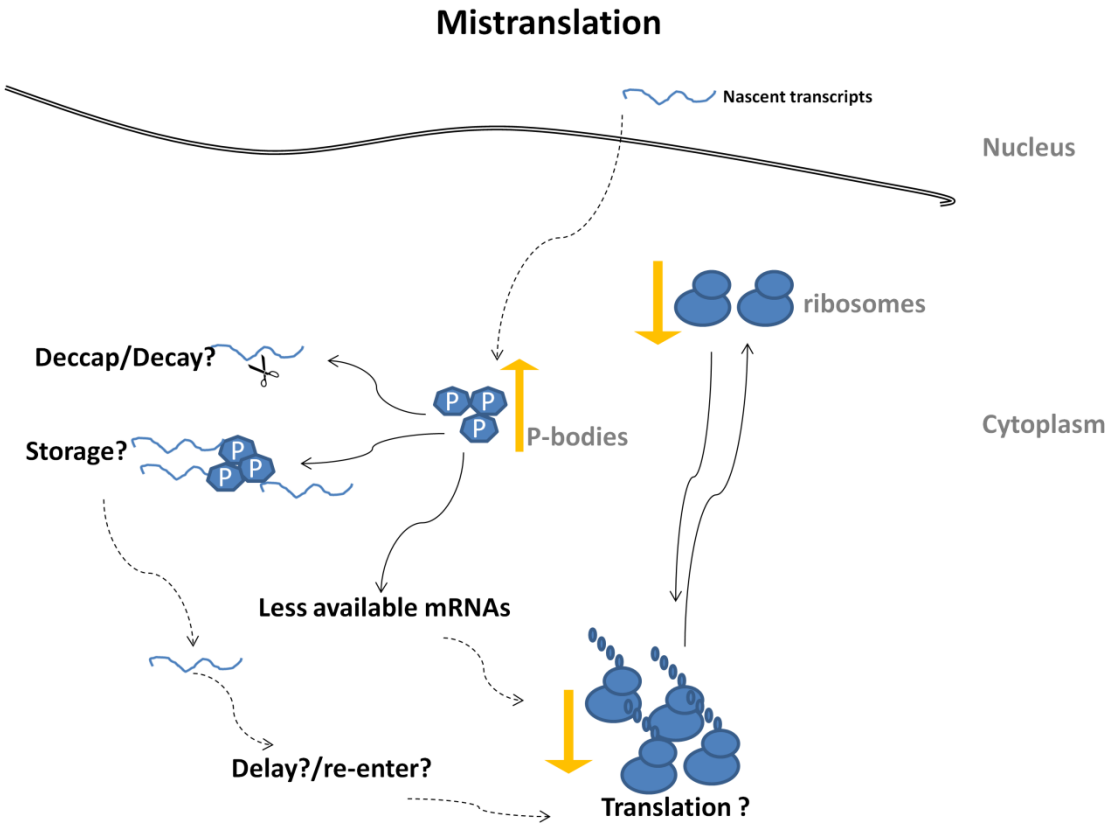

Figure 43- Integration of p-body formation in mistranslating cells - mRNA mistranslation leads to lower ribosome content, which may contribute to lower translation rates, which in turn, lowers even further ribosome biosynthesis, in negative a feedback mechanism. On the other hand, mRNA mistranslation induces p-body assembly which sequesters mRNAs in the cytoplasm which also influences translation rate. P-body formation can be important for mRNA degradation or storage. Stored mRNAs can be later released for delayed translation.

Materials and methods

Strains and growth conditions

S.cerevisiae strain BY4743 was used in this study. Cells were co-transformed using standard techniques with pRS plasmids plus p147 or pRP1657 plasmids described in

Table 12 . For this, cells were grown to early log phase (OD_{600} =0.3) at 30°C, using constant agitation at 180 rpm, in synthetic medium lacking leucine and uracil in order to ensure plasmids maintenance. Stationary phase tests were carried out in cells grown for 36h.

Detection of P-Bodies and Stress Granules

For each strain and treatment, 1.5 ml of culture were decanted and divided into two eppendorf tubes and centrifuged for 30s at 13000 rpm. Culture media was carefully removed and pellets were resuspended SMD-leu-ura (glucose), SMD-leu-ura (glucose) + drug or SMD-leu-ura (glucose free), depending on the test. This washing step was repeated and cells were finally resuspended in the media of interest, then decanted to 50 ml flasks and incubated with shacking at 30°C for the appropriate time. In general, 2h treatments were applied, in the presence of 2mg/ml of canavanine, 2.5 mM of paromomycin and 20mM of L-azetidine-2-carboxylic-acid (AZC). For glucose starvation tests, cells were grown for 10 min in SD-N medium. Microscopic observations were made using a Zeiss Axio Imager Z1 (software Axio Vision 4.5 – multichannel module) with optimized conditions with cells embedded in agarose coated slides. At least two independent experiments were carried for each condition tested and more than 150 cells were observed and counted for each treatment. Foci were counted manually.

Table 12- Plasmids used in this study

Name	Description	Source
pRS715	*C.albicans* Ser-tRNA$_{CAG}$ G$_{33}$	our laboratory, described in Santos *et al* 1996 and elsewhere in this thesis
pRS315	Empty plasmid	our laboratory, described in Santos *et al* 1996 and elsewhere in this thesis
p147	Dcp2-GFP fusion	kind gift from Dr. D.Teixeira , (Dr.Roy Parker's lab), Teixeira *et al* 2005
pRP1657	Pab1-GFP+Edc3-mCherry fusion	kind gift from Dr. J.Buchan , (Dr.Roy Parker's lab), Buchan *et al* 2008, Buchan *et al* 2010
pcK5	pRS316 based plasmid harboring RPL25-GFP fusion	kind gift from Dr. Claudine Kraft (Dr Mathias Petter's lab)

Microarray Analysis

DNA microarrays

RNA preparation

Cells (25 OD_{600} units) were harvested by centrifugation at 4000 rpm for 5 minutes, immediately frozen in liquid nitrogen and stored at -80ºC until further use. Frozen pellets were resuspended in 500 µl Acidic Phenol-Chlorophorm (5:1, pH4.7; Sigma), heated at 65ºC prior use. The same volume of hot TES buffer (10 mM Tris, pH 7.5; 10 mM EDTA, 0.5%SDS) was added. Pellets were resuspended by vortexing for 20 seconds and were immediately incubated at 65°C for 1 hour with vortexing every 10 min, in order to maintain a homogeneous suspension. The extracts were then transferred to clean microfuge tubes and cells debris and organic phase were separated from upper aqueous phase by centrifugation at 14000 rpm for 20 minutes at 4°C. The upper phase

was collected and extracted twice with 1 volume of Phenol: Chlorophorm (5:1, pH 4.7; Sigma) and once with Chlorophorm:Isoamyl-alcohol (25:1; Sigma). At each step, extracts were centrifuged at 14000 rpm for 10 minutes at 4°C. The RNA was precipitated by addition of 1 volume of 3M sodium acetate (pH 5.2) plus 3 volumes of ice-cold absolute ethanol, followed by an overnight incubation at -20°C . The RNA was pelleted by centrifugation at 14000 rpm for 5 minutes at 4°C, washed once with 70% ethanol and again pelleted by centrifugation. The remaining alcohol was evaporated using a speed-vac (Savant) and the RNA pellets were dissolved in 50 µl of RNase-free water. RNA concentration was determined by OD_{260} using a Nanodrop 1000 (ThermoScientific) (van de et al., 2003) .

Data Analysis and Statistical Analysis

DNA-microarrays were scanned using an Agilent G2565AA laser scanner, and images were processed using QuantArray® software package (Packard BioChip Technologies). The slides background was subtracted and bad spots were excluded after manual inspection. Slides were normalized using standard ratio-based methods (print-tip lowess normalization within arrays) as implemented in Biometric Research Branch BRB-Array Tools v3.4.0 software. Experiments were performed in two independent assays, corresponding to two different clones for each strain, with dye-swapping. Microarray data analyses were performed using MEV software (TM4 Microarray Software Suite) (Saeed et al., 2006; Saeed et al., 2003). Data were analyzed based on $\log_2$ ratio (M) values. Genes included in the final dataset exhibited significance based on a FDR median< 0.05, in a SAM 1-class analysis (Salin 2008, Tusher 2001, Saeed 2003, van Helden 2003).

Quantification of ribosomal proteins

Yeast cells expressing the $tRNA_{CAG}^{Ser}$ and the Rpl25-GFP fusion (pCK5; kind gift from C.Kraft and M.Petter laboratory) were grown at 30^{o}C until late exponential phase. Cells were then poured onto a microscope slide previously coated with a bed of 1% of agarose. Observations were carried out using an Zeiss Axiovision imager Z1 microscope equipped with a 63X Plan-apochromat objective with 10X ocular (Zeiss). GFP tagged proteins were monitored using a GFP filter (38HE, Zeiss) and were photographed with an AxioCam HRC camera (Zeiss). Image J software was used to determine the mean intensity of cytoplasmic fluorescence for each strain. Microscope fields were randomly chosen and at least 150 cells were analyzed per sample.

Protein extraction, preparation and SDS-PAGE were carried out according to standard laboratory methods. For western-blotting, Rpl25p-GFP was detected using a rabbit anti-GFP primary antibody (Santa-Cruz) and detection was carried out using an IRDye600 Goat anti-rabbit secondary antibody (Li-cor Biosciences). For sample loading normalization, membranes were stripped and re-incubated with an anti-ADH antibody followed by detection with IRDye600 Goat anti-rabbit secondary antibody (Li-cor Biosciences). Detection was performed using an Odyssey Infrared Imaging system. Rpp0 was detected using an anti Rpp0 antibody, a kind gift from Dr. Juan P.G.Ballesta.

Aknowledgements: The authors would like to thank to Dr. Claudine Kraft, Dr. Mathias Petter, Dr. Roy Parker and J.Ross Buchan for strains and plasmids and to Professor JPG Ballestra, Professor Sabine Rospert and Dr. Mathias Seedorf for antibodies.

Supplementary *Data*

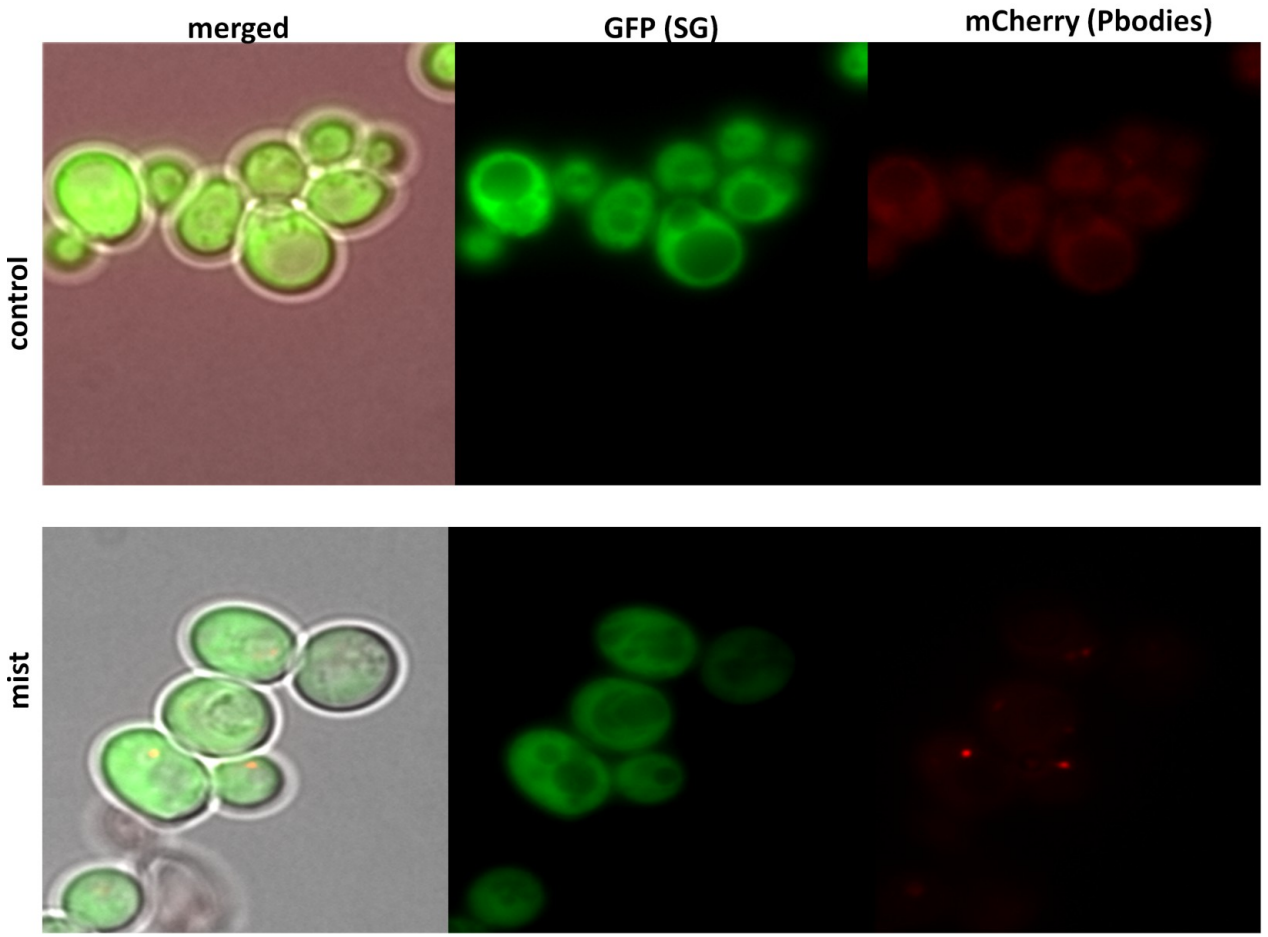

Supp.Figure 20- Enlarged view of image shown in figure 38 (cells grown in glucose rich medium)

References

1. Amsterdam, A., K.C.Sadler, K.Lai, S.Farrington, R.T.Bronson, J.A.Lees, and N.Hopkins. 2004. Many ribosomal protein genes are cancer genes in zebrafish. *PLoS Biol* 2:E139.
2. Andrei, M.A., D.Ingelfinger, R.Heintzmann, T.Achsel, R.Rivera-Pomar, and R.Luhrmann. 2005. A role for eIF4E and eIF4E-transporter in targeting mRNPs to mammalian processing bodies. *RNA.* 11:717-727.
3. Aragon, A., G.Quinones, E.Thomas, S.Roy, and M.Werner-Washburne. 2006. Release of extraction-resistant mRNA in stationary phase Saccharomyces cerevisiae produces a massive increase in transcript abundance in response to stress. *Genome Biology* 7:R9.
4. Arimoto, K., H.Fukuda, S.Imajoh-Ohmi, H.Saito, and M.Takekawa. 2008. Formation of stress granules inhibits apoptosis by suppressing stress-responsive MAPK pathways. *Nat Cell Biol* 10:1324-1332.
5. Balagopal, V. and R.Parker. 2009. Polysomes, P bodies and stress granules: states and fates of eukaryotic mRNAs. *Curr. Opin. Cell Biol* 21:403-408.
6. Baker, K. and J.Coller. 2005. The many routes to regulating mRNA translation. *Genome Biology*
7. Belin, S., A.Beghin, E.Solano-Gonzalez, L.Bezin, S.Brunet-Manquat, J.Textoris, A.C.Prats, H.C.Mertani, C.Dumontet, and J.J.Diaz. 2009. Dysregulation of ribosome biogenesis and translational capacity is associated with tumor progression of human breast cancer cells. *PLoS One.* 4:e7147.
8. Bernstein, K.A., F.Bleichert, J.M.Bean, F.R.Cross, and S.J.Baserga. 2007. Ribosome biogenesis is sensed at the Start cell cycle checkpoint. *Mol. Biol Cell* 18:953-964.
9. Bhattacharyya, S.N., R.Habermacher, U.Martine, E.I.Closs, and W.Filipowicz. 2006a. Relief of microRNA-mediated translational repression in human cells subjected to stress. *Cell* 125:1111-1124.
10. Bhattacharyya, S.N., R.Habermacher, U.Martine, E.I.Closs, and W.Filipowicz. 2006b. Stress-induced reversal of microRNA repression and mRNA P-body localization in human cells. *Cold Spring Harb. Symp. Quant. Biol* 71:513-521.
11. Brengues, M. and R.Parker. 2007. Accumulation of Polyadenylated mRNA, Pab1p, eIF4E, and eIF4G with P-Bodies in Saccharomyces cerevisiae. *Mol. Biol. Cell*E06-E12.
12. Brengues, M., D.Teixeira, and R.Parker. 2005. Movement of Eukaryotic mRNAs Between Polysomes and Cytoplasmic Processing Bodies. *Science* 310:486-489.
13. Buchan, J.R., T.Nissan, and R.Parker. 2010. Analyzing P-bodies and stress granules in Saccharomyces cerevisiae. *Methods Enzymol.* 470:619-640.
14. Buchan, J.R. and R.Parker. 2009. Eukaryotic stress granules: the ins and outs of translation. *Mol Cell* 36:932-941.
15. Buchan, J.R., J.H.Yoon, and R.Parker. 2011. Stress-specific composition, assembly and kinetics of stress granules in Saccharomyces cerevisiae. *J Cell Sci* 124:228-239.
16. Buchan, J.R., D.Muhlrad, and R.Parker. 2008. P bodies promote stress granule assembly in Saccharomyces cerevisiae. *J. Cell Biol.* 183:441-455.
17. Cassola, A., J.G.De Gaudenzi, and A.C.Frasch. 2007. Recruitment of mRNAs to cytoplasmic ribonucleoprotein granules in trypanosomes. *Molecular Microbiology* 65:655-670.
18. Eilers, M. and R.N.Eisenman. 2008. Myc's broad reach. *Genes Dev.* 22:2755-2766.
19. Franks, T.M. and J.Lykke-Andersen. 2008. The control of mRNA decapping and P-body formation. *Mol Cell* 32:605-615.
20. Fujii, K., M.Kitabatake, T.Sakata, A.Miyata, and M.Ohno. 2009. A role for ubiquitin in the clearance of nonfunctional rRNAs. *Genes Dev.* 23:963-974.
21. Gasch, A., P.Spellman, C.Kao, O.Carmel-Harel, M.Eisen, G.Storz, D.Botstein, and P.Brown. 2000. Genomic Expression Programs in the Response of Yeast Cells to Environmental Changes. *Mol. Biol. Cell* 11:4241-4257.
22. Geslain, R., L.Cubells, T.Bori-Sanz, R.varez-Medina, D.Rossell, E.Marti, and L.R.de Pouplana. 2010. Chimeric tRNAs as tools to induce proteome damage and identify components of stress responses. *Nucleic Acids Res.* 38:e30.
23. Hamilton, B., Y.Dong, M.Shindo, W.Liu, I.Odell, G.Ruvkun, and S.S.Lee. 2005. A systematic RNAi screen for longevity genes in C. elegans. *Genes Dev.* 19:1544-1555.
24. Hoyle, N.P. and M.P.Ashe. 2008. Subcellular localization of mRNA and factors involved in translation initiation. *Biochem Soc. Trans.* 36:648-652.
25. Hoyle, N.P., L.M.Castelli, S.G.Campbell, L.E.Holmes, and M.P.Ashe. 2007. Stress-dependent relocalization of translationally primed mRNPs to cytoplasmic granules that are kinetically and spatially distinct from P-bodies. *J Cell Biol* 179:65-74.
26. Jorgensen, P., J.L.Nishikawa, B.J.Breitkreutz, and M.Tyers. 2002. Systematic identification of pathways that couple cell growth and division in yeast. *Science* 297:395-400.
27. Jorgensen, P., I.Rupes, J.R.Sharom, L.Schneper, J.R.Broach, and M.Tyers. 2004a. A dynamic transcriptional network communicates growth potential to ribosome synthesis and critical cell size. *Genes Dev.* 18:2491-2505.

28. Jorgensen, P., I.Rupes, J.R.Sharom, L.Schneper, J.R.Broach, and M.Tyers. 2004b. A dynamic transcriptional network communicates growth potential to ribosome synthesis and critical cell size. *Genes Dev.* 18:2491-2505.
29. Jorgensen, P. and M.Tyers. 1999. Altered states: programmed proteolysis and the budding yeast cell cycle. *Curr. Opin. Microbiol.* 2:610-617.
30. Kanki, T. and D.J.Klionsky. 2008. Mitophagy in yeast occurs through a selective mechanism. *J Biol Chem* 283:32386-32393.
31. Kedersha, N., G.Stoecklin, M.Ayodele, P.Yacono, J.Lykke-Andersen, M.J.Fritzler, D.Scheuner, R.J.Kaufman, D.E.Golan, and P.Anderson. 2005. Stress granules and processing bodies are dynamically linked sites of mRNP remodeling. *J Cell Biol* 169:871-884.
32. Lackner, D.H. and J.B□hler. 2008. Chapter 5 Translational Control of Gene Expression: From Transcripts to Transcriptomes. *In* International Review of Cell and Molecular Biology. W.J.Kwang, editor. Academic Press, 199-251.
33. Lin, C.J., R.Cencic, J.R.Mills, F.Robert, and J.Pelletier. 2008a. c-Myc and eIF4F are components of a feedforward loop that links transcription and translation. *Cancer Res* 68:5326-5334.
34. Lin, M.D., S.J.Fan, W.S.Hsu, and T.B.Chou. 2006. Drosophila decapping protein 1, dDcp1, is a component of the oskar mRNP complex and directs its posterior localization in the oocyte. *Dev. Cell* 10:601-613.
35. Lin, M.D., X.Jiao, D.Grima, S.F.Newbury, M.Kiledjian, and T.B.Chou. 2008b. Drosophila processing bodies in oogenesis. *Dev. Biol* 322:276-288.
36. McCarthy, J.E.áG. 1998. Posttranscriptional Control of Gene Expression in Yeast. *Microbiol. Mol. Biol. Rev.* 62:1492-1553.
37. Pluta, K., O.Lefebvre, N.C.Martin, W.J.Smagowicz, D.R.Stanford, S.R.Ellis, A.K.Hopper, A.Sentenac, and M.Boguta. 2001. Maf1p, a negative effector of RNA polymerase III in Saccharomyces cerevisiae. *Mol. Cell Biol* 21:5031-5040.
38. Ruggero, D. and P.P.Pandolfi. 2003. Does the ribosome translate cancer? *Nat Rev. Cancer* 3:179-192.
39. Saeed, A.I., N.K.Bhagabati, J.C.Braisted, W.Liang, V.Sharov, E.A.Howe, J.Li, M.Thiagarajan, J.A.White, and J.Quackenbush. 2006. TM4 microarray software suite. *Methods Enzymol.* 411:134-193.
40. Saeed, A.I., V.Sharov, J.White, J.Li, W.Liang, N.Bhagabati, J.Braisted, M.Klapa, T.Currier, M.Thiagarajan, A.Sturn, M.Snuffin, A.Rezantsev, D.Popov, A.Ryltsov, E.Kostukovich, I.Borisovsky, Z.Liu, A.Vinsavich, V.Trush, and J.Quackenbush. 2003. TM4: a free, open-source system for microarray data management and analysis. *Biotechniques* 34:374-378.
41. Santos, M.A., V.M.Perreau, and M.F.Tuite. 1996. Transfer RNA structural change is a key element in the reassignment of the CUG codon in Candida albicans. *EMBO J* 15:5060-5068.
42. Silva, R.M., I.C.N.Duarte, J.A.Paredes, T.Lima-Costa, M.Perrot, H.Boucherie, B.J.Goodfellow, A.C.Gomes, D.D.Mateus, G.R.Moura, and M.A.S.Santos. 2009. The Yeast PNC1Longevity Gene Is Up-Regulated by mRNA Mistranslation. *PLoS ONE* 4:e5212.
43. Silva, R. Reconstrução molecular de uma alteração ao código genético / Molecular reconstruction of a genetic code alteration. 2005. Biologia Universidade de Aveiro.
44. Steffen, K.K., V.L.MacKay, E.O.Kerr, M.Tsuchiya, D.Hu, L.A.Fox, N.Dang, E.D.Johnston, J.A.Oakes, B.N.Tchao, D.N.Pak, S.Fields, B.K.Kennedy, and M.Kaeberlein. 2008b. Yeast life span extension by depletion of 60s ribosomal subunits is mediated by Gcn4. *Cell* 133:292-302.
45. Steffen, K.K., V.L.MacKay, E.O.Kerr, M.Tsuchiya, D.Hu, L.A.Fox, N.Dang, E.D.Johnston, J.A.Oakes, B.N.Tchao, D.N.Pak, S.Fields, B.K.Kennedy, and M.Kaeberlein. 2008a. Yeast life span extension by depletion of 60s ribosomal subunits is mediated by Gcn4. *Cell* 133:292-302.
46. Teixeira, D., U.Sheth, M.A.Valencia-Sanchez, M.Brengues, and R.Parker. 2005. Processing bodies require RNA for assembly and contain nontranslating mRNAs. *RNA.* 11:371-382.
47. Teixeira, D. and R.Parker. 2007. Analysis of P-Body Assembly in Saccharomyces cerevisiae. *Mol. Biol. Cell*E07-03.
48. van de, P.J., P.Kemmeren, B.H.van, M.Radonjic, L.D.van, and F.C.Holstege. 2003. Monitoring global messenger RNA changes in externally controlled microarray experiments. *EMBO Rep.* 4:387-393.
49. van Dijk, E., N.Cougot, S.Meyer, S.Babajko, E.Wahle, and B.Seraphin. 2002. Human Dcp2: a catalytically active mRNA decapping enzyme located in specific cytoplasmic structures. *EMBO Journal* 21:6915-6924.

Chapter 5

General discussion, conclusions and future perspectives

The mechanistic aspects of protein synthesis have been a hot topic in the molecular biology field, being intensively studied both at biochemical and structural levels. However, there are many aspects of quality control processes that remain obscure and the biological relevance of mRNA mistranslation is one of them. Mistranslation is an intrinsic property of the protein synthesis process with an average basal error rate in the order of 10^{-4} errors/codon decoded (Reynolds et al., 2010). More importantly, there is growing experimental evidence that mistranslated proteins are not always eliminated and may even be functionally relevant. For example, yeast strains displaying high levels of natural mistranslation express large quantity of heat shock proteins and have a constitutive stress response that preadapt cells to survive in harsh environmental conditions. Also, mammalian cells and in particular dendritic cells, take advantage of mistranslated protein (DRiPs) to produce antigens which are presented by the MHC class I pathway to cytotoxic T cells (Lelouard et al., 2004). Connections between mRNA mistranslation and several illnesses have been uncovered during the last few years and, therefore, a better understanding of the accuracy of protein synthesis is essential to unravel the biology of neurodegeneration, cancer and aging. The initial goal of this PhD thesis was to shed new light on how cells eliminate aberrantly synthesized proteins under conditions where the proteome quality control systems become saturated, and evaluate the consequences of such saturation on cell degeneration.

In the first chapter, we have shown that mistranslation leads to the accumulation of insoluble (aggregated) proteins and to significant cellular ultrastructural alterations namely vacuolar fragmentation and ER expansion. ImmunoTEM analysis revealed that

mistranslating cells tended to accumulate the ubiquitin signal in the vacuoles and we were able to establish a link between mistranslation, autophagy and proteasome activity. Additionally, we have shown that the longevity *PNC1/SIR2* pathway is involved in regulation of autophagy, but these genes are not involved in starvation induced autophagy, conversely to mammalian cells (Lee et al., 2008).

In the second chapter, we have evaluated the effect of mistranslation on oxidative stress and we have demonstrated that mRNA mistranslation increases ROS accumulation, up-regulates antioxidant defenses at the transcriptome level and that Sir2p plays an important role in mistranslating cells, at least under certain conditions. Deep disruption of the mitochondrial network was also observed in mistranslating cells, suggesting a strong increase in the activity of the mitochondrial fission machinery or, on the other hand, impairment of the fusion apparatus. These alterations did not lead to selective degradation of mitochondria (mitophagy) and may explain the observed respiratory deficiency of mistranslating cells.

Finally, this work provides insight into the connections between mRNA (mis)translation and regulation of mRNA of translation and turnover, by showing that mistranslation leads to P-body assembly. Our data also show that mistranslation does not affect stress granule formation, but increases selective ribosomal degradation and strongly down regulates ribosomal protein expression.

Physiology of mistranslating cells - general features

The utilization of knockout strains harbouring deletions in sir2Δ, pnc1Δ, rpn4Δ, atg1Δ, atg5Δ, yap1Δ,yap2Δ, yap1Δ yap2Δ, provided insight on the role of these genes on the cellular responses to mistranslation. Our data show clearly that cells are able to compensate the inactivation or overloading of each of the quality control processes by up-regulating others, highlighting significant redundancy in protein quality control mechanisms. Those knockout strains showed similar responses to mistranslation, namely growth rate and viability. However, the sir2Δ strain showed stronger accumulation of insoluble proteins and higher ROS accumulation in particular in what O_2^- is concerned (in stationary phase), suggesting that Sir2p plays an important role in the cellular responses to protein aggregation and ROS detoxification activity. Another important gene in ROS detoxification was shown to be *PNC1*.

Two physiological parameters that we studied in detail were growth rate and stress resistance. Growth rate consistently decreased in all mistranslating strains (chapter 3), likely due to the need to deviate large quantities of energy to protein degradation and protein folding pathways, which, under normal circumstances, would be committed to growth. Slow growth has recently been pointed out as being advantageous when cells are challenged with heat shock, as it may provide cross-protection (Lu et al., 2009). Apparently there is an inverse relationship between the rate of cell division and their resistance to heat stress (Lu et al., 2009). Therefore, the slow growth of mistranslating cells may be advantageous over extended periods of mistranslation. Alternatively, slow growth and short-term viability loss could also be caused by ROS accumulation, as discussed below. Still, the phenotypic similarities between control and knockout mistranslating cells, was surprising because the knockouts involved longevity, protein quality control and responses to oxidative stress genes. For instance, the lack of increased proteasome activity or increased level of insoluble proteins in mistranslating

cells with impaired autophagy was surprisingly. This leads to several questions, namely how do these cells get rid of the damaged/misfolded proteins? It will be interesting to study whether mistranslation induces major alterations (enlargement) in the vacuoles which could indicate alternative targeting of proteins to these organelles.

In general, mistranslation conferred increased sensitivity to menadione, but apparently increased resistance to H_2O_2. The *SIR2* deletion did not significantly affect stress tolerance (chapter 3) but, the pnc1Δ mistranslating strain had higher resistance to menadione (chapter 3). A different scenario was observed in the yap1Δ and yap2Δ mistranslating strains which showed increased sensitivity to exogenous oxidative stressors. As expected, *YAP1* deletion leads to increased sensitivity to exogenous oxidative stressors, which was increased by mistranslation. The yap2Δ strain was less sensitive to oxidative stress than the yap1Δ strain, while double yap1Δyap2Δ strain showed the highest sensitivity to oxidative stress, as it was completely unable to grow in the presence of H_2O_2 (a slight increase in tolerance to menadione was observed). In other words, mistranslation produced the expected results in these genetic backgrounds, showing that *YAP1* and *YAP2* genes are relevant to the response to oxidative stress generated by mistranslation. This is consistent with induction of the stress master regulator *MSN4* gene (Martinez-Pastor et al., 1996) in the mistranslating cells. Indeed, strains lacking Msn4p have major defects in acquired stress resistance, but no observed sensitivity to single dose of acute stress. We have not observed upregulation of the other stress master regulator *MSN2*, however, activation of Msn4 and/or Msn2 is implicated in cross-protection. In order to further unveil the specific role of each of these transcription factors in the mistranslation context, physiological

characterization of single and double *MSN2/MSN4* mistranslating mutants should be performed.

The fact that different mistranslating yeast strains show different stress resistance patterns challenges previous work that suggested that mistranslation increased stress resistance of yeast cells through stress pre-adaption mechanisms (Santos et al., 1999). This phenomenon is known as hormesis, a positive effect that is attributed to the stimulation and priming of the stress responses pathways by a mild stressor. In multicellular organisms, this can be of relevance, as it suggests that different tissues/cell types may react differently to mistranslation.

Microarray data showed that there is a considerable overlap between the profiles of cells exposed to mistranslation and those exposed to environmental stressors. Indeed, mistranslation deregulated approximately 900 genes which are also deregulated by environmental stressors (Gasch et al., 2000). Some global differences were noticed, in particular one third of the genes was down-regulated while two thirds were up-regulated (data not shown), while in the ESR higher number of genes was down-regulated (Gasch et al., 2000). Therefore, mistranslation does not trigger a true environmental stress response, suggesting that, despite resulting in marked growth defects, mistranslation may be sensed as a mild stress. This observation can be related with the kind of stress that our mistranslating cells are subjected to, namely chronic stress rather than an acute stress, meaning that cells have readapted their transcriptome to a new constitutive physiological condition and reached a new physiological “steady-state”.

mRNA mistranslation and proteostasis: effects on protein aggregation and UPS

Protein homeostasis (proteostasis) is a *bona fide* condition for proper cellular functioning. The functionality of proteins depends on two apparent opposite characteristics: the need for a stable and defined native structure and maintaining at the same time conformational flexibility. Ultimately, imbalances between these two properties result in abnormal misfolded proteins that can aggregate. The causes and consequences of protein aggregation in cellular physiology is a topic that has been intensively debated over the last few years as it is a hallmark of several diseases and has been implicated in natural aging processes (David et al., 2010). In addition to the potential harmful effect of protein insoluble aggregates, these structures can also have a protective function as they may trap damaged proteins that can be harmful to the cell. This has been suggested in both neurodegeneration and aging (Kourtis and Tavernarakis, 2011; Ross and Poirier, 2005). We have observed increased insoluble proteins in mistranslating cells and, in particular, in sir2Δ mistranslating cells, as discussed below. The increase of insoluble protein content is in line with the observed up-regulation of heat-shock proteins, in particular *HSP104*. This chaperone works together with Ssa1p (Hsp70) and Ydj1p (Hsp40), in order to disassemble protein aggregates that accumulate during stress (Parsell et al., 1994; Glover et al., 1998). Furthermore the strong up-regulation of Hsps indicates that they are one of the primary defence lines against the proteolytic stress imposed by mRNA mistranslation and that this can be one of the major cellular deregulatory events associated to chronic mRNA mistranslation. Despite the fact that mistranslating cells have a growth defect their viability is only slightly affected. Together, these observations strength the

idea that cells are able to adjust their metabolism to cope with proteostasis perturbations induced by protein conformational alterations.

The stronger protein aggregation observed in the sir2Δ strain can be related to the recent findings that sir2p is a key element of the so called spatial quality control. Indeed, it has been shown that oxidatively damaged proteins do not diffuse freely in the cytoplasm, but rather, are spatially controlled in such way that during cytokinesis the mother cell inherits the damaged proteins while the daughter cells remains virtually protein damage free (Erjavec and Nystrom, 2007; Liu et al., 2010b). Indeed, aggregates of oxidatively damaged proteins aggregates are recognized by Hsp104p, and are then tethered to the actin cables and microtubules avoiding retention in the daughter cells (Erjavec et al., 2007; Erjavec and Nystrom, 2007; Liu et al., 2010a). It is tempting to speculate, therefore, that the abrogation of this process is the cause of increased insoluble protein content in the sir2Δ mistranslating cells. Interestingly, overexpression or activation of the mammalian homologue of Sir2 increases the heat-shock response by increasing the time of binding of Hsf1p to the target promoters (Westerheide et al., 2009). Our results are in line with these observations and further support the hyphothesis that sir2p plays a role in PQC, which is of particular relevance since sirtuins apparently delay age-related neurodegeneration (Nystrom, 2011). It would be interesting to further explore the role of this gene in the cellular response to mistranslation in particular clarify whether Sir2p affects Sod1p or Ctt1p activity? acts on the signal transduction pathways that activate the misfolding sensors? clarify whether in mistranslating cells the activity of the chaperonin Cct1p, which is regulated by Sir2p and is required for actin and tubulin folding, is affected? Analysis of the

cytoskeleton of mistranslating cells and a detailed study of the kinetics of protein aggregation and the structure of these aggregates could also be informative. However, the observation that sir2Δ mistranslating strains have similar viability to wild type mistranslating cells, together with the observation that Sir2 may have a pivotal role in dilution of the protein aggregates points to a minor role of aggregation in the loss of viability observed in mistranslating cells, suggesting that other types of metabolic deregulation may be more important .

Recent studies show that protein aggregates partition between the JUNQ and IPOD cellular compartments. Indeed, the ubiquitination state of the aggregates and their status may dictate their partioning into these discrete compartments. Soluble misfolded proteins appear to accumulate in a juxtanuclear compartment named JUNQ, where proteasomes are concentrated, while the insoluble aggregates are sequestered to a perivacuolar inclusion (IPOD). It is tempting to speculate that mistranslation leads to the formation of aggresomes, which have been observed in a yeast model of huntington disease. These juxtanuclear aggregates are in line with our observations that mistranslation activates autophagy (discussed below) since agressomes sequester the misfolded toxic proteins and facilitate their removal by autophagy (Johnston et al., 1998; Kopito, 2000; Wang et al., 2009).

Our data showed that accumulation of insoluble proteins was accompanied by increased proteasome activity and autophagy. However, the majority of the knockout mistranslating strains, in exponential growth showed no increase in proteasomal activity. A decline in proteasome activity could be due to increased oxidative stress

caused by mistranslation or to the direct inhibition of the proteasome by the oxidized or damaged proteins. Indeed, we have observed that mRNA mistranslation leads to ROS accumulation (chapter 3 and below). Similar levels of the two ROS species analysed were observed between wild-type mistranslating cells and sir2Δ mistranslating cells, in exponential phase. However, in pnc1Δ mistranslating cells the two species were detected in abnormally high amounts, which support the above hypothesis. In addition, the observed decrease in this protease activity can be explained by the abrogation of functionally relevant interactions between Sir2p/Pnc1p and proteasome regulatory proteins (Guerrero et al., 2008; Darst et al., 2008).

Another interesting feature of mistranslating cells was the lack of polyubiquitinated proteins in the cytoplasm and increased ubiquitin accumulation in vacuoles, strongly suggesting that autophagy play a major role in the clearance of mistranslated proteins. This may also lead to the ubiquitin stress response (Hanna and Finley, 2007; Hanna et al., 2007) (due to ubiquitin depletion) which is characterized by increased loading of the proteasome with the deubiquitinating enzyme Ubp6p, that increases recycling of ubiquitin by this organelle. It would be of relevance, therefore, to clarify whether this stress response is activated mistranslating cells.

mRNA mistranslation and autophagy

This study shows that autophagy is up-regulated in response to mistranslation, likely due to accumulation of misfolded proteins rather than increased accumulation of dysfunctional organelles as we have only detected minor up-regulation of ribophagy and failed to detect mitophagy in mistranslating cells. The detection of ubiquitin in

vacuoles supports this hypothesis that autophagy is the preferred degradative pathway for aggregated proteins in mistranslating cells, which is in line with previous studies that proposed that autophagy may represent the last line of defence against toxic aggregates (Pan et al., 2008; Madeo et al., 2009). Despite this, impairment of autophagy does not compromise viability of mistranslating cells since cells blocked in the autophagic pathway and control cells mistranslating constitutively have similar viability and longevity. However, our studies should be complemented with additional studies using strains harbouring multiple knockouts in the autophagy pathway. For example the multiple knockout strain (MKO) constructed by Cao and co-workers (Cao et al., 2008; Cao et al., 2009; Cao and Klionsky, 2008) could be a good option for these studies. This could allow clarifying how mistranslated proteins are targeted to the vacuole.

Remarkably, there is high similarity between the phenotypes displayed by mistranslating cells and those of yeast growing under starvation conditions. In this context, it is most interesting that previous studies strongly suggest that mistranslation may generate an amino acid starvation phenotype (Silva, 2005). For example, mistranslation reduces PKA signalling even in the presence of glucose since mistranslating cells accumulate threalose and glycogen (Silva, 2005), whose biosynthesis is dependent on the activation of STRE-containing genes, and down-regulate expression of ribosomal protein genes (Silva, 2005). Medverik and collegues (Medvedik et al., 2007) have shown that calorie restriction (CR) and the TOR pathway induce Msn2p and Msn4p re-localization to the nucleus resulting in increased expression of *PNC1* with consequent increase in replicative life span. Therefore, the

upregulation of the *PNC1/SIR2* pathway may be dependent on PKA signalling and may contribute to maintain viability of mistranslating cells. We have shown that mistranslation-induced autophagy is Sir2p dependent but our data also show that Sir2p does not play a role in autophagy under starvation conditions (Figure 44). This result should however be confirmed because the yeast Hst1p and Hst2p sirtuins can replace Sir2p function (Lamming et al., 2005). Since our data do not clarify the full role of *PNC1* and *SIR2* in the response to mistranslation, it would be interesting to investigate if *PNC1* regulates the master stress regulators *MSN2/MSN4* and whether regulation of the response to mistranslation happens upstream or downstream of TOR and PKA.

Other studies from our laboratory showed that mistranslation decreased expression of ribosomal protein genes (Silva, 2005; Silva RM et al., 2007; Paredes JA, 2010) and reduces the polysomal fraction but the expected increase in free ribosome (80S) was not observed. These data prompt some questions, namely 1) whether down regulation of ribosomal genes has a negative impact on the cellular level of ribosomal proteins 2) whether ribosomes are degraded selectively by ribophagy? Our data revealed that ribophagy was not significantly up-regulated in response to mistranslation, suggesting that ribosomes are degraded by a ribophagy independent.

According to the mitochondria dysfunction phenotype (discussed below), one would expect that mitophagy would be up-regulated in mistranslating cells, as damaged mitochondria represent an additional risk to the cell. In other words, efficient elimination of damaged mitochondria should be important to maintain cellular

homeostasis. Furthermore, we have detected a consistent overexpression of the *CIT2* gene, which encodes for the Cit2p, a target of the retrograde signaling pathway (RTG), which is involved in mitophagy induction (Journo et al., 2009). Despite this, we did not detect mitophagy in mistranslating cells. However, mitophagy in yeast as so far been detected in cells grown in a nonfermentable carbon source and/or in post-log phase, which is not the case of our mistranslating cells (Kanki et al., 2009b; Kanki et al., 2010; Kanki and Klionsky, 2008; Kanki et al., 2009a). Moreover, several other factors have been described to induce mitophagy, namely osmotic swelling of mitochondria caused by loss of Mdm38p (Nowikovsky et al., 2007), mitochondrial depolarization (in mammalian, but not in yeast cells) (Kissova et al., 2004; Kanki and Klionsky, 2009; Sandoval et al., 2008), nitrogen starvation or rapamycin treatment (Tal et al., 2007; Kanki et al., 2009b; Kanki and Klionsky, 2008) and we did not verify whether mistranslation affected these factors. On the other hand, it is also known that mitophagy can be blocked in the presence of strong macroautophagy inducing conditions (nitrogen starvation) if mitochondria are essential for cell survival in such conditions (Kanki and Klionsky, 2008). Several groups have also shown that impairment of mitophagy could be achieved through redox imbalance caused by alterations in the cellular reduced gluthatione pool (Deffieu et al., 2009; Kissova and Camougrand, 2009). Therefore, increased gluthatione levels could explain the lack of mitophagy in mistranslating cells. Finally, mistranslating cells may degrade mitochondria by a non-selective pathway, namely microautophagy, or instead of degrading entire mitochondria, they may degrade mitochondrial proteins and, rely on the activity of intrinsic mitochondrial proteases like Oma1p or Yme1p or ubiquitin-proteasome dependent degradation of mitochondrial proteins (Bestwick et al., 2010). In any case,

impairment of mitochondria degradation should lead to accumulation of misfolded and ubiquitinated proteins in the mitochondria, causing progressive mitochondrial dysfunction.

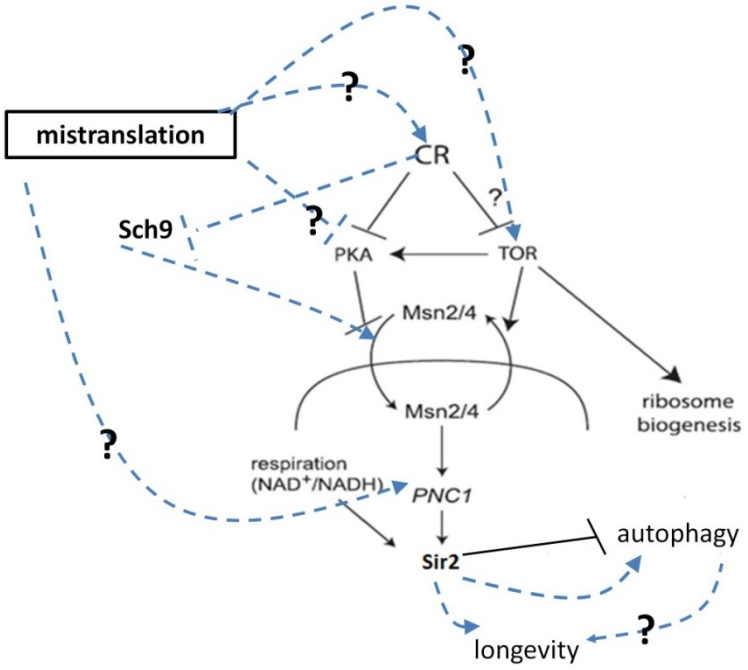

Figure 44-Under CR conditions PKA and TOR are blocked. These pathways act on Msn2/4 which are relocated to the nucleus where they regulate *PNC1* expression. The *PNC1* nicotinamidase activity leads to a decrease in nicotinamide (NAM) which in turn results on higher Sir2p activity, but does not increase autophagic activity. For reasons that remain unclear, under mistranslation conditions, Sir2p up-regulates autophagy. Dashed lines indicate mistranslation relations while full lines represent CR described relations (adapted from Medvedik 2007)

The impact of mistranslation on oxidative stress and respiration

Intracellular generation of ROS is an intrinsic process of aerobic organisms and is intrinsically linked to oxidative stress. The latter defines several interrelated phenomena, namely elevated generation of ROS and oxidative damage to cell components. There are several factors that have been described as oxidative stress triggers and our study identified mistranslation as one of them. Indeed, mistranslating cells accumulated ROS and up-regulated genes involved in the oxidative stress

response. While we have observed the up-regulation of most of the antioxidant defences, namely *CTT1*, *SOD1*, *TRX1*, *TSA1*, etc, mistranslation did not increase expression of the *YAP1* gene and we did not find enrichment for transcriptional binding sites for Yap1p in the set of deregulated genes. This result was quite unexpected as Yap1p activates the transcription of anti-oxidant genes and is the central regulator of the oxidative stress response in *S.cerevisiae*. Therefore, it is possible that mistranslating cells may activate alternative ROS scavenging mechanisms, namely increasing the level of methionine incorporation into proteins. Mammalian cells respond to oxidative stress generated by environmental stressors by misacylating different tRNAs with methionine (Met) (Netzer et al., 2009). The mechanisms by which the MetRS loses its specificity in presence of ROS are not yet known. However Met is a ROS scavenger and its misincorporation into proteins is likely beneficial under oxidative stress (Netzer et al., 2009).

ROS accumulation may also reflects the need for regulation of the cellular response to mistranslation, as H_2O_2 and other ROS species are also important secondary messengers that regulate several physiological processes in mammalian cells (Linnane et al., 2007; Scherz-Shouval et al., 2007; Scherz-Shouval and Elazar, 2007). Protein damage by ROS depends on several factors, namely the relative protein content of oxidation-sensitive amino acid residues (methionine, for instance), having or not metal-binding sites, the localization of proteins in the cell, their conformation and degradation rate. More importantly, newly synthesized proteins are more prone to oxidative damage, suggesting that mistranslated proteins may be more prone to oxidative damage than wild-type proteins that fold correctly during synthesis. In other

words, ROS may damage mistranslated proteins due to their inability to fold properly as they exit from the ribosome. Such oxidative damage may therefore promote protein aggregation. ROS have also been implicated in apoptosis induction, but we did not detected increased apoptosis in mistranslating cells.

The ROS detected in mistranslating cells may be related to UPR induction or to mitochondrial dysfunction. High protein folding and refolding activity in the ER, which are highly redox-dependent processes, may lead to ROS generation and oxidative stress. This hypothesis is in line with previous studies which show that upon a threshold, the UPR causes the accumulation of reactive oxygen species (ROS), contributing to cell death (Haynes et al., 2004; Santos et al., 2009). Mitochondria are also ROS producers and structural damage caused by mistranslated proteins may compromise mitochondrial function, increasing ROS production (Andreyev et al., 2005). In this study we have shown that mistranslation affects the mitochondrial network, leading to mitochondrial fragmentation. Furthermore, mistranslation impairs yeast growth in the presence of respiratory substrates, which provides strong evidence for major mitochondrial dysfunction in these cells. Such mitochondrial fragmentation supports the hypothesis that mistranslation deeply affects mitochondrial fusion or fission (or both). However, their inability to grow in the presence of respiratory substrates suggests that they are also unable to produce ROS. If so, ROS are most likely produced in the ER rather than in the mitochondria.

Finaly, our data seem to indicate that mistranslating cells rely on glycolysis rather than on oxidadative phosphorylation to produce ATP. This may happen to compensate

mitochondrial dysfunction and to lower global ROS production, i.e. lowering the mitochondrial contribution to ROS production, to maintain the latter within tolerable levels.

Mistranslation, P-bodies and translation

Our data showed that mistranslation induces formation of P-bodies and does not affect formation of stress granules. The observation that mistranslation leads to P-body assembly, indicates that it generates a stress condition (as expected) and suggests that microarray data may not reflect the full picture of gene deregulation because some of the mRNAs are trapped in the P-bodies and are not available to translation (Teixeira et al., 2005;Balagopal and Parker, 2009; Parker and Sheth, 2007). This may explain some discrepancies between the transcriptomic and the proteomic data obtained in our laboratory (Silva, 2005). If so proteomics analysis of mistranslating cells may provide a more accurate view of the cellular response to this form of stress. Alternatively, profiling of polysome-associated mRNA may provide a more accurate view of the cellular response to mistranslation, as these mRNAs are effectively translated

P-body formation may be related to the down regulation of ribosomal protein genes, and consequently to a predictable decrease in translational rate, as P-body accumulation is known to be a consequence of translational shut-down (Eulalio et al., 2007; Teixeira et al., 2005). The expected lower translation rate can also be related to increased oxidative stress as it has been shown that both oxidative stress and mistranslation impair translation initiation and protein synthesis, which may alleviate

the deleterious effects of continuous mRNA mistranslation allowing for reprogramming of proteins synthesis in order to respond to the stressful conditions imposed by protein misfolding. Alternatively, it is possible to rationalize the down-regulation of ribosomal proteins in terms of energetic costs. Indeed, the cell invests approximately 90% of the total cellular energy available to synthesize proteins and assigns 80% of the transcriptional machinery to rRNA synthesis. Therefore, the energetic requirement of mistranslating cells for protein degradation, folding and refolding, may force a strong reduction in protein synthesis, in particular because mistranslating cells likely produce ATP less efficiently than control cells due to mitochondrial dysfunction.

Conclusion and Perspectives

This study contributes to the characterization of the cellular response to aberrant protein synthesis. Errors in translation decrease growth rate, increase in the amount of insoluble proteins and lead to accumulation of ubiquitinated proteins in vacuoles, upregulate autophagy, accumulation of ROS and induce mitochondrial dysfunction and P-body formation. The study highlights how several stress response pathways work in a coordinated and interactive manner, to prevent a general collapse of cellular homeostasis. Therefore, the identification of the main regulators of the stress response induced by mistranslation is of paramount importance. Given that the TOR pathway stands on the crossroads of growth, metabolism, translational control, autophagy, this would be a good starting point to dissect the signaling pathway that control the cellular response to mistranslation. Also, attention should be paid to the role of HSPs and, therefore, it would be important to study how HSPs are induced in

mistranslating cells. The mitochondrial associated defects should also be addressed in further detail and the ROS sources should be identified. Although our study indicates that yeast is an excellent model system to study mistranslation and its physiological consequences, these studies should be extended to a vertebrate model, like zebrafish or mouse. These models would provide additional information on the effects of mistranslation in human diseases namely neurodegeneration, autoimmune diseases and aging.

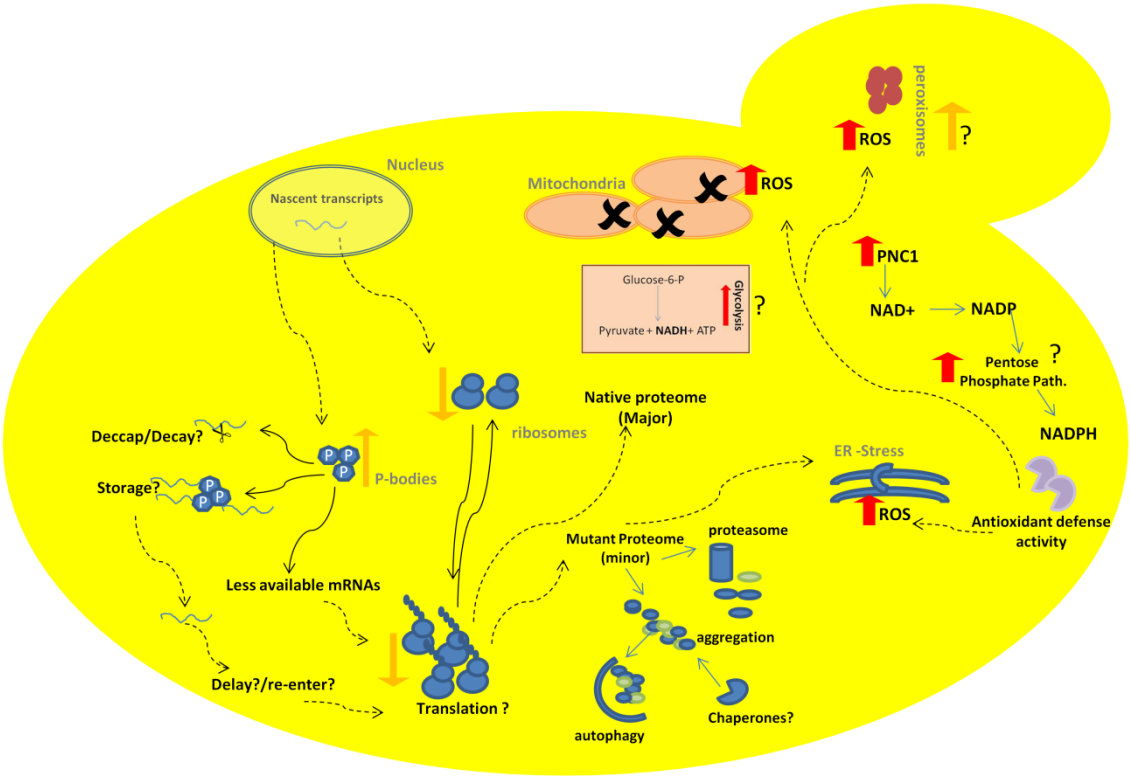

Figure 45- Overall aspects of constitutive mRNA mistranslation in yeast cells. The major physiological alterations caused by mistranslation are shown. For simplicity, not all relations are shown. mRNAs are correctly transcribed in the nucleus and either redirected to P-bodies were they can be degraded or temporarly stored or to the ribosomes, for translation. Storage of mRNAs in the P-bodies may have to do with the need of transcribing specific mRNAs at certain time points. Decreased ribosome synthesis results in expected lower translation rates. During translation, erroneous incorporation of serine at leucine CUG codon sites leads to the appearance of misfolded proteins, which aggregate and induce ER-stress, UPR, autophagy, proteasome activity and chaperone activity. On the other hand, ER-stress may lead to increased ROS production. Mistranslation also leads to mitochondrial dysfunction that may be related to increased glycolysis, in order to minimize ROS production. It is likely that mistranslation deregulates peroxisome number and metabolism. Mistranslation also upregulates *PNC1*, which is important to increase NAD^+ production and for autophagy control. Increased NAD^+ production ensures high levels of NADPH in mistranslating cells, in order to allow for an effective antioxidant response.

References

1. Andreyev, A.Y., Y.E.Kushnareva, and A.A.Starkov. 2005. Mitochondrial metabolism of reactive oxygen species. *Biochemistry (Mosc.)* 70:200-214.
2. Balagopal, V. and R.Parker. 2009. Polysomes, P bodies and stress granules: states and fates of eukaryotic mRNAs. *Curr. Opin. Cell Biol* 21:403-408.
3. Bestwick, M., M.Y.Jeong, O.Khalimonchuk, H.Kim, and D.R.Winge. 2010. Analysis of Leigh syndrome mutations in the yeast SURF1 homolog reveals a new member of the cytochrome oxidase assembly factor family. *Mol. Cell Biol* 30:4480-4491.
4. Cao, Y., H.Cheong, H.Song, and D.J.Klionsky. 2008. In vivo reconstitution of autophagy in Saccharomyces cerevisiae. *J. Cell Biol* 182:703-713.
5. Cao, Y. and D.J.Klionsky. 2008. New insights into autophagy using a multiple knockout strain. *Autophagy.* 4:1073-1075.
6. Cao, Y., U.Nair, K.Yasumura-Yorimitsu, and D.J.Klionsky. 2009. A multiple ATG gene knockout strain for yeast two-hybrid analysis. *Autophagy.* 5:699-705.
7. Darst, R.P., S.N.Garcia, M.R.Koch, and L.Pillus. 2008. Slx5 promotes transcriptional silencing and is required for robust growth in the absence of Sir2. *Mol. Cell Biol* 28:1361-1372.
8. David, D.C., N.Ollikainen, J.C.Trinidad, M.P.Cary, A.L.Burlingame, and C.Kenyon. 2010. Widespread protein aggregation as an inherent part of aging in C. elegans. *PLoS Biol* 8:e1000450.
9. Deffieu, M., I.Bhatia-Kissova, B.Salin, A.Galinier, S.Manon, and N.Camougrand. 2009. Glutathione participates in the regulation of mitophagy in yeast. *J. Biol Chem.* 284:14828-14837.
10. Erjavec, N., L.Larsson, J.Grantham, and T.Nystr+Âm. 2007. Accelerated aging and failure to segregate damaged proteins in Sir2 mutants can be suppressed by overproducing the protein aggregation-remodeling factor Hsp104p. *Genes & Development* 21:2410-2421.
11. Erjavec, N. and T.Nystrom. 2007. Sir2p-dependent protein segregation gives rise to a superior reactive oxygen species management in the progeny of Saccharomyces cerevisiae. *PNAS* 104:10877-10881.
12. Eulalio, A., I.Behm-Ansmant, and E.Izaurralde. 2007. P bodies: at the crossroads of post-transcriptional pathways. *Nat Rev Mol Cell Biol* 8:9-22.
13. Gasch, A., P.Spellman, C.Kao, O.Carmel-Harel, M.Eisen, G.Storz, D.Botstein, and P.Brown. 2000. Genomic Expression Programs in the Response of Yeast Cells to Environmental Changes. *Mol. Biol. Cell* 11:4241-4257.
14. Guerrero, C., T.Milenkovic, N.Przulj, P.Kaiser, and L.Huang. 2008. Characterization of the proteasome interaction network using a QTAX-based tag-team strategy and protein interaction network analysis. *Proc. Natl. Acad. Sci. U. S. A* 105:13333-13338.
15. Hanna, J. and D.Finley. 2007. A proteasome for all occasions. *FEBS Lett.* 581:2854-2861.
16. Hanna, J., A.Meides, D.P.Zhang, and D.Finley. 2007. A ubiquitin stress response induces altered proteasome composition. *Cell* 129:747-759.
17. Haynes, C.M., E.A.Titus, and A.A.Cooper. 2004. Degradation of misfolded proteins prevents ER-derived oxidative stress and cell death. *Mol. Cell* 15:767-776.
18. Johnston, J.A., C.L.Ward, and R.R.Kopito. 1998. Aggresomes: A Cellular Response to Misfolded Proteins. *J. Cell Biol.* 143:1883-1898.
19. Journo, D., A.Mor, and H.Abeliovich. 2009. Aup1-mediated regulation of Rtg3 during mitophagy. *J. Biol Chem* 284:35885-35895.
20. Kanki, T., D.Kang, and D.J.Klionsky. 2009a. Monitoring mitophagy in yeast: the Om45-GFP processing assay. *Autophagy.* 5:1186-1189.
21. Kanki, T. and D.J.Klionsky. 2008. Mitophagy in yeast occurs through a selective mechanism. *J Biol Chem* 283:32386-32393.
22. Kanki, T. and D.J.Klionsky. 2009. Atg32 is a tag for mitochondria degradation in yeast. *Autophagy.* 5:1201-1202.
23. Kanki, T., K.Wang, Y.Cao, M.Baba, and D.J.Klionsky. 2009b. Atg32 is a mitochondrial protein that confers selectivity during mitophagy. *Dev. Cell* 17:98-109.
24. Kanki, T., K.Wang, and D.J.Klionsky. 2010. A genomic screen for yeast mutants defective in mitophagy. *Autophagy.* 6:278-280.
25. Kissova, I., M.Deffieu, S.Manon, and N.Camougrand. 2004. Uth1p is involved in the autophagic degradation of mitochondria. *J. Biol Chem* 279:39068-39074.
26. Kissova, I.B. and N.Camougrand. 2009. Glutathione participates in the regulation of mitophagy in yeast. *Autophagy.* 5:872-873.
27. Kopito, R.R. 2000. Aggresomes, inclusion bodies and protein aggregation. *Trends Cell Biol* 10:524-530.
28. Kourtis, N. and N.Tavernarakis. 2011. Cellular stress response pathways and ageing: intricate molecular relationships. *EMBO J.* 30:2520-2531.
29. Lamming, D.W., M.Latorre-Esteves, O.Medvedik, S.N.Wong, F.A.Tsang, C.Wang, S.J.Lin, and D.A.Sinclair. 2005. HST2 mediates SIR2-independent life-span extension by calorie restriction. *Science* 309:1861-1864.

30. Lee, I.H., L.Cao, R.Mostoslavsky, D.B.Lombard, J.Liu, N.E.Bruns, M.Tsokos, F.W.Alt, and T.Finkel. 2008. A role for the NAD-dependent deacetylase Sirt1 in the regulation of autophagy. *PNAS* 105:3374-3379.
31. Lelouard, H., V.Ferrand, D.Marguet, J.Bania, V.Camosseto, A.David, E.Gatti, and P.Pierre. 2004. Dendritic cell aggresome-like induced structures are dedicated areas for ubiquitination and storage of newly synthesized defective proteins. *J. Cell Biol* 164:667-675.
32. Linnane, A.W., M.Kios, and L.Vitetta. 2007. The essential requirement for superoxide radical and nitric oxide formation for normal physiological function and healthy aging. *Mitochondrion.* 7:1-5.
33. Liu, B., L.Larsson, A.Caballero, X.Hao, D.Oling, J.Grantham, and T.Nystrom. 2010b. The polarisome is required for segregation and retrograde transport of protein aggregates. *Cell* 140:257-267.
34. Liu, B., L.Larsson, A.Caballero, X.Hao, D.Oling, J.Grantham, and T.Nystrom. 2010a. The polarisome is required for segregation and retrograde transport of protein aggregates. *Cell* 140:257-267.
35. Lu, C., M.J.Brauer, and D.Botstein. 2009. Slow growth induces heat-shock resistance in normal and respiratory-deficient yeast. *Mol. Biol Cell* 20:891-903.
36. Madeo, F., T.Eisenberg, and G.Kroemer. 2009. Autophagy for the avoidance of neurodegeneration. *Genes Dev.* 23:2253-2259.
37. Martinez-Pastor, M.T., G.Marchler, C.Schuller, A.Marchler-Bauer, H.Ruis, and F.Estruch. 1996. The Saccharomyces cerevisiae zinc finger proteins Msn2p and Msn4p are required for transcriptional induction through the stress response element (STRE). *EMBO J.* 15:2227-2235.
38. Medvedik, O., D.W.Lamming, K.D.Kim, and D.A.Sinclair. 2007. MSN2 and MSN4 link calorie restriction and TOR to sirtuin-mediated lifespan extension in Saccharomyces cerevisiae. *PLoS Biol* 5:e261.
39. Netzer, N., J.M.Goodenbour, A.David, K.A.Dittmar, R.B.Jones, J.R.Schneider, D.Boone, E.M.Eves, M.R.Rosner, J.S.Gibbs, A.Embry, B.Dolan, S.Das, H.D.Hickman, P.Berglund, J.R.Bennink, J.W.Yewdell, and T.Pan. 2009. Innate immune and chemically triggered oxidative stress modifies translational fidelity. *Nature* 462:522-526.
40. Nowikovsky, K., S.Reipert, R.J.Devenish, and R.J.Schweyen. 2007. Mdm38 protein depletion causes loss of mitochondrial K+/H+ exchange activity, osmotic swelling and mitophagy. *Cell Death. Differ.* 14:1647-1656.
41. Nystrom, T. 2011. Spatial protein quality control and the evolution of lineage-specific ageing. *Philos. Trans. R. Soc. Lond B Biol Sci.* 366:71-75.
42. Pan, M., V.Maitin, S.Parathath, U.Andreo, S.X.Lin, G.C.St, Z.Yao, F.R.Maxfield, K.J.Williams, and E.A.Fisher. 2008. Presecretory oxidation, aggregation, and autophagic destruction of apoprotein-B: a pathway for late-stage quality control. *Proc. Natl. Acad. Sci. U. S. A* 105:5862-5867.
43. Paredes JA. Estudo molecular da degeneração e evolução celular induzidas por erros na tradução do mRNA / Molecular study of cell degeneration and evolution induced by mRNA mistranslation. 2010. University of Aveiro.
44. Parker, R. and U.Sheth. 2007. P bodies and the control of mRNA translation and degradation. *Mol. Cell* 25:635-646.
45. Reynolds, N.M., B.A.Lazazzera, and M.Ibba. 2010. Cellular mechanisms that control mistranslation. *Nat Rev Microbiol.* 8:849-856.
46. Ross, C.A. and M.A.Poirier. 2005. Opinion: What is the role of protein aggregation in neurodegeneration? *Nat Rev. Mol. Cell Biol* 6:891-898.
47. Sandoval, H., P.Thiagarajan, S.K.Dasgupta, A.Schumacher, J.T.Prchal, M.Chen, and J.Wang. 2008. Essential role for Nix in autophagic maturation of erythroid cells. *Nature* 454:232-235.
48. Santos, C.X., L.Y.Tanaka, J.Wosniak, and F.R.Laurindo. 2009. Mechanisms and implications of reactive oxygen species generation during the unfolded protein response: roles of endoplasmic reticulum oxidoreductases, mitochondrial electron transport, and NADPH oxidase. *Antioxid. Redox. Signal.* 11:2409-2427.
49. Santos, M.A., C.Cheesman, V.Costa, P.Moradas-Ferreira, and M.F.Tuite. 1999. Selective advantages created by codon ambiguity allowed for the evolution of an alternative genetic code in Candida spp. *Mol Microbiol.* 31:937-947.
50. Scherz-Shouval, R. and Z.Elazar. 2007. ROS, mitochondria and the regulation of autophagy. *Trends Cell Biol* 17:422-427.
51. Scherz-Shouval, R., E.Shvets, E.Fass, H.Shorer, L.Gil, and Z.Elazar. 2007. Reactive oxygen species are essential for autophagy and specifically regulate the activity of Atg4. *EMBO J.* 26:1749-1760.
52. Silva, R.M., J.A.Paredes, G.R.Moura, B.Manadas, T.Lima-Costa, R.Rocha, I.Miranda, A.C.Gomes, M.J.Koerkamp, M.Perrot, F.C.Holstege, H.Boucherie, and M.A.Santos. 2007. Critical roles for a genetic code alteration in the evolution of the genus Candida. *EMBO J.* 26:4555-4565.
53. Silva,R. Reconstrução molecular de uma alteração ao código genético / Molecular reconstruction of a genetic code alteration.2005.Biologia Universidade de Aveiro.
54. Tal, R., G.Winter, N.Ecker, D.J.Klionsky, and H.Abeliovich. 2007. Aup1p, a yeast mitochondrial protein phosphatase homolog, is required for efficient stationary phase mitophagy and cell survival. *J Biol. Chem.* 282:5617-5624.

55. Teixeira, D., U.Sheth, M.A.Valencia-Sanchez, M.Brengues, and R.Parker. 2005. Processing bodies require RNA for assembly and contain nontranslating mRNAs. *RNA.* 11:371-382.
56. Wang, Y., A.B.Meriin, N.Zaarur, N.V.Romanova, Y.O.Chernoff, C.E.Costello, and M.Y.Sherman. 2009. Abnormal proteins can form aggresome in yeast: aggresome-targeting signals and components of the machinery. *FASEB J* 23:451-463.
57. Westerheide, S.D., J.Anckar, S.M.Stevens, Jr., L.Sistonen, and R.I.Morimoto. 2009. Stress-inducible regulation of heat shock factor 1 by the deacetylase SIRT1. *Science* 323:1063-1066.